The role of PTEN as a PI(3,4)P_2 lipid phosphatase in Class I phosphoinositide 3-kinase signalling

This dissertation is submitted to the University of Cambridge
for the degree of Doctor of Philosophy

Anna Jadwiga Kielkowska

Darwin College
University of Cambridge
September 2017

Blank

Summary

Name: Anna Jadwiga Kielkowska

Dissertation title: The role of PTEN as a PI(3,4)P_2 lipid phosphatase in Class I phosphoinositide 3-kinase signalling

Class I phosphoinositide 3-kinases (Class I PI3Ks) are essential players involved in the signalling events in the cell and are critical promoters of cellular growth, survival and metabolism. Once activated by environmental stimuli such as growth factors, cytokines or antigens, they exert their catalytic activity by phosphorylating phosphatidylinositol (4,5)-bisphosphate (PI(4,5)P_2) to yield a second messenger - PI(3,4,5)P_3. Unrestrained PI(3,4,5)P_3 signalling has been classically associated with hyperactivation of the Class I PI3K/AKT pathway and has been shown to be a molecular trigger of many pathophysiologies in humans, including autoimmune disorders, respiratory diseases and cancer. To date, two classes of lipid phosphatases SHIP1/2 and PTEN have been reported, which dephosphorylate PI(3,4,5)P_3 on positions 5' and 3' of the inositol ring to generate PI(3,4)P_2 and PI(4,5)P_2 respectively, and thus quench Class I PI3K signalling. Moreover, PI(3,4)P_2 levels in the cell are regulated by two important lipid 4-phosphatases - INPP4A/B. While the role of PTEN as a tumour suppressor is well established, functions of SHIP1/2 and INPP4A/B are just starting to emerge. A major barrier to progress in this field has been the lack of high quality measurements of PI(3,4)P_2, to assess the impact it may have on shaping cellular behaviour.

This dissertation summarises the work performed to develop a novel, HPLC-ESI MS/MS based method, in order to measure the product of PI(3,4,5)P_3 5-dephosphorylation, PI(3,4)P_2, separated from its more abundant regioisomer in cells - PI(4,5)P_2. This and an existing HPLC-ESI MS/MS method for measuring PI(3,4,5)P_3, have enabled us to describe the fluxes through Class I PI3K-controlled PI(3,4,5)P_3 generation and its subsequent 3- and 5- dephosphorylation pathways in human mammary epithelial cells (Mcf10a) stimulated with epidermal growth factor (EGF). By means of genetic suppression of PTEN and INPP4B, we revealed an unexpectedly high level of PI(3,4)P_2 that accumulates in EGF-stimulated PTEN-INPP4B-KO Mcf10a cells. Further, an *in vitro* biochemical assay suggested a novel role for PTEN as a direct PI(3,4)P_2 3-phosphatase in Mcf10a cells. This important observation was supported by *in sillico*

phosphatidylinositol lipid modelling of the relevant pathways. In an effort to understand its potential physiological significance, we demonstrated that PI(3,4)P_2 accumulation correlates with the ability of genetically modified Mcf10a cells to form gelatin-degrading invadopodia. Finally, we used a mouse prostate cancer model to show PTEN's importance in controlling PI(3,4)P_2 levels *in vivo*, pointing to a potential role for PI(3,4)P_2 in PTEN-dependent tumourigenesis. I hope that the work described in this dissertation will contribute to the current knowledge of phosphatidylinositol lipid biology in the context of Class I PI3K signalling and will simulate future efforts to gain an in-depth understanding of the roles of PTEN and PI(3,4)P_2 in cellular physiology.

Declaration

The work presented in this dissertation was undertaken in the Inositide Laboratory, under the supervision of Dr Phillip T. Hawkins FRS, at the Babraham Institute. This dissertation is the result of my own work and includes nothing which is the outcome of work done in collaboration except as declared in the Preface and specified in the text.

It is not substantially the same as any that I have submitted, or, is being concurrently submitted for a degree or diploma or other qualification at the University of Cambridge or any other University or similar institution except as declared in the Preface and specified in the text. I further state that no substantial part of my dissertation has already been submitted, or, is being concurrently submitted for any such degree, diploma or other qualification at the University of Cambridge or any other University or similar institution except as declared in the Preface and specified in the text.

It does not exceed the prescribed word limit set out by the Biology Degree Committee.

Anna Jadwiga Kielkowska

September 2017

Blank

Nothing in life is to be feared, it is only to be understood.

- Maria Skłodowska-Curie -

Blank

Acknowledgements

I would like to thank my supervisors Phill and Len for accepting me as a group member and for their continuous support during the course of my PhD. The way they approach science has become my 'gold standard' which I will try to apply throughout my professional career. It has also been amazing to work in such a stimulating environment, and the team spirit that exists within our group is without doubt thanks to them. At this stage, I could not forget about Jonathan, who was my first supervisor at Babraham and who, by employing me six years ago, has initiated the UK chapter of my life. Jonathan has had a great contribution to shaping me as a scientist and I will continue to admire him for his patience which I quite often lack.

My PhD would not be possible if it wasn't for a huge help from people in the lab and others at Babraham Institute. I would like to thank Malek for being a great teacher during the initial stages of my PhD, hours spent working as a team and for inspiring discussions. Special thanks to Tamara, Karen and Natalie, for their contribution to the project, patience in answering my questions and offering help and advice during the intense periods of this PhD. Simon Walker is another person with a huge input to the outcome of this work and his expertise in imaging and patience have been invaluable. Special thanks to Dominik, whose knowledge and positive approach to life have been equally important during the critical moments of this project. I would also like to acknowledge Veronique's contribution and thank her for fighting through generating the CRISPR/Cas9 knock-out cell lines. Barzan, Vishnu and Piotrek have been amazing to spend time with at work and outside the lab. Finally, I would like to thank other lab members, our collaborators and people who at different stages shared their advice, opinion and offered help, all of which has been invaluable in progressing the science forward.

I would like to thank my best friend Magda, who has been a continuous source of support and inspiration since we met in Lausanne and whose critical and honest opinions have helped me navigate through life and avoid making mistakes. Iza and Dorota have been two closest to my heart people in the UK and I am grateful for their friendship, time spend together and help they offer every day.

I am eternally grateful to my parents for their support throughout my life, for showing me the World and making me the person who I am today. They have always been the best support team and the largest driving force in my life. My brother Marek is a person who has been part of my life since we were born and is both one of my greatest friends and honest critics.

I've been lucky enough to meet people in my life who brought values which have become my values and who inspired me to doing things I would never think were possible. As there are not enough words to properly say thank you, I believe that inspiring others, by achieving more and reaching further, is the best way to return what we receive from life and it is what I will continue doing.

Table of acknowledgement of assistance

1. Initial training in techniques and laboratory practice and subsequent mentoring:

Dr J. Clark – PhD mentoring (development of HPLC-ESI MS/MS methodology)
Dr S. Beinke – PhD mentoring (GSK)
Dr K. Anderson – PhD mentoring (Babraham Institute)
Dr M. Malek – initial laboratory training
Dr S. Walker – training (microscopy and imaging)
Dr E. Ivanova – training (mouse prostate cryosections)
Dr N. Rynkiewicz – training (H&E staining of mouse prostate cryosections)

2. Data obtained from a technical service provider (e.g. DNA sequencing, illustrations, simple bioinformatics information etc)

N/A

3. Data produced jointly (e.g. where it was necessary or desirable to have two pairs of hands)

Dr M. Malek – co-performance of *in vitro* biochemical assay, imaging of 12 week mouse prostate and mass spectrometry experiments
Dr K. Anderson – co-performance of mass spectrometry experiments in human prostate cell lines

4. Data/materials provided by someone else (e.g. one-off analysis, bioinformatics analysis, where parallel data or technical provision in a very different area is needed to provide a connected account in the thesis)

Dr J. Clark and Dr I. Niewczas – synthesis and provision of mass spectrometry standards
Dr J. Clark – development of HPLC-ESI MS/MS method for PI3P/PI4P separation
Dr V. Juvin and Dr D. Spensberger – CRISPR knockout Mcf10a cell lines
Dr P. Pir, Dr N. le Novère and Dr V. Kiselev – *in sillico* phosphatidylinositol lipid modelling
Dr M. Malek and Dr K. Anderson – pAKT time courses in Mcf10a cells
Dr T. Sasaki – provision of [*Pten*$^{flox/flox}$, *PbCre*$^{-/-}$, *Inpp4b*$^{-/-}$] and [*Pten*$^{flox/flox}$, *PbCre*$^{+/-}$ *Inpp4b*$^{-/-}$] mouse prostate tissue; mass spectrometry analysis of WT and [*Pten*$^{flox/flox}$, *PbCre*$^{+/-}$] 10 week mouse prostates
Dr S. Felisbino – histopathological analysis of H&E stained mouse prostate sections
Dr T. Chessa – Western Blot analysis of mouse prostate and human prostate cell lines
Dr T Durrant – provision of human platelet samples
Dr G. Masson – provision of recombinant PTEN
Dr A. Segonds-Pichon – statistical analysis

Blank

List of abbreviations

3-phosphatase	-	inositol polyphosphate 3-phosphatase
4-phosphatase	-	inositol polyphosphate 4-phosphatase
5-phosphatase	-	inositol polyphosphate 5-phosphatase
acetyl CoA	-	acetyl coenzyme A
AKT	-	human homologue of serine/theonine kinase in transforming virus Akt-8
APDS	-	activated p110δ syndrome
AR	-	androgen receptor
BTK	-	Bruton's tyrosine kinase
C2 domain	-	conservation domain 2 in calcium activated protein kinase C
CCP	-	clathrin coated pit
CCV	-	clathrin coated vesicle
CID	-	collision induced dissociation
CL	-	cardiolipin
CLL	-	chronic lymphocytic leukemia
CME	-	clathrin mediated endocytosis
DAG	-	diacylglycerol
DC	-	direct current
DMS	-	dimethyl sulphide
ECM	-	extracellular matrix
EEA1	-	early endosomal antigen 1
EMT	-	epithelial-to-mesenchymal transition
ER	-	estrogen receptor
ESI	-	electrospray ionisation
FA	-	focal adhesion
FEME	-	fast endophilin-mediated endocytosis
fMLP	-	formyl peptide f-MetLeuPhe
FTC	-	follicular thyroid carcinoma
FWHM	-	full width at half maximum
FV-PTC	-	follicular variant of papillary thyroid carcinoma
G-3-P	-	glycerol-3-phosphate
GAB	-	GRB2-associated binder
GEF	-	guanine nucleotide exchange factor

GFP	-	green fluorescent protein
GLUT4	-	glucose transporter 4
GPCR	-	G protein coupled receptor
GRP1	-	general receptor for phosphoinositides 1
GSK3	-	glycogen synthase kinase 3
HMEC	-	human mammary epithelial cells
HPLC	-	high performance liquid chromatography
IHC	-	immunohistochemistry
INPP4A	-	inositol polyphosphate-4-phosphatase type I
INPP4B	-	inositol polyphosphate-4-phosphatase type II
IRS1	-	insulin receptor substrate 1
ITAM	-	immunoreceptor tyrosine-based activation motif
ITIM	-	immunoreceptor tyrosine-based inhibitory motif
LPIAT1	-	lysophosphatidylinositol acyltransferase 1
MEF	-	mouse embryonic fibroblast
MMP	-	matrix metalloproteinase
MRM	-	multiple reaction monitoring
mTORC1	-	mammalian target of rapamycin complex 1
mTORC2	-	mammalian target of rapamycin complex 2
N-WASP	-	neural Wiskott–Aldrich syndrome protein
PA	-	phosphatidic acid
PB-Cre4	-	ARR_2PB-Cre recombinase strain 4
PC	-	phosphatidylcholine
PDGF	-	platelet derived growth factor
PDK1	-	phosphoinositide-dependent kinase 1
PE	-	phosphatidylethanolamine
PG	-	phosphatidylglycerol
PgR	-	progesterone receptor
PH domain	-	pleckstrin homology domain
PI	-	phosphatidylinositol
PI3K	-	phosphoinositide 3-kinase
PID	-	primary immunodeficiency
PIN	-	prostatic intraepithelial neoplasia
PIP 5-kinase	-	phosphatidylinositol phosphate 5-kinase
PIPP	-	proline-rich inositol polyphosphate 5-phosphatase
PKB	-	protein kinase B
PLA1	-	phospholipase A1

PLA2	-	phospholipase A2
PLC	-	phospholipase C
PS	-	phosphatidylserine
PSS1	-	phosphatidylserine synthase 1
PSS2	-	phosphatidylserine synthase 2
PTEN	-	phosphatase and tensin homologue deleted on chromosome 10
PTP	-	protein tyrosine phosphatase
PX domain	-	PHOX homology domain
PyMT	-	polyoma middle T antigen
RBD	-	RAS-binding domain
RF	-	radiofrequency current
RNAi	-	RNA interference
ROS	-	reactive oxygen species
RTK	-	receptor tyrosine kinase
scF_v	-	single chain variable fragment
SH2 domain	-	Src homology 2 domain
SH3 domain	-	Src homology 3 domain
SHIP1	-	SH2-containing inositol polyphosphate phosphatase 1
SHIP2	-	SH2-containing inositol polyphosphate phosphatase 2
shRNA	-	small hairpin RNA
siRNA	-	small interfering RNA
SOS	-	son of sevenless
Src	-	cellular homologue of the product of the transforming oncogene in Rous sarcoma virus
TAG	-	triacylglycerol
TAPP1	-	tandem PH-domain containing protein 1
TAPP2	-	tandem PH-domain containing protein 2
TGFβ	-	transforming growth factor β
TLC	-	thin layer chromatography
TMS	-	trimethylsilyl
Vps34	-	vacuolar protein sorting defective mutant 34

List of figures

Figure 1.1 Lipid components of mammalian membranes 3

Figure 1.2 Enzymatic pathways for de novo synthesis of glycerophospholipids 5

Figure 1.3 Phosphatidylinositol lipids in mammals 6

Figure 1.4 Remodelling of acyl chains by the Lands cycle 7

Figure 1.5 Phosphatidylinositol lipid remodelling by kinases and phosphatases 8

Figure 1.6 Protein effectors of 3-phosphorylated phosphatidylinositol lipids 10

Figure 1.7 The complex nature of signalling through class IA and class IB PI3Ks 14

Figure 1.8 Class IA PI3K domain architecture 15

Figure 1.9 Class IB PI3K domain architecture 17

Figure 1.10 Class II PI3K domain architecture 18

Figure 1.11 Class III PI3K domain architecture 20

Figure 1.12 Physiological processes controlled by the class I PI3K/AKT signalling pathway 22

Figure 1.13 PTEN domain architecture 24

Figure 1.14 Mammalian lipid 5-phosphatases 28

Figure 1.15 INPP4A/B domain architecture 31

Figure 3.1 Glycerolphospholipids generated in stimulated human neutrophils 73

Figure 3.2 An example of chromatographic separation of phosphatidylinositol lipids by anion-exchange HPLC 74

Figure 3.3 A schematic representation of ion generation by electrospray ionisation 75

Figure 3.4 Fragmentation of PI(3,4,5)P_3 aldehyde in a triple quadrupole mass spectrometer 76

Figure 3.5 Structures of C38:4 PIP_2 and deuterated-C38:4 PIP_2 regioisomers 79

Figure 3.6 Separation of PI(3,4)P_2 and PI(4,5)P_2 with C18:0-C20:4 or C17:0-C20:4 acyl chains 80

Figure 3.7 Ozonolysis of C38:4 PI(4,5)P_2 81

Figure 3.8 The effect of MeOH on the stability of PI(4,5)P_2 aldehyde 82

Figure 3.9 The effect of column length on the separation efficiency between PI(3,4)P_2 aldehyde and PI(4,5)P_2 aldehyde 83

Figure 3.10 The presence of deuterated-C18:0 acyl chain affects PIP_2 separation 84

Figure 3.11 The effect of deuterium on the retention time of HPLC column 84

Figure 3.12 The effect of column temperature on retention time 85

Figure 3.13 The effect of increasing aqueous content of the mobile phase on peak separation 86

Figure 3.14 Comparison between the isocratic and gradient HPLC conditions 87

Figure 3.15 The effect of c18 HPLC column functionalisation 88

Figure 3.16 HPLC-ESI MS/MS method validation in human platelets stimulated with thrombin 89

Figure 4.1 Calibration curve for PI(3,4,5)P_3 95

Figure 4.2 Calibration curves for PI(3,4)P2 and PI(4,5)P2 in Mcf10a cells 95
Figure 4.3 PI(3,4,5)P_3 levels in Mcf10a cells 97
Figure 4.4 PI(3,4)P_2 and PI(4,5)P_2 levels in Mcf10a cells 99
Figure 4.5 PIP levels in Mcf10a cells with altered phosphatase expression 100
Figure 4.6 Phosphorylation of the EGFR in genetically modified Mcf10a cells 101
Figure 4.7 Expression of phosphatases in cell populations treated with siRNA 102
Figure 4.8 Expression of phosphatases in Mcf10a clones derived by CRISPR/Cas9 gene editing 103
Figure 5.1 Inhibition of class I PI3K in [PTEN-KO, INPP4A/B-KD] Mcf10a cells 109
Figure 5.2 The effect of PI-103 on the accumulation of PI(3,4,5)P_3 and PI(3,4)P_2 in EGF-stimulated [PTEN-KO, INPP4A/B-KD] Mcf10a cells 110
Figure 5.3 The effect of Byl-719 on the accumulation of PI(3,4,5)P_3 and PI(3,4)P_2 in EGF-stimulated [PTEN-INPP4B-KO] Mcf10a cells 110
Figure 5.4 PI3K-C2α and PI3K-C2β suppression in Mcf10a cells 111
Figure 5.5 The effect of siRNA-directed suppression of Class II PI3Kα or β on the accumulation of PI(3,4,5)P_3 and PI(3,4)P_2 in EGF-stimulated Mcf10a cells 112
Figure 5.6 The effect of reduced 5-phosphatase expression on EGF-stimulated PI(3,4,5)P_3 and PI(3,4)P_2 accumulation in EGF-stimulated [PTEN-SHIP2-KO, INPP4A/B-KD] Mcf10a cells 113
Figure 5.7 Timecourses of PI(3,4)P_2 and PI(3,4,5)P_3 hydrolysis in Mcf10a cells in response to PI-103 114
Figure 5.8 Comparison between HPLC-ESI MS/MS and ^{33}P-labelling: example HPLC traces 117
Figure 5.9 Comparison of [^{33}P]P_i-labelling and HPLC-ESI MS/MS methods for phosphatidylinositol lipid quantitation 118
Figure 5.10 Comparison between different mass spectrometry methods 119
Figure 6.1 Dephosphorylation of PI(3,4,5)P_3 by Mcf10a cytosol 125
Figure 6.2 Dephosphorylation of PI(3,4)P_2 by Mcf10a cytosol 126
Figure 6.3 Recombinant PTEN acts as PI(3,4)P_2 phosphatase in Mcf10a cytosol 127
Figure 6.4 Identification of PIP derived from PI(3,4)P_2 by Mcf10a cytosol as PI4P 128
Figure 7.1 AKT phosphorylation in Mcf10a cells 134
Figure 7.2 Identification of invadopodia in Mcf10a cells 135
Figure 7.3 Invadopodia quantification in Mcf10a cells 136
Figure 8.1 Model of cancer progression in mouse prostate 140
Figure 8.2 Phosphatidylinositol lipid levels in mouse prostate measured by HPLC-ESI MS/MS 141
Figure 8.3 PI(3,4)P_2 staining in 12 week mouse prostate cryosections 142
Figure 8.4 The impact of deleting Pten and Inpp4b in mouse prostate 143

Figure 8.5 PI(3,4)P_2 and pAKT levels in 16 week mouse prostate 144
Figure 8.6 H&E staining and PI(3,4)P_2 levels in WT mouse prostate 145
Figure 8.7 H&E staining and PI(3,4)P_2 levels in PTEN and PTEN-INPP4B-KO mouse prostate 146
Figure 8.8 PI(3,4,5)P_3 and PI(3,4)P_2 in prostate cancer cells 148

Contents

Title page		i
Summary		iii
Declaration		v
Acknowledgements		ix
Table of acknowledgement of assistance		xi
List of abbreviations		xiii
List of figures		xvi
Contents		xix
Chapter 1	**Introduction**	1
1.1	The biology of a lipid bilayer	1
1.1.1	Lipids that make up the biological membranes	1
1.1.2	Phospholipid biosynthetic pathways	4
1.1.3	Phosphatidylinositol lipids - a non-structural role of lipids in the cell	6
1.1.3.1	Phosphatidylinositol lipid signalling at the plasma membrane	7
1.1.4	Membrane linked proteins	10
1.2	PI3K/AKT signalling pathway	12
1.2.1	Class I PI3K	14
1.2.1.1	Activation and regulation of class IA PI3K	15
1.2.1.2	Activation and regulation of class IB PI3K	17
1.2.2	Class II PI3K	18
1.2.3	Class III PI3K	19
1.2.4	AKT/PKB - a major effector downstream of PI3K activity	21
1.2.5	PTEN - the primary tumour suppressor of the PI3K/AKT signalling pathway	24
1.2.6	5-phosphatases	27
1.2.7	INPP4A/B - PI(3,4)P_2 specific 4-phosphatases	31
1.3	PI3K/AKT signalling pathway in tumorigenesis	33
1.3.1	Class I PI3K alterations in human cancer	33
1.3.2	AKT isoform-specific roles in tumour initiation and progression	35

1.3.3 Role of PTEN in tumorigenesis 37
1.3.4 INPP4B as a tumour suppressor 39
1.3.5 5-phosphatases and their role in cancer 42

1.4 Physiological roles of $PI(3,4)P_2$ in PI3K-regulated signalling 45
1.4.1 The role of TAPP1/2 in class I PI3K signalling 46
1.4.2 $PI(3,4)P_2$ at the centre of cell migration and invasion 47
1.4.2.1 The role of invadopodia in transformed cells 47
1.4.2.2 The role of class II PI3K in clathrin mediated endocytosis 50
1.4.2.3 FEME - a fast track to receptor internalisation 51

1.5 Aims 52

Chapter 2 Materials and methods 53

2.1 Materials 53
2.1.1 Key resources 53
2.1.2 Mice 57
2.1.3 Cell lines 58
2.1.4 Human platelets 58

2.2 Methods 60
2.2.1 Preparation of platelets for $PI(3,4)P_2$ measurement 60
2.2.2 siRNA suppression 60
2.2.3 Gene editing of Mcf10a cell lines using CRISPR/Cas9 60
2.2.4 Western-Blot 61
2.2.5 Lipid extraction 62
2.2.6 Measurement of $PI(3,4)P_2$ and $PI(4,5)P_2$ 63
2.2.7 Measurement of PI3P and PI4P 65
2.2.8 $[^{33}P]P_i$ labelling of Mcf10a cells 66
2.2.9 *In vitro* phosphatase assay 66
2.2.10 Invadopodia assay 67
2.2.11 Mouse prostate dissection and processing 68
2.2.12 Mouse prostate imaging 68
2.2.13 HPLC-ESI MS/MS measurement of mouse prostate phophatidylinositiol lipids 69
2.2.14 Experimental design 69
2.2.15 Statistics 70

Chapter 3 Development of an HPLC-ESI MS/MS method to measure $PI(3,4)P_2$ *in vivo* 71

3.1 Introduction 71

3.1.1 The variety of *in vitro* and *in vivo* techniques used to study phosphatidylinositol lipids 71

3.1.2 Lipidomics - measurement of lipids by mass spectrometry 74

3.1.2.1 Electrospray ionisation mass spectrometry 75

3.1.2.2 Reverse phase chromatography 77

3.1.2.3 Quantification of phosphatidylinositol lipids by HPLC-ESI MS/MS 77

3.2 Results 79

3.2.1 Separations of full length C38:4 PIP_2 regioisomers 79

3.2.2 Ozonolysis 80

3.2.3 HPLC method optimization 82

3.2.3.1 Solvent effect 82

3.2.3.2 Length of the HPLC column 83

3.2.3.3 The role of internal standards in mass spectrometry - deuterium effect 83

3.2.3.4 Temperature effect 85

3.2.3.5 Different modes of HPLC runs 87

3.2.3.6 Functionalised reverse phase HPLC columns 87

3.2.3.7 Method validation in human platelets 88

3.3 Discussion 90

Chapter 4 PTEN and INPP4B synergistically regulate the accumulation of $PI(3,4)P_2$ in EGF-stimulated Mcf10a cells 92

4.1 Introduction 92

4.2 Results 94

4.2.1 Calibration curves for quantitative measurement of $PI(3,4)P_2$, $PI(4,5)P_2$ and $PI(3,4,5)P_3$ in Mcf10a cells 94

4.2.2 The contribution of PTEN and INPP4B to the accumulation of $PI(3,4)P_2$ in EGF-stimulated Mcf10a cells 96

4.2.2.1 $PI(3,4,5)P_3$ dephosphorylation is shared between the 3- and 5-phosphatases 97

4.2.2.2 Unexpectedly high levels of PI(3,4)P_2 accumulate in EGF-stimulated Mcf10a cells depleted of PTEN and INPP4B 99
4.2.3 Phosphorylation levels of EGFR in genetically modified Mcf10a cells 101
4.2.4 The effect of siRNA suppression and CRSIPR/Cas9 gene editing on the expression level of phosphatases in Mcf10a cells 102
4.3 Discussion 104
Chapter 5 EGF stimulates PI(3,4)P_2 accumulation via 5-phosphatase-mediated dephosphorylation of PI(3,4,5)P_3 in Mcf10a cells 106
5.1 Introduction 106
5.2 Results 108
5.2.1 The effect of isoform-selective and pan-class I PI3K inhibitors on the accumulation of PI(3,4,5)P_3 and PI(3,4)P_2 in EGF-stimulated Mcf10a cells 108
5.2.2 The effect of class II PI3K suppression on PI(3,4)P_2 and PI(3,4,5)P_3 accumulation in EGF-stimulated Mcf10a cells 111
5.2.3 The role of 5-phosphatases in PI(3,4,5)P_3 hydrolysis in Mcf10a cells 112
5.2.4 The kinetics of EGF-mediated PI(3,4,5)P_3 and PI(3,4)P_2 dephosphorylation in Mcf10a cells 114
5.2.5 Comparison between HPLC-ESI MS/MS and ^{33}P labelling methods 116
5.2.6 Different mass spectrometry approaches for measuring PI(3,4)P_2 levels in Mcf10a cells 119
5.3 Discussion 120
Chapter 6 PTEN acts as a direct PI(3,4)P_2 3-phosphatase in Mcf10a cytosol 122
6.1 Introduction 122
6.2 Results 124
6.2.1 Dephosphorylation of PI(3,4,5)P_3 and PI(3,4)P_2 by Mcf10a cytosol 124
6.2.2 PTEN's activity towards PI(3,4)P_2 is related to its intrinsic lipid phosphatase identity 127
6.2.3 PTEN is a PI(3,4)P_2 3-phosphatase 128
6.3 Discussion 129

Chapter 7 PTEN and INPP4B regulate invadopodia formation in Mcf10a cells 131

7.1 Introduction 131

7.2 Results 133

7.2.1 AKT phosphorylation levels in Mcf10a mutant cells 133

7.2.2 Invadopodia formation in Mcf10a cells 134

7.3 Discussion 137

Chapter 8 PTEN regulates the accumulation of PI(3,4)P_2 in mouse prostate 138

8.1 Introduction 138

8.2 Results 140

8.2.1 Phosphatidylinositol lipid quantitation in mouse prostate by HPLC-ESI MS/MS 140

8.2.2 The impact of deleting PTEN and INPP4B in mouse prostate 141

8.2.3 Pathophysiological significance of PTEN deletion in mouse prostate 144

8.2.4 Role of PTEN as a PI(3,4)P_2 phosphatase in human prostate cancer cell lines 147

8.3 Discussion 149

Chapter 9 General discussion 151

References 157

Blank

Chapter 1 Introduction

1.1 The biology of a lipid bilayer

Since the introduction of a 'fluid mosaic model' of a biological membrane in 1970's (Singer and Nicolson 1972) our knowledge about lipids and proteins, the two major players that govern membrane biology, has significantly advanced. The ever growing body of evidence suggests that lipids, apart from their generally accepted role as bilayer building blocks, possess a very important function in signal transduction in the cell. Eukaryotic cells designate around 5% of their genes to contribute to lipid synthesis, which together with more than 1000 structurally unique members identified by lipidomics, suggests, that an evolutionary pressure must have existed that caused this diversification (van Meer, Voelker et al. 2008). Biological membranes are defined by their characteristic lipid composition and cells invest a lot of energy to maintain polarity at the organelle, bilayer and transmembrane level. What is more, proteins embedded in the membrane are able to form well defined domains which serve specific functions and confine the biological events in space (Engelman 2005). Lipid-lipid, lipid-protein and protein-protein interactions enforce membrane heterogeneity by changing the bilayer's thickness, curvature and fluidity, and therefore make some of its regions less accessible. Finally, a membrane's temporal composition is a result of constant remodelling in response to signalling inputs from the environment, as it becomes a focal point of events essential for cellular proliferation, growth, defence and survival.

1.1.1 Lipids that make up the biological membranes

Lipids as biomolecules support many crucial functionalities of our bodies. Triacylglycerol stored in the adipose tissue forms energy reservoirs, galactocerebroside is the main component of nerve-insulating myelin sheath and brown fat plays an important role in thermoregulation. Moreover, phospholipids, sphingolipids and cholesterol form the building blocks of biological membranes and regulate cell permeability. Lipids can also act as activators or important components of cellular signalling pathways. All lipids which make up biological membranes are amphiphilic in

nature, i.e. they consist of a hydrophobic tail and a hydrophilic headgroup. Formation of a lipid bilayer in the aqueous environment is a spontaneous, entropically driven process that results in the lipid tails buried away from the cytosol and the headgroups exposed to the environment. This property of lipids was the original driving force of cell formation and is the basic mechanism for cellular compartmentisation. Thus, structural lipids form the physical barrier that gives the cell its rigidity and encompasses the cellular content but also protects the cell from invasion by pathogens. The presence of specialised organelles, on the other hand, is utilised by the cell to restrict proteins and cytosol components to certain regions and allow for spatial segregation of biochemical processes. Moreover, the ability to 'self-heal', generate potential gradients or aid in cytoskeleton remodelling are among many membrane properties which are central to the processes which happen in the cell - from cellular division and movement to signal transmission in neurons and muscle contraction.

Mammalian membranes are composed of three major classes of lipids – sphingolipids, glycerophospholipids (also called phosphoglycerides or phospholipids) and sterols (Figure 1.1). Diacylglycerol (DAG) forms a hydrophobic backbone of glycerophospholipids and consists predominantly of a *sn1* saturated and *sn2* cis-unsaturated fatty acyl chains of different length. Phosphatidylcholine (PC) and phosphatidylethanolamine (PE) are the two most abundant phosphoglycerides, with the total lipid abundance in most mammalian cells reaching 40-50% and 20-30%, respectively (Vance 2015). The other members are predominantly phosphatidylserine (PS), phosphatidic acid (PA) and phosphatidylinositol (PI), which possess crucial structural and signalling functions but their relative abundance in the cell does not exceed 10%. Sphingolipids share the ceramide backbone which can be bound to a sugar (a group of glycosphingolipids) or to a choline moiety (sphingomyelin). Sphingomyelin intercalates into the structure of glycerophospholipids and contributes to a tight packing of the membrane. Cholesterol, the most common sterol of mammalian membranes, is a non-polar polycyclic compound and an important precursor of many hormones and vitamin D. Within the membranes, cholesterol interacts with sphingomyelin and phospholipids to maintain an appropriate membrane fluidity.

Lipid composition is a unique feature of each of the cellular bilayers which implies the existence of tight control mechanisms for lipid synthesis and trafficking. Endoplasmic reticulum is the primary site of the *de novo* synthesis of

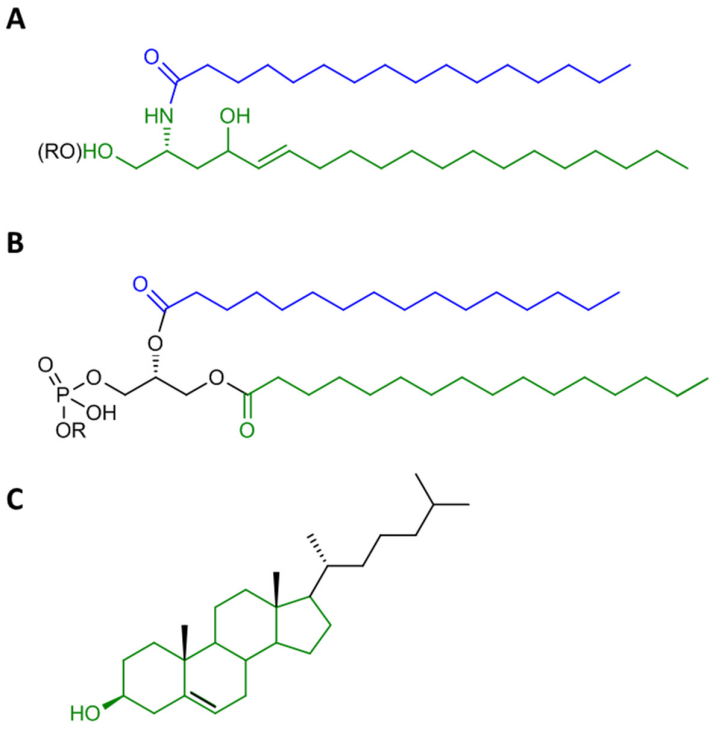

Figure 1.1 Lipid components of mammalian membranes

*(**A**) Sphingolipids are based on a sphingosine moiety (green), which when N-acetylated with fatty acids (blue) forms the ceramide backbone. This can be further modified to a sphingomyelin (R = phosphocholine) or to glycerolsphingolipids (R = sugar(s)). (**B**) Glycerophospholipids are based on a glycerol backbone with fatty acyl chains at positions sn1 (green) and sn2 (blue). The glycerol backbone, via a phosphodiester bond, can be further modified to form phosphatidylcholine (R = choline), phosphatidylethanolamine (R = ethanolamine), phosphatidylserine (R = serine), phosphatidic acid (R = H) or phosphatidylinositol (R = myo-inositol). (**C**) Cholesterol is a member of the sterol (green) family of lipids, modified with aliphatic chains (black).*

glycerophospholipids and cholesterol, while the ceramide backbone exits the endoplasmic reticulum and is 'capped' with the polar headgroup in the Golgi apparatus to give sphingolipids (van Meer, Voelker et al. 2008). Cholesterol and sphingolipids are actively transported to the plasma membrane to regulate its rigidity and fluid like character. Bilayer asymmetry is another property which contributes to the biological properties of a cellular membrane. While in the endoplasmic reticulum, newly synthesised lipids are equally distributed between the two leaflets and the 'flip-flop' between them is nonspecific and facilitated by the action of a group of proteins called lipid flippases (Pomorski and Menon 2006). The situation radically changes in the plasma membrane. Here, the negatively-charged inner leaflet is enriched in aminophospholipids, PS and PE, while sphingolipids and PC are restricted to the outer leaflet. In order to maintain this asymmetry, floppases and ABC transporters in an ATP-

driven process actively transport PC outside, whereas PS and PE are translocated towards the inside by another group of ATP-dependent proteins, i.e. P4-ATP type flippases (Hankins, Baldridge et al. 2015), hence creating and maintaining membrane polarity. Thus, phosphatidylserine under physiological conditions is found exclusively on the inner, cytosolic part of the membrane. During apoptosis, non-specific transport mechanisms of scramblases start to predominate and PS becomes exposed on the outer leaflet, where it marks the cell for non-inflammatory clearance by phagocytosis (Bratton, Fadok et al. 1997).

1.1.2 Phospholipid biosynthetic pathways

The *de novo* synthesis of fatty acids starts in the cytosol, where a product of glycolysis, acetyl coenzyme A (acetyl CoA), is converted into palmitic acid (C16:0; where total number of carbon atoms : number of double bonds, $\Delta^{\text{double bond positions}}$) in a sequence of reactions catalysed by fatty acid synthase. The subsequent reactions carried out by elongases and desaturases lead to longer and/or unsaturated fatty acids, with some exceptions, e.g. linoleic acid (C18:2, $\Delta^{9,12}$), which represents a building block for arachidonic acid (C20:4, $\Delta^{5,8,11,14}$), which needs to be provided by the diet. Alternatively, free fatty acids can be released from triacylgylcerol stored in the adipose tissue by adipolysis or during digestion by pancreas-specific lipases. Prior to entering biosynthetic pathways, fatty acids are converted into acyl-CoAs.

Phosphatidic acid is the common precursor in the *de novo* synthesis of all major phospholipids. The primary route of PA synthesis is a two-step reaction during which saturated acyl-CoA is added to position *sn1* of glycerol-3-phosphate (G-3-P), followed by acylation of lyso-PA with saturated/unsaturated acyl-CoA on position *sn2*. At this stage, the pathway diverges and phospholipid synthesis follows one of the two routes - the so-called Kennedy pathway or the CDP-DAG pathway (Figure 1.2). In 1956, Kennedy and co-workers described a mechanism of PC synthesis from DAG and phosphocholine with cytidine trisphosphate as the preferential energy source (Kennedy and Weiss 1956). The Kennedy pathway is considered the primary route for synthesis of PC, PE and triacylglycerols. The major step includes PA dephosphorylation into diacylglycerol by PA-phosphatase. DAG can then be acylated to produce triacylglycerol (TAG) or react with CDP-activated choline or ethanolamine to yield PC or PE, respectively. The final

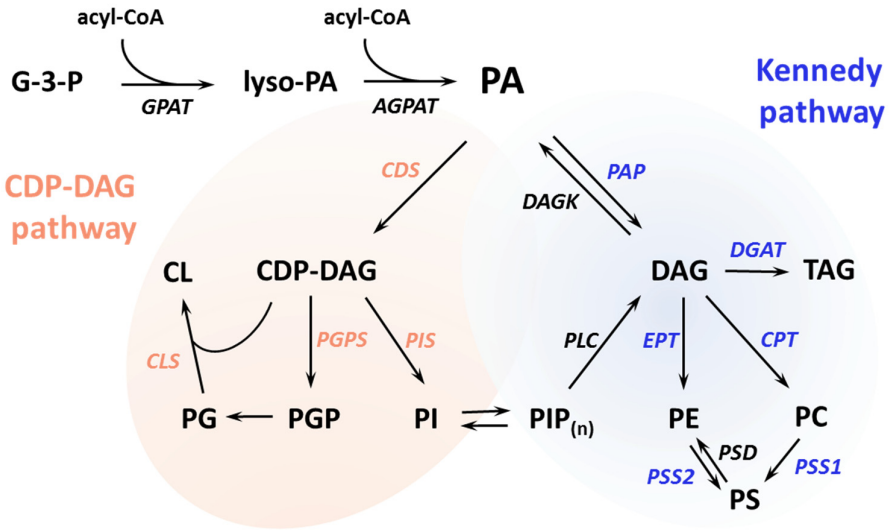

Figure 1.2 Enzymatic pathways for de novo synthesis of glycerophospholipids

Phosphatidic acid (PA) is the common precursor for de novo synthesis of glycerophospholipids. The Kennedy pathway is utilised by mammalian cells to produce phosphatidylcholine (PC), phosphatidylethanolamine (PE) and triacylglycerol (TAG); major enzymes involved in the pathway are depicted in blue. The CDP-DAG pathway is the primary route for synthesis of phosphatidylinositol (PI), phosphatidylglycerol (PG) and cardiolipins (CL); major enzymes involved in the pathway are depicted in red.

reaction takes place at the surface of the endoplasmic reticulum and is catalysed by choline- or ethanolamine-phosphotransferase. The remaining pool of PA produced in the cell undergoes a condensation reaction with CTP to produce CDP-DAG. This process was described by Agranoff et al. as the initial stage required for the synthesis of PI (Agranoff, Bradley et al. 1958). Unlike synthesis of PC or PE, *myo*-inositol does not require prior activation, but in the process controlled by phosphatidylinositol synthase reacts with CDP-DAG and releases CMP as a by-product. The CDP-DAG pathway is described as the principal mechanism for the production phosphatidylglycerol (PG) and cardiolipins (CL). Surprisingly, lipid measurements show that the cellular levels of the rate limiting substrates, i.e. PA, DAG and CDP-DAG are very low, which suggests a very rapid turnover that occurs through both pathways. The additional explanation may be that PA and DAG are signalling molecules, hence regulatory mechanism are required to reduce this potential. Interestingly, phosphatidylserine is the only phospholipid that cannot be synthesised *de novo* via a CDP-activation pathway but relies on a source of PC and PE. Phosphatidylserine synthase 1 (PSS1) catalyses headgroup exchange with PC while phosphatidylserine synthase 2 (PSS2) uses PE as a substrate. Both reactions are ATP-independent and are tightly regulated by product inhibition. Moreover, the newly

synthesised PS can be readily transported between the endoplasmic reticulum and mitochondria, where it is accessed by a decarboxylase that converts PS back to PE.

1.1.3 Phosphatidylinositol lipids - a non-structural role of lipids in the cell

Myo-inositol is the most abundant of the nine naturally occurring stereoisomers of inositol in nature and an essential building block of bioactive molecules, many of which possess important signalling functions. The mammalian phosphatidylinositol family consists of eight members, i.e. PI, P3P, P4P, P5P, PI(3,4)P_2, PI(3,5)P_2, PI(4,5)P_2 and PI(3,4,5)P_3 (Figure 1.3). The glycerol moiety forms a core of each of the

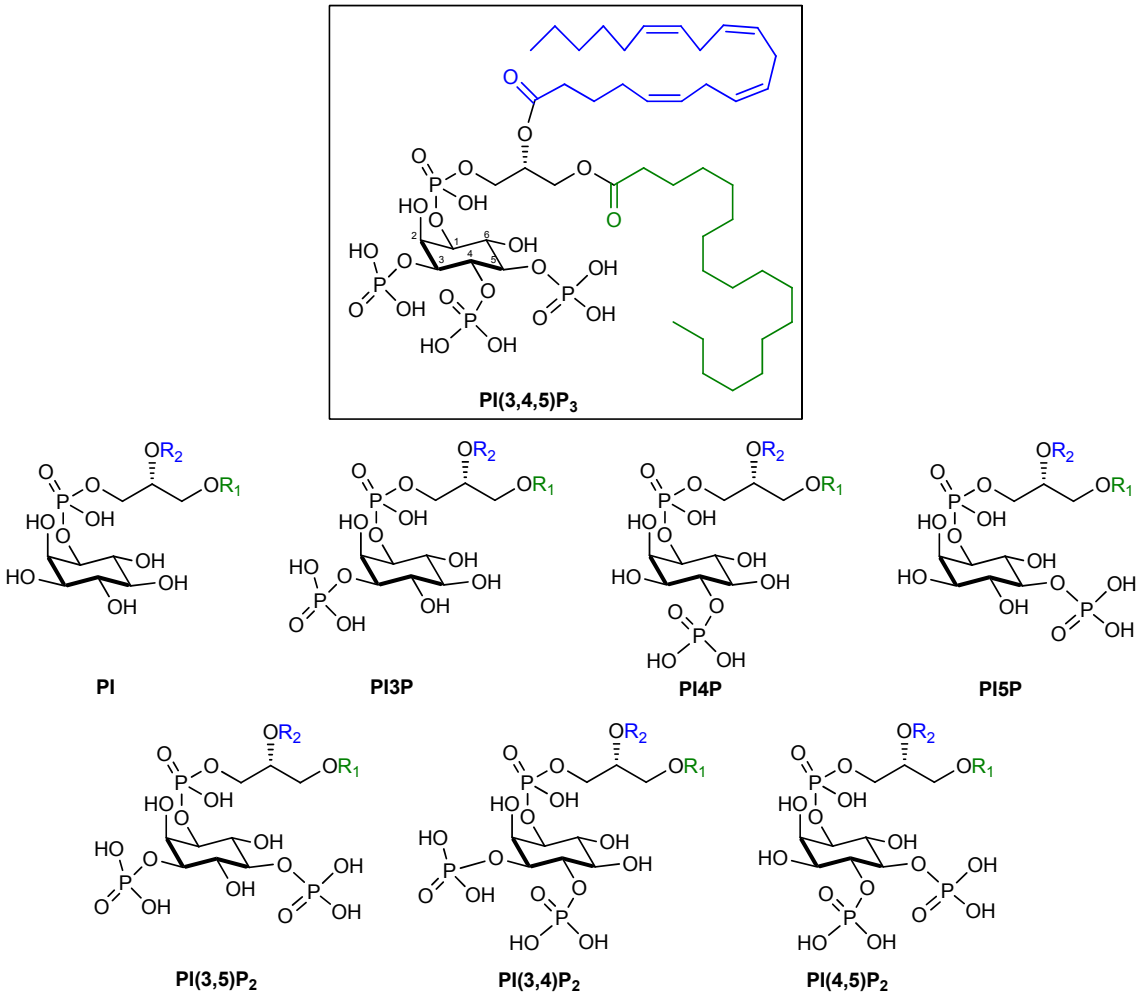

Figure 1.3 Phosphatidylinositol lipids in mammals

The chemical structures of phosphatidylinositol lipids present in mammalian cells. The structure of PI(3,4,5)P_3 is shown with 18:0 (stearoyl, green) and 20:4 (arachidonoyl, blue) acyl groups at the sn-1 and sn-2 positions, respectively, as an example of the major molecular species found in mammalian cells.

phosphatidylinositols, with fatty acyl chains at positions *sn1* and *sn2*, and a *myo*-inositol linked via a phosphodiester bond to position *sn3*. Ether and diether phosphatidylinositol variants have been observed in organisms like *D. discoideum* but are not abundant in mammals (Clark, Kay et al. 2014). Specific groups of enzymes have the ability to remodel these lipids, either by changing the acyl chain composition or the level of phosphorylation of the inositol headgroup. The process of deacylation/reacylation of the glycerol backbone is known as Land's cycle and was defined by showing that the rate of remodelling is lower in triacylglycerols (storage molecules) compared to biologically active phosphatidylcholine (Lands 1958) (Figure 1.4). Phospholipase A2 (PLA2)

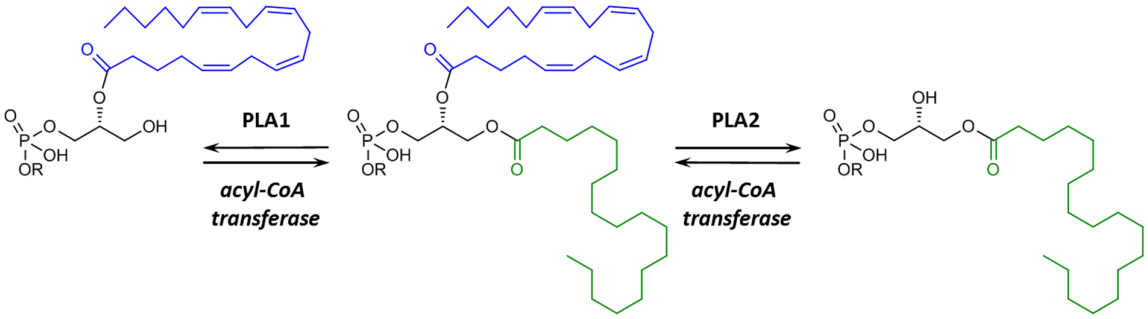

Figure 1.4 Remodelling of acyl chains by the Lands cycle

Glycerophospholipid remodelling at the level of the glycerol backbone is carried out by specialised phospholipases, which have the ability to cleave fatty acids at the position sn1 (PLA1) or sn2 (PLA2), respectively. The reverse reacylation reaction is carried out by a group of acyl-CoA transferases.

specifically hydrolyses position *sn2* of the phosphatidylinositol to yield lyso-PI and fatty acid. The reverse reaction is catalysed by a group of acyltransferases, with lysophosphatidylinositol acyltransferase 1 (LPIAT1) recently shown to contribute to the enrichment of phosphatidylinositol lipids in arachidonic acid in mice (Lee, Inoue et al. 2008, Anderson, Kielkowska et al. 2013). This result may partly explain why mammalian tissues and primary cells are highly enriched in *sn1* stearoyl (C18:0) : *sn2* arachidonoyl (C20:4) fatty acyl chains (referred to as C38:4) (Clark, Anderson et al. 2011).

1.1.3.1 Phosphatidylinositol lipid signalling at the plasma membrane

The most studied and at the same time, the most remarkable role of phosphatidylinositol lipids is in cellular signalling. In contrast to fatty acyl chains that grant anchorage in the plasma membrane, polyanionic inositol headgroups are the

structural motifs that interact with proteins by electrostastic interactions or via specialised domains. Thus, a large group of lipid kinases and phosphatases have evolved that selectively phosphorylate/dephosphorylate specific positions on the *myo*-inositol ring, to efficiently modulate the lipid's signalling potential (Figure 1.5). Upon signalling

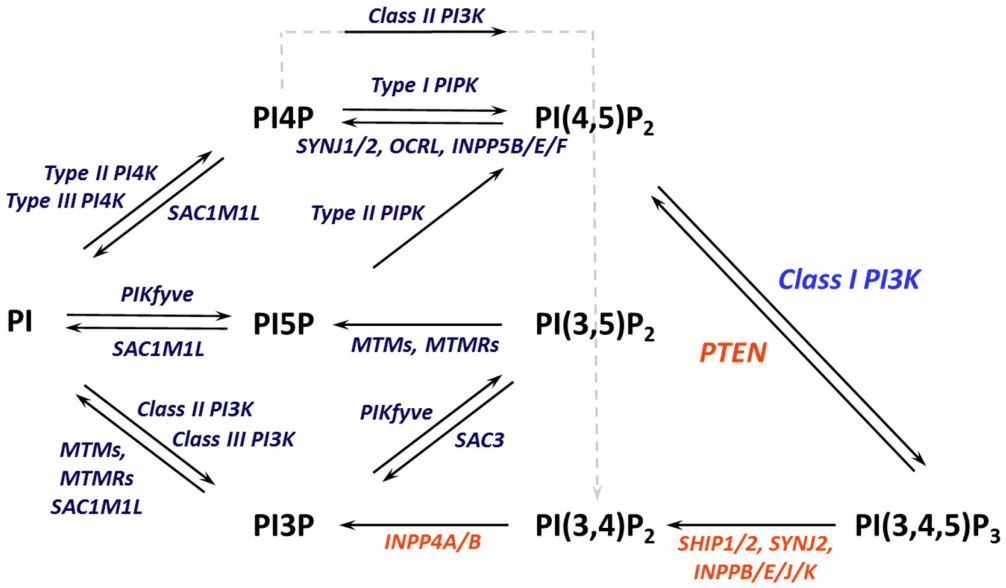

Figure 1.5 Phosphatidylinositol lipid remodelling by kinases and phosphatases

Schematic representation of routes for phosphatidylinositol lipids' headgroup remodelling by phosphorylation/dephosphorylation with lipid kinases and phosphatases that catalyse the reactions. Enzymes depicted in red are lipid phosphatases with a reported 'molecular quenching' function in class I PI3K/AKT signalling. Key sources: (Balla 2013, Hawkins and Stephens 2016).

events, like the class I PI3K-induced appearance of $PI(3,4,5)P_3$, dynamic changes in phosphatidylinositol lipid levels at the cellular membrane dramatically alter its local environment. Proteins, which normally reside in the cytosol, are recruited to the membrane's surface, via interaction of their lipid binding domains with the specific type of phosphatidylinositol. This spatio-temporal confinement brings together components of the signalling machinery which, by conformational changes, phosphorylation events and catalytic activity propagates the initial signal to the cellular interior. The diversity of proteins able to interact with these phosphorylated headgroups include cytoskeletal regulators, phospholipases, membrane trafficking proteins, lipid phosphatases and protein kinases. Phosphatidylinositol lipids can thus be seen as regulatable 'interaction platforms', with the ability to segregate cellular components, in favour of quick and efficient signal transduction.

The discovery of the pleckstrin homology (PH) domain, as ~120 amino acid domain of pleckstrin able to bind PI(4,5)P_2 vesicles, suggested a mechanism which proteins that lack lipid anchors may utilize to bind to the plasma membrane (Harlan, Hajduk et al. 1994). The interaction between the PH domain and phosphatidylinositol lipid is stereospecific, i.e. it is determined by the number of phosphate groups on the inositol ring and their relative position. The X-ray crystal structure of the PLCδ1 PH domain showed that hydrogen bonds between two adjacent phosphates on the inositol ring and conserved, basic amino acids are required for interaction specificity (Ferguson, Lemmon et al. 1995). However, very few out of several hundreds of PH domain-containing proteins identified so far, can be considered as strong and selective binders. This suggests that the electrostatic interactions are essential but not sufficient to provide the unique recognition and that it is difficult to 'score' proteins based solely on their amino acid sequence or even the results from *in vitro* assays. Indeed, dynamin oligomerisation was shown to induce stronger interaction with PI(4,5)P_2-rich domains *in vitro* and N-WASP seems to require synergistic input from CDC42 and PI(4,5)P_2 for activation (Klein, Lee et al. 1998, Papayannopoulos, Co et al. 2005). These additional regulatory mechanisms invalidate the simple 'on/off switch' theory but on the other hand may provide the systems with a higher level of flexibility or tuneability (Hammond and Balla 2015). Despite this, several important phosphatidylinositol lipid effectors have been identified with confirmed specificity and selectivity, including Bruton's tyrosine kinase (BTK) and general receptor for phosphoinositides 1 (GRP1) that bind specifically PI(3,4,5)P_3, a unique PI(3,4)P_2 binder, tandem PH-domain containing protein 1/2 (TAPP1/2) and dual PI(3,4)P_2/PI(3,4,5)P_3 binders, e.g. the serine/threonine protein kinases AKT (also known as PKB) and phosphoinositide-dependent kinase 1 (PDK1) (Figure 1.6). Two other protein domains with well-characterised phosphatidylinositol lipid binding selectivity for PI3P have been described. The highly specific FYVE domain was first identified in early endosomal antigen 1 (EEA1), as a PI3P-specific effector with roles implied in endosomal fusion (Gaullier, Simonsen et al. 1998, Patki, Lawe et al. 1998). Several years later, a more promiscuous PHOX (PX) domain was reported as a component of cytosolic proteins involved in the assembly of NADPH oxidase complex at the phagosome membrane (Ellson, Gobert-Gosse et al. 2001, Kanai, Liu et al. 2001). Interestingly, $p40^{phox}$ and $p47^{phox}$ are thought to rely on different interaction partners - PI3P and PI(3,4)P_2 ,respectively - suggesting that several classes of PI3K are needed to shape neutrophil's responses to pathogen infection. In contrast to PH domains, PX and

FYVE domains have limited ability to form hydrogen bonds with a sole 3-phosphate of the inositol ring and to increase binding specificity, they engage in hydrophobic interactions with the membrane and glycerol backbone (Lemmon 2007).

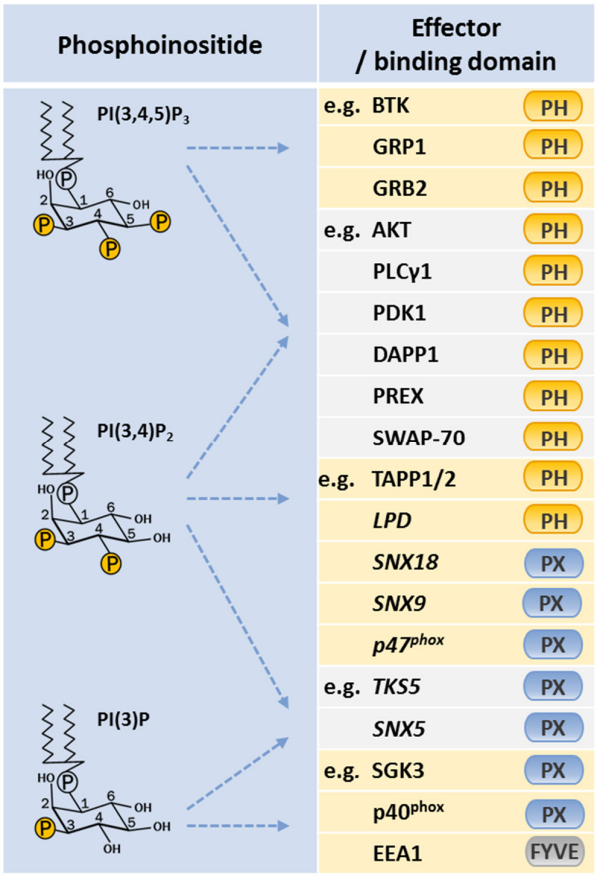

Figure 1.6 Protein effectors of 3-phosphorylated phosphatidylinositol lipids

A table with examples of PH-, PX- or FYVE-domain containing proteins and their binding specificities towards 3-phospohorylated phosphatidylinositol lipids. Proteins in italics are effectors for which binding selectivity has not been fully validated. Key sources: (Blero, Payrastre et al. 2007, Li and Marshall 2015, Hawkins and Stephens 2016).

1.1.4 Membrane linked proteins

The plasma membrane can be viewed as a ~100Å thick physical barrier that separates the aqueous cellular content from the environment. If lipids were the only membrane's constituents, the cell would be impermeable to the vast majority of macromolecules. Membrane proteins comprise around 50% of the total membrane mass and fulfil extremely diverse functions, e.g. they serve as ion pumps, are an attachment point of the cytoskeleton to the membrane and are a source of epitopes recognized by antibodies. In the context of cellular homeostasis, membrane proteins are at the origin of each signalling event as they interact directly with the 'molecular triggers' present in the environment, whether they are small molecules, peptides or other proteins.

A number of ways exist in which proteins interact with the cellular membrane. Transmembrane proteins such as porins or GPCRs possess hydrophobic domains (typically α-helices or β-barrels) which cross the bilayer and permanently lock a protein in place. Other proteins utilize electrostatic forces or specific anchors to make a transient interaction, as is the case of phosphatidylinositol binding proteins or RAS. Membrane proteins whose domains extend into the extracellular space are modified with a large variety oligosacharides. These carbohydrate-rich surfaces form a shield that protects the cell from chemical and mechanical stress, keeps away the pathogens and is involved in the cell-recognition processes.

Plasma membrane undergoes continuous remodelling which requires a tight control over its protein and lipid composition. Membrane heterogeneity has been credited to the presence of lipid rafts - highly dynamic nanodomains enriched in cholesterol and sphingolipids, which form in the inner and outer leaflet by protein-lipid and protein-protein interactions (Sezgin, Levental et al. 2017). These nanodomains are small (<200nm), short-lived and highly mobile which makes them hard to study. Nevertheless, our current understanding is that lipid rafts can preferentially recruit proteins to form spatio-temporally confined regions in the plasma membrane that possess a defined biological activity. Despite that, solid proofs are still missing that would complement the predominating set of *in vitro* models with real time observations in the cells.

1.2 PI3K/AKT signalling pathway

The story of what we now call a phosphoinositide 3-kinase (PI3K) signal transduction pathway is a fascinating journey of over 30 years of scientific research that due to its significance has resulted in many ongoing clinical studies and the first FDA-approved drug administered to patients. It is also a beautiful example of how biological questions that puzzle scientists become a driving force for developing new techniques, in order to be able to capture events in real time and at a molecular level. As in any other research field, cell biology has now advanced by joined efforts of biologists, chemists, clinicians, bioinfomaticians and engineers, whose expertise allows to continually cross the barriers leading to better understanding of the complex nature of signal transduction in the cell.

Before PI3Ks were defined as a family of lipid kinases with catalytic ability to transfer the γ-phosphate from a molecule of ATP to a phosphatidylinositol lipid substrate with a free 3D-OH position on the inositol ring, several groundbreaking discoveries were made. In one of the pioneering papers, Whitman et al. showed that the PI3K activity, related in earlier work to viral oncoproteins' transforming function, was due to its *in vitro* ability to phosphorylate phosphatidylinositol (PI) and generate PI(3)P (Whitman, Downes et al. 1988). This work not only shifted focus on the cellular events away from the cytosol to the plasma membrane but also separated PI3K's lipid kinase activity from that of phospholipase C (PLC). Around the same time, two types of mechanisms were shown to regulate PI3K activity in cells, which lead to production of lipids with analogous, 3D-phosphorylated characteristics. Stimulation of human neutrophils with a GPCR peptide agonist resulted in transient (within 12 sec) generation of a phosphatidylinositol lipid which, after deacylation and HPLC analysis, turned out to be PI(3,4,5)P_3 (Traynor-Kaplan, Harris et al. 1988). In the second study, lysates derived from platelet derived growth factor (PDGF)-stimulated smooth muscle cells after P-Tyr-specific immunoprecipitation, were shown to generate three 3-phopshorylated phosphatidylinositol lipids – PI3P, PI(3,4)P_2 and PI(3,4,5)P_3 – from their synthetic substrates – PI, PI4P and PI(4,5)P_2, respectively (Auger, Serunian et al. 1989). Additionally, traces of two of those lipids, PI(3,4)P_2 and PI(3,4,5)P_3 were directly measured in cells only upon PDGF-stimulation and were absent in quiescent cells. These revolutionary studies not only discovered two new lipid second messengers that

transiently appear downstream of PI3K activity but introduced two distinct regulation mechanisms by which these molecules can be produced. Subsequently, studies on PDGF-stimulated 3T3 cells and neutrophils activated by formyl peptide f-MetLeuPhe (fMLP) were instrumental in showing that activated PI3K uses $PI(4,5)P_2$ as a substrate to directly produce $PI(3,4,5)P_3$ (Stephens, Hughes et al. 1991, Hawkins, Jackson et al. 1992). Comparison between the radioactivity levels of analogous [^{32}P]-phosphates of $PI(3,4)P_2$ and $PI(3,4,5)P_3$ and the apparent lag in production between the two, contributed to the argument in support of the hypothesis that $PI(3,4)P_2$ is generated as a consequence of $PI(3,4,5)P_3$ dephosphorylation. Finally, no obvious change in the levels of PI3P suggested that, in opposition to what was initially thought, this phospholipid is not produced in response to receptor stimulation and implied the presence of another type of PI3K.

The attempts to purify PI3K from cells became a natural consequence of the initial discoveries and were led by a desire to confirm its kinase activity and to identify the genes that encode the protein sequence. It soon became apparent that the first candidate, an 85 kDa protein found to associate with P-Tyr motifs, when purified showed no kinase activity. In 1992, purification, cloning and expression of an associated p110 protein confirmed that it is the p110 protein that carries the kinase catalytic activity and that active PI3Ks exist only as p85-p110 heterodimers (Hiles, Otsu et al. 1992). This essential work fuelled the discovery of remaining PI3K isoforms as well as structural studies aimed at characterising domain architecture and interaction sites between the subunits that comprise PI3K heterodimers. Importantly, p110 was shown to possess significant homology to a protein encoded by a mutant previously identified in the yeast vacuolar protein sorting pathway, VPS34p (Schu, Takegawa et al. 1993). Since then, PI3Ks are defined as a family of lipid kinases that share catalytic selectivity towards the 3D position of phosphatidylinositol lipids but differ in substrate specificity, mode of activation and protein architecture (Vanhaesebroeck, Stephens et al. 2012). Thus, a natural division into three main classes has been agreed on, that takes into consideration this evolutionary diversity. Mammalian cells express seven different PI3K members while *C elegans* and *D. melanogaster* possess one representative of each class. A sole class III PI3K is expressed in yeast and plants.

1.2.1 Class I PI3K

Class I PI3K comprises a group of obligate heterodimers and is subdivided into two subclasses, class IA and class IB, which historically was related to activation by receptor tyrosine kinases (RTKs) or G-protein coupled receptors (GPCRs), respectively. However, more recent studies suggest that signalling through class I PI3K is a lot more complex and requires integration of multiple signalling inputs, i.e. direct/indirect interactions with GPCRs/RTKs, tyrosine-phosphorylated adaptor proteins or RAS superfamily of small G proteins (Burke and Williams 2015) (Figure 1.7). Thus, only a multi-component stimulus results in what we perceive as class I PI3K isoform 'activity'. This implies that interpretation of the cause-biological effect relation is almost never straightforward and requires more in-depth studies using genetically modified mouse models or isoform-specific inhibitors, among many others. The repertoire of stimuli that can act via specific cell surface receptors to activate class I PI3Ks includes growth factors (e.g. EGF, PDGF, IGF), hormones (e.g. insulin), inflammatory stimuli (e.g. fMLP, cytokines), antigens and neurotransmitters. The hallmark of class I PI3K activity is related to its ability to directly phosphorylate $PI(4,5)P_2$ and produce $PI(3,4,5)P_3$. This reaction leads to first amplification of initial stimulus and $PI(3,4,5)P_3$, due to its unique properties, propagates the signal within the cell.

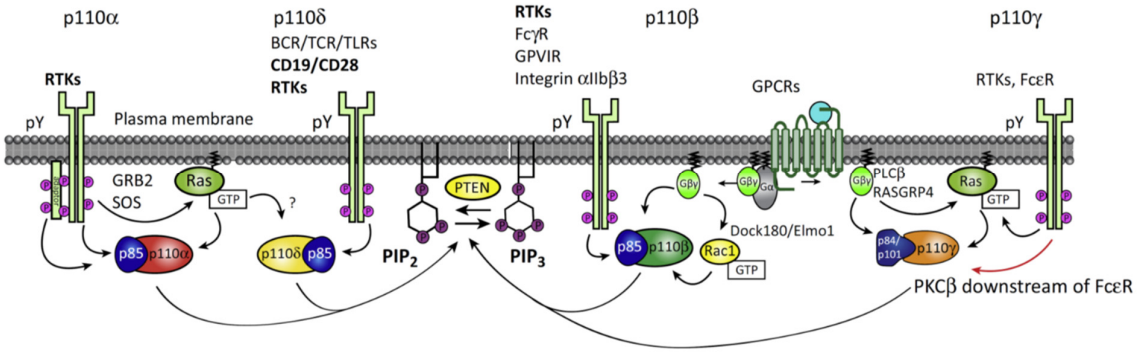

Figure 1.7 The complex nature of signalling through class IA and class IB PI3Ks

Schematic representation of diverse mechanisms that lead to stimulus-driven potentiation of class I PI3K catalytic activity. Depending on the type of stimulus, activated cell-surface receptors, membrane-bound small proteins and tyrosine-phosphorylated protein adaptors, cooperate to trigger catalytic activity of specific class I PI3K isoforms and result in $PI(3,4,5)P_3$ synthesis at the inner leaflet of the plasma membrane. From (Burke and Williams 2015).

1.2.1.1 Activation and regulation of class IA PI3K

Class IA PI3K is represented by three catalytic subunits: ubiquitously expressed p110α and p110β, and p110δ which is enriched in haematopoietic cells. Each catalytic subunit can form heterodimers with one of the five regulatory subunits: p85α, p55α and p50α, which are a product of alternative transcription initiation at the same gene locus, as well as p85β and p55γ (Figure 1.8). Although kinase characteristics are largely determined by the catalytic subunit, regulatory subunits are also important. Functional studies of these proteins provided us with a better understanding of how the two

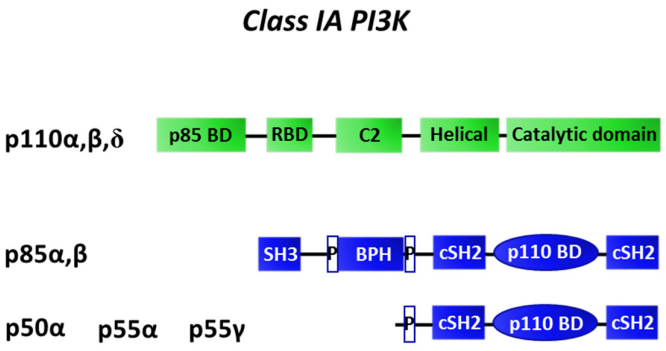

Figure 1.8 Class IA PI3K domain architecture

Class IA PI3K's core is composed of C2, helical and catalytic domains which provides enzymatic activity and, through interaction with SH2 domains, regulate dimer activity. SH2 domains in the regulatory subunit are responsible for the interaction with tyrosine-phosphorylated receptors or adaptor proteins, while the RBD can bind active RAS or RHO family members. Additional contacts are formed between the regions on p85- and p110-binding domains. Key sources: (Vanhaesebroeck, Guillermet-Guibert et al. 2010, Burke and Williams 2015).

subunits contribute to the overall kinase stability, activity and localisation within the cell. Direct contact between the regulatory and catalytic subunit is established between Src homology 2 (SH2) domains of p85 and specific regions on the helical, catalytic and C2 domain of p110 (Burke and Williams 2015). These interactions not only provide heterodimer stability but, most importantly, keep class IA PI3K in an auto-inhibited conformation.

A classical mechanism of class IA PI3K regulation takes place via activation of RTK by agonists such as EGF, IGF or PDGF. This initiates autophosphorylation of a receptor's cytosolic tails or phosphorylation of adaptor proteins such as GAB or IRS that associate with these receptors. Both types of events involve phosphorylation of tyrosine residues present on specific peptides called YXXM consensus motifs. Subsequently, SH2 domains

of the regulatory subunit bind to these pTyr motifs with high affinity and selectivity (Hawkins, Anderson et al. 2006). This results in class p85-p110α dimer recruitment to the plasma membrane and conformational changes that activate the protein. As a consequence of this recruitment, p110α catalytic subunit is also found in proximity to its substrate and can initiate $PI(3,4,5)P_3$ production. An example of indirect class IA PI3K activation is via RAS, which becomes 'GTP loaded' by a RAS GEF, for example son of sevenless (SOS), downstream of tyrosine phosphorylated GRB2 (Burke and Williams 2015). Active RAS-GTP then co-activates p110α by direct interaction with its RAS-binding domain (RBD). The importance of this signalling input is exemplified in mice, which become resistant to tumorigenesis by oncogenic RAS, when site-specific mutations disrupt RAS interaction with p110α-RBD.

p110β, on the other hand, is an isoform that can be co-regulated by GPCRs and RTKs. It responds to direct binding of a Gβγ dimer to its linker region, or to RHO family members (like RAC1 or CDC42), which when activated downstream of a GPCR interact with its RBD. While both inputs can be necessary for complete p110β activation, the latter is an example of 'modulatory exclusiveness' between class IA PI3K isoforms, as p110β does not respond to RAS. The mechanism of p110β regulation by RTKs appears to be analogous to regulation of p110α, but seems to co-operate with GPCRs and RAC1 or CDC42 to provide a non-redundant role for p110β in more specific circumstances, such as platelet activation during thrombosis (Gratacap, Guillermet-Guibert et al. 2011). Moreover, comparison between p110β knock-out and kinase-dead knock in transgenic mice suggests potential kinase-independent functions of this PI3K isoform (Jia, Liu et al. 2008).

Finally, receptors of the haematopoietic cells are predominantly involved in modulating the activity of p110δ. Thus, FcεR, cytokine and Toll-like receptors integrate extracellular signals that trigger tyrosine phosphorylation and in effect tune B- and T-cell responses (Hawkins and Stephens 2015). In addition, RAS members R-RAS and R-RAS2 may once again serve as additional signalling inputs, via direct interaction with p110δ-RBD.

1.2.1.2 Activation and regulation of class IB PI3K

Members of class IB PI3K are characterised as two heterodimers that form by interaction of p110γ catalytic subunit with one of the two regulatory subunits - p84 or p101 (Figure 1.9). Similar to p110δ, p110γ-containing complexes are widely expressed in the cells of haematopoietic origin. A canonical pathway of class IB PI3K activation is

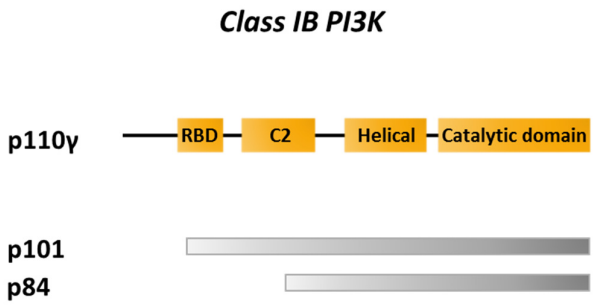

Figure 1.9 Class IB PI3K domain architecture

Class IB PI3K is represented by two dimers – p110γ/p84 and p110γ/p101 – and p110γ shares the core domains, i.e. C2, helical and catalytic with other members of PI3K. Although domain architecture of p101 and p84 is still vague, Gβγ activates p110γ/p101 through interaction with regions on both catalytic and regulatory subunits. RAS can activate p110γ through interaction with its RBD. Key sources: (Vanhaesebroeck, Guillermet-Guibert et al. 2010, Burke and Williams 2015).

through GPCRs responding to agonists such as fMLP or C5a (Hawkins, Anderson et al. 2006). These extracellular events cause GTP loading of the Gαi subunit and heterotrimer dissociation with subsequent release of Gβγ. Membrane-anchored Gβγ can then directly interact with the linker region on p110γ and C-terminal region on p101 - a process required for full activation of the p110γ-p101 dimer. RAS on the other hand, seems to be more important in activation of p110γ in complex with p84 regulatory subunit. This process requires active RAS-GTP, which is provided downstream of Gβγ-activated RASGRP4 or downstream of RTK receptors such as FcεR. The non-redundant role of p84 and p101 regulatory subunits was shown in studies on mouse neutrophils (Deladeriere, Gambardella et al. 2015). Although both contribute equally to total PI(3,4,5)P_3 which accumulates in response to GPCR signalling, the authors suggest that only p84-containing p110γ molecules are found in the spatio-temporal context that allows them to control PI(3,4,5)P_3-dependent ROS formation. This may be related to the availability of RAS-GTP 'microdomains' as well as proximity of other signalling inputs necessary for this physiological process. In contrast, *in vivo* and trans-well migration assays showed

that neutrophils from *p101*$^{-/-}$ and *p110γ*$^{-/-}$ mice exhibited reduced migratory capability, while this of *p84*$^{-/-}$ mice was unaffected.

The extensive cross talk that emerges from regulation of different class I PI3K isoforms is a picture far more complex than it was first imagined. In many cases, a certain level of synergy is required for effective protein activation and translation into intended biological function. This comes partly from cellular heterogeneity, which correlates with different expression levels of p110 catalytic subunits, relevant receptors, adaptors and modulators of class I PI3K activity. The other very important reason is that the presence of PI(3,4,5)P_3, as one of the most versatile signalling lipids known, needs to be tightly regulated in time and coincide with the appearance of its specific effectors. Thus, the multi-layered control brought by direct and indirect interactions originating at cell surface receptors seems to be the necessary strategy to provide the system with the right amount of plasticity and redundancy. However, it then becomes a great challenge to target one of the class I PI3K isoforms in a context-dependent manner and without inducing too many side effects.

1.2.2 Class II PI3K

Mammalian class II PI3K was initially discovered by sequence similarity to its *Drosophila* homologue and is represented by three monomeric proteins: PI3K-C2α, PI3K-C2β and PI3K-C2γ (Figure 1.10) (Domin, Pages et al. 1997). The first two isoforms, although not ubiquitous, are expressed in a broad variety of cells, while the presence of PI3K-C2γ is rather limited (Vanhaesebroeck, Guillermet-Guibert et al. 2010). The protein architecture involves a core catalytic domain flanked by C2, PX, helical and RAS-binding

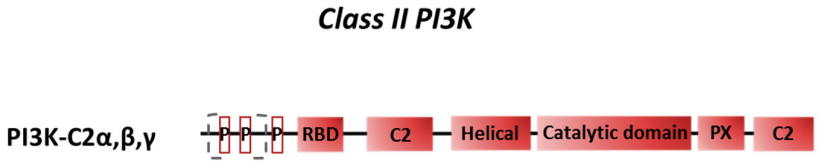

Figure 1.10 Class II PI3K domain architecture

Members of class II PI3K are monomers, whose PI3K core (consisting of C2, helical and catalytic domain) is flanked at the N-terminal end by RBD and proline-rich regions, and at the C-end by PX and C2 domains. This extended structure is thought to offer additional protein-protein interactions, which in class I and class III PI3Ks are granted by regulatory domains. Key source: (Vanhaesebroeck, Guillermet-Guibert et al. 2010).

domains. This multi-domain structure is suggested to be a substitute and have a role of the missing regulatory domain. In quiescent cells, members of class II PI3K are thought to be constitutively associated with cellular membranes and can be activated by association to RTK adaptors or by the interaction of GTPases with their RBD in response to GPCR activation. *In vitro*, class II PI3K members show affinity towards PI and PI4P. This is the least studied class of PI3K and the extent to which it contributes to PI3P versus PI(3,4)P_2 formation in cells is still not clear. Some early cell biology studies suggested roles in processes like cell migration and glucose metabolism but the most convincing evidence for a physiological role has come from a recent study of clathrin mediated endocytosis (CME). PI(4,5)P_2 has been long known for its recruitment of PH domain-containing proteins such as dynamin during early stages of clathrin coated pit (CCP) nucleation (Klein, Lee et al. 1998). The outstanding question was however related to the 'catalytic bridge' that would convert the maturating CCP into PI3P-rich endosomes. Posor et al. revealed a wortmannin-insensitive PI(3,4)P_2 pool, that localised to CCPs and depended on PI3K-C2α catalytic activity to maintain uninterrupted CME (Posor, Eichhorn-Gruenig et al. 2013). Thus, these studies point to at least one important context in which a class II PI3K is responsible for localised synthesis of PI(3,4)P_2. This and other processes that engage PI(3,4)P_2 will be discussed in more detail in later Chapters.

1.2.3 Class III PI3K

After p110α was cloned, it was noted that it possessed substantial sequence homology to VPS34, a *S. cerevisiae* kinase involved in protein targeting to the yeast vacuole (Hiles, Otsu et al. 1992). This then paved the way for the identification of a class III PI3K gene that is conserved across Eukaryotes and unlike other members, does not directly respond to growth-factor stimulation. Instead, Vps34 forms a heterodimer with myristoylated Vps15 that anchors it at the cellular membranes and its catalytic function is largely modulated by protein-protein interactions in which it participates (Figure 1.11). Vps34 is an exclusive PI-selective 3-kinase and is thought to be the major regulator of the steady state levels of cellular PI3P. The major roles of class III PI3K are in endosomal trafficking, phagocytosis and autophagy (Vanhaesebroeck, Guillermet-Guibert et al. 2010). The original role identified for Vps34 in endocytic sorting of cellular

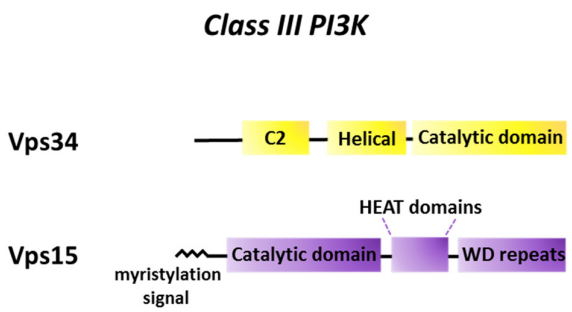

Figure 1.11 Class III PI3K domain architecture

The catalytic subunit of class III PI3K - Vps34 - binds Vps15 which anchors the heterodimer at the membrane via a myristoyl group. Vps15 possesses an inactive catalytic domain as well as WD repeats and HEAT domains that engage in important protein-protein interactions. Vps34, Vps15, BECLIN and UVRAG are core members of Complex 1 that regulates the induction of autophagy; Vps34, Vps15, BECLIN and ATG14 are core members of Complex II that regulates endocytosis. Key source: (Vanhaesebroeck, Guillermet-Guibert et al. 2010).

receptors relies on Vps15 and Vps34 interaction with RAB proteins. RAB5-GTP recruits class III PI3K to the early endosomes that form from the plasma membrane, with their embedded cargo. PI3P-positive membranes allow assembly of the endocytic machinery, which drives endosome maturation and receptor recycling or conversion into RAB7-GTP enriched late endosomes. The final stage of endocytosis is marked by endosome fusion into lysosomes and cargo degradation. In autophagy, amino acid starvation drives Vps34 interaction with ATG14L and BECLIN1 at membranes associated with the ER and leads to localised PI3P production in so-called 'omegosomes' (Axe, Walker et al. 2008). PI3P-rich membranes provide a positive feedback loop for omegasome formation that eventually transforms into an autophagosome and can become a source of nutrients upon fusion with the lysosome. PI3P is also produced during phagocytosis – a specialised form of endocytosis utilised by phagocytic cells to remove pathogens and cellular debris. Phagosome formation is initiated by class I PI3K activation in response to inflammatory stimuli while Vps34 acts during the maturation process. Dynamin coordinates class III PI3K interaction with RAB5-GTP that stimulates lipid kinase activity and localised PI3P synthesis. The latter has been shown to contribute to NADPH oxidase complex assembly and ROS production by association with PX domain-containing $p40^{phox}$ in neutrophils responding to infection by *E. coli* (Anderson, Boyle et al. 2008).

1.2.4 AKT/PKB - a major effector downstream of PI3K activity

Realisation that class I PI3K activity is inherently related to transforming oncoproteins and growth factor receptors created a large pressure to determine its downstream effectors. In 1995, two independent groups discovered that the ser/thr protein kinase AKT is activated in PI3K-dependent manner, downstream of active RTKs (Burgering and Coffer 1995, Franke, Yang et al. 1995). AKT contains a ~120aa plekstrin homology (PH) domain, which had previously been suggested to bind phosphatidylinositol lipids and hence the link between PH domains and D3-phosphorylated phosphatidylinositol lipids was first suggested. This for the first time placed AKT as an important element of the signal transduction pathway, regulated by growth factor receptors. It took the effort of several groups to fully appreciate the mechanism by which AKT is activated. The role that PI(3,4,5)P_3 plays in AKT translocation to the plasma membrane and phosphorylation on a residue essential for catalytic activity (^{308}Thr) was discovered by two groups (Alessi, James et al. 1997, Stokoe, Stephens et al. 1997, Stephens, Anderson et al. 1998). Meanwhile, work on purified AKT and its isolated PH domain showed, that the protein binds PI(3,4)P_2 and PI(3,4,5)P_3 with 1:1 stoichiometry, high affinity and specificity (Frech, Andjelkovic et al. 1997). Finally, several years later, the work performed by Sarbassov et al. identified mammalian target of rapamycin complex 2 (mTORC2) as the kinase that phosphorylates AKT on a second residue required for maximal activity - ^{473}Ser (Sarbassov, Guertin et al. 2005).

This work identified the PH domain as a direct target of PI(3,4,5)P_3 signalling and AKT is now considered as one of the major effectors downstream of PI3K signalling, and plays a critical role in some of the most crucial cellular processes such as cell growth, survival and metabolism (Figure 1.12). The AKT family consists of three isoforms expressed in mammalian cells (AKT1/PKBα, AKT2/PKBβ and AKT3/PKBγ) that share sequence homology with other AGC-family protein kinases, i.e. PKA or PKC. Structural studies on glycogen synthase kinase 3 (GSK3) defined a minimal recognition motif that is required for phosphorylation by AKT and is shared by many of its substrates (Manning and Cantley 2007). Bioinformatics tools helped identify over 100 potential, non-redundant AKT protein targets but many of them still require rigorous *in vitro* and *in vivo* studies before their function can be confirmed. Unphosphorylated AKT's

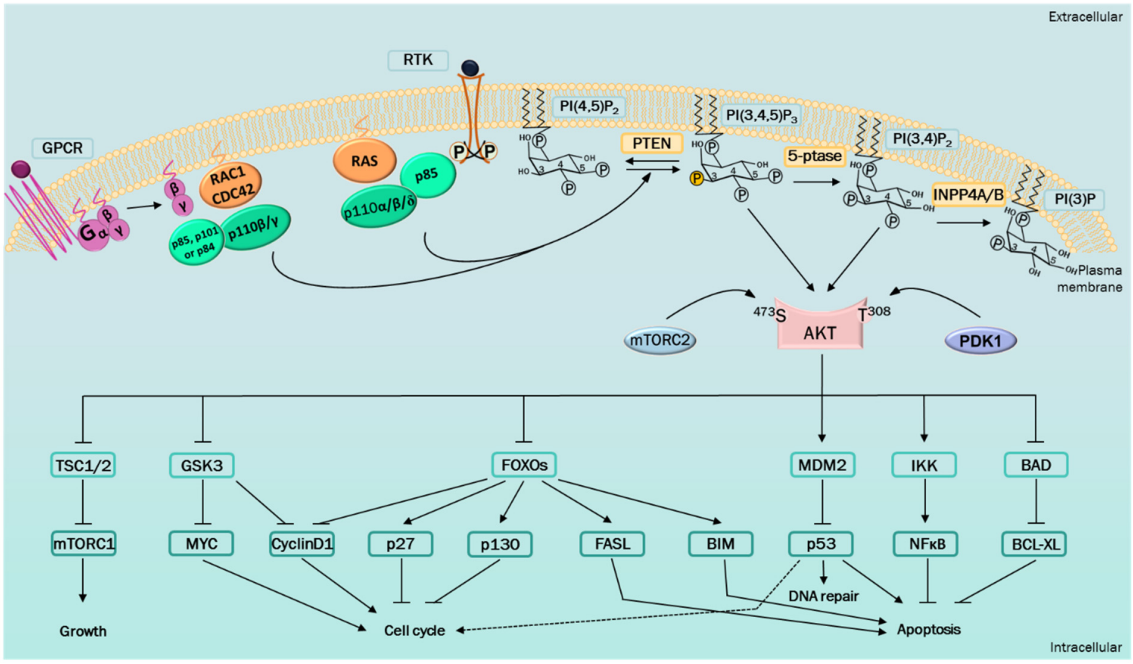

Figure 1.12 Physiological processes controlled by the class I PI3K/AKT signalling pathway

A schematic representation of class I PI3K activation downstream of GPRCs and RTKs in cooperation with RAS and RHO proteins, and their effect on the physiological processes controlled by activated AKT. $PI(3,4,5)P_3$ transiently generated at the plasma membrane from $PI(4,5)P_2$ is sequentially dephosphorylated by 5-phosphatases into $PI(3,4)P_2$ and by INPP4A/B into PI3P. PTEN dephosphorylates $PI(3,4,5)P_3$ into $PI(4,5)P_2$. $PI(3,4,5)P_3$ and $PI(3,4)P_2$ recruit PH domain-containing AKT and enable its phosphorylation on ^{308}Thr (by PDK1) and ^{473}Ser (by mTORC1). Active AKT dissociates into cytosol and by phosphorylation of its downstream effectors activates/inhibits important cellular processes including cell cycle, DNA repair and protein expression, cell survival, growth and metabolism. Key source: (Vadas, Burke et al. 2011).

localisation is mainly cytosolic and changes upon class I PI3K activation by external stimuli. The process is initiated by protein translocation to the plasma membrane enriched in the newly-synthesised $PI(3,4,5)P_3$ and interaction of its PH domain with this highly acidic phosphatidylinositol lipid. Conformational changes that take place in the protein's kinase domain, expose ^{308}Thr which becomes phosphorylated by phosphoinositide-dependent kinase 1 (PDK1), anchored at the plasma membrane by the same PH domain - $PI(3,4,5)P_3$ interaction. The second phosphorylation event takes place on ^{473}Ser located on the C-terminal hydrophobic motif and is controlled by mTORC2. Although each phosphorylation occurs independently, i.e. the absence of PDK1 or mTORC2 activity does not completely abrogate the process, a concomitant ^{308}Thr/^{473}Ser phosphorylation is required for full activation of AKT (Guertin and Sabatini 2007). The importance of this dual activation is emphasized by the action of phosphatases PHLPP1/2, which quench activity of AKT by dephosphorylation of ^{473}Ser.

The myriad of downstream targets that become phosphorylated by AKT makes it one of the most significant decision-making centres in the cell and reinforces its role as a proto-oncogene (Figure 1.12). Activated AKT dissociates from the plasma membrane into the cytosol, ready to phosphorylate its downstream targets. Cell growth is one of the canonical processes modulated by availability to growth factors and nutrients, with AKT's role intrinsically related to mammalian target of rapamycin complex 1 (mTORC1) activity. AKT phosphorylates two negative regulators of mTORC1 – TSC2 and PRAS40 – that support the pro-growth status of the cell and enable mTORC1-regulation of ribosome biogenesis and translation initiation (Manning and Cantley 2007). AKT is also a negative regulator of the pro-apoptotic protein BAD and its transcriptional regulator FOXO1, that results in promotion of cellular survival. Another important contribution is in AKT's control of metabolism. Positive signalling via growth factors (e.g. insulin), stimulates nutrient uptake and upregulates glucose and lipid metabolism. AKT promotes expression of glucose transporter 4 (GLUT4) on the surface of insulin-sensitive cells - a protein involved in uptake of glucose from blood. Central to this metabolic process, is inhibition by phosphorylation of GSK3 that releases active glycogen synthase and allows glucose conversion into glycogen. Moreover, pGSK3 regulates transcriptional processes that promote synthesis of enzymes involved in cholesterol and fatty acid synthesis. Finally, AKT, on its own or in cooperation with other protein kinases, controls additional processes such as cell proliferation, angiogenesis or migration. This very often leads to substantial cross talk between pathways, creating a complex signalling network in which different AKT isoforms can show differential contributions or even oppose each other in a context-dependent manner. Although a certain level of redundancy is expected from the structural similarity between AKT isoforms, studies on knockout mice revealed different developmental and metabolic deficiencies (Manning and Cantley 2007). This suggests that the intricacy, with which every process is controlled within the global signalling network, depends greatly on the type of stimulus, cell-specific AKT expression levels, as well as substrate availability and the presence of redundant protein kinases. A further complication starts to arise from the work on different cancer models. Our understanding more often points towards substantial rewiring processes that take place upon oncogenic transformation and AKT, due to high functional pressure, is potentially one such candidate.

1.2.5 PTEN - the primary tumour suppressor of the PI3K/AKT signalling pathway

The discovery of phosphatase and tensin homologue deleted on chromosome 10 (PTEN), and the majority of the work that followed, has been fundamentally related to its function as a tumour suppressor. In 1997, two groups identified a gene on chromosome 10, which correlated with a hotspot for loss of heterozygosity and was shown to be mutated in many advanced tumours (Li, Yen et al. 1997, Steck, Pershouse et al. 1997). Moreover, patients with Cowden disease, a rare autosomal cancer predisposition syndrome, were shown to be targeted by *PTEN* germline mutations (Liaw, Marsh et al. 1997). Generation of the first *Pten*$^{-/-}$ mice turned out to be embryonically lethal and *Pten*$^{+/-}$ animals exhibited loss of heterozygosity and related to it, a susceptibility to developing tumours (Di Cristofano, Pesce et al. 1998, Suzuki, de la Pompa et al. 1998). PTEN's relationship to PI3K activity was investigated in mouse embryonic fibroblasts (MEFs) from homozygous *Pten*-mutant mice. MEFs showed decreased responses to apoptotic stimuli like UV irradiation or osmotic stress and had constitutively raised AKT phosphorylation levels (Stambolic, Suzuki et al. 1998). Exogenous expression of PTEN re-sensitised the cells and normalised the levels of phosphorylated AKT.

PTEN was the first tumour suppressor discovered to bear phosphatase activity; a feature determined by its domain architecture (Figure 1.13). PTEN is a 403 aa protein and shares structural similarity of its catalytic motif, so called C(X)$_5$R, with the group of

Figure 1.13 PTEN domain architecture

PTEN is a 403 aa protein with five functional domains: an N-terminal PI(4,5)P$_2$-binding domain (PBD), a phosphatase domain with a C(X)$_5$R catalytic active site, a C2 domain, a carboxy-terminal tail (C-tail) and a PDZ-binding domain. Key sources: (Song, Salmena et al. 2012, Worby and Dixon 2014).

protein tyrosine phosphatases (PTPs) (Lee, Yang et al. 1999). C(X)$_5$R is part of the P loop formed at the bottom of a wide active-site pocket and gives PTEN its dual specificity, first described against acidic phosphorylated serine/threonine and tyrosine peptides (Myers, Stolarov et al. 1997). Recombinant PTEN was then shown to act as an inositol polyphosphate 3-phosphatase (3-phosphatase) towards synthetic substrates PI(3,4,5)P$_3$

and Ins(1,3,4,5)P_4 (Maehama and Dixon 1998). Moreover, the authors showed that PTEN overexpression in HEK293 cells led to a decrease in PI(3,4,5)P_3 levels upon insulin stimulation, without affecting the activity of PI3K. Finally, overexpression of a C124S PTEN mutant lacking the essential 'catalytic' cysteine, caused accumulation of PI(3,4,5)P_3 even in the absence of stimulus. This important work ratified PTEN's role as PI(3,4,5)P_3 phosphatase *in vitro* and *in vivo*. Finally, Myers et al. correlated PTEN's phosphoinositide 3-phosphatase function with the G129E missense mutation that occurs in patients with Cowden disease (Myers, Pass et al. 1998).

In most cells, cytosolic PTEN is thought to fulfil the majority of its physiological roles by transient association with the plasma membrane and co-localisation with its substrate, PI(3,4,5)P_3. This association is driven largely by non-substrate interactions with membrane lipids, which include interactions with the C2 domain on PTEN and also an N-terminal PI(4,5)P_2-binding domain (Worby and Dixon 2014). These interactions enhance stability and regulate activity through both local substrate concentration and allosteric effects. Further, residues found on the C2-catalytic interface are among the most commonly mutated in cancer (Worby and Dixon 2014). PTEN also undergoes extensive post-translational modification, including phosphorylation, ubiquitination, SUMOylation, oxidation and acetylation. In most cases, the precise roles of these modifications have yet to be fully elucidated. Phosphorylation of C-terminal tail residues creates an intramolecular association with the C2 domain and promotes an inactive PTEN conformation (caused by limited interaction with the plasma membrane); auto-dephosphorylation of these residues and subsequent activation of PTEN's lipid phosphatase activity is now thought to be the main function of PTEN's protein phosphatase activity (Tibarewal, Zilidis et al. 2012). Poly-ubiquitylation can mediate PTEN's proteasomal degradation, while mono-ubiquitylation and SUMOylation are thought to act as signals for nuclear translocation (Bassi, Ho et al. 2013, Leslie, Kriplani et al. 2016). PTEN's localisation and activity can be also modulated through incorporation into multiprotein complexes - a process often facilitated by its C-terminal PDZ binding domain (PDZ-BD) (Worby and Dixon 2014). Although its association with the p85 regulatory subunit of PI3K, PREX2 or, formation of a ternary PDGF-NHERF-PTEN complex have been reported, it is difficult to speculate on the universal character of these observations. Despite what was originally thought, PTEN is not constitutively and ubiquitously expressed and important mechanisms that can alter its cellular

concentration operate at the transcriptional level. As an example, PTEN provides a positive-feedback mechanism by binding to the p53 transcription factor, thus supporting its association with PTEN's promotor region (Song, Salmena et al. 2012). Transcriptional repression through aberrant hypermethylation of the *PTEN* encoding gene has also been observed in metabolic disorders and cancers (Garcia, Silva et al. 2004, Alvarez-Nunez, Bussaglia et al. 2006).

The physiological roles of PTEN are most clearly associated with its 3-phosphatase activity in the regulation of class I PI3K-synthesised levels of $PI(3,4,5)P_3$. As such, PTEN is defined as one of the most important molecular quenchers of class I PI3K signalling. Chemotaxis, the property of cells to sense and migrate along chemoattractant gradients like fMLP, is one of the processes in which localised activity of specific proteins is needed to establish cell polarity and support the process. In *Dictyostelium discoideum*, a GPCR-stimulated $PI(3,4,5)P_3$ anterior-posterior gradient is maintained by selective dephosphorylation of this lipid at the sides and rear of the cell due to PTEN activity (Funamoto, Meili et al. 2002). At the leading edge, guanine exchange factors (GEFs) binding to $PI(3,4,5)P_3$ and activation of GTPases initiate F-actin polymerisation. This creates lamellipodia that act in concert with acto-myosin contraction towards the rear to propel the cell forward. In contrast to *D. discoideum*, chemotaxis in mouse neutrophils seems to be primarily controlled by another $PI(3,4,5)P_3$ phosphatase - SH2-containing inositol phosphatase 1 (SHIP1). *Pten*$^{-/-}$ neutrophils showed no abnormalities while deletion of *Ship1* reduced the neutrophil's polarity and impaired its migratory potential (Nishio, Watanabe et al. 2007). PTEN's impact on cellular growth and metabolism is closely related to downregulation of the canonical insulin/PI3K/AKT signal transduction pathway. Therefore, mice with liver-specific *Pten* deletion showed increased sensitivity to insulin and enhanced glycogen storage (Knobbe, Lapin et al. 2008). PTEN is also a negative regulator of the Warburg effect – a metabolic process utilised by many cancer cells to produce ATP (Song, Salmena et al. 2012). In an oxygen-deprived environment, cancer cells can upregulate the rate of glycolysis through activation of specific effectors downstream of the activated PI3K/AKT pathway. Many tumours are thus able to reprogram metabolic pathways to sustain the elevated need for biomolecule production, including lipids and proteins. Insufficient downregulation of PI3K/AKT pathway by PTEN may result in abnormal cell-cycle progression - another hallmark of rapidly proliferating cancer cells. In the absence of this 'enzymatic break', G1 -> S phase

transition escapes control by hormones and mitogenic factors, which can lead to abnormal cellular division and accumulation of DNA mutations.

It is now well established that a pool of PTEN can also be detected in the nucleus, where it appears to carry out functions distinct from its 3-phosphatase activity. $PI(3,4,5)P_3$ produced in the nucleus in response to class I PI3K activity is insensitive to alterations in PTEN levels and a role for another enzyme , possibly a 5-phosphatase, has been suggested for its dephosphorylation in this organelle (Lindsay, McCoull et al. 2006). Instead, nuclear PTEN is suggested to engage in DNA repair processes and regulation of cell-cycle progression (Song, Salmena et al. 2012). This may explain why complete loss of *PTEN* is related to triggering cellular senescence, as opposed to *PTEN* deregulation (due to heterozygous loss or mutation), that promotes pro-growth and pro-survival signalling.

1.2.6 5-phosphatases

Apart from PTEN, a group of phosphatases that share inositol polyphosphate 5-phosphatase (5-phosphatase) activity can dephosphorylate $PI(3,4,5)P_3$, transiently generated in response to hormone-activated class I PI3Ks (Figure 1.5 and Figure 1.12). The product of this reaction, $PI(3,4)P_2$, shows some analogous properties to $PI(3,4,5)P_3$, i.e. it can control the distribution and activity of some PH domain-bearing proteins. The best studied example is the apparently similar ability of $PI(3,4,5)P_3$ and $PI(3,4)P_2$ to stimulate PDK1-dependent phosphorylation and activation of AKT (Alessi, James et al. 1997). Here, a second dephosphorylation reaction, performed e.g. by a $PI(3,4)P_2$ 4-phosphatase INPP4B, is required to efficiently quench PI3K/AKT signalling. However, several studies have suggested an AKT-inhibitory role for 5-phosphatases, while others go one step further and point towards AKT-independent properties of $PI(3,4)P_2$ (Hawkins and Stephens 2016). The potential signalling roles for $PI(3,4)P_2$ are discussed in more detail below.

In mammals, ten members of the 5-phosphatase family have been sequenced; each showing a unique affinity towards 5-phosphate containing inositol lipids or phosphates (Figure 1.14). SHIP1/2, INPP5E, SKIP and PIPP/INPP5J belong to class II 5-phosphatases and are proteins with described *in vivo* $PI(3,4,5)P_3$ 5-phosphatase activity (Eramo and

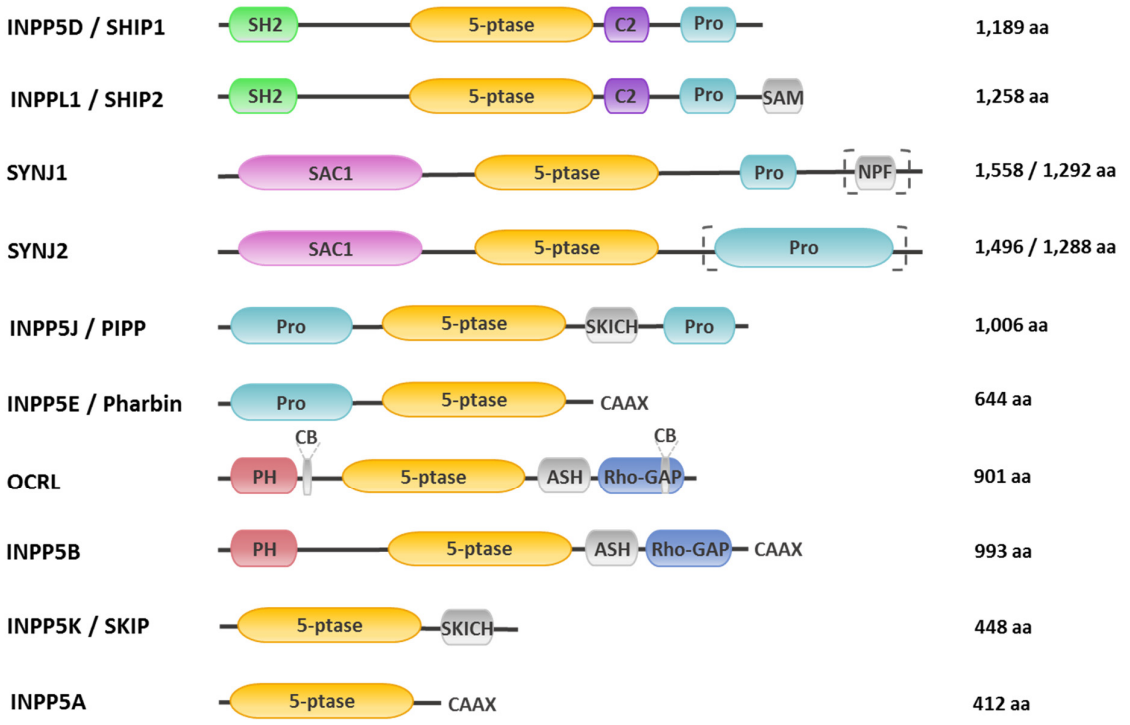

Figure 1.14 Mammalian lipid 5-phosphatases

Domain organisation of mammalian 5-phosphatases is diverse but all members share a central 5-phosphatase (5-ptase) catalytic domain. The SH2 domain of SHIP1/2 is responsible for protein recruitment to the plasma membrane, while the SAC1 domain provides SYJN1/2 with additional phosphatase activity. Cellular localisation of 5-phosphatases is controlled by the SKICH domain and CAAX motifs whereas protein-protein interactions are mediated e.g. by ASH, Rho-GAP, SAM or proline-rich motifs. Key sources: (Ooms, Horan et al. 2009, Balla 2013).

Mitchell 2016). Their central catalytic core possesses conserved arginines that coordinate PI(3,4,5)P_3 or Ins(1,3,4,5)P_4 and is sandwiched by a selection of different domains, such as SH2, SH3, SKICH or Pro-rich regions. Each of them contributes to the large diversity of the family by bringing properties such as protein scaffolding or cellular localisation.

SH2 (Src homology 2)-containing inositol phosphatase 1 (SHIP1) was discovered as 145 kDa protein predominantly expressed in haematopoietic cells and is an exclusive PI(3,4,5)P_3 5-phosphatase (Damen, Liu et al. 1996). Two types of immune signalling complexes can form on the surface of immune cells when the Fc portions of antibodies are recognised by appropriate receptors (FcγRs); each possess cytosolic, tyrosine-containing motifs which upon phosphorylation act as adaptors/activators for effector proteins. Immunoreceptor tyrosine-based activation motifs (ITAMs) activate downstream effectors (like PI3K, PLC or RAS) and trigger immune defence. Inhibitory

motifs (ITIMs) co-cluster with ITAMs and, by 'overpowering' their activatory potential, silence the immune response. SHIP1 function is thought to be executed by colocalisation; upon interaction of its SH2 domain with the phospho-tyrosine-containing ITIM motif of FcγRIIB it is recruited to the plasma membrane, where it can degrade $PI(3,4,5)P_3$, and thus quench signalling of this second messenger. SHIP1 is also an example of an allosterically regulatable enzyme; its activity is upregulated upon binding of its $PI(3,4)P_2$ product to a C2 domain. Finally, SHIP1's proline-rich regions enable interaction with SH3 domain-containing partners and may contribute to the protein-substrate co-localisation. The multiple non-catalytic interactions of SHIP1 suggest that its activity is tightly regulated and heavily context dependent. Indeed, *Ship1-null* mice show significant abnormalities in immune cell number and function that cause massive infiltration of myeloid cells into lungs and results in a very short lifespan, with mortality at 14 weeks reaching 60% (Helgason, Damen et al. 1998). B cells from these animals are characterised by raised AKT activity, related to enhanced $PI(3,4,5)P_3$ and lowered $PI(3,4)P_2$ levels post B-cell receptor stimulation. As a result, cells proliferate and mature at a much faster rate, and become resistant to cell death (Brauweiler, Tamir et al. 2000). In agreement, studies on leukemic T-cells with *SHIP1* loss-of-function mutation showed decreased basal AKT phosphorylation upon expression of constitutively active SHIP1 (Freeburn, Wright et al. 2002).

SH2 (Src homology 2)-containing inositol phosphatase 2 (SHIP2) is a product of a different gene and an ubiquitous homologue of SHIP1 with *in vivo* preference for $PI(3,4,5)P_3$ over other phosphatidylinositol lipids (Pesesse, Deleu et al. 1997). Although 'catalytically equivalent' to SHIP1, the presence of a SAM domain, unique proline-rich motif and phosphorylation sites, determine SHIP2's engagement in interactions with specific proteins and has an impact on its subcellular localisation and activities (Ooms, Horan et al. 2009). Therefore, SHIP2 in resting cells is detected mainly in the cytosol and upon stimulation translocates to relevant membrane-containing cellular regions. The first discovered and one of the key functions of SHIP2 is in the control of metabolism; a property explained by its predominant expression in insulin-sensitive tissues like skeletal muscles, heart, brain or adipose tissue (Thomas, Erneux et al. 2017). *Ship2-null* mice fail to develop dietary obesity despite observed increased insulin tolerance and glucose uptake that result from enhanced insulin-induced AKT activation (Sleeman, Wortley et al. 2005). In contrast, mice expressing germ-line catalytically-inactive SHIP2

are affected by developmental abnormalities and metabolic disorders (like lipid metabolism and insulin secretion) but do not show changes in AKT phosphorylation or glucose tolerance. Finally, SHIP2 overexpression in 3T3-L1 adipocytes, reduces insulin-induced AKT activity, $PI(3,4,5)P_3$ levels and translocation of GLUT4 transporters (Wada, Sasaoka et al. 2001). The observed effects are reversed in adipocytes expressing 5-phosphatase-defective SHIP2. It seems that our lack of full understanding of the metabolic process regulated by SHIP2 may come from the complex nature of catalytic and non-catalytic roles it has in the insulin-mediated PI3K/AKT signalling. Similar to SHIP1, SHIP2 utilizes its SH2 domain to interact with phosphorylated-ITIM motifs of FcγRIIB adaptor proteins in immune cells, but for efficiency requires association with adaptors such as GRB2 (Blero, Payrastre et al. 2007). SHIP2's role has also been associated with actin cytoskeleton organisation. It's protein's scaffolding properties and localised synthesis of $PI(3,4)P_2$ provide elements essential for formation of specialised structures like lamellipodia and invadopodia (Thomas, Erneux et al. 2017).

The other members of 5-phosphatases are more promiscuous and, apart from $PI(3,4,5)P_3$, are able to hydrolyse other inositol lipids and phosphates. SKIP is a small 5-phosphatase found in heart, kidney and muscles, with functions similar to those of SHIP2. It seems to play an inhibitory role in growth factor-stimulated insulin signalling and by dephosphorylation of $PI(4,5)P_2$ contributes to actin rearrangements and cellular migration (Eramo and Mitchell 2016). INPP5E is enriched in brain and testes and shows affinity towards all of the 5-phosphate-containing phosphatidylinositol lipids. This 5-phosphatase plays a critical role during embryonic development, with mutations causing severe developmental abnormalities, collectively related to as ciliopathies. PIPP/INPP5J is a dual $PI(3,4,5)P_3$/$PI(4,5)P_2$ 5-phosphatase with a role implied in neural development as negative regulator of active AKT levels (Ooms, Fedele et al. 2006). Moreover, PIPP was shown to suppress tumour growth in mouse xenografts when overexpressed in human melanoma cell line and was recently defined as a bona fide tumour suppressor in breast tumorigenesis (Ye, Jin et al. 2013, Ooms, Binge et al. 2015).

1.2.7 INPP4A/B - PI(3,4)P_2 specific 4-phosphatases

Two PI(3,4)P_2 - specific phosphatases have been convincingly characterised so far - inositol polyphosphate-4-phosphatase type I (INPP4A) and type II (INPP4B), respectively (Figure 1.15). Analogously to PTEN, they belong to the protein tyrosine phosphatase (PTP) family, with the catalytic ability provided by a conserved cysteine located within the C-terminal C(X)$_5$R motif. INPP4A and INPP4B show only ~37%

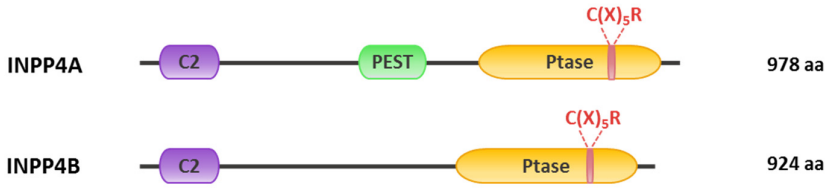

Figure 1.15 INPP4A/B domain architecture

Functional domains of INPP4A/B include a lipid binding domain (C2) and a phosphatase domain with a C(X)$_5$R catalytic active site. INPP4A has an additional PEST (proline, glutamate/aspartate, serine/threonine rich) motif. Key sources: (Agoulnik, Hodgson et al. 2011, Li and Marshall 2015).

sequence homology, which points to differential functions and may explain the fact that INPP4B is ubiquitously expressed while INPP4A is mainly restricted in the brain. They both possess an N-terminal lipid binding domain which however seems to drive interaction with a different group of lipids; that of PI(3,4)P_2, PI4P and PS with INPP4A and PA or PI(3,4,5)P_3 with INPP4B (Li and Marshall 2015). INPP4A/B's significance in quenching PI(3,4)P_2-driven processes at the plasma membrane is conveyed by the intrinsic ability to specifically hydrolyse position 4D on the inositol ring of this lipid. The PI3P produced at the plasma membrane by this process however, seems to make a negligible contribution to whole cell steady-state PI3P levels (Posor, Eichhorn-Gruenig et al. 2013), which in the cell are mainly controlled by class III, and possibly class II, PI3Ks within the endolysosomal system. Despite this, one cannot exclude context-dependent or spatially-confined functions of pools of PI3P at the plasma membrane that may be controlled by these enzymes.

INPP4A's importance in brain development has been realised through generation of genetically modified animal models (Sasaki, Kofuji et al. 2010). *Inpp4a-null* mice experienced severe neurodegeneration that affected their motor ability and cognitive potential. Moreover, mechanistic studies on cultured neurons in which 4-phosphatase

expression was supressed by small hairpin RNA (shRNA), revealed SHIP1's protective role against glutamate excitotoxicity and, related to it, neuronal death. This pro-death signalling was reproduced when neurons were incubated with $PI(3,4)P_2$ but not $PI(3,4,5)P_3$.

INPP4B is expressed in a wide variety of human tissues, including heart, muscle, brain and epithelial cells of the breast and prostate. Unlike INPP4A, no severe developmental changes have been observed in mice expressing INPP4B with a truncated phosphatase domain. Instead, animals develop osteoporosis characterised by reduced bone mass, with INPP4B having a protective effect against dysregulated osteoclast differentiation and maturation (Ferron, Boudiffa et al. 2011). In addition, a predominant role for INPP4B as a tumour suppressor has recently started to emerge with the original work by Gewinner et al., who showed its physiological relevance in the context of breast tumorigenesis (Gewinner, Wang et al. 2009). Moreover, the work in human prostate cancer cell lines identified two androgen receptor binding sites on the *INPP4B* locus, suggesting a multilayer regulation mechanisms of INPP4B protein levels (Hodgson, Shao et al. 2011). The role of INPP4B as a tumour suppressor is discussed in more detail below.

1.3 PI3K/AKT signalling pathway in tumorigenesis

The work until the late 90s was led by mechanistic studies trying to establish the fundamentals of PI3K signalling and its link to phosphatidylinositol lipids. Therefore, a lot of research was based on cell-based assays, cloning and expression of PI3K family isoforms or developing the first synthetic PI3K inhibitor - LY294002. A full circle was made in 1998, when the focus on PI3K switched back to the context of its original discovery in cell transformation driven by viral oncoproteins. Establishing the functional link between deregulation of a tumour suppressor PTEN, earlier shown to be associated with multiple hamartoma syndrome, and PI3K/AKT hyperactivation created a natural direction for future scientific investigations (Stambolic, Suzuki et al. 1998). Moreover, a short report by Samuels et al., described the high frequency of somatic mutations in patients with solid tumours in the gene encoding p110α (*PIK3CA)* (Samuels, Wang et al. 2004). This further emphasized the importance of PI3K-centred signalling in pathophysiology and justified its role as a drug target. Since then, many proteins with critical roles in the homeostatic control of PI3K/AKT pathway activity have been reported to be dysregulated in cancer, with modifications ranging from homozygous deletions and LOH to gene amplifications, transcriptional and epigenetic silencing. It has been estimated, that alterations at the genomic level in the components of the PI3K/AKT pathway occur in around 70% of breast and in 42% / 100% of localized / metastatic prostate cancers (Taylor, Schultz et al. 2010, Koren and Bentires-Alj 2013).

1.3.1 Class I PI3K alterations in human cancer

The majority of class I PI3K activating somatic mutations occur in p110α and result in enhanced lipid kinase activity. Two particularly well studied hotspots on the *PIK3CA* gene - E545K on exon 9 and H1047R on exon 20 - are gain-of-function mutations, which imitate the protein's active conformation. The presence of ^{545}K in the helical domain of p110α disrupts the inhibitory conformation imposed by the p85 regulatory subunit and makes it independent of phosphotyrosine docking to the N-SH2 domain in p85, but the enzyme probably still needs input from RAS or translocation to the membrane. Activation induced by ^{1047}R, on the other hand, is achieved through changes occuring in p110α catalytic domain, similar to those that take place upon RAS binding (Zhao and

Vogt 2008). Both mutations are thought to provide enhanced basal activity and signal-independence, by reducing the number of components required for p110α full activation. Moreover, the unique regulatory mechanisms that emerge from the individual mutations, if they co-occur during tumour progression, can potentiate the cells with a great growth advantage. Despite this, several studies in mouse models suggest that p110α activating mutations must act in cooperation with other oncogenic factors that accumulate to support tumour development, including loss of *PTEN* and *p53* mutations in ovarian and breast cancer, respectively (Kinross, Montgomery et al. 2012, Koren and Bentires-Alj 2013).

The frequency of activating mutations in p110β is low and its connection to cancer came from the studies on PTEN's role in mouse prostate homeostasis. Targeted deletion of *Pten* from prostatic epithelium is achieved by probasin-driven Cre recombinase expression in *Pten*$^{flox/flox}$ mice. Such animals show signs of epithelial hyperplasia already at 4 weeks, which by 6 weeks develops into murine prostatic intraepithelial neoplasia (mPIN) (Wang, Gao et al. 2003). Later, the disease progresses through invasive adenocarcinoma and eventually leads to metastasis in the lungs. Therefore, this mouse model is a useful tool to study the molecular mechanisms that occur during prostatic tumorigenesis as it follows the stages and similar kinetics observed in humans. In order to fully understand the mechanisms of PTEN-regulated tumorigenesis, different class I PI3K isoforms were tested for their relative contribution to the process. Thus, crossing *Pten*$^{flox/flox}$ with *p110α*$^{flox/flox}$ or *p110β*$^{flox/flox}$ animals was performed to generate double knockout mutants (Jia, Liu et al. 2008). Surprisingly, ablation of p*110β* but not *p110α* inhibited tumorigenesis triggered by *Pten* loss and normalised the previously raised levels of pAKT^{473}. The authors propose that tumorigenic transformation in the mouse prostate is potentiated by the permanent increase in the pool of basal PI(3,4,5)P_3 levels produced by p110β, as opposed to transient PI(3,4,5)P_3 generated downstream of RTK-controlled p110α activity.

The effects of p110γ and p110δ dysregulation are primarily manifested in the development of primary immunodeficiencies (PIDs) and autoimmune disorders. The hereditary E1021K mutation in the p110δ kinase domain has been identified in 10% of patients suffering from PIDs; called activated p110δ syndrome (APDS) (Angulo, Vadas et al. 2013). The clinical symptoms of APDS include abnormalities in B and T lymphocytes and impaired immune response to bacterial infections that predispose these patients to

chronic respiratory infections. The presence of enhanced p110δ activation, led to increased basal and stimulated $PI(3,4,5)P_3$ levels in T cells isolated from patient's peripheral blood (compared to control group) and raised AKT phosphorylation. Further studies reinforced the initial observations and supported the hypothesis that the E1021K gain-of-function mutation causes increased activity of p110δ and its downstream effectors. Moreover, one of the patients identified with APDS developed lymphoma, which may support the previously reported ability of p110δ to transform cells.

Idelalisib (formerly known as GS-1101 or CAL-101), the first FDA approved drug targeting a member of class I PI3K, is a selective p110δ inhibitor currently administered to patients with diagnosed lymphoid cancers like chronic lymphocytic leukemia (CLL) (Brown, Byrd et al. 2014). In contrast to the initial aim of inhibiting p110δ-dependent growth in the lymphoid tumour cells themselves, idelalisib probably acts primarily by interfering with lymphoid-stromal cell interactions, which leads to the ejection of the tumour cells from their protective lymphoid niche (Fruman and Rommel 2011). Further, a great deal of the current focus in this area is on the development of p110γ and p110δ inhibitors that target immune suppressor cells in the tumour microenvironment that allow solid tumours to escape cytotoxic T-cell attack (e.g. regulatory T cells, myeloid-derived suppressors) (Okkenhaug, Graupera et al. 2016).

1.3.2 AKT isoform-specific roles in tumour initiation and progression

AKT/PKB is a major effector that transduces aberrant PI3K signalling and by this promotes carcinogenesis. The risk of tumour development due to abnormal AKT activity is intrinsically related to the spectrum of functions that it regulates, including cellular motility and metabolism as well as growth, proliferation and survival. The three isoforms (AKT1-AKT3) expressed in humans are translation products of different genes and despite high sequence identity, show a surprising functional diversity and, quite often, limited level of redundancy (Manning and Cantley 2007).

Somatic mutations that localize mainly to the PH and catalytic domain of AKT are estimated to occur in 5% of human cancers, with some cases leading to constitutive recruitment of the protein at the plasma membrane (Rodgers, Ferguson et al. 2017). 16% of ER-positive breast cancer patients bearing an E17K mutation in the PH domain

of *AKT1* have not been identified with any additional genetic alterations, suggesting AKT's role as *bona fide* oncogene in this context (Rudolph, Anzeneder et al. 2016). The initial data postulated AKT1^{E17K} as a negative prognostic factor, emerging from the increased death rate observed at the early stage of disease in AKT1^{E17K} versus control cohorts.

Gene amplification of *AKT* isoforms is not very common in human cancer and AKT hyperactivation is often a result of alterations that occur upstream. Indeed, amplification of *PDK1* and amplification/overexpression of RICTOR (member of the mTORC2 complex) - two regulators of AKT's phosphorylation status, have been identified in various types of tumours (Rodgers, Ferguson et al. 2017).

Opposing roles of AKT1 and AKT2 in cancer initiation and progression were revealed during studies on mammary tumorigenesis in polyoma middle T (PyMT) mice. Expression of activated AKT1 or AKT2 alone did not lead to malignancy formation in the mammary epithelium of wild type animals. However, transgenically expressed AKT1 was found to promote tumour incidence in PyMT oncogene-driven transformation, while AKT2's role in the process was dispensable (Dillon, Marcotte et al. 2009). Interestingly, an AKT2-stimulating (and an AKT1-inhibitory) function was associated with tumour progression, with higher frequency of metastasis in the lungs occurring in the animals with constitutively active AKT2. The pro-migratory role of AKT seems to be heavily cell- and context-dependent. In the prostate cancer cell line PC3, both AKT1 and AKT2 isoforms control cell proliferation, whereas knocking down AKT2 promoted, but knocking down AKT1 impeded, cell migration (Cariaga-Martinez, Lopez-Ruiz et al. 2013).

The knowledge coming from the *Akt3*$^{-/-}$ mouse model and the preferential expression of AKT3 in the brain may correlate with its critical function in developing brain malignancies. Primary murine astrocytes, derived from the model that recapitulates the common mutations occurring during gliomagenesis in humans, showed AKT3-dependent development of anchorage-independent growth; a phenotype that wasn't observed even after combined deletion of *Akt1* and *Akt2* and could not be rescued by exogenous AKT1 expression (Endersby, Zhu et al. 2011).

1.3.3 Role of PTEN in tumorigenesis

The tumour-suppressive power of a protein has been associated with the observation that heterozygous genetic alterations 'prime' the cells for malignant transformation. Thus, tumours were initially thought to develop following a *two-hit model*, in which loss of one allele triggers cancer susceptibility and loss of the second, induces cancer (Song, Salmena et al. 2012). Generation of *Pten*$^{-/-}$ mice by several labs demonstrated the importance of PTEN in embryonic development, whereas genomic analysis of cancers which spontaneously developed in *Pten*$^{+/-}$ animals supported the hypothesis that PTEN is a haploinsufficient tumour suppressor (Di Cristofano, Pesce et al. 1998). The work on hypermorphic PTEN mice, which retain 80% of the original protein levels, revealed that subtle modulation in PTEN's expression implies serious physiological consequences (Alimonti, Carracedo et al. 2010). Interestingly, *Pten*$^{hy/+}$ animals, similar to *Pten*$^{+/-}$, experienced premature lethality and developed tumours, while retaining a functional wt allele. Breast and uterus were among the organs most susceptible to subtle changes in PTEN expression and showed the highest incidence of cancer development. Comparing the data from existing mouse models, it becomes apparent that PTEN 'dosing' and activity is tissue-specific and essential to preserve cellular homeostasis. Therefore, a *continuum model*, in which a gradual reduction in the amount of functional PTEN predisposes different tissues to tumorigenesis, appears to be a more plausible way of looking at the 'onco-protective' potential of tumour suppressors (Carracedo, Alimonti et al. 2011).

PTEN regulation in the context of carcinogenesis is multifaceted and appears at the gene, mRNA and protein level. As well as gene deletion, the efficiency of transcription/translation can be dysregulated by promoter methylation, transcription factors and miRNAs, whereas posttranslational modifications such as phosphorylation or acetylation can aberrantly reduce PTEN protein levels (Hollander, Blumenthal et al. 2011). Therefore, genetic screens for the presence of point mutations or gene alterations do not dismiss PTEN's role in tumour formation and cannot serve as a universal diagnostic tool.

The incidence of breast cancer appears to be most strongly correlated with subtle alterations in PTEN levels in mice and human females with Cowden syndrome carry a high, 25-50% risk of developing this disease during their lifetime (Alimonti, Carracedo

et al. 2010). PTEN protein levels are very commonly decreased in sporadic mammary tumours (estimated to happen in around 40% of cases) which, when compared with 5% of *PTEN* mutations, strongly suggests the presence of more complex mechanisms that become activated in the course of tumour progression (Hollander, Blumenthal et al. 2011). The frequently occurring *PTEN* LOH and promoter methylation, the fact that *PTEN* loss correlates with downregulation of other tumour suppressors resulting in hyperactivated PI3K/AKT, and the identification of breast cancer 1/2 (*BRCA1/2*) genes, are the likely explanation to why breast cancer is one of the most prevalent types of tumours in humans. Immuno-oncology is one of the most quickly developing areas of science in defying cancer, which aims to study the role the immune system plays in supporting tumour growth and protecting it from therapeutic intervention. PTEN's importance as a tumour suppressor has been implicated in the communication that occurs between the fast proliferating malignant cells and their environment. Genetic ablation of *Pten* in mouse stromal fibroblasts, the component cells of stroma that provide the tumour with essential growth factors and chemokines, triggered activation of secretion, vascularisation and macrophage recruitment, which together accelerated transformation processes in the epithelial cells of mammary gland (Trimboli, Cantemir-Stone et al. 2009). The mechanisms that PTEN utilizes as a 'protection shield' have been proposed to be through AKT, RAS and JNK signalling networks.

Prostate cancer is the most common malignancy occurring in men and its incidence largely increases with age. PTEN, in this context, has been extensively studied and defined as haploinsufficient, with genetic alterations detected from early stage to metastatic adenocarcinomas. Thus, *PTEN* inactivating missense or truncation mutations, LOH and homozygous deletions have been reported in patient cohorts by several groups, with the numbers reaching 30% in primary and 63% in metastatic cancers (Wang, Gao et al. 2003, Sarker, Reid et al. 2009). Associated with *PTEN* loss, increased levels of phosphorylated AKT1 have been suggested as a promising clinicopathological marker in predicting the biochemical recurrence in prostate cancer. ^{473}Ser-AKT1 staining was found to positively correlate with high Gleason grade in advanced tumours and shorter recurrence-free survival in patients after the primary treatment (Ayala, Thompson et al. 2004). In parallel, multiple transgenic mouse models have been generated to follow the molecular mechanism underlying initiation and development of prostatic malignancies. Unlike in breast tissue, *Pten*$^{+/-}$ mice very rarely develop prostate carcinoma and instead

slowly evolve into high grade PIN, suggesting the need for additional mutations for the disease to progress into the malignant state. Tissue-specific *Pten* deletion, on the other hand, starts with hyperplasic growth of epithelial cells, which at 6-8 weeks of age is followed by PIN to eventually evolve into adenocarcinomas by 4 months, where tumour progression is fastest in the lateral and slowest in the ventral prostate ((Wang, Gao et al. 2003); C. Sandi and S. Cosulich, personal communication). As discussed above, one of the consequences of *Pten* ablation is unrestrained AKT signalling and studies in the *Pten*$^{flox/flox}$ mouse showed a unique role of p110β in the process of tumorigenesis in prostatic epithelial cells (Jia, Liu et al. 2008).

1.3.4 INPP4B as a tumour suppressor

INPP4B, due to its demonstrated 4-phosphatase hydrolytic activity towards PI(3,4)P_2, had been suspected to exert a tumour suppressive function by negatively regulating the PI3K/AKT pathway (Norris, Atkins et al. 1997). Similar to PTEN, the initial genomic analyses reported on LOH in the region encoding INPP4B in breast cancer cell lines and primary breast tumours (Naylor, Greshock et al. 2005). The first solid confirmation of this hypothesis came with the study by Gewinner et al., in which human mammary epithelial cells (HMEC) were transformed with retroviruses (using shRNA) to stably suppress INPP4B levels (Gewinner, Wang et al. 2009). Interestingly, when grown in soft agar, INPP4B-KD HMEC cells showed characteristics of anchorage-independent growth, phenocopying the effect of PTEN-KD in the same cells. Moreover, knocking down INPP4B showed similar effect to knocking down PTEN in stimulating the migratory potential of HMECs, with the effect inhibited by the pan-PI3K inhibitor LY294002 and unaffected by overexpression of catalytically-inactive INPP4B, therefore linking increased motility with raised levels of PI(3,4)P_2 or PI(3,4,5)P_3. An additive effect of PTEN and INPP4B suppression was demonstrated by higher and sustained AKT phosphorylation levels compared to suppression of individual phosphatases alone. Finally, wild type INPP4B impeded growth of tumorigenic SUM149 cells injected in nude mice and, when overexpressed in 3T3-L6 cells, caused a decrease in PI(3,4)P_2, leaving the levels of PI(3,4,5)P_3 unaffected. *In vitro* assays formally confirmed that INPP4B is a preferential PI(3,4)P_2 4-phosphatase. The analysis of publically available data on advanced breast cancer revealed that *INPP4B* allelic loss is most common in patients

carrying the *BRCA1* germline mutation and in triple-negative tumours. The fact that the correlation frequency in each case reached over 55% and that clinical data describes the triple-negative breast cancer as highly metastatic, and with poor outcome in patients, became a reason for further analysis. Immunohistochemical (IHC) staining of INPP4B levels in breast and ovarian cancer tissues confirmed the relationship between reduced phosphatase expression and poor patient outcome and underscored the importance of INPP4B in controlling AKT activity and as a tumour suppressor in these types of cancers.

Another important contribution to understanding INPP4B's function in breast cancer biology was the work performed by Fedele et al. (Fedele, Ooms et al. 2010). In normal human breast, INPP4B appears to be expressed only in the oestrogen receptor (ER) positive cells, where it performs a proliferation-suppressive function. A similar observation was made in breast cancer cell lines, with low or undetectable INPP4B levels in the majority of cell lines lacking ER expression. ER-positive Mcf7 cells with INPP4B knock down showed increased proliferation and raised, basal and stimulated ^{473}Ser-AKT phosphorylation levels. Moreover, the cells were characterised by higher colony number in soft agar and larger tumour size in nude mice. When overexpressed in ER-negative MDA-MB-231 cells, INPP4B caused a reduction in EGF-stimulated ^{308}Thr- and ^{473}Ser-AKT phosphorylation levels. Finally, scoring two independent sets of primary breast carcinoma samples for INPP4B expression levels, indicated a positive correlation between the loss of both ER and progesterone receptor (PgR) with INPP4B deficiency. Compared to the previous analysis, at least 80% of tumours classified as triple-negative in both groups, were associated with loss of INPP4B expression. What is more, an in-depth analysis of a cohort of 267 ductal breast carcinomas indicated that the frequency of INPP4B loss of expression is highly similar to that occurring in PTEN or when compared against frequency of mutations in *PIK3CA*. Importantly, loss of INPP4B expression was shown in 49% of *PTEN-null* tumours and only 14% of PTEN-positive tumours. Thus, the results presented in this study supported the previously published work by Gewinner et al., confirmed INPP4B's role as a negative regulator of AKT *in vivo* and suggested its significance as a molecular marker of basal-like breast carcinomas. Further, the concomitant loss of the two tumour suppressors *PTEN* and *INPP4B* that occurs with relatively high frequency, may suggest selection mechanisms occur to favour cells with highly aggressive phenotypes characterised by hyperactivated AKT.

Patients with diagnosed advanced prostate cancer are routinely subject to androgen-ablation therapy, in order to systemically suppress the levels of testicular androgen. Unfortunately, after initial regression the disease very often progresses into an aggressive, castration-resistant form. Androgen receptor (AR) signalling supports prostatic growth, survival and differentiation and thus shows significant functional overlap with the PI3K/AKT pathway. The relapse observed in androgen-resistant tumours has been related to increased AKT1 signalling and likewise, androgen-starvation of LNCaP prostate cancer cells leads to upregulation of PI3K/AKT activity (Rokhlin, Taghiyev et al. 2002, Ayala, Thompson et al. 2004). Hodgson et al. found that the mRNA levels of INPP4B increase in a time and dose dependent manner when LNCaP cells were treated with synthetic androgen following starvation, suggesting AR-driven transcriptional regulation of this phosphatase (Hodgson, Shao et al. 2011). Indeed, two unique binding-sites were identified in the *INPP4B* locus with increased recruitment of AR observed in androgen-treated LNCaP cells. More importantly, androgen starvation led to a decrease in INPP4B levels in LNCaP (PTEN-null) and VCaP (PTEN-positive) prostate cancer cell lines with parallel increases in ^{308}Thr-AKT phosphorylation. This was followed by analogous observations made in INPP4B-KD LNCaP cells, which additionally showed an increased rate of proliferation. Finally, a corepressor NCoR was identified to positively regulate INPP4B transcription via direct interaction and modulation of AR activity. Similar to the studies on breast cancer, the analysis of prostate cancer tissues from patients showed a substantial decrease in epithelial INPP4B expression compared to healthy prostate. This further correlated with high tissue-proliferating status, as judged by Ki67 staining, and decreased relapse-free survival time. Although similar trends were observed for PTEN, no correlation analysis was performed for those two phosphatases.

The cooperative role of PTEN and INPP4B in restricting excessive PI3K/AKT signalling was investigated in the context of thyroid cancer development. Although patients with Cowden syndrome have been associated with higher risk of developing benign and malignant thyroid lesions, transgenic mice with heterozygous deletion of *Pten* do not develop thyroid cancers (Liaw, Marsh et al. 1997, Stambolic, Tsao et al. 2000). This may suggest that PTEN deficiency is not a strong enough driver of tumour progression in thyroid and additional factors are required to trigger malignant transformations in the cells. Generation of *Inpp4b*$^{\Delta/\Delta}$ mice, with a mutation in the

phosphatase domain, gave healthy offspring without major abnormalities, implying that INPP4B does not play a significant tumour suppressive role in the presence of PTEN (Kofuji, Kimura et al. 2015). However, when *Inpp4b*$^{\Delta/\Delta}$ and *Pten*$^{+/-}$ mice were crossed, the lethality of the double mutants substantially increased and by 32 weeks, the animals developed thyroid tumours with metastases in the lungs. At the molecular level, hyperactivation of the PI3K/AKT pathway was observed by raised phosphorylated AKT levels in the double-mutant compared to *Inpp4b*$^{\Delta/\Delta}$ or *Pten*$^{+/-}$ controls and the AKT2 isoform was identified as the primary downstream effector contributing to the phenotype. *In vitro* assays showed a weak PI(3,4,5)P_3 phosphatase activity of INPP4B under 'overexpression' conditions. More importantly, however, a significant increase in PI(3,4,5)P_3 was measured in the thyroid tissue from the double-mutant mice, compared to *Pten*$^{+/-}$ mice and low levels of PI(3,4,5)P_3 in *Inpp4b*$^{\Delta/\Delta}$ mice. To gain a clinical perspective, INPP4B was shown to be downregulated in 30% of patients with a follicular variant of papillary thyroid carcinoma (FV-PTC). This was then supported by IHC analysis, with 7/8 patients with follicular thyroid carcinoma (FTC) showing low levels of INPP4B, 3 of which coincided with reduced levels of PTEN. Finally, a careful analysis of two databases revealed a strong correlation between INPP4B and PTEN downregulation in thyroid cancers and common alterations in *INPP4B* and *PTEN* genes in endometrial tumours. This work supported the need for mouse model generation to delineate more complex biological mechanisms and for the first time revealed a redundant role for INPP4B, which can prevent PI3K/AKT hyperactivation under PTEN-deficient conditions. Outstanding questions remain, as to what position on the PI(3,4,5)P_3's inositol ring is hydrolysed by INPP4B *in vitro* and to what extent, and in which context, this activity may be directly relevant to controlling levels of PI(3,4,5)P_3 *in vivo* e.g. in the presence of activating mutations in class I PI3K members.

1.3.5 5-phosphatases and their role in cancer

PIPP/INPP5J is the first of the inositol polyphosphate 5-phosphatase members that has been shown to act as a putative tumour suppressor. Genetic alterations in *PIPP* that lead to LOH or allelic loss of chromosome, as well as lower mRNA levels associated with the more aggressive ER-negative subtype, have all been reported to occur in breast tumours (Rodgers, Ferguson et al. 2017). Driven by PIPP's role as a PI(3,4,5)P_3 5-

phosphatase and the fact that its overexpression in human melanoma cell lines was shown to suppress ^{473}Ser-AKT levels and proliferation in mouse xenografts (Ye, Jin et al. 2013), transgenic mice with systemic deletion of *Pipp* were generated to progress our understanding of its function in breast carcinogenesis in a physiologically isolated setting. *Pipp*$^{-/-}$ mice were viable with no hyperplasia or other abnormalities observed during mammary gland development, emphasizing a dispensable role of PIPP in normal breast homeostasis (Ooms, Binge et al. 2015). However, deletion of *Pipp* in mice expressing the oncogene polyoma middle T (PyMT) had a significant impact on tumour initiation and progression, showing enhanced hyperplasia and faster tumour growth. Studies in the MDA-MB-231 cell line and cell lines developed from transgenic mice, showed loss of *PIPP* increased plasma membrane recruitment of a PI(3,4,5)P_3-specific reporter (based on the BTK-PH domain) and decreased recruitment of a PI(3,4)P_2-specific reporter (based on the PH domain of TAPP1). Surprisingly, *Pipp* deletion delayed metastasis formation in mice, while in MDA-MB-231 cells, PIPP-KD caused an AKT1-driven loss of directional migration with an apparent increase in cell proliferation and survival. Further experiments linked the increased AKT1 activity with downregulation of NFAT1 and TSC2 – two transcription factors involved in pro-invasive processes. Thus, PIPP deregulation in the breast cancer may activate a dual role of AKT1, possibly through activation of a different group of downstream effectors, i.e. the ones that promote tumour proliferation and growth and others that restrict its invasive potential.

Although SHIP1/2 regulate PI(3,4,5)P_3 cellular levels and SHIP2 is a ubiquitous 5-phosphatase, ablation of these proteins in mouse models did not lead to cancer development. In the case of *Ship1*$^{-/-}$ mice, an explanation may be their early lethality (Helgason, Damen et al. 1998). Another factor may be the domain architecture of 5-phosphatase members, which outside of the conserved phosphatase domain is quite divergent and determines non-catalytic functions of these proteins. The C-terminal SKITCH domain of PIPP is thought to facilitate its constitutive plasma membrane localisation in resting and stimulated cells, which potentially affects its substrate availability (Gurung, Tan et al. 2003). SHIP1/2, on the other hand, are predominantly cytosolic and upon stimulation become recruited by the interaction with ITIM motifs and other adaptor proteins, suggesting a more complex regulation, possibly depending on the type and strength of stimulus. Finally, it is possible that the level of redundancy

between ten members of the 5-phosphatase family is an evolutionarily-developed buffer, that allows efficient control over PI(3,4,5)P_3 levels even in the absence of several 5-phosphatases.

1.4 Physiological roles of PI(3,4)P_2 in PI3K-regulated signalling

The classical and best established role of PI(3,4)P_2 is its ability to co-regulate the activity of AKT downstream of class I PI3K in response to wide variety of cellular stimuli. PI(3,4,5)P_3 and PI(3,4)P_2 are produced at the plasma membrane as an outcome of this primary signalling event and engage in intermolecular interactions with the PH domain of AKT and its kinase, PDK1. This, and subsequent phosphorylation by mTORC2, are the well-defined steps necessary to fully activate AKT's kinase capacity. Once activated, AKT executes its function by phosphorylation of cytosolic or nuclear target proteins (Li and Marshall 2015). Thus, the phosphorylation level of the two sites, ^{308}Thr & ^{473}Ser, has become one of the most robust readouts of the PI3K/AKT status in the cell and has been routinely used to study physiological events and pathophysiological transformations that occur in biological systems.

A contradictory argument exists, that advocates for the ability of PI(3,4)P_2 to control the extent of ^{473}Ser phosphorylation by mTORC2, while giving PI(3,4,5)P_3 the primary role in promoting ^{308}Thr phosphorylation by PDK1. Human B cell line (BJAB) expressing membrane-bound, constitutively active SHIP1, when stimulated with antibodies, showed a significant decrease in PI(3,4,5)P_3 levels and ^{308}Thr phosphorylation and a surprising lack of effect on ^{473}Ser phosphorylation or PI(3,4)P_2 (Ma, Cheung et al. 2008). In another study, bone marrow-derived *Ship1*$^{-/-}$ mast cells were pre-treated with LY294002, followed by exogenous addition of synthetic PI(3,4)P_2 and stimulation with stem cell factor (Scheid, Huber et al. 2002). This resulted in apparent increase in ^{473}Ser phosphorylation and no change in ^{308}Thr phosphorylation. On the other hand, a different set of studies suggested a non-discernible role for PI(3,4)P_2 in affecting the levels of relative ^{308}Thr/^{473}Ser phosphorylation. INPP4B, when overexpressed in MDA-MB-231 cells caused a simultaneous reduction in EGF-stimulated ^{308}Thr- and ^{473}Ser-AKT phosphorylation levels and when depleted in LNCaP cells caused the opposite effect (Fedele, Ooms et al. 2010, Hodgson, Shao et al. 2011). A similar lack of specificity was observed when 5-phosphatase PIPP knock down in MDA-MB-231 cells led to elevated levels of phospho-^{308}Thr and phospho-^{473}Ser AKT (Ooms, Binge et al. 2015). Thus, the data obtained from breast and prostate cell lines is in accordance with the early *in vitro* assays, where the affinity of a series of synthetic phosphatidylinositol lipids and inositol phosphates was tested against purified AKT or its PH domain, clearly demonstrating the

highest and comparable affinity towards PI(3,4,5)P_3 and PI(3,4)P_2 (Franke, Kaplan et al. 1997, Frech, Andjelkovic et al. 1997). Finally, PDK1 is thought to bind PI(3,4,5)P_3 and PI(3,4)P_2 with comparable affinity to AKT but only PI(3,4,5)P_3 was tested for its ability to regulate mTORC2 kinase activity *in vitro* (Stokoe, Stephens et al. 1997, Gan, Wang et al. 2011).

1.4.1 The role of TAPP1/2 in class I PI3K signalling

The array of phosphatidylinositol lipids generated in the cell by cooperative action of PI3K and lipid phosphatases creates regions on cellular membranes with unique composition and discrete functions. PI(3,4,5)P_3 and PI(3,4)P_2 transduce the extracellular signal by binding effector proteins with specialised PH or PX domains. Some of the 'binders' are sufficiently selective that they are thought to bind only one phosphatidylinositol *in vivo* (e.g. GRP1 and BTK bind only PI(3,4,5)P_3), while some, like AKT and PDK1, show less specificity and have been suggested to bind both PI(3,4,5)P_3 and PI(3,4)P_2. Tandem PH-domain containing protein 1/2 (TAPP1/2) contains two PH domains, one of which possesses a thus far uniquely defined binding specificity for PI(3,4)P_2 (Dowler, Currie et al. 2000). The architecture of the TAPP1 binding pocket is common with other PH domains and the PI(3,4)P_2 specificity is assured by ^{203}Ala that spatially restricts the 5-phosphate of PI(3,4,5)P_3 (Thomas, Dowler et al. 2001). The *in vitro* specificity was further validated in various experiments, where cells expressing fluorescently-tagged TAPP-PH showed fluorescent patterns aligning with the expected changes in PI(3,4)P_2 levels. As a result, TAPP1-PH has become an accepted and widely used construct to detect cellular levels of PI(3,4)P_2 . The physiological role of TAPP was studied by the generation of mice expressing TAPP1/2 mutants, unable to bind PI(3,4)P_2 (Landego, Jayachandran et al. 2012). B cells extracted from these animals showed elevated levels of phosphorylated AKT and enhanced proliferation. This suggests that activated TAPP provides a silencing role in B cell receptor signalling and the possible mechanism may be through competing with AKT for the limited PI(3,4)P_2 produced as a result of class I PI3K activation. A scaffolding role for TAPPs has also been implied through binding to proteins such as syntrophin, MUPP1 or PTPL1, thus providing access to target proteins in the vicinity of PI(3,4)P_2 rich membranes, with some proposed to generate a PI3K/AKT negative feedback loop (Li and Marshall 2015).

1.4.2 $PI(3,4)P_2$ at the centre of cell migration and invasion

The cellular cytoskeleton is formed of a dense meshwork of actin filaments and microtubules that fill the cytoplasm, provide the cell with shape and rigidity, and serve as a machinery for cellular movement. Proteins involved in the cytoskeleton play diverse roles, e.g. fascin links linear actin filaments into bundles, motor proteins that control muscle contraction and chromosome segregation or integrin receptors that provide and initiate a link with the cellular membrane. Within the cytoskeleton, dynamic actin polymerisation/depolymerisation is regulated by specialised protein complexes that, in response to a constantly changing environment, promote formation of structures such as lamellipodia, focal adhesions, ruffles or podosomes at defined places inside the cell. Therefore, the actin cytoskeleton is essential in supporting physiological processes such as immune cell chemotaxis to the site of infection, cell polarity during embryonic development or vesicle formation in endocytosis. In cancer cells, dynamic structures specialised in enzymatic degradation of extracellular matrix (ECM) have been observed, that equip transformed cells with the invasive apparatus which defines their metastatic phenotype.

1.4.2.1 The role of invadopodia in transformed cells

Invadosomes were first observed as rosettes forming on the ventral membranes in Src-transformed embryonic fibroblasts (David-Pfeuty and Singer 1980). Later, podosomes and invadopodia were defined as actin-rich membrane protrusions that, by localised release of specialised proteases, are able to degrade the ECM and drive the process of cellular invasion (Chen 1989). Despite a large degree of structural and functional similarity, invadopodia rely on unique proteins (e.g. TKS5), are long-lived and can penetrate much deeper into the ECM, which classically associates them with a characteristic of metastatic cancer cells (Revach and Geiger 2013).

The mechanism of invasion is governed by the coordinated assembly of protein complexes into three functional domains, i.e. proteolytic, adhesive and invasive. ECM *degradation potential* is controlled by the recruitment of cytosolic and membrane-bound matrix metalloproteinases (MMPs), which along with other proteases hydrolyse the components of ECM. Although the regulatory mechanisms of MMPs' localisation are not fully understood, the use of specific inhibitors or siRNA-mediated downregulation have

demonstrated a reduction in invadopodium-mediated matrix degradation (Revach and Geiger 2013). Furthermore, multiple clinical studies have reported on elevated plasma and tissue levels of MMPs in cancer patients, but whether this can become a reliable biomarker is still under debate. Real-time observations of invadopodia dynamics confirmed that an *adhesion ring* forms around the actin core that assists in invadosome initial assembly but is probably less stable compared to that forming in the more stationery podosomes. Integrin receptors, apart from their established role as mechano-sensory likers between the ECM and cell interior, are thought to engage in interactions with metalloproteinases and enhance their proteolytic activity (Branch, Hoshino et al. 2012). Moreover, breast epithelial cell treatment with transforming growth factor β (TGFβ), induces invadopodia formation through upregulation of adaptor protein and focal adhesion marker HIC5 (Pignatelli, Tumbarello et al. 2012).

The nanomechanical force created by continuous actin polymerisation at the tip of a growing invadopodium is responsible for gradual *invasion* into proteolytically-degraded matrix. Although proteins that mark invadopodia were among the first elements that contributed to its discovery, signalling pathways that initiate the process and the sequence of events that lead to a mature invadopodium have only recently been studied in more detail. External stimuli like growth factors or serum were known to promote invadopodia formation but the intellectual link to class I PI3K came from the clinical studies on breast carcinoma patients that correlated mutations in *PI3KCA* with metastatic phenotype (Saal, Holm et al. 2005). The intrinsic ability of MDA-MB-231 breast cancer cells to form invadopodia was abolished within 1 min post treatment with PI3K inhibitors - LY294002 or wortmannin (Yamaguchi, Yoshida et al. 2011). Further, sequential suppression of PI3K isoforms, use of isoform-selective inhibitors and assessment of phospho-AKT levels, confirmed a decisive role of p110α in the process. Finally, generation of MDA-MB-231 mutants with alterations in two hotspots of p110α, E545K or H1047R, lead to enhanced matrigel invasion and was functionally linked to PDK1 and AKT activity.

TKS5 was first described as a protein whose PX domain is necessary for translocation from the cytosol to invadopodia in Src-treated fibroblasts, possibly via interaction with $PI(3,4)P_2$ (Abram, Seals et al. 2003). The fact that localisation of ADAM family proteases relied on interaction with TKS5's SH3 domains further implied its role in invadopodium function and/or creation. Later, TKS5 knock down in Src-fibroblasts

abolished invadopodia formation, which contrasted with the 'invadopodia-positive' phenotype induced by microinjection of active Src and TKS5 into nontransformed cells (Seals, Azucena et al. 2005). Elevated TKS5 levels were shown in the invasive MDA-MB-231 cell line (compared to Mcf7 control) and the protein positively stained paraffin sections from skin and breast cancer patients. This suggested that TKS5 functions through clustering and/or activation of proteins critical for invadopodium formation. The use of high-resolution microscopy techniques was thus pivotal in following the order and kinetics of molecular interactions that underlay invadopodium initiation and maturation. Spatio-temporal tracking of proteins at nascent invadopodia of rat mammary MTLn3 cells revealed ~20 sec delay in the arrival of TKS5 compared to other essential components like cortactin, N-WASP or actin (Sharma, Eddy et al. 2013). Upon TKS5 depletion, a severe defect in invadopodia stability was observed, with 50% of structures surviving less than 10 min. More importantly, expression of a TKS5-PX mutant unable to bind $PI(3,4)P_2$ showed a substantial drop in the number of long-lived invadopodia and a similar effect was observed when $PI(3,4)P_2$ was sequestered by overexpressed TAPP1. The use of $PI(3,4)P_2$- and $PI(3,4,5)P_3$-specific reporters showed enrichment of these lipids at the invadopodium core and adhesion ring, respectively. Finally, SHIP2's appearance coincided with the spatial enrichment in $PI(3,4)P_2$ and SHIP2 suppression phenocopied depletion of TKS5.

The process of cancer cell extravasation through capillaries, combined with high-resolution intravital imaging, were used as tools to investigate the role of invadopodia in an *in vivo* model (Leong, Robertson et al. 2014). Protrusions projecting through the endothelial layer were observed from the early stages of extravasation and disruption of any of the essential components, such as cortactin or TKS5, resulted in the inhibition of primary metastases formation. Thus, direct evidence was provided for the functional significance of invadopodia and its protein components to drive metastasis in a physiological context. Overall, the results emphasize the importance of class I PI3K signalling in the dynamic process of invasion with the specific role of p110α, which may be explained by its preferential activation downstream of RTKs. Although p110α activating mutations alone are insufficient to promote invadopodia in non-transformed cells, PI3K/AKT provides the substrates and processes necessary to maintain the invasive phenotype in the cancer cells.

1.4.2.2 The role of class II PI3K in clathrin mediated endocytosis

Endocytosis, in its classical understanding, describes the processes that involve complete internalisation of a section of plasma membrane together with extracellular liquid and cargo of different size and physico-chemical properties. The physiological processes that rely on some form of endocytosis are numerous and encompass continuous probing of the environment by pinocytosis, phagocytic engulfment of apoptotic cells or recycling of ligand-bound receptors by clathrin-mediated endocytosis (CME). Thus, some of the processes are nonspecific and permanent, while some become initiated by the external cues that switch on relevant biochemical pathways.

The structural intermediates that form during CME are initiated by the assembly and growth of a clathrin coated pit (CCP), surrounded by the polymerising clathrin cage and a selection of adaptor and accessory proteins that assist the process, e.g. SNX9 that supports the increasing membrane curvature via its BAR domain (Doherty and McMahon 2009). Next, a clathrin coated vesicle (CCV) forms from the mature CCP by dynamin-mediated scission and subsequent clathrin dissociation releases the endocytic vesicle into the cytosol. Coordinated with this process, is the gradual change in phosphatidylinositol lipid composition taking place at the inner leaflet of nucleating CCP en route to fusing with an early endosome. Several lipid kinases and phosphatases have been implied in controlling these transformations, and a role for PI(3,4)P_2 and class II PI3K has emerged from recent studies in Cos7 cells (Posor, Eichhorn-Gruenig et al. 2013). Until recently, PI(4,5)P_2 has been reported to form from the PI4P-rich membranes of nucleating CCP due to the catalytic activity of phosphatidylinositol phosphate 5-kinase (PIP 5-kinase). Mature endosomes, on the other hand, are particularly enriched in PI3P. However, no link had been established that would lead to formation of PI3P from a plasma membrane originally rich in PI4P and PI(4,5)P_2. A combinatorial use of anti-PI(3,4)P_2 antibody and a PI(3,4)P_2-specific TAPP1(PH)-RFP reporter enabled accurate and reliable localization of this phosphatidylinositol during the process of endosome formation and maturation. Further, overexpression of the 4-phosphatase INPP4B slowed CCP formation. PI(3,4)P_2 has thus been assigned an intermediary role in CME - between that of PI(4,5)P_2 and PI3P. Surprisingly, PI3K-C2α-depleted Cos7 cells and MEFs derived from *PI3K-C2α*$^{-/-}$ mice showed elevated transferrin levels at the plasma membrane due to impaired endocytosis. Further studies proposed SNX9 as PI(3,4)P_2 effector in CCPs and associated the defect with dynamin 2

arrest prior to CCP scission due to lack of accumulated SNX9. Thus, it has been determined that the pool of $PI(3,4)P_2$ comes from the activity of the class II isoform C2α and not, as might be expected, that of class I PI3K. Overall, this suggests that during CME PI4P is converted to $PI(3,4)P_2$, which is then dephosphorylated to PI3P.

1.4.2.3 FEME - a fast track to receptor internalisation

Recently, a novel endocytic pathway has been associated with fast GPCR and RTK recycling at the edge of protruding cells (Boucrot, Ferreira et al. 2015). Surprisingly, fast endophilin-mediated endocytosis (FEME) turns out to be independent of the classical components such as clathrin or AP2 but instead relies on endophilin. The endophilin-rich tubular structures were observed at the leading edge of the cell together with dynamin and F-actin, and were unaffected by siRNA suppression of AP2 or clathrin. Next, the effect of growth factor stimulation was tested in various mammalian cell lines. The number of endophilin-positive structures increased with increasing EGF concentration, suggesting that only activated receptors can be recognised as potential FEME cargo. Moreover, FEME vesicles formed within seconds of growth factor stimulation and were of comparable size (<1 μm) to CCVs. The observation that class I PI3K inhibition abrogated endophilin-rich vesicles combined with their characteristic localisation at the lamellipodia, led to the hypothesis that FEME may be controlled by the lipid second messenger $PI(3,4,5)P_3$. Subsequent inhibition of SHIP1/2 or INPP4A/B had a more profound effect compared to PTEN inhibition and thus pointed towards $PI(3,4)P_2$ as the phosphatidylinositol lipid involved in FEME. Finally, lamellipodin was suggested to be the direct $PI(3,4)P_2$ effector, which binds endophilin and allows FEME vesicle maturation and scission by dynamin. Collectively, two parallel endocytic processes seem to exist in the cell that are spatially separated, recycle different types of cargo and rely on different endocytic proteins and yet share a common regulator $PI(3,4)P_2$ which is synthesised by two different families of PI3K.

1.5 Aims

The role of $PI(3,4)P_2$ within the class I PI3K signalling pathway is currently enigmatic. Some studies point to a specific signalling role, whilst others suggest its formation simply represents an alternative pathway for $PI(3,4,5)P_3$ removal. There is no clear evidence for effectors with both selectivity for $PI(3,4)P_2$ and a clear physiological role. There are also no quantitative studies describing the relative flux through 5- versus 3-dephosphorylation of $PI(3,4,5)P_3$, nor any clear understanding of the relative contributions of individual enzymes to the control of $PI(3,4)P_2$ levels.

A major problem in moving this field forward is the difficulty in accurately measuring $PI(3,4)P_2$ in cells and tissues. The initial aim of my thesis was to develop a reliable method for quantifying $PI(3,4)P_2$ in biological samples and then, if successful, to apply this method to understand the relative contribution of PTEN, INPP4A and B, and various 5-phosphatases, to the formation of $PI(3,4)P_2$ during growth factor stimulation of class I PI3K.

Chapter 2 Materials and methods

2.1 Materials

2.1.1 Key resources

REAGENT or RESOURCE	SOURCE	IDENTIFIER
ANTIBODIES		
anti-phospho-Akt-S473	Cell Signaling	D9E, 4060
anti-phospho-Akt-T308	Cell Signaling	5106
anti-β-COP	Babraham Institute	Nick Ktistakis, BI
anti-βactin	Abcam	Ab6276
anti-INPP4A	Santa Cruz	Sc-12314
anti-INPP4B	Santa Cruz	Sc-12318
anti-SHIP1	Cell Signaling	2728
anti-PTEN	Cell Signaling	9188
anti-EGFR	Cell Signaling	4267
anti-phospho-EGFR	Cell Signaling	3777
Anti-Cortactin	Abcam	Ab33333
Biotinylated anti-PI(3,4)P_2	Echelon Biosciences	z-B034b
Alexa Fluor 568 goat anti Mouse	Life Technologies	A11004
Alexa Fluor 568 goat anti Rabbit	Life Technologies	A11036
Alexa Fluor 647 goat anti Mouse	Life Technologies	A21235
Alexa Fluor 647 goat anti Rabbit	Life Technologies	A21244
Steptavidin-Alexa 647	Life Technologies	S32357
IRdye 680 goat anti Rabbit IgG	Licor	926-68071
IRdye 800 goat anti Mouse IgG	Licor	926-32210
Goat anti-Mouse antibody HRP	BioRad	170-6516
Goat anti-Rabbit antibody HRP	BioRad	170-6515
anti-SHIP2	Cell Signaling	2730
BIOLOGICAL SAMPLES		
Human Platelets	Dr Ingeborg Hers	University of Bristol

CHEMICALS, PEPTIDES AND RECOMBINANT PROTEINS		
TMS-diazomethane	Sigma-Aldrich	362832
Fatty acid free BSA	Sigma-Aldrich	A7906
Dulbecco's phosphate buffered saline	Sigma-Aldrich	D8537
Human insulin	Sigma-Aldrich	I9278
Human EGF	Sigma-Aldirch	E9644
Hydrocortisone	Sigma-Aldrich	H0888
PBS 10x	Life Technologies	70011-036
DMEM/F12	Life Technologies	31330-038
RPMI-1640	Sigma-Aldrich	R8758
Insulin-Transferrin-Selenium	ThermoFischer	41400045
Dihydrotestosterone	Sigma-Aldrich	D-073-1ML
Fetal Bovine Serum	ThermoFischer	10270106
Distilled water	Life Technologies	15230-089
rhTGF-β1	R&D systems	240-B
Gelatin from pig skin- Oregon Green 488	Fisher Scientific	11594856
[33]P-γATP	Perkin Elmer	NEG602H250UC
TGX115	Abcam	142078
PI-103	Cayman Chemicals	10009209
PIK75	Axon MedChem	1334
BYL719	Biochem Inhibitor	A-1214
1-heptadecanoyl-2-hexadecanoyl-sn-glycero-3-(phosphoinositol 3,4,5-trisphosphate) (C17:0/C16:0-PI(3,4,5)P_3)	Biological Chemistry Department, Babraham Institute	
C17:0/C16:0-PI	Biological Chemistry Department, Babraham Institute	
D6- C18:0/C20:4-PI(3)P	Biological Chemistry Department, Babraham Institute	
D6-C18:0/C20:4-PI(4)P	Biological Chemistry Department, Babraham Institute	
D6-C18:0/C20:4-PI(3,4)P_2	Biological Chemistry Department, Babraham Institute	
D6-C18:0/C20:4- PI(4,5)P_2	Biological Chemistry Department, Babraham Institute	

D6-C18:0/C20:4-PI(3,4,5)P_3	Biological Chemistry Department, Babraham Institute	
C18:0/C20:4-PI(3,4)P_2	Biological Chemistry Department, Babraham Institute	
C18:0/C20:4 PI(3,5)P_2	Biological Chemistry Department, Babraham Institute	
C18:0/C20:4 PI(4,5)P_2	Biological Chemistry Department, Babraham Institute	
C18:0/C20:4 PI(3,4,5)P_3	Biological Chemistry Department, Babraham Institute	
C17:0/C20:4-PI	Avanti Polar Lipids	LM-1502
Horse serum	PAA	B15-021
penicillin/streptomycin	Life Technologies	15140-122
CS-FBS	Life Technologies	12676-029
cholera toxin	Sigma-Aldrich	C8052
DharamaFECT1	GE Dharmacon	T-2001-04
Optimem	Life Technologies	31985-047
lipofectamine 2000	Invitrogen	11668-019
Polybrene used at 4ug/ml	Sigma-Aldrich	TR-1003-G
Tris	Melford	B2005
NaCl	VWR Chemicals	27810.295
EDTA	Sigma-Aldrich	E5134
EGTA	Sigma-Aldrich	E4378
Triton	Sigma-Aldrich	T9284
Anti-protease leupeptin	Sigma-Aldrich	L8511
Anti-protease Aprotinin	Sigma-Aldrich	A1153
Anti-protease antipain	Sigma-Aldrich	A6191
Anti-protease pepstatin	Sigma-Aldrich	P5318
PMSF	Sigma-Aldrich	78830
$Na_4P_2O_7$	Sigma-Aldrich	P8010
β- glycerolphosphate	Calbiochem	35675
Na_3VO_4	Sigma-Aldrich	S6508

NaF	Sigma-Aldrich	S7920
PVDF membranes (immobilon P)	Millipore	IPVH00010
DTT	Melford	MB1015
Tris-HCl	Sigma-Aldrich	T3253
Glycerol	Invitrogen	15514-011
Bromophenol Blue	Sigma-Aldrich	B8026
Methanol	Romil	H410
Chloroform	Romil	H140
Acetone	VWR chemicals	20066.330
Dimethyl sulphide	Sigma-Aldrich	34869
Formic acid	Fisher Scientific	F/1900/PB08
Acetonitrile	Romil	M050
Hepes	Sigma-Aldrich	H3375
$MgCl_2$	VWR Chemicals	25108.295
Protease inhibitor cocktail	Roche	11836170001
Bovine Serum Albumin	Sigma-Aldrich	A7906
KCl	VWR Chemicals	26764.260
Trichloroacetic acid 6.1N	Sigma-Aldrich	T0699
Embedding medium	Thermo Scientific	1310
Mayer's hematoxylin solution	Sigma Aldrich	SLBP6175V
Eosin Y solution	Sigma-Aldrich	SLBP1949V
Critical Commercial Assays		
AMAXA nucleofection system	Lonza	Kit T
Lasky ozone generator	AirTree Ozon technology	C-L010-DT
Experimental Models: Cell Lines		
$PTEN^{-/-}$ and Parental Mcf10a	Horizon Discovery	HD101-006
Experimental Models: Organisms/Strains		
PB-Cre4 mice	JAX ®	Strain 026662
$PTEN^{loxP/loxP}$ mice	JAX ®	Strain 004597
'WT' ($PTEN^{loxP/loxP}$, $PbCre^{-/-}$) mice	Signalling Programme, Babraham Institutte	
'PTEN-KO' ($PTEN^{loxP/loxP}$, $PbCre^{+/-}$) mice	Signalling Programme, Babraham Institutte	
$INPP4B^{-/-}$ mice	(Kofuji, Kimura et al. 2015)	
BPH-1	DSMZ	ACC143
DU-145	Dr Scholes	ex Tenovus Institute

PC3	ATCC	CRL 1435
LNCaP95	Dr Meeker	John Hopkins University
LNCaP	ATCC	CRL 1740
Oligonucleotides		
INPP4B knockout sgRNA	designed by https://chopchop.rc.fas.harvard.edu	5'-GATCTCCGTAATCCACCCCG-3'
SHIP2 knockout sgRNA	designed by https://chopchop.rc.fas.harvard.edu	5'-GTGCAGGCCTTTGAGGTACA-3'
Recombinant DNA		
pSpCas9(BB)-2A-GFP	Addgene	48138
Software		
FIJI	NIH	
Imaris	Bitplane	
AxioVision 4	Zeiss	
Velocity	Perkinelmer	
Adobe Photoshop		
Image Studio 2.1	LI-COR	
Aida	Raytest	
Prism	Graph Pad	

2.1.2 Mice

PB-Cre4 mice (Trotman, Niki et al. 2003) and $PTEN^{loxP/loxP}$ mice (Wang, Gao et al. 2003) have been described previously. PbCre4 mice and $PTEN^{loxP/loxP}$ mice were interbred to generate 'WT' ($PTEN^{loxP/loxP}$, $PbCre^{-/-}$) and 'PTEN-KO' ($PTEN^{loxP/loxP}$, $PbCre^{+/-}$) mice and backcrossed to the C57BL/6J strain for at least 4 generations; these mice were housed in the Biological Support Unit at The Babraham Institute. $INPP4B^{-/-}$ mice have been described previously (Kofuji, Kimura et al. 2015) and were interbred with PTEN-KO mice to generate 'PTEN-INPP4B-KO' ($PTEN^{loxP/loxP}$, $PbCre^{+/-}$, $INPP4B^{-/-}$) mice; these mice were housed in the Akita University Animal House. Prostates from several naïve male mice of identical genotype from the same litter were analysed and multiple independent experiments were carried out, using several biological replicates specified

in the legends to figures. The animals were kept under specific-pathogen-free conditions and the animal facilities where the mice were kept were regularly checked for standard pathogens. All animal experiments at The Babraham Insitute were reviewed and approved by The Animal Welfare and Ethics Review Body and performed under Home Office Project license PPL 70/8100. Animal experiments in Akita were reviewed and approved by the Akita University Institutional Committee for Animal Studies, Akita University.

2.1.3 Cell lines

Mcf10a cells are non-transformed human female breast epithelial cells. PTEN$^{-/-}$ Mcf10a cell lines were generated by targeted homologous recombination and were obtained from Horizon Discovery Ltd together with their parental cell lines. All Mcf10a cell lines were maintained at 37°C with 5% CO_2 in DMEM/F12 supplemented with 5% horse serum, 10 ng/ml EGF, 10 μg/ml insulin, 0.1 μg/ml cholera toxin, 0.5 μg/ml hydrocortisone, 1% w/v penicillin/streptomycin (complete medium). Starvation medium consisted of DMEM/F12 supplemented with 1% charcoal/dextran treated foetal bovine serum, 0.1 μg/ml cholera toxin, 0.5 μg/ml hydrocortisone, 1% penicillin/streptomycin.

Human prostate cancer cells (DU-145, BPH-1, LNCaP, LNCaP 95 and PC-3) were obtained from the AstraZeneca cell bank and had been previously authenticated using DNA fingerprinting short tandem repeat assays. All revived cells were used within 10 passages and cultured at 37°C with 5% CO_2 for less than 2 months. Benign prostatic hyperplasia epithelial cell line BPH-1 was cultured in RPMI-1640 supplemented with 20% FBS, 10 μg/ml insulin, 6.7 ng/ml sodium selenite, 5.5 μg/ml transferrin, 0.5 nM dihydrotestosterone and 1% w/v penicillin/streptomycin. The remaining prostate and breast cancer cell lines were grown in RPMI-1640 with 10% FBS and 1% w/v penicillin/streptomycin.

2.1.4 Human platelets

Venous blood was obtained from a healthy female human volunteer with the approval of the local research ethics committee at the University of Bristol, UK. The

donor provided written informed consent, and reported as not having taken medication in the 14 days prior to donation. Blood was drawn into 4% trisodium citrate (1:9, v/v), and acidified with acidic citrate dextrose (1:7, v/v; 120 mM sodium citrate, 110 mM glucose, 80 mM citric acid). Platelet-rich plasma (PRP) was obtained by centrifugation of the blood at 180xg for 17 minutes at room temperature. Platelets were subsequently pelleted by centrifugation of the PRP at 650 x g for 10 minutes at room temperature in the presence of 10 μM indomethacin and 0.02 U / mL apyrase (grade VII). Platelets were resuspended at 4 x 10^8 / mL in HEPES–Tyrode buffer (145 mM NaCl, 3 mM KCl, 0.5 mM Na_2HPO_4, 1 mM $MgS0_4x7H_2O$, 10 mM HEPES, pH 7.2) supplemented with 0.1% [w/v] D-glucose, 10 μM indomethacin and 0.02 U/mL apyrase, and allowed to rest at 30 °C for 30 minutes prior to experimentation.

2.2 Methods

2.2.1 Preparation of platelets for PI(3,4)P_2 measurement

1 x 10^8 platelets were preincubated with DMSO or 100 nM wortmannin for 10 minutes, before treatment with HEPES–Tyrode buffer or 0.5 U / ml thrombin for 3 minutes under stirring at 1200 r.p.m using a Chronolog 490-4D aggregometer at 37°C (Labmedics, Abingdon-on-Thames, UK). Treatment was stopped by the addition of 750 µl ice-cold 1 M HCl and samples were centrifuged at 12000 x g for 10 minutes at 4°C. Resulting pellets were frozen until lipid extraction.

2.2.2 siRNA suppression

1.6×10^5 cells were seeded per 35 mm dish, and were subject to reverse transfection (using transfection agent DharamaFECT1) with a pool of 4 different siRNA (40 nM per target; ON-Target-plus pooled siRNA.) in Optimem and 10% complete medium, according to manufacturer's instructions. Media was changed after 16 hr and replaced with complete medium for 32 hr, after which cells were washed with dPBS and maintained in starvation media for 16 hr. Cells were stimulated with 10 ng/ml of EGF for the indicated times. Where indicated, cells were pre-incubated with inhibitors for 20 min prior to EGF stimulation. Stimulations were terminated by aspiration of media and washing with ice-cold PBS, prior to processing of the cells for lipid or Western-Blot analysis as described below.

2.2.3 Gene editing of Mcf10a cell lines using CRISPR/Cas9

sgRNAs were designed using https://chopchop.rc.fas.harvard.edu/ or http://crispr.mit.edu/ and cloned into all-in-one pSpCas9(BB)-2A-GFP plasmid as described previously (Ran, Hsu et al. 2013). To generate an INPP4B knockout, sgRNA 5'-GATCTCCGTAATCCACCCCG-3' targeting exon 7 was used. SHIP2 knockout was generated using sgRNA 5'-GTGCAGGCCTTTGAGGTACA-3' directed against exon 8. Mcf10a cells were transfected with 4 µg DNA using the AMAXA nucleofection system. After 24-48 hr, GFP positive cells were FACS sorted and seeded at the density of up to 1

cell per well in a 96 well plate using a conditioned medium (1:1 mix of fresh Mcf10a medium and conditioned medium harvested after 3 days in culture with Mcf10a cells and 0.45 µm filtered). Single clones were picked after 7 days, expanded and analysed for loss of protein by Western blot using anti-INPP4B and anti-SHIP2 antibodies.

2.2.4 Western-Blot

Mcf10a: Cells were scraped and lysed in 150 µl of ice-cold lysis buffer (20 mM Tris, pH 7.5; 150 mM NaCl; 1 mM EDTA, pH 7.5; 1 mM EGTA, pH 7.5; 0.1% v/v Triton-X100 supplemented with anti-proteases: 10 µg/ml leupeptine, 10 µg/ml aprotinin, 10 µg/ml antipain, 10 µg/ml pepstatin A, 0.1 mM PMSF and anti-phosphatases: 2.5 mM $Na_4P_2O_7$, 5 mM β- glycerolphosphate, 1 mM Na_3VO_4, 25 mM NaF). After 30 min solubilisation at 4°C with agitation, lysates were centrifuged (15,000 x g, 10 min, 4°C) and the supernatants collected and diluted in SDS-PAGE sample buffer. Proteins (45 µg/well, or 15 µg/well, where indicated) were resolved on a SDS-PAGE gel, transferred to PVDF membranes and blotted with the indicated primary antibodies at 4°C overnight. They were then washed in TBS (40 mM Tris/HCl, pH 8.0, 22°C; 0.14 M, NaCl) containing 0.1% v/v Tween 20 and incubated with a mix of Infrared Dye coupled secondary antibodies. The membranes were imaged with the Li-Cor Odyssey Infrared Imaging System using the 700 nm and 800 nm channels. Signals were quantified using the Image Studio software. Alternatively, membranes were washed and incubated with HRP-conjugated secondary antibodies and signals detected using the ECL detection system. Signals from the HRP-incubated membranes were quantified using the Aida software. Irrespective of technique used, the amount of protein loaded, antibody dilution as well as exposure times were selected to provide a linear detection range. During quantitation, signal intensity of individual bands was corrected for variations in the local background followed by a normalisation step with respect to selected housekeeping proteins.

Mouse tissues: Tissues were pulverized under a continuous flow of $N_{2(l)}$. 1x reducing SDS sample buffer (0.4 M DTT, 160 mM Tris-HCl pH 6.7, 50% glycerol, 0.012% Bromophenol Blue) was pre-warmed to 70°C and 750 µl of sample buffer was added per 50 mg tissue to yield an approximate final protein concentration of 4 mg/ml. Lysates were homogenized by vortexing for 15 sec followed by a sequential syringe step through a 21G needle (3x), followed by a 23G needle (3x). Proteins were denatured by boiling at

95°C for 5 min. Lysates were cleared by centrifugation for 5 min at 20,238 x g, after which the syringe and centrifugation steps were repeated. Proteins were resolved by SDS-PAGE (20 µg estimated total protein per lane) and immunoblotted for the indicated antibodies.

2.2.5 Lipid extraction

750,000 Mcf10a cells grown on a 35 mm dish were killed in 750 µl ice-cold 1M HCL, then scraped and collected into an Eppendorf tube. Each sample was then split into three separate 2 ml polypropylene Eppendorf tubes; 250 µl for PI, PIP, PIP2, PIP3 measurement, 250 µl for PI(3,4)P_2/PI(4,5)P_2 measurement, and the remaining cells were kept for analysis by Western-Blot. Cells were pelleted in a microfuge (15,000 x g, 10 min at 4°C), the supernatant removed and cell pellets either processed immediately or snap-frozen in liquid nitrogen and stored at -80°C for up to two weeks.

For human prostate cancer cell lines, 250,000 cells were seeded into 35 mm dishes and grown in the medium optimal for each cell line for 32h. Cells were then starved for 16h by replacing the medium with starvation medium – a phenol red-free RPMI 1640 supplemented with 2mM glutamax. Following stimulation and / or inhibition with appropriate reagents, medium was removed by aspiration and cells killed with 750 µl ice-cold 1M HCL. Cells were then scraped, collected into Eppendorf tubes, pelleted and snap-frozen, as described above.

920 µl of a solvent mixture containing 2:1:0.79 (v/v) MeOH:$CHCl_3$:$H_2O_{(acidic\ pH)}$ was added to the cell pellets and the mixture vortexed thoroughly for 10 sec. Relevant internal standards were then added:10 ng C17:0/C16:0-PI(3,4,5)P_3, 100 ng C17:0/C16:0-PI, 250 ng D6-C18:0/C20:4-PI(4,5)P_2 for routine analysis of PI, PIP, PIP_2 and PI(3,4,5)P_3; 50 ng C17:0/C20:4 PI, 50 ng D6-C18:0/C20:4-PI(3,4)P_2, 250 ng D6-C18:0/C20:4-PI(4,5)P_2 for routine analysis of PI, PI(3,4)P_2 and PI(4,5)P_2. Lipids were then extracted using an acidified Folch phase partition and derivatised with TMS-diazomethane (Clark, Anderson et al. 2011).

Molecules derived from PI, PIP, PIP2, and PIP3 were measured by HPLC-ESI MS/MS (Kielkowska, Niewczas et al. 2014). Response ratios were calculated for the endogenous species of these lipids divided by their relevant C17:0/C16:0 internal standard. We

routinely analysed 5 molecular species of these lipids but present here data for the C38:4 species only, to align with data presented for the C38:4 species of PI(3,4)P_2 and PI(4,5)P_2 (see below). The C38:4 species of PIP_2 and PIP_3 represent approx. 10-15% of the total species of these lipids in Mcf10a cells and all species behave very similarly upon stimulation with EGF (Anderson, Juvin et al. 2016). In some experiments, absolute amounts of C38:4 PI(3,4,5)P_3 were generated by reference to standard curves previously generated for this molecular species (Figure 4.1) (Kielkowska, Niewczas et al. 2014). Three technical replicates were routinely analysed for each experiment and, unless stated otherwise, data is presented as means ±SD of three biological replicates.

Molecules derived from PI, PI(3,4)P_2 and PI(4,5)P_2 were analysed by a new HPLC-ESI-MS/MS method, see below. Response ratios were calculated for the endogenous C38:4 species of these lipids divided by their relevant D6-labelled internal standard. In some experiments, absolute amounts of these lipids were generated by reference to standard curves (Figure 4.2). Three technical replicates were routinely analysed for each experiment and, unless stated otherwise, data is presented as means ±SD of three biological replicates.

2.2.6 Measurement of PI(3,4)P_2 and PI(4,5)P_2

Sample preparation: Lipids were extracted and derivatized with TMS-diazomethane; we added 2M TMS-diazomethane in hexane (50 µl) to lipid extracts prepared as described above (approx. 1 ml of 'lower phase'), to give a yellow solution, and then allowed the reaction to proceed for 10 min, RT. We quenched reactions with glacial acetic acid (6µl), which removed the sample's yellow colour (this reaction releases $N_{2(g)}$, thus care should be taken). We added post-derivatisation wash solution (700 µl) to the organic solution, and mixed the samples, which we then centrifuged (5000 rpm, 3 min), and collected the resultant lower phase. We repeated the wash step, and then added MeOH:H_2O (9:1 v:v, 100 µl) to the final collected lower phase. The samples were then dried down under a stream of nitrogen at room temperature without warming until dry. 160 µl methanol was then added and sonicated briefly, then left at RT for about 30 min prior to ozonolysis. A C-Lasky ozone generator was used in the following procedure. The unit was set to use air as the oxygen source at a flow rate of 4 dm^3/min and the flow was split after the ozone generator so that approximately 75 to 90% of the flow went to an

ozone destruction unit and the remaining fraction was used to bubble through the solution containing the samples. The power level on the ozone generator was set to about 60% of the maximum level. The ozonolysis procedure started by placing the glass sample vials containing the methylated lipid solutions in an aluminium block which was cooled in an acetone/dry ice bath to a temperature of about -70°C. Ozone was then bubbled through the solutions for 5 min. Dimethyl sulphide (2 µl) was then added to each sample and allowed to warm up to RT. Water (40 µl) was then added to each sample which was then ready to be submitted for analysis by UPLC, using the following conditions for $PI(3,4P)_2$/$PI(4,5P)_2$ separation:

UPLC parameters:

Solvent A: Water, 0.1% formic acid

Solvent B: (40% acetonitrile/60% methanol), 0.1% formic acid

Column temperature: 60°C

Injection volume 45 µl

Gradient:

Time (min)	Flow rate (ml/min)	%A	%B	Curve
0	0.4	30	70	
18.99	0.4	30	70	6
19.00	0.4	20	80	1
22.00	0.4	20	80	6
24.00	0.4	0	100	6
29.00	0.4	0	100	6
30.00	0.4	30	70	6
35.00	0.4	30	70	6

QTRAP4000 mass spectrometer parameters:

Positive mode, Q1 and Q3 unit resolution, Turbo Spray source

CUR	20		CAD	Medium
IS	4500		DP	100
TEM	300		EP	10
GS1	18		CE	35

GS2	20		CXP	10
ihe	ON			

Transitions:

Analyte	Q1 mass (Da)	Q3 mass (Da)	Dwell (ms)
D6-SA-PIP_2-aldehyde product	935.4	445.3	50
endogenous SA PIP_2-aldehyde product	929.4	439.3	50
endogenous SA PI-aldehyde product	713.38	439.3	50
17:0-20:4 PI-aldehyde product	699.4	425.3	50

2.2.7 Measurement of PI3P and PI4P

Precisely the same conditions were used for the measurement of $PI(3,4)P_2$ and $PI(4,5)P_2$ described above, except for the following UPLC-MS/MS conditions:

UPLC conditions for PI3P/PI4P separation:

Additional sample preparation: Take 40 µl of sample prepared as above and add to 200µl 70% methanol /30% water. Inject 5 µl

Column: ACE Excel 2 C18-Amide, 150 mm x 0.5 mm
Solvent A: Water, 0.1% formic acid
Solvent B: (40% acetonitrile/60% methanol), 0.1% formic acid
Column temperature: 60°C

Gradient:

Time (min)	Flow rate (ul/min)	%A	%B	Curve
0	10	30	70	
5	10	30	70	6
10	10	22	78	1
35	10	22	78	6
36	10	0	100	6
45	10	0	100	6
46	10	30	70	6

60	10	30	70	6

QTRAP4000 mass spectrometer parameters: as above

Transitions:

Analyte	Q1 mass (Da)	Q3 mass (Da)	Dwell (ms)
D6-SA-PIP-aldehyde product	827.4	445.3	50

2.2.8 [^{33}P]P_i labelling of Mcf10a cells

We added 0.1 ml of 1.5M NaCl to 1 ml of [^{33}P]P_i and then diluted this mixture into a phosphate-depleted medium (GIBCO) and supplemented with (20 mM Hepes, 1% Dialysed FBS, 500 ng/ml hydrocortisone, 100 ng/ml cholera toxin) to reach a final concentration of 250 µC/ml. After siRNA transfection, as described above, cells were starved for 16 hr, then washed twice with phosphate-depleted medium before adding the [^{33}P]P_i-containing medium for 90 min. Then we stimulated the cells with 10 ng/ml hEGF. We aspirated the medium then stopped the reaction with ice-cold 1M HCl. We extracted and deacylated the lipids, and analysed the glycerophoinositides by strong anion-exchange chromatography (Guillou, Stephens et al. 2007).

2.2.9 *In vitro* phosphatase assay

Mcf10a cells (1x10^6) were seeded in 15 cm tissue culture dishes and grown for 64 hr, then washed twice with ice-cold PBS prior to lysis with 1 ml of lysis buffer (10 mM Tris pH7.4, 1.5 mM $MgCl_2$, 5 mM KCl, 1 mM DTT, anti-proteases (1 tablet Roche inhibitor cocktail per 50 ml lysis buffer)) on ice. Cells were then scraped on ice, collected in 2 ml safe lock Eppendorf tubes, vortexed and kept on ice for 5 min. The lysate was sonicated on ice (4 x 10 sec; probe sonication) and then ultracentrifuged (10,000 x g for 30 min at 4°C). A 50 µl aliquot was taken for subsequent protein analysis and this, along with the remainder of the sample, were snap frozen in liquid N_2 and stored at -80°C. Protein determination was performed on the 50 µl aliquots. The remainder of each sample was then thawed and all samples normalized to the same protein concentration with lysis

buffer. The lysates were then divided into 100 µl aliquots and frozen at -80°C. For in-lysate phosphatase assays, a 100 µl aliquot was thawed on ice, then an aliquot containing 20 µg of protein was diluted to 20 µl with a solution containing 2 mg/ml of BSA, 160 mM KCl, 1 mM $MgCl_2$, 20 mM Hepes pH7.3 and 1 mM EGTA. These 20 µl aliquots of cytosol were then used directly in the phosphatase assays, see below.

Micelles consisting of a mixture of lipids and a D6-phosphatidylinositol lipid substrate were prepared at RT as follows. A lipid solution containing liver PI, brain PE, brain PC, brain PS, sphingomyelin, cholesterol, brain PI(4,5)P_2 and either D6-C18:0/C20:4-PI(3,4)P_2 or, D6- C18:0/C20:4-PI(3,4,5)P_3, was prepared in a glass vial at 32.4:23.2:10.5:23.7:2.6:0.9:2.9:3.7 (w/w) ratio (all lipids in their respective solvents) and solvents evaporated under vacuum. In order to reconstitute the lyophilized lipid mixture into micelles, 200 µl of a solution containing 20 mM Hepes pH7.3, 0.1 mM EDTA and 1 mM EGTA was added and the lipid solution bath sonicated for 1 min and divided into 20 µl aliquots.

A 20 µl aliquot of diluted cell lysate was then added to 20 µl micellar solutions (yielding 0.5 µg/µl total protein concentration and 200-500 µM DTT per reaction) and incubated at 30°C for the indicated times. Reactions were terminated by the addition of 920µl of a solvent mixture containing 2:1:0.79 (v/v) MeOH:$CHCl_3$:$H_2O_{(acidic\ pH)}$. The resultant solution was processed for lipid analysis as described above.

2.2.10 Invadopodia assay

Slides and cells preparation: Prior to the experiment, 13 mm coverslips were pre-coated with gelatin enriched with fluorescently labeled Oregon Green 488 gelatin (Martin, Hayes et al. 2012). Mcf10a cells were grown for 6 days in complete medium supplemented with 10 ng/ml rhTGF-β1. $5x10^4$ cells were seeded in complete medium on the fluorescent gelatin surface and left to adhere (between 2-2.5 hr). Next, cells were washed with PBS, starved for 4 hr, and then stimulated with 20 ng/ml hEGF for another 6 hr. Both complete and starvation media were supplemented with 10 ng/ml rhTGF-β1. After washing with PBS and fixing in 3.7% PFA (15 min at RT), cells were labelled for cortactin following a previously described protocol (Gligorijevic, Bergman et al. 2014) and the nuclei (Hoechst dye, 0.8 ng/ml added to a PBS wash).

Invadopodia imaging and data analysis: In each experiment, 3 coverslips were prepared per condition. Fixed and labelled cells were imaged using a confocal Nikon A1R microscope with a 60x oil objective. 15 images were obtained per coverslip with an average of 15 cells per field of view. Invadopodia quantitation was done blind, by manually scoring the cells for the instances in which cortactin labelling aligned with a hole created in the gelatin. These were then normalized to the number of nuclei per field of view. Such approach was applied due to inability of the semi-automated methods developed in the lab to reliably identify invadopodia from images, while minimising the number of false positives.

2.2.11 Mouse prostate dissection and processing

Mice were sacrificed using Schedule 1 methods, in agreement with the Animals (Scientific Procedures) Act 1986 (ASPA) and tissues rapidly dissected. Prostates, consisting of anterior, ventral and dorsolateral lobes (one pair of each lobe), were dissected intact and one set of anterior, dorsolateral and ventral lobes was used for Western-Blot, while the other set was used for IHC. For Western-Blot and measurements of phosphatidylinositol lipids, tissues were rinsed in PBS and flash-frozen in $N_{2(l)}$. For IHC, prostates were rinsed in PBS and fixed in 4% paraformaldehyde for 1 hr at room temperature. Prostates were then cryo-protected by immersion in 30% w/v sucrose in PBS, while rotating at 4°C, for 1 hr for WT prostates, and for 2-3 hr for PTEN-KO prostates. Prostates were then immersed in embedding medium and slowly frozen on dry ice. Embedded prostates were stored at -80°C until use. 12 µm cryosections were prepared on charged glass slides using Leica CM1850 cryostat. INPP4B-KO and PTEN-INPP4B-KO prostates were dissected intact and prepared for measurements of phosphatidylinositol lipids or for immunofluorescence on site at Akita University.

2.2.12 Mouse prostate imaging

H&E staining: H&E staining of prostate cryosections prepared on glass slides was performed using Mayer's hematoxylin and Eosin Y solutions, following a standard protocol. Images were acquired using Zeiss Laser Microdissection microscope (20x or 40x air objectives), stitched with AxioVision4 software (5% overlap) and gaps

automatically filled with Adobe Photoshop. Alternatively, Olympus BX41 microscope equipped with a 40x oil objective was used to obtain higher resolution images. These were then manually stitched using Velocity software with brightness correction.

Immunofluorescence: 12 µm mouse prostate cryosections prepared on glass slides were stained for PI(3,4)P_2 by permeabilising the sections with saponin (30 min at RT in 0.5% saponin, 1% BSA in PBS). Cells were labelled with anti-PI(3,4)P_2 antibody at 1:150 dilution for 2 hours at RT, then sections were washed 3 times with PBS and incubated with streptavidin-Alexa Fluor674 for 1 hour at RT, in a humid dark container. In some experiments, an additional labelling with anti-phospho-^{473}Ser-Akt antibody was performed, according to the manufacturer's instructions (Cell Signalling). After triple washing with PBS, sections were incubated with Hoechst / PBS solution for 10 minutes, washed again with PBS and mounted with a hard-set medium. Sections were imaged using wide field Nikon Live Cell Imager microscope and 20x air objective. Multiple fields of view were stitched automatically with 10% overlap using NIS-Elements software integrated with the microscope.

2.2.13 HPLC-ESI MS/MS measurement of mouse prostate phophatidylinositiol lipids

Unpublished work from our laboratory and that of Takehiko Sasaki (Akita, Japan) had indicated that the most predominant molecular species of PI(3,4,5)P_3 and PI(3,4)P_2 which accumulate in mouse prostate on deletion of PTEN were the shorter chain, more saturated species. We therefore used a new HPCL-ESI MS/MS method (Sasaki, manuscript in preparation) to analyse 17 different species of phosphatidylinositol lipids in this tissue and present results for the combined total of all species measured (C32:0; C32:1; C34:0; C34:1; C34:2; C36:0; C36:1; C36:2, C36:3; C36:4; C38:3; C38:4; C38:5; C38:6; C40:4; C40;5; C40:6). Data were corrected for wet weight of tissue. At least three individual mice were used per genotype.

2.2.14 Experimental design

A strategy for randomization or stratification of samples has not been carried out. Sample sizes were not chosen based on pre-specified effect size. Instead, multiple

independent experiments were carried out using several sample replicates as detailed in the figure legends. Technical replicates refer to samples analysed in parallel within a single experiment and biological replicates refer to experiments separated in time and performed on separate passages (cell lines) or animals (mice).

2.2.15 Statistics

Unless stated otherwise, data are means ± SD of at least three biological replicates, *P < 0.05, **P < 0.01, ***P < 0.005, and ****P < 0.0001. For the phosphatidylinositol lipid quantitation by HPLC-ESI MS/MS, the variable displayed a very large range and there was every reason to expect heterogeneous error and thus, that the assumptions for parametric tests were not met. In order to stabilise the errors, a logarithmic transformation of the data was carried prior to analysis. Next, a one-way repeated measures ANOVA analysis was performed followed by post-hoc Dunnett's multiple comparisons test to compare the groups of interest against control. For the invadopodia assay in Mcf10a clones, a two-way repeated measures ANOVA analysis was performed followed by post-hoc Tukey's multiple comparisons test to look for the effect of EGF on each genotype and to compare the genotypes, with and without EGF.

Chapter 3 Development of an HPLC-ESI MS/MS method to measure PI(3,4)P_2 *in vivo*

3.1 Introduction

The wealth of knowledge which has been gained in the field of phosphatidylinositol lipid biology over the years has come in parallel with the development of various techniques that allow lipid measurements. Although phosphatidylinositols comprise the minority of phospholipids that populate the lipid bilayer, their extreme importance in cellular signalling and the level of accuracy to which they are regulated is unarguable. Therefore the need for robust, inexpensive, widely applicable and, if used *in vivo*, non-invasive methods is part of the challenge faced by the scientists who study lipids. Unfortunately, no ideal method exists and each of the currently available techniques has its strengths and weaknesses.

3.1.1 The variety of *in vitro* and *in vivo* techniques used to study phosphatidylinositol lipids

The processes driven by PI3K signalling such as neutrophil chemotaxis or cancer cell invasion are not easy to study *in vivo*. Although intra vital microscopy in conjugation with complex biological models has enabled visualization of leukocyte rolling and arrest in different knockout mice (Mueller, Stadtmann et al. 2010), and for the first time linked the function of invadopodia with cell extravasation during metastasis (Leong, Robertson et al. 2014), the techniques require hours of preparation, specialised equipment and for ethical reasons do not have a high-throughput potential. Moreover, such a functional approach does not give an insight into the molecular basis of the process and needs to be complemented by biochemical techniques. A lot of our 'functional' knowledge comes from the phenotype studies of various knockout/knockin mice bearing mutations in selected classes of PI3K, PTEN and other important phosphatidylinositol lipid phosphatases, or major downstream effectors such as AKT, and combining these with PI3K-catalytic site inhibitors.

One of the major breakthroughs in cell biology came with the discovery of autofluorescent proteins and nobody these days can imagine science without the green fluorescent protein (GFP) or its spectral variants. Generation of a fusion protein between GFP and a domain specific for binding a certain phosphatidylinositol lipid is in most cases relatively easy, which makes this approach among one of the most commonly used in spatiotemporal tracking experiments. Fluorescence imaging, however, has its inherent problems, with loss of function due to improper protein folding, spectral crosstalk or photobleaching being just the examples. Moreover, generation of transgenic mice expressing fluorescent bioprobes is an extremely time consuming process and thus the method remains mostly used in various cell-based assays. Phosphatidylinositol lipid quantification using these methods, due to common problems of poor signal-to-noise ratio and background fluorescence, is rarely done. Nevertheless, the PH domain of TAPP1 is accepted as a reliable, PI(3,4)P_2-specific domain, and has therefore been used as bioprobe to study the cellular roles of this bisphosphate (Dowler, Currie et al. 2000, Posor, Eichhorn-Gruenig et al. 2013). Finally, taking into account the variety of techniques available (like confocal microscopy, STORM or TIRFM) and the still underrated potential of FRET sensors, fluorescence imaging, if complemented with good quality quantitative measurements, can be used as a perfect duet to study phosphatidylinositol lipid biology.

Another approach which has dominated biological sciences is generation of specific antibodies, which when coupled to secondary chromophores or fluorophores, report on the presence/absence of their ligand. The biggest challenge in this field is the development of a monoclonal antibody with high binding affinities and good selectivity and stability. Although the variety of antibody products is overwhelming, ranging from humanized antibodies to single chain variable fragments (scF_v), development of antibodies that exhibit specificity towards PIP_2 regioisomers is not a trivial task. A murine, IgG based antibody has been developed by Echelon Biosciences which offers specificity towards PI(3,4)P_2. The work done in Cos7 cells, where the antibody was used to track lipid localization in maturating endosomes, seems to support its specificity (Posor, Eichhorn-Gruenig et al. 2013). In order for the antibody to penetrate the membrane and bind PI(3,4)P_2, prior cell fixation and permeabilization is needed. Therefore, immunocytochemistry, although extremely informative, gives only a

snapshot of what happens in the cell and a series of experiments are normally necessary to see the bigger picture.

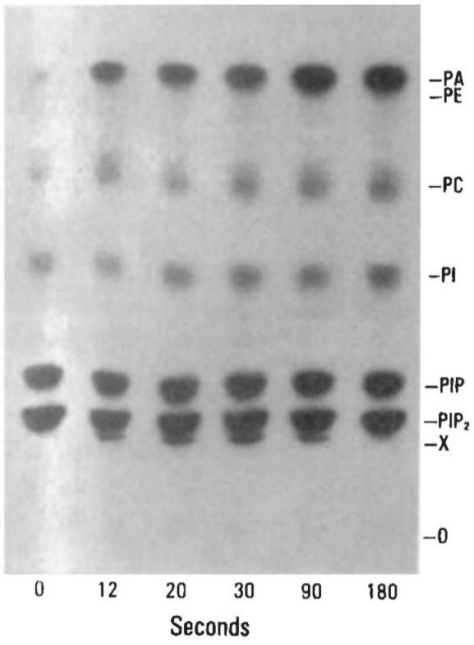

Figure 3.1 Glycerolphospholipids generated in stimulated human neutrophils

Autoradiograph of TLC-separated glycerolphospholipids extracted from human neutrophils. Cells were equilibrated with [^{32}P]-P_i and stimulated with 10nM FLPEP (hexapeptide) for the indicated times. X was later confirmed to correspond to PI(3,4,5)P_3 generated in these cells. From (Traynor-Kaplan, Harris et al. 1988).

The identification of a phosphatidylinositol trisphosphate in formylpeptide-stimulated human neutrophils relied on thin-layer chromatography (TLC) - a semi-quantitative method to measure the levels of phosphatidyinositol lipids extracted from cells stably labelled with radioactive isotopes (Figure 3.1). This method was crucial in identifying PI(3,4,5)P_3 as a lipid product transiently generated in stimulated human neutrophils and in showing PTEN's and SHIP's phosphatase activity towards PI(3,4,5)P_3 *in vitro* (Traynor-Kaplan, Harris et al. 1988, Auger, Serunian et al. 1989, Myers, Pass et al. 1998). This method however has poor resolving power and can only quantify PI(3,4,5)P_3 when it is present in relatively high proportions compared to other labelled lipids.

The most successful attempts to globally quantify phosphatidylinositol lipids has so far been achieved through radioactivity measurements of [^{32}P]-Pi or [^{3}H]-inositol labelled lipid headgroups (Stephens, Hughes et al. 1991, Guillou, Stephens et al. 2007). Cells are first labelled with a radioactive precursor, treated with agonist and/or inhibitor, followed by lipid extraction by a Folch phase separation and deacylation by a transesterification reaction with methylamine (Clarke and Dawson 1981). Finally, a mixture of radiolabelled glycerophosphatidylinositol headgroups is separated by anion

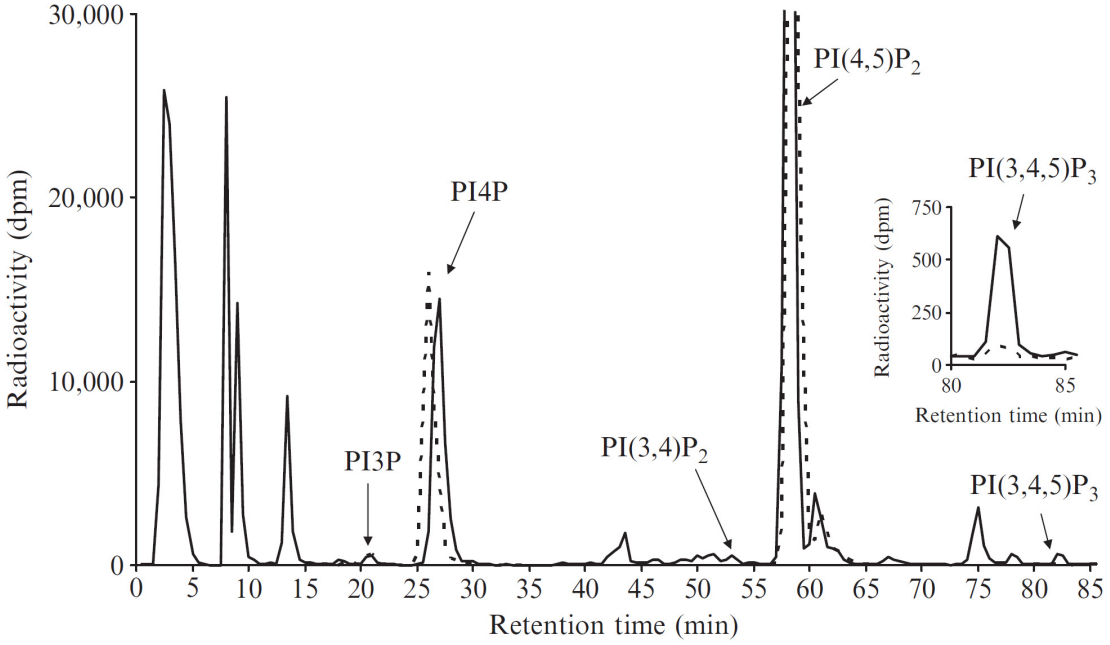

Figure 3.2 An example of chromatographic separation of phosphatidylinositol lipids by anion-exchange HPLC

[^{32}P]P_i-labelled mouse neutrophils were stimulated (continuous line) or not (dotted line) for 10 min with 10μM fMLP. Next, phosphatidylinositol lipids were extracted, deacylated, and run on the HPLC column followed by scintillation counting. From (Guillou, Stephens et al. 2007).

exchange HPLC and each lipid fraction is quantified by scintillation counting (Figure 3.2). Although the technique allows detection of low abundant PI(3,4)P_2 and PI(3,4,5)P_3, it suffers from several drawbacks. In order to achieve good resolving power, a long HPLC gradient is needed, which results in collecting nearly 200 samples per experiment and as such becomes a major limiting factor. Moreover, the essential radiolabelling step limits applicability of this technique and measurements are not easily achieved *in vivo*. Finally, preparation of methylamine and handling radioactive ^{32}P requires care and a significant amount of expertise. Taken together, the above approach has contributed greatly to understanding PI3K-centered processes but a more sensitive, low cost, high-throughput method for phosphatidylinositol lipid quantification is still highly desired.

3.1.2 Lipidomics - measurement of lipids by mass spectrometry

Mass spectrometry, since the development of the first modern machines in 1910's, has been primarily used as an analytical tool for structure determination of newly synthesized compounds. With the emergence of new ionisation techniques, accurate

mass analysers and easy to operate machines, its applications today range from chemistry, life- and forensic science to the pharmaceutical industry. While studies of protein structure and function by mass spectrometry (proteomics) is a well-established field of science, with a variety of reliable methods and databases available, metabolomics and lipidomics are still very young disciplines.

3.1.2.1 Electrospray ionisation mass spectrometry

Measurement of lipids by mass spectrometry requires mild ionisation techniques in order to leave molecules intact as they enter the mass analyser. To achieve this, electrospray ionisation (ESI) is very commonly a method of choice (Figure 3.3). Liquid containing analyte molecules is passed from the HPLC through a metal capillary with a high voltage applied to it. High voltage and the presence of conductive solvents (like formic or acetic acid) cause liquid ionisation and formation of a fine aerosol. The Coulombic repulsive forces and desolvation by the nebuliser gas (e.g. N_2) trigger dispersion of analyte into smaller droplets and eventually lead to formation of charged lipid molecules in the gas phase. The stream of ionised gas is then accelerated to the entrance of the mass analyser.

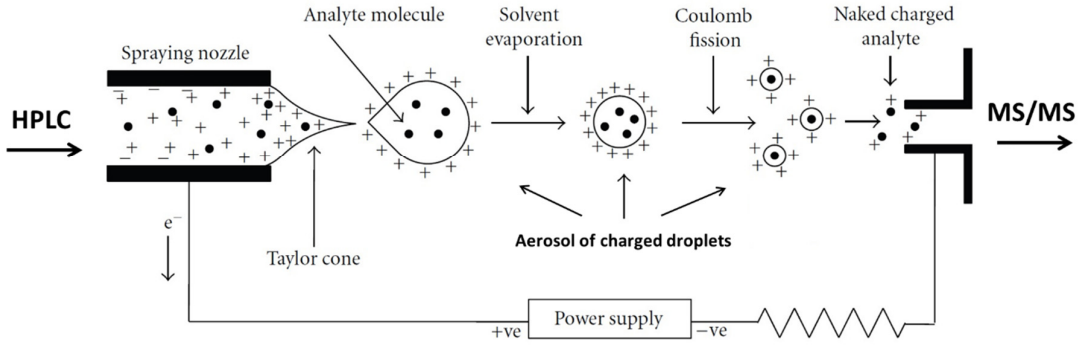

Figure 3.3 A schematic representation of ion generation by electrospray ionisation

Analyte solution at the edge of a metal capillary forms a Taylor cone, which due to the high-density of positive charge and applied voltage becomes destabilized and produces an aerosol of charged droplets. Solvent evaporation is accompanied by increasing repulsive forces, which eventually leads to formation of the analyte in the gas phase that enters the source of the mass spectrometer. Adapted from (Banerjee and Mazumdar 2012).

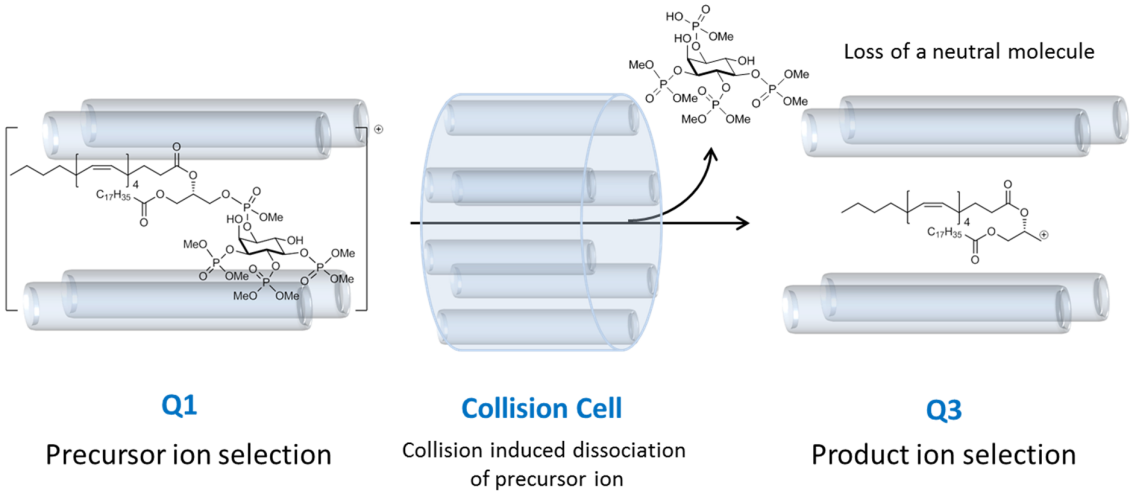

Figure 3.4 Fragmentation of PI(3,4,5)P_3 aldehyde in a triple quadrupole mass spectrometer

A precursor ion selected in the first quadrupole (Q1) enters a collision chamber where it collides with a neutral gas and produces a collection of secondary ions. A product ion of a certain m/z is selected in the third quadrupole (Q3) and passed onto the detector.

Depending on the type of mass analyser, electric field, magnetic field or the kinetic energy of the accelerated ions are used as a force to control trajectories and the time it takes for the ions to reach the detector. In the triple quadrupole system, the first quadrupole (Q1) is kept at high vacuum to maximize the mean free path of analyte molecules and minimize collisions between them (Figure 3.4). Four parallel, metal rods are subject to constant direct current (DC) and radiofrequency current (RF) of alternating polarity, which together form a mass filter, that stabilizes the trajectory of a precursor ion (the ion of certain m/z), while rejecting the rest. Next, the precursor ion enters the collision chamber (a multipole, Q2), where fragmentation is facilitated by interaction with the collision gas, in the process known as collision induced dissociation (CID). Finally, a mixture of product ions and neutral fragments is passed through the third quadrupole (Q3), which works in an analogous way to Q1. When Q3 is set to a scanning mode, all daughter ions reach the detector and a classic MS/MS spectrum is obtained. In multiple reaction monitoring (MRM) experiments, Q3 is fixed to filter the most abundant fragment, which allows monitoring multiple Q1/Q3 ion pairs in a short period of time.

3.1.2.2 Reverse phase chromatography

Reverse phase chromatography is a technique used to separate components from a mixture of analyte molecules suspended in a common solvent. The separation itself is a result of competition between the non-polar, stationary phase and the mobile phase of changing composition for the analyte molecule. Thus, the more hydrophobic the character of the analyte is, the more retained it becomes on the column and the more nonpolar the solvent needs to be to elute it from the column support. Columns used in reverse phase chromatography are most commonly based on silica functionalised with hydrocarbon chains of various length, e.g. c4, c8, c18 columns. Further functionalisation with phenyl- amide- or chiral molecules is chosen when specific types of interactions have the potential to dominate the separation, or when analytes in the mixture have high levels of similarity. The mobile phase is the crucial element of the separation process as its primary function is to overcome the retentive power of the column. Most commonly used solvent systems are blends of organic solvents such as MeCN or MeOH with water. If HPLC is used in-line with the mass spectrometer, additives like organic acids are used to facilitate analyte ionisation.

3.1.2.3 Quantification of phosphatidylinositol lipids by HPLC-ESI MS/MS

Several mass spectrometry lipidomics approaches have been developed in the recent years, but none of the techniques provided good enough sensitivity and reliability to measure Class I PI3K's catalytic product - PI(3,4,5)P_3. A method recently developed at Babraham is based on chemical modification of phospholipids, with the aim to allow detection of low-abundant PI(3,4,5)P_3 with high specificity and good signal-to-noise ratio (Clark, Anderson et al. 2011). Prior to the analysis by mass spectrometry, lipids from homogenised tissues or cells are extracted using an acid Folch extraction method and reacted with trimethylsilyl diazomethane (TMS-diazomethane). Methylation of the acidic phosphates is a crucial step, as it reduces the net charge of molecules and thus significantly improves the detection sensitivity of the highly phosphorylated phosphatidylinositol lipids. Finally, a mixture of methylated phospholipids is separated by reverse phase HPLC and analysed by an in-line ESI-MS/MS in positive-ion mode, using neutral loss of the defined mass of a methylated headgroup coupled with detection of a positively charged glycerol-lipid backbone for selectivity (Figure 3.4). The biggest

advantage of using this mass spectrometry approach is that tissues and cells from a wide variety of organisms can be profiled for the existence of novel species or biomarkers that report on the activity of specific signalling pathways. Moreover, utilisation of mass-differentiated internal standards allows quantification of phosphatidylinositol lipids and helps to interpret the data coming from *in vitro* and biochemical studies. Finally, the triple quadrupole mass spectrometer is a low maintenance machine and the rate-limiting step becomes the time of sample preparation and data acquisition. This HPLC-ESI MS/MS method, however, suffers from a major drawback - it is unable to distinguish between regioisomers of the same mass that are normally found in cells e.g. $PI(3,4)P_2$ and $PI(3,5)P_2$ from the usually much more abundant $PI(4,5)P_2$. The latter is the necessary condition for quantitative $PI(3,4)P_2$ measurements – classically associated with combined class I PI3K – 5-phosphatase activity, decoupled from the $PI(4,5)P_2$ background.

The initial phase of this PhD project was focused on developing a quantitative, mass spectrometry based method, to measure the low abundant $PI(3,4)P_2$ relative to ubiquitous $PI(4,5)P_2$ with high accuracy and reliability.

3.2 Results

For the purpose of HPLC - mass spectrometry method development, synthetic C38:4 PIP_2 lipids as well as their deuterated equivalents (referred to in the text as D6-PIP_2) were used (Figure 3.5). Each compound was synthesised to a high purity and stored in the form of a lyophilised ammonium salt.

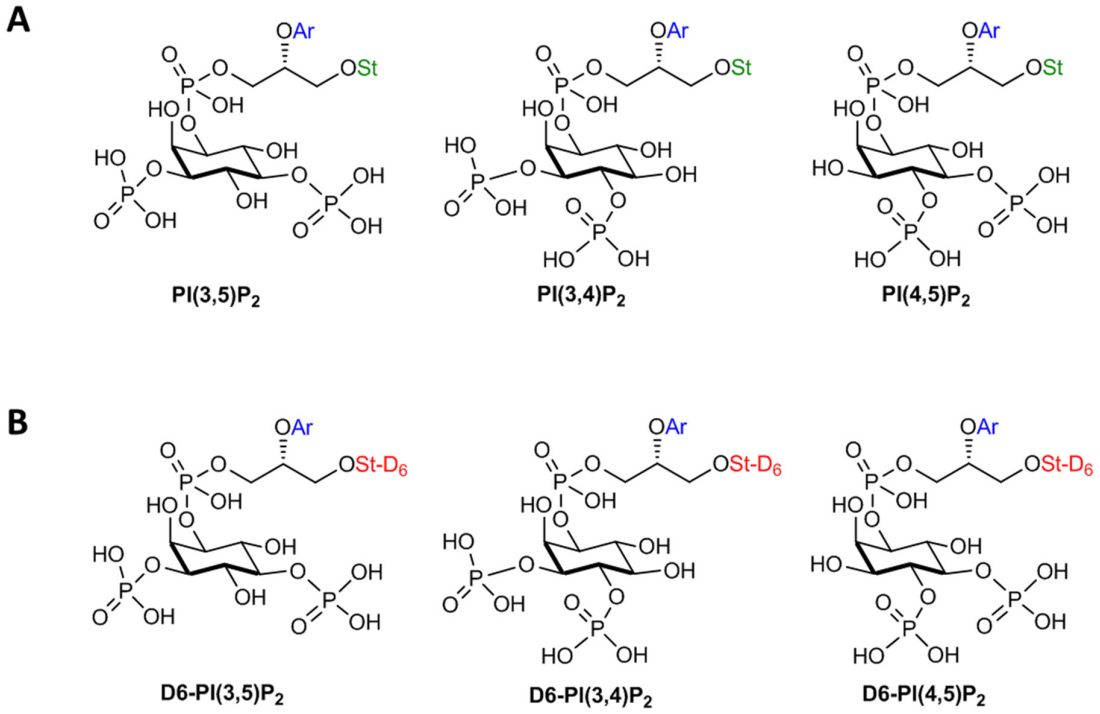

Figure 3.5 Structures of C38:4 PIP_2 and deuterated-C38:4 PIP_2 regioisomers

*Structure of three regioisomers of C38:4 PIP_2 (**A**) and of three deuterated-C38:4 PIP_2 (**B**); St = stearoyl (C18:0; green) and Ar = arachidonoyl (C20:4, blue) fatty acyl chain. "St-D6" (**B**, red), represents where six atoms of hydrogen in the stearoyl acyl chain were chemically replaced by the heavier deuterium atoms yielding a deuterated equivalent.*

3.2.1 Separations of full length C38:4 PIP_2 regioisomers

Before the start of this PhD project, a significant amount of work had been put into trying to separate by HPLC full length C38:4 PIP_2 regioisomers. The approaches taken included 1) alternative headgroup modifications (e.g. benzylation of the phosphate hydroxyl groups), 2) using various blends of HPLC solvents and 3) different reverse phase columns. Unfortunately, none of the strategies led to a quantifiable separation of

$PI(3,4)P_2$ and $PI(4,5)P_2$ (one of the best separations achieved is shown in Figure 3.6A). Intriguingly, when C37:4 PIP_2 lipids were passed through the HPLC-ESI MS/MS system, a much better separation was observed (Figure 3.6B). This may suggest that the 3D structure of stearoyl/arachidonoyl chains shields lipid headgroups and thus hinders their interaction with the column support.

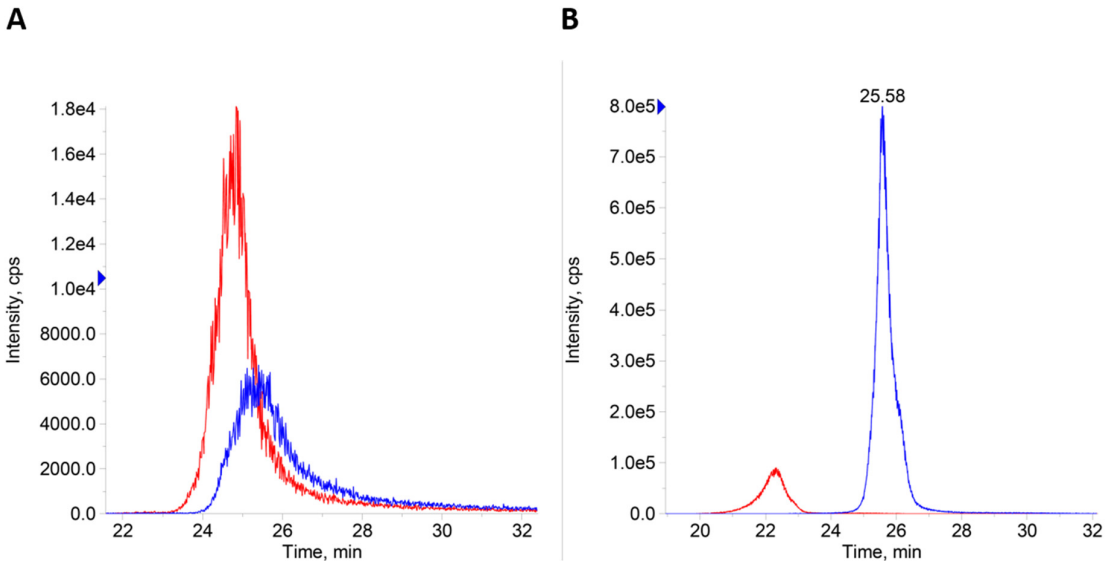

Figure 3.6 Separation of $PI(3,4)P_2$ and $PI(4,5)P_2$ with C18:0-C20:4 or C17:0-C20:4 acyl chains

*(**A**) Chromatogram of C18:0-C20:4 $PI(3,4)P_2$ (red) and C18:0-C20:4 $PI(4,5)P_2$ (blue) synthetic lipids, chiral CHS column (TCI) 40min 35-80% MeCN/H_2O gradient; (**B**) Chromatogram of C17:0-C20:4 $PI(3,4)P_2$ (red) and C17:0-C20:4 $PI(4,5)P_2$ (blue) synthetic lipids (Avanti), chiral MBS column (TCI) isocratic at 45% MeCN/H_2O.*

3.2.2 Ozonolysis

Due to lack of success in separating full length C38:4 PIP_2 regioisomers a new strategy was needed. We hypothesised, that shortening the arachidonoyl acyl chain, provided that a selective cleavage of its C=C bond is achieved, might favour interaction of the PIP_2 headgroup with the column support and potentially lead to a better separation between $PI(3,4)P_2$ and $PI(4,5)P_2$. The idea came from another project, in which identifying the position of a double bond was necessary for structure determination of an unusual PIP_2 in *D. discoideum* (Clark, Kay et al. 2014).

An oxidative cleavage of C=C bonds via reaction with ozone is one of the strategies used in chemistry for determining positions of unsaturated bonds. The mechanism proposed by Criegee starts with 1,3-dipolar addition of an ozone molecule to a π bond and, via several rearrangements, leads to formation of an ozonide. Next, dimethyl sulphide (DMS) is used as reducing agent to give DMSO and an aldehyde derivative as reaction products. By analogy, a reaction of C38:4 PI(4,5)P_2 with the ozone, followed by the DMS reduction step, leads to formation of 1-stearoyl-2-(5'-oxo-valeroyl)-*sn*-glycero-3-phospho-(1'-myo-inositol-4',5'-bisphosphate) (Figure 3.7; for simplicity 'PI(4,5)P_2 aldehyde' is used in the text). Indeed, initial ozonolysis experiments performed on synthetic C38:4 PIP_2 regioisomers in solution confirmed a selective and complete conversion of full length lipids to their respective aldehyde derivatives (data not shown).

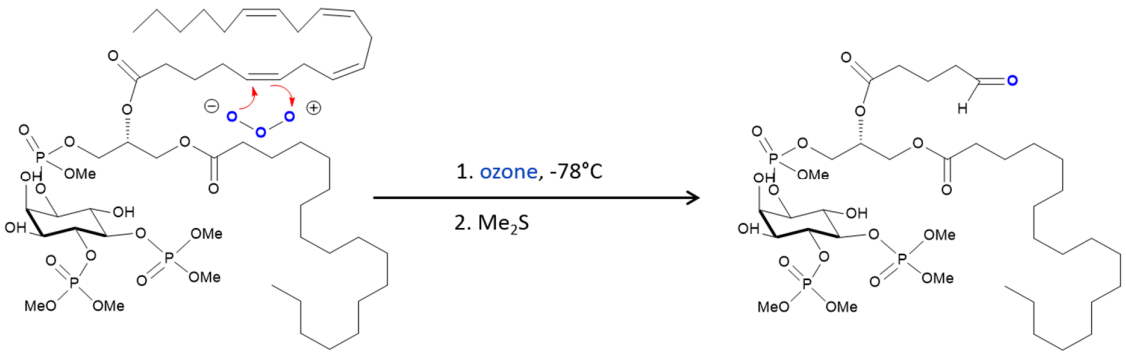

Figure 3.7 Ozonolysis of C38:4 PI(4,5)P_2

C38:4 PI(4,5)P_2 exposure to ozone leads to oxidative cleavage of the arachidonoyl chain and yields an aldehyde derivative.

An HPLC-ESI MS/MS system was used throughout this project as a tool to measure ozonolysed lipids in solution or in the cellular extracts. As described earlier, mass spectrometry is a technique that offers quantitative measurements of lipids in a robust and sensitive manner. Moreover, the method established at Babraham for measuring PI(3,4,5)P_3, could be easily adapted to measure ozonolysed PIP_2's and serve as a starting point for future developmental work. Similar to the full length lipids, fragmentation of a PIP_2 aldehyde in the collision cell of a triple quadrupole mass analyser causes a loss of a neutral headgroup and yields a glycerol cation (see Figure 3.4).

3.2.3 HPLC method optimization

The most important part of the method development process was to optimize the HPLC conditions to enable PI(3,4)P_2 aldehyde and PI(4,5)P_2 aldehyde separation. Moreover, several parameters had to be adjusted to improve sample stability and signal intensity. The approach which led to a satisfactory regioisomer separation will be discussed below, followed by method validation in a biological system.

3.2.3.1 Solvent effect

The HPLC solvent system used in the initial measurements of ozonolysed lipids was the same as for the full length lipids, i.e. it was based on a mixture of acetonitrile and water. As it turned out, the system under such conditions is highly unstable, with multiple peaks appearing on the chromatogram (Figure 3.8; left panel), probably as a result of phosphate migration around the inositol ring. Phosphate migration was minimised by increasing the methanol content in the organic part of the binary mix. The final HPLC solvent composition used throughout the study was: solvent A = H_2O, solvent B = 40% MeCN/MeOH; both solvents supplemented with 0.1% formic acid. The small peak that elutes first (e.g. the peak at 2.92 minutes in the last panel of Figure 3.8) is probably a contaminant resulting from the organic synthesis.

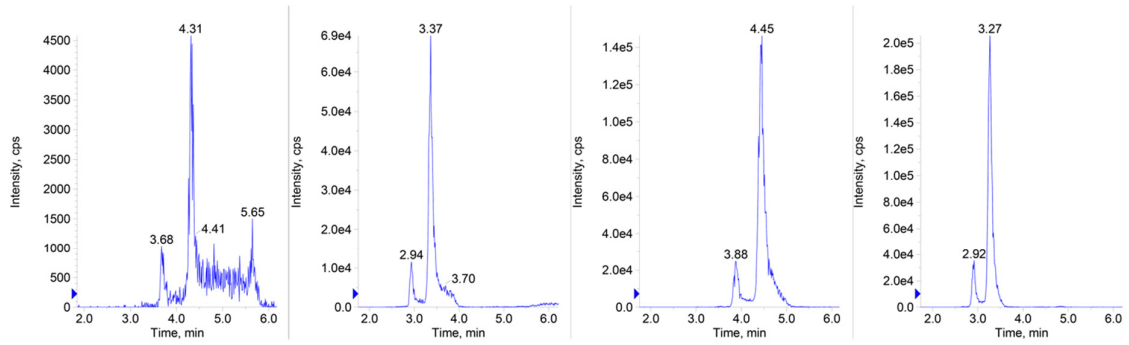

Figure 3.8 The effect of MeOH on the stability of PI(4,5)P_2 aldehyde

Isocratic HPLC runs of synthetic PI(4,5)P_2 aldehyde in a solvent system of increasing methanol content (conditions used in later experiments). Composition of inorganic (A) and organic (B) part of the binary solvent mix is indicated below each chromatogram; A and B solvents were supplemented with 0.1% formic acid.

3.2.3.2 Length of the HPLC column

A longer HPLC column, tested to allow extended interaction time between the lipid headgroups and the support, showed an improved separation (Figure 3.9). Although resulting peak broadening is one of the factors that may affect sensitivity, it was not identified as a serious problem in our case.

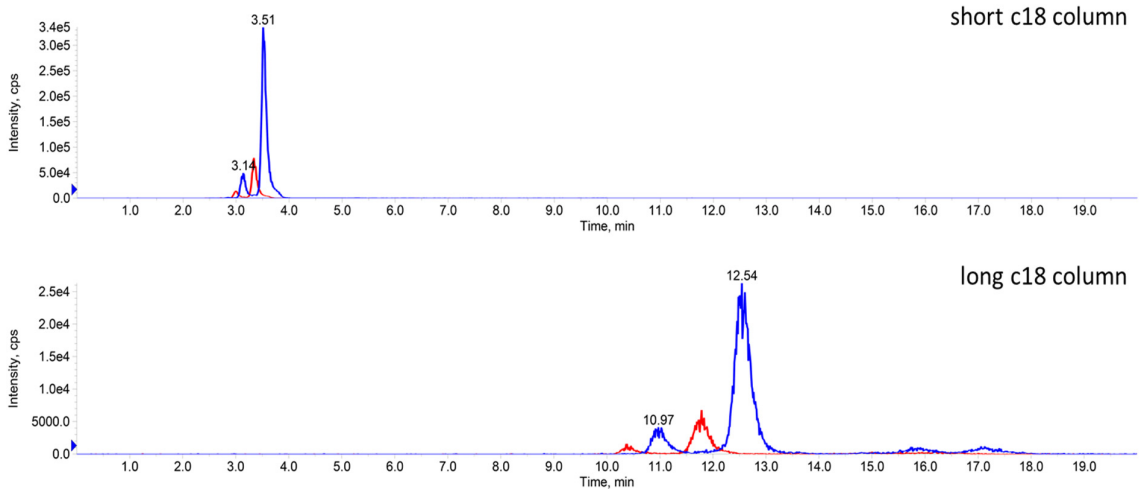

Figure 3.9 The effect of column length on the separation efficiency between PI(3,4)P_2 aldehyde and PI(4,5)P_2 aldehyde

Chromatograms of D6-PI(3,4)P_2 aldehyde (red) coeluted with PI(4,5)P_2 aldehyde (blue) during isocratic runs (86% B; A = H_2O, B = 40% MeCN/MeOH; A and B solvents were supplemented with 0.1% formic acid) through a short c18 column (10 cm, top) and long c18 column (15 cm, bottom).

3.2.3.3 The role of internal standards in mass spectrometry - deuterium effect

Deuterated phosphatidylinositol lipid internal standards are considered superior to shorter-chain lipid equivalents due to their comparable physicochemical properties. According to current knowledge, deuterated standards are indistinguishable from their 'light' equivalents by mass spectrometry, except by mass. The first stage of HPLC conditions optimization was done with a pair of synthetic inositol lipids: D6-PI(3,4)P_2 and non-deuterated PI(4,5)P_2. The above choice was dictated by the lack of mass overlap between the two species, which helped to monitor separation progress. To our surprise, separation between the two regioisomers was much poorer when synthetic PI(3,4)P_2 was coeluted with the endogenous PI(4,5)P_2, i.e. when the pair of monitored lipids was of the same m/z (Figure 3.10). In these and subsequent studies, we used both WT and

[PTEN-KO + siRNA INPP4A&B] Mcf10a cells to provide a source of endogenous PIP_2 comprising < 5% or approximately 20% $PI(3,4)P_2$, respectively (see later Chapters for a fuller explanation).

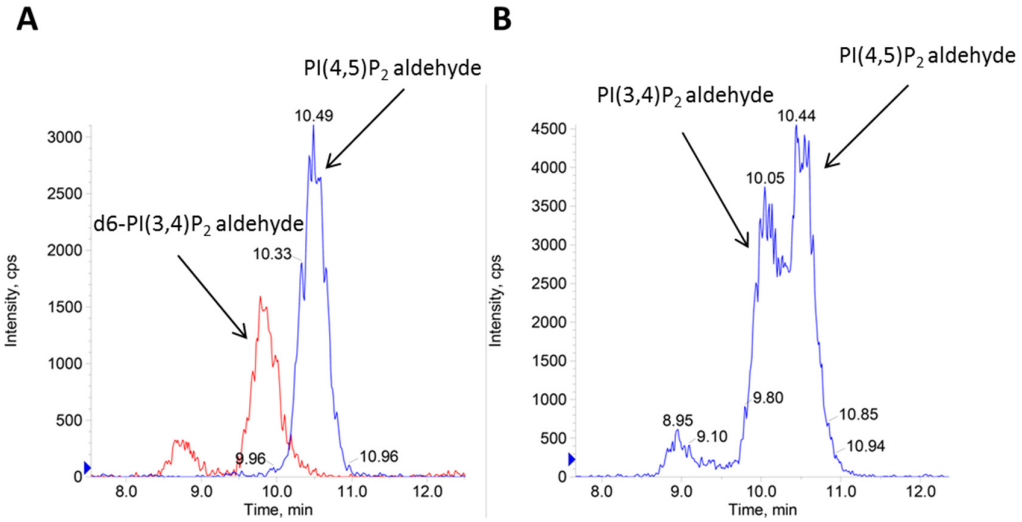

Figure 3.10 The presence of deuterated-C18:0 acyl chain affects PIP_2 separation

*(**A**) Chromatogram of endogenous $PI(4,5)P_2$ aldehyde (blue) coeluted with synthetic D6-$PI(3,4)P_2$ aldehyde (red); (**B**) Chromatogram of endogenous $PI(4,5)P_2$ aldehyde (blue, right peak) coeluted with synthetic $PI(3,4)P_2$ aldehyde (blue, left peak). HPLC conditions: 86% B; A = H_2O, B = 40% MeCN/MeOH; A and B solvents were supplemented with 0.1% formic acid. Endogenous $PI(4,5)P_2$ was a component of lipid extract from WT Mcf10a cells that contains very little $PI(3,4)P_2$.*

When chromatograms of $PI(3,4)P_2$ with an increasing number of deuterium atoms are overlapped, a decrease in retention time is observed (Figure 3.11). This suggests, that the energy of interactions between the heavier, deuterium-containing stearoyl

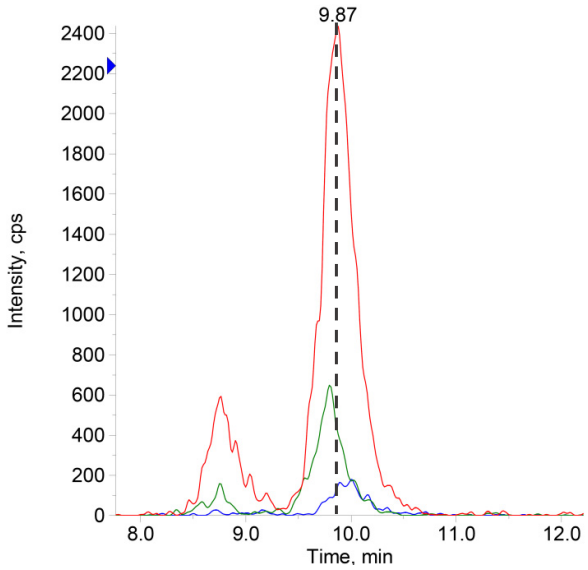

Figure 3.11 The effect of deuterium on the retention time of HPLC column

Chromatogram of synthetic D3- (blue, RT = 10.00 min), D6- (red, RT = 9.87 min) and D9-$PI(3,4)P_2$ aldehyde (green, RT = 9.80 min). HPLC conditions: 86% B; A = H_2O, B = 40% MeCN/MeOH; A and B solvents were supplemented with 0.1% formic acid.

chain and the column support is weaker and thus a "peak drift" on the HPLC column is observed for D3-, D6- and D9-enriched molecules.

3.2.3.4 Temperature effect

Column temperature is another parameter which influences the overall performance of chromatographic separations. At higher temperatures, intensified translational, rotational and vibrational motion raises the thermal energy of molecules and the system becomes more fluid. Flexible lipid hydrocarbon chains can squeeze through the column support more easily and as a result the peaks become sharper (Figure 3.12). This in turn, causes a drop in the column back pressure, which allows starting the HPLC elution with a higher aqueous content and further increases separation (Figure 3.13).

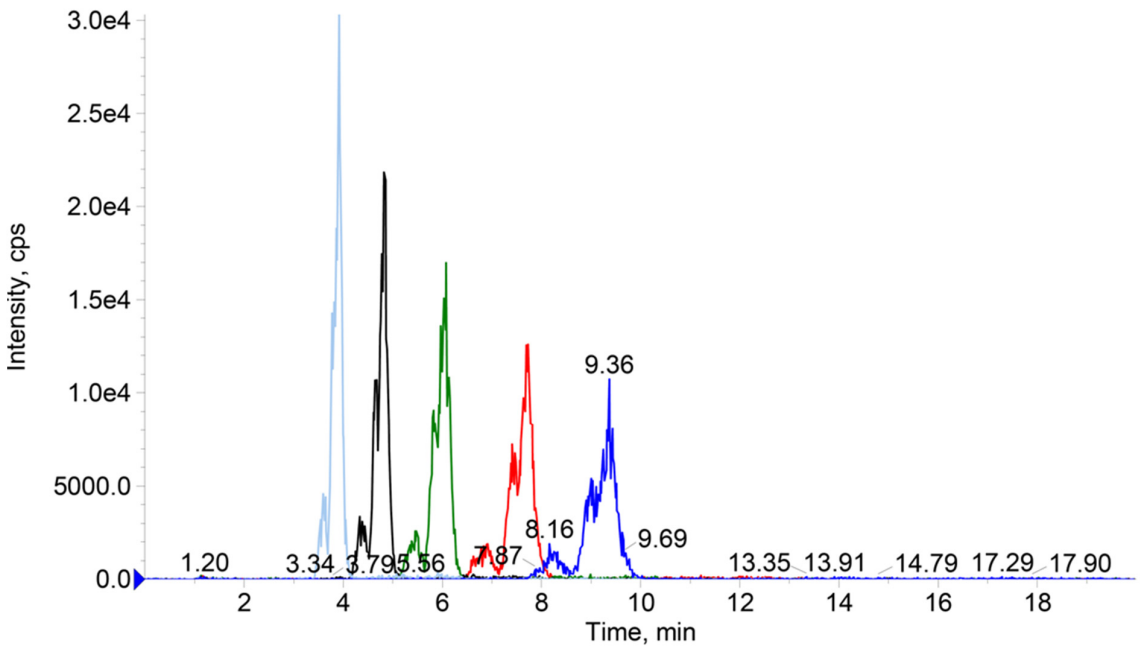

Figure 3.12 The effect of column temperature on retention time

Isocratic HPLC runs at 86% B and varying column temperature (RT - blue, 30°C - red, 40°C - green, 50°C - black, 60°C - light blue) of a mixture of synthetic PI(3,4)P_2 aldehyde and PI(4,5)P_2 aldehyde. HPLC conditions: 86% B; A = H_2O, B = 40% MeCN/MeOH; A and B solvents were supplemented with 0.1% formic acid.

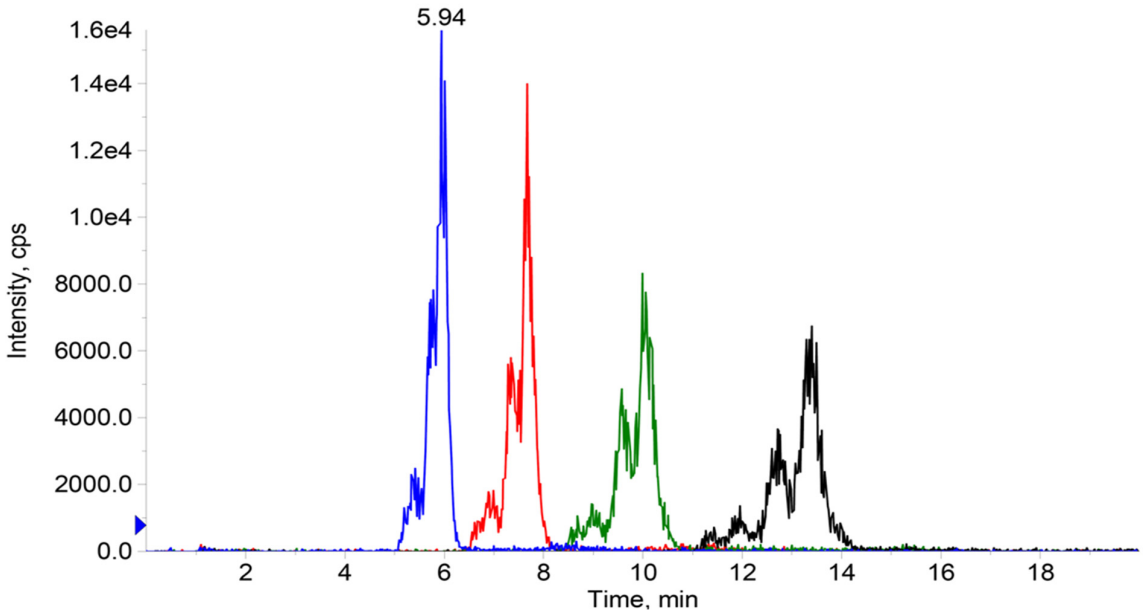

Figure 3.13 The effect of increasing aqueous content of the mobile phase on peak separation

Isocratic HPLC runs at 60°C and varying %B solvent composition (82% B - blue, 80% B - red, 78% B - green, 76% B - black) of a mixture of synthetic PI(3,4)P_2 aldehyde and PI(4,5)P_2 aldehyde. HPLC conditions: varying % B; A = H_2O, B = 40% MeCN/MeOH; A and B solvents were supplemented with 0.1% formic acid.

3.2.3.5 Different modes of HPLC runs

The separation progress between PI(3,4)P_2 aldehyde and PI(4,5)P_2 aldehyde was initially monitored under isocratic HPLC conditions, i.e. with composition of A and B solvents kept constant. Once a satisfactory separation was achieved, gradient HPLC conditions were used to increase the signal-to-noise ratio of measured analytes (Figure 3.14).

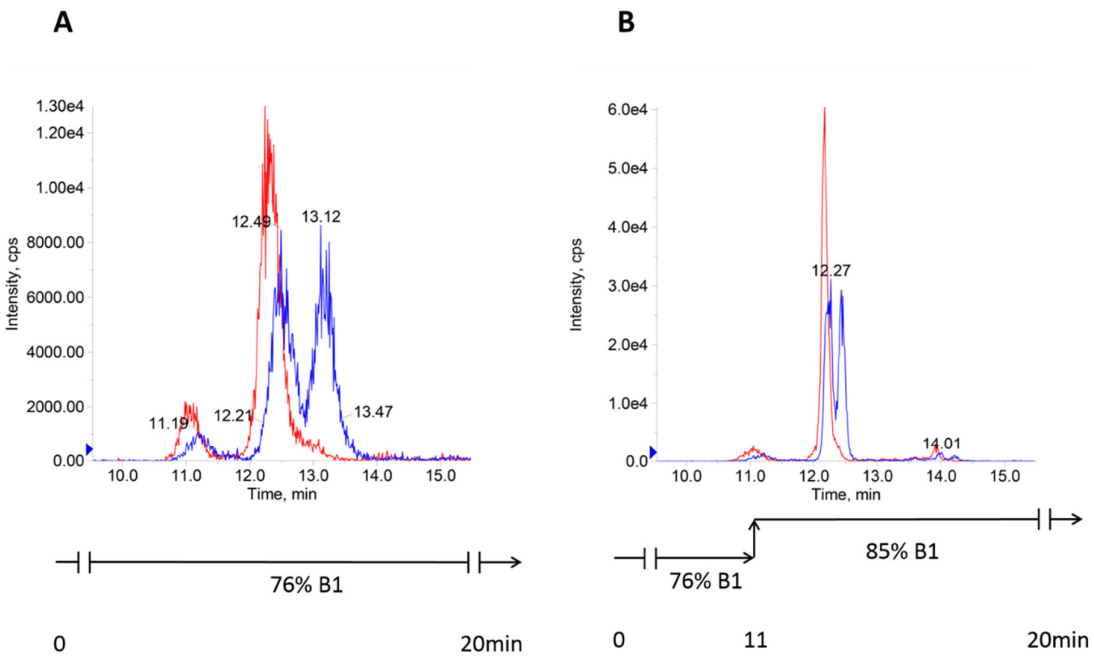

Figure 3.14 Comparison between the isocratic and gradient HPLC conditions

*Chromatograms of endogenous PI(4,5)P_2 aldehyde (blue, right peak) and synthetic PI(3,4)P_2 aldehyde (blue, left peak) coeluted with D6-PI(3,4)P_2 (red, left peak) during a 20min isocratic run (**A**) or a 20min gradient run (**B**); WT unstimulated Mcf10a cells (containing very little endogenous PI(3,4)P_2). HPLC solvent composition: A = H_2O, B = 40% MeCN/MeOH; A and B solvents were supplemented with 0.1% formic acid. Endogenous PI(4,5)P_2 was a component of lipid extract from WT Mcf10a cells that contains very little PI(3,4)P_2.*

3.2.3.6 Functionalised reverse phase HPLC columns

One of the important stages in HPLC method development is to test the quality of measurements on different reverse phase columns. This is done not only to improve separations between the peaks and their shape but also to check for contaminants, which may coelute with the analyte peaks and skew the data. A c18 amide column was found to retain the peak shapes of the two regioisomers but, most importantly, to

provide additional interaction sites and by this significantly improved the relative separation between the aldehydes (Figure 3.15).

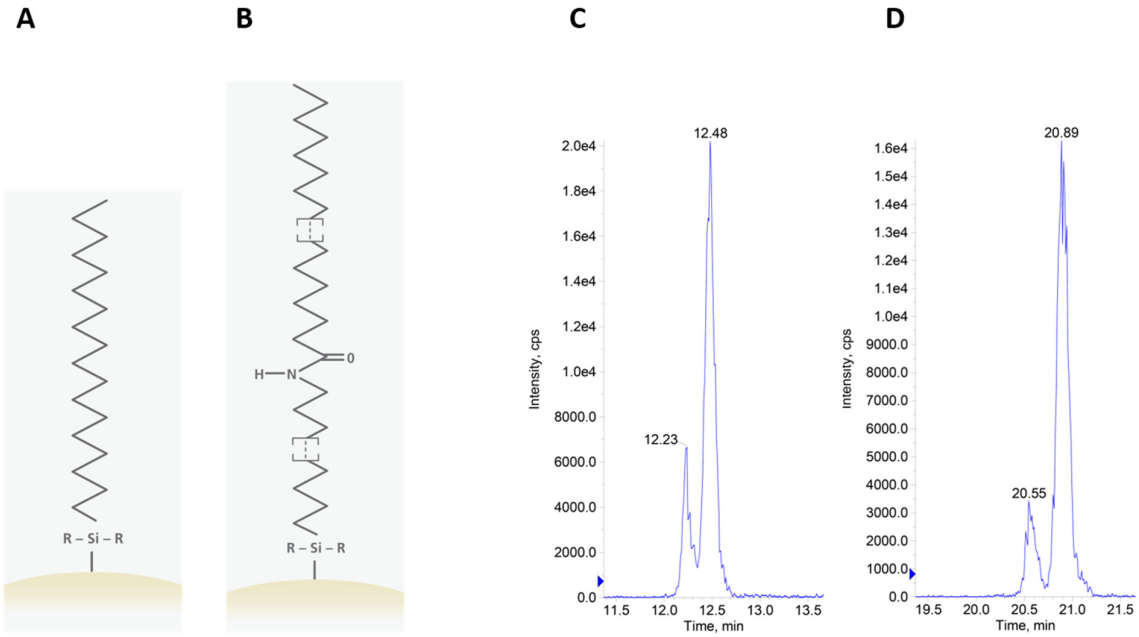

Figure 3.15 The effect of c18 HPLC column functionalisation

*Architecture of a c18 (**A**) and c18 amide (**B**) reverse phase column. Chromatograms of endogenous PIP_2 aldehydes showing $PI(3,4)P_2$ (left) regioisomer separated from $PI(4,5)P_2$ (right) run through a c18 (**C**) and c18 amide (**D**) column. HPLC conditions: see Materials and Methods section (Chapter 2.2.6). Lipid extracts were from PTEN-KO + siRNA INPP4A&B Mcf10a cells stimulated with EGF for 5min.*

3.2.3.7 Method validation in human platelets

Platelets are an important member of the haematopoietic cell lineage and in the body control the process of haemostasis. Upon arrival at the site of injury, platelets adhere and become activated by multiple agonists (such as integrins, ADP or thrombin) binding to specific cellular receptors. This activation triggers several signalling cascades, which initiate substantial actin rearrangement processes leading to a shape change and platelet aggregation. $PI(3,4,5)P_3$ production by class I PI3K is one of the hallmarks of activated platelets and SHIP1 has been defined as the major 5-phosphatase that regulates the levels of $PI(3,4,5)P_3$ and $PI(3,4)P_2$ in the mouse platelets responding to stimulation by thrombin (Giuriato, Pesesse et al. 2003) or integrin (Maxwell, Yuan et al. 2004). Due to the fact that thrombin-stimulated platelets have been shown to accumulate pronounced levels of $PI(3,4)P_2$, this system was used to validate the newly

developed mass spectrometry method. Indeed, thrombin stimulation of platelets isolated from human blood led to a substantial accumulation of $PI(3,4)P_2$, estimated to amount to ~40% of total $PI(4,5)P_2$ measured in these cells (Figure 3.16A). Moreover, preincubation of human platelets with wortmannin – a nonspecific PI3K inhibitor, significantly decreased the levels of measured $PI(3,4)P_2$, hence authenticating the origin of the chromatographic peak at RT = 20.59 min, which we earlier assigned to be indicative of the presence of $PI(3,4)P_2$ in the system. A fixed amount of synthetic, deuterated phosphatidylinositol bisphosphates, i.e. D6-$PI(3,4)P_2$ and D6-$PI(4,5)P_2$, were spiked into each sample and used to correct for any material loss and as a quality control of the HPLC system (Figure 3.16B).

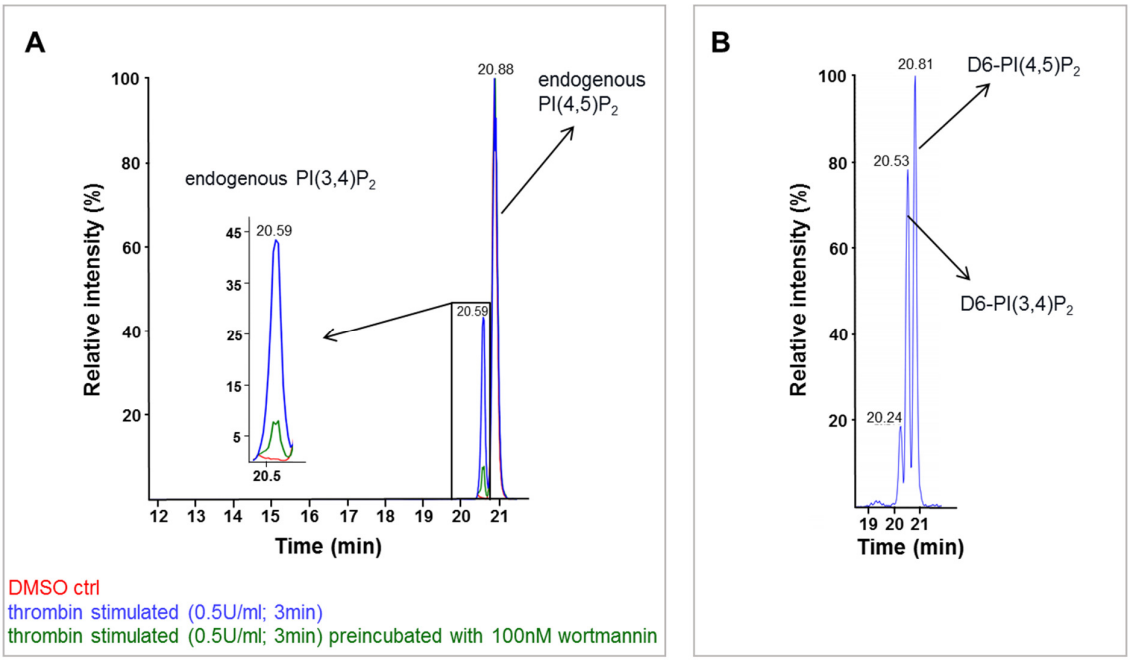

Figure 3.16 HPLC-ESI MS/MS method validation in human platelets stimulated with thrombin

*(**A**) Chromatograms showing endogenous levels of $PI(3,4)P_2$ alddhyde and $PI(4,5)P_2$ aldehyde in human platelets subject to stimulation with thrombin (blue), compared to DMSO control (red). Preincubation with wortmannin substantially abrogated the $PI(3,4)P_2$ levels that accumulated in these cells upon thrombin stimulation (green). (**B**) Representative chromatogram of synthetic C38:4 D6-$PI(3,4)P_2$ and C38:4 D6-$PI(4,5)P_2$ spiked into cellular extracts prior to lipid extraction and ozonolysis. HPLC conditions: see Materials and Methods (Chapter 2.2.6). Cell pellets were provided by Tom Durrant, University of Bristol UK.*

3.3 Discussion

We have managed to develop a novel ESI-HPLC MS/MS method, which can be used to measure levels of PI(3,4)P_2 decoupled from the PI(4,5)P_2 background. Reaction with ozone led to a selective and complete conversion of C38:4 PIP_2's to their respective aldehyde derivatives. Moreover, the strategy of shortening the arachidonoyl acyl chain to favour PIP_2 headgroup interactions with the HPLC column proved to be successful, i.e. the initial experiments showed improved separation compared to that observed in full length PIP_2 regioisomers. Further, several optimisation approaches were used to enhance the system's stability and sensitivity. Presence of methanol in the binary HPLC mix diminished separation to a certain extent, but at the same time minimised phosphate migration around the inositol ring and improved the peak shape. Switching to a longer c18 column with an amide spacer (c18 amide column), created additional interaction sites for phosphatidylinositol lipid headgroups and helped in their differential interaction with the column support. Finally, running the HPLC methods at high temperatures sharpened the peaks and further increased separation without losing sensitivity.

Method validation in human platelets suggests, that the levels of PI(3,4)P_2 and PI(4,5)P_2 aldehydes are quantifiable at both basal (unstimulated) and thrombin-stimulated conditions, and that their dynamic range lies within the machines' linear response. Deuterated PIP_2 equivalents, despite the deuterium effect observed, are still useful internal standards and can be used to correct for extraction errors, and serve as a reference to identify endogenous PIP_2 peaks. Limitation of this mass spectrometry technique comes from the fact, that the product of C38:4 PI(3,4,5)P_3 ozonolysis gave a multi-peak chromatogram and we were unable to resolve why this was or to prevent it occurring (data not shown). Therefore, whenever the levels of PI(3,4,5)P_3 are to be compared to its dephosphorylation products, PI(3,4)P_2 and PI(4,5)P_2, two separate methods must be run in parallel for confident quantification.

Previous work in our group has indicated that the third phosphatidylinositol bisphosphate regioisomer found in cells, PI(3,5)P_2, elutes slightly later than PI(4,5)P_2 under the HPLC conditions used in the studies described above (data not shown). However, the resolution of this regioisomer from PI(4,5)P_2 was sufficiently poor, and its concentration is sufficiently small in mammalian cells (Dove, Dong et al. 2009), that we

consider it to make an insignificant contribution to the 'PI(4,5)P_2 peak' identified here. Moreover, the HPLC conditions were designed to ensure no overlap between the chromatographic peaks of PI(3,4)P_2 and PI(3,5)P_2 and hence allow PI(3,4)P_2 quantitation without contamination from the two other regioisomers, PI(4,5)P_2 and PI(3,5)P_2. Nevertheless, further modification of the current HPLC conditions will be required if one wants to reliably quantify PI(3,5)P_2.

Finally, our method for separating PI(3,4)P_2 and PI(4,5)P_2 aldehydes relies on ozone-catalysed cleavage of the C38:4 molecular species of this lipid. This means further HPLC conditions would need to be developed to separate other molecular species. However, previous work has indicated that the most abundant molecular species of phosphatidylinositol lipids in primary mammalian tissues is C38:4, and further, that different molecular species of PI(3,4,5)P_3 behave similarly when cells in culture are stimulated by receptors coupled to class I PI3Ks (Anderson, Juvin et al. 2016).

Chapter 4 PTEN and INPP4B synergistically regulate the accumulation of $PI(3,4)P_2$ in EGF-stimulated Mcf10a cells

4.1 Introduction

After achieving the first goal of this PhD project, we were equipped with two mass spectrometry-based methods, optimised to quantitatively measure three phosphatidylinositol lipids of interest: $PI(3,4)P_2$, $PI(4,5)P_2$ and $PI(3,4,5)P_3$. The next big question that we decided to address was to find a suitable biological system in which we could follow enzymatic conversions of these phosphatidylinositols in the context of class I PI3K signalling, with a particular interest in $PI(3,4)P_2$. Currently, distinct points of view dominate the literature, when it comes to the physiological roles of $PI(3,4)P_2$ in the cell (refer to Chapter 1.4 for more detailed discussion). One point of view is that $PI(3,4)P_2$ is solely a dephosphorylation product of $PI(3,4,5)P_3$, en route to silencing class I PI3K-triggered signalling. Another point of view suggests $PI(3,4)P_2$ in this setting is 'equivalent to $PI(3,4,5)P_3$' in the activation of AKT. Finally, another group of scientists is of the opinion that the apparent bifurcation of the dephosphorylation pathway at the level of $PI(3,4,5)P_3$, i.e. the reason for evolutionary development of $PI(3,4,5)P_3$-specific 3- and 5-phosphatases, is that it provides the cell with a mechanism to diverge the class I PI3K signalling away from the canonical PI3K/AKT axis, hence implying AKT-independent roles of $PI(3,4)P_2$. Evidence in support of this hypothesis has started to emerge with the discovery of the first $PI(3,4)P_2$-specific PH-domain containing proteins TAPP1/2, which unfortunately have not yet been linked to a unique and clear physiological role. Further, LPD, TKS5 and SNX9 are PH or PX domain-containing proteins which have been implicated in regulation by $PI(3,4)P_2$, but, thus far, the evidence provided for their $PI(3,4)P_2$-selectivity is unconvincing. Thus, in most cases, we have ended up in a 'grey zone', trying to define how essential/dispensable $PI(3,4)P_2$ is in contributing to the physiological processes being observed.

Irrespective of the precise role that $PI(3,4)P_2$ plays, in order to better understand the dynamics of processes regulated by class I PI3K, it will be important to model the

relative fluxes of its catalytic product PI(3,4,5)P_3 through 3- versus 5-dephosphorylation pathways. The initial 'on/off' switch model of PH domain - phosphatidylinositol lipid binding has evolved into an 'avidity binding' model, in which this initial interaction is in many cases insufficient and must be accompanied by additional protein-protein interactions to grant efficient signal transduction. Moreover, time-controlled 'bursts' or sustained, elevated levels of certain phosphatidylinositol lipids are now thought to be necessary to trigger certain biological responses. Therefore, the ability to quantify the appearance of PI(3,4,5)P_3 and PI(3,4)P_2 in the cell in a time-resolved manner, will advance our understanding of some of these dependencies. Further, such quantification will help assess the relative roles of enzyme activities considered to catalyse PI(3,4,5)P_3 3-dephosphorylation, such as the well described tumour suppressor PTEN, and put them into perspective with the relevant 5-phosphatases, such as SHIP1/2, that convert this second messenger into PI(3,4)P_2.

We initially embarked on a characterisation of PI(3,4,5)P_3 and PI(3,4)P_2 accumulation in response to EGF-stimulation of Mcf10a cells. These cells are an immortalised, non-transformed human breast epithelial cell line that many laboratories have used as a model for understanding the role of class I PI3K signalling in breast cancer. The original Mcf10 cells were isolated from a mammary gland of a 36 year old woman with fibrocystic disease, characterised by several abnormalities and hyperplasia but no tumorigenic potential. Among the three known sublines of Mcf10 cells, two underwent a spontaneous immortalisation in culture - the floating Mcf10f and adherent Mcf10a subtype (Soule, Maloney et al. 1990). The fact that Mcf10a cells retain the ability to form acini when grown in collagen, their tendency to form monolayers when grown on support and reliance on growth factors and hormones, makes Mcf10a cells an ideal model cell line of human breast epithelium and a suitable non-transformed control, when used in conjunction with a panel of breast cancer cell lines. The parental Mcf10a cells (referred to as 'WT' Mcf10a cells) have also been subject to homozygous knockout of *PTEN*, via deletion of exon 2, thus generating an isogenic *PTEN*$^{-/-}$ Mcf10a cell line (referred to as 'PTEN-KO' Mcf10a cells; Horizon Drug Discovery), making them an ideal starting point for characterising the impact of PTEN on this pathway.

4.2 Results

During the initial phase of this project, an extensive siRNA genetic screen was performed in our laboratory to identify the major lipid phosphatases that significantly contribute to $PI(3,4,5)P_3$ hydrolysis during EGF-stimulation of Mcf10a cells. Only depletion of PTEN or SHIP2 lead to significant changes in $PI(3,4,5)P_3$ accumulation (data not shown). INPP4A and INPP4B have previously been identified as 4-phosphatases acting on $PI(3,4)P_2$. Therefore, we initially chose to evaluate the impact of genetically manipulating the expression of PTEN, SHIP2, INPP4A and INPP4B by homologous gene deletion (PTEN), siRNA knock-down (PTEN, SHIP2, INPP4A and INPP4B) or CRISPR/Cas9 editing (SHIP2, INPP4B) on $PI(3,4,5)P_3$ and $PI(3,4)P_2$ accumulation in these cells.

4.2.1 Calibration curves for quantitative measurement of $PI(3,4)P_2$, $PI(4,5)P_2$ and $PI(3,4,5)P_3$ in Mcf10a cells

Generation of calibration curves is the prerequisite of any quantitative mass spectrometry analysis that involves absolute quantitation. The use of internal standards in mass spectrometry is a powerful tool, provided that several conditions are met. In lipidomics, the use of short chain, synthetic phospholipids with an odd number of carbon atoms on one of the acyl chains has been the most common practice. Such molecules are in general more stable and easier to synthesise, and, most importantly, provide a spectral separation from the naturally occurring analogues. However, the physicochemical character of such standards may differ, which implies the requirement for additional tests to compare their solubility in the mobile phase, ionisation efficiency and fragmentation patterns. Therefore, generation of heavier, deuterium-substituted lipid analogues has been accepted as the strategy that provides the 'ideal' internal standards, which fulfil all the requirements and circumvent the need for laborious characterisation.

For the purpose of the planned experiments, a series of calibration curves was prepared in Mcf10a cells for each of the phosphatidylinositol lipids that we intended to quantify, i.e. $PI(3,4)P_2$, $PI(4,5)P_2$, and $PI(3,4,5)P_3$. This involved preparation of cells depleted of endogenous PIP_2 lipids to minimize the background signal and generation of a series of primary lipid extracts. Next, specific amounts of C38:4 phosphatidylinositol

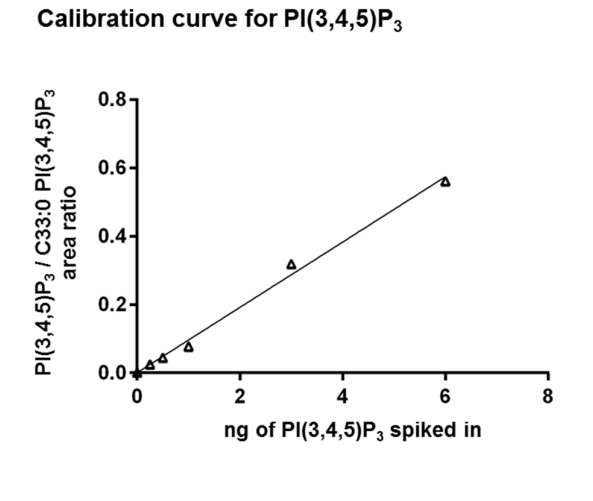

Figure 4.1 Calibration curve for PI(3,4,5)P3

Mcf10a cells were incubated with rotenone and CCCP decoupler for 24 hrs to reduce endogenous levels of polyphosphatidylinositol lipids. The indicated quantities of synthetic C38:4 PI(3,4,5)P3 and a fixed quantity of C33:0 PI(3,4,5)P3 were then added to the primary lipid extracts, processed and analysed by ESI-HPLC MS/MS on the c4 column.

lipids and their respective internal standards were added to each sample, followed by lipid extraction to obtain a calibration curve for $PI(3,4,5)P_3$ (Figure 4.1), or lipid extraction and ozonolysis to obtain calibration curves for $PI(3,4)P_2$ and $PI(4,5)P_2$ (Figure 4.2).

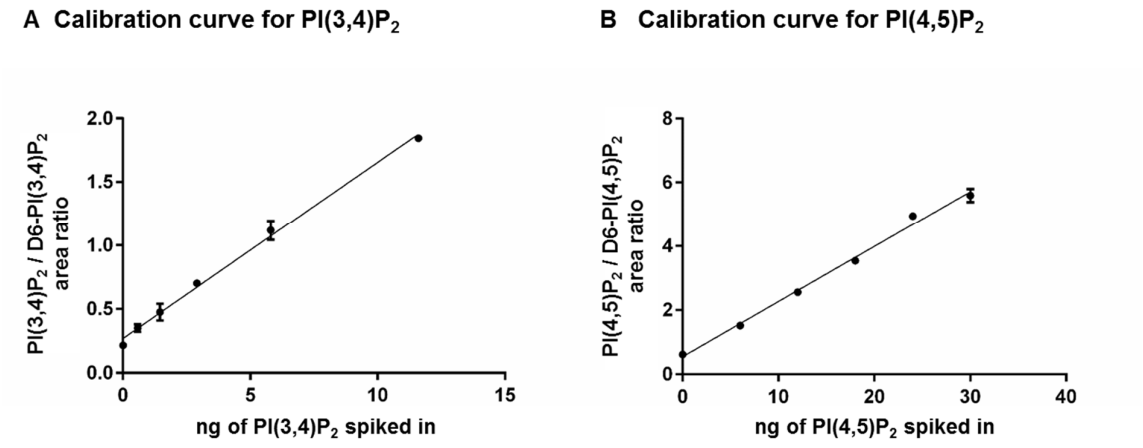

Figure 4.2 Calibration curves for PI(3,4)P2 and PI(4,5)P2 in Mcf10a cells

*(**A**) Calibration curve for $PI(3,4)P_2$ and (**B**) for $PI(4,5)P_2$. Mcf10a cells were incubated with rotenone and CCCP decoupler for 24 hrs to reduce endogenous levels of polyphosphatidylinositol lipids. The indicated quantities of synthetic C38:4 $PI(3,4)P_2$ or $PI(4,5)P_2$ and a fixed quantity of D6-C38:4 $PI(3,4)P_2$ and $PI(4,5)P_2$ were then added to the primary lipid extracts, processed, ozonolysed and analysed by ESI-HPLC MS/MS on the c18 amide column.*

4.2.2 The contribution of PTEN and INPP4B to the accumulation of PI(3,4)P_2 in EGF-stimulated Mcf10a cells

PI(4,5)P_2 is the most abundant of all phosphorylated inositol lipids and in quiescent cells is estimated to represent 2-5% of the total lipid content (Hammond and Balla 2015). Its levels in the plasma membrane are thought to be kept within tight margins by active PI4P 5-kinases and PI(4,5)P_2 5-phosphatases, which allow fast replacement of the PI(4,5)P_2 used by PLC and class I PI3K. The levels of PI(3,4)P_2 and PI(3,4,5)P_3, on the other hand, are much smaller and in the resting cells amount to <5% relative to cellular PI(4,5)P_2 levels. This makes both of these phosphatidylinositol lipids virtually invisible to detection by semi-quantitative methods like TLC, specific fluorescently-tagged PH domains or antibodies. The situation dramatically changes when the cell responds to extracellular agonists that activate class I PI3K. Consequently, a burst of PI(3,4,5)P_3 is generated at the plasma membrane (in some cells appearing within seconds after stimulation), which rapidly disappears, as a result of two mechanisms: PI(3,4,5)P_3 hydrolysis by specialised phosphatases and desensitisation/recycling of the activated receptor. Therefore, what we observe is transient accumulation of PI(3,4,5)P_3 that is a result of several catalytic reactions which, in a coordinated way, synthesise (class I PI3K) and hydrolyse (e.g. PTEN and SHIP2) PI(3,4,5)P_3. In a similar fashion, several enzymatic reactions can be drawn as inputs/outputs that affect the temporal accumulation of PI(3,4)P_2 in stimulated cells. Although the physiological roles of the major phosphatases implicated in these processes have been widely assumed, relatively little is known about their relative contribution to shaping the actual amounts of PI(3,4,5)P_3 and PI(3,4,)P_2 that accumulate downstream of class I PI3K activation.

We monitored the levels of PI, PIP, PI(3,4)P_2, PI(4,5)P_2 and PI(3,4,5)P_3 in starved and EGF-stimulated Mcf10a cells. The levels of the three most important phosphatidylinositol lipids to this study, i.e. PI(3,4)P_2, PI(4,5)P_2 and PI(3,4,5)P_3, were read off the previously prepared calibration curves and converted into nmoles. Next, we corrected these numbers for varying cell number between individual samples and experiments by using a ratio to the levels of PI (i.e. PI(3,4)P_2/PI, PI(4,5)P_2/PI and PI(3,4,5)P_3/PI), and then used an average correction factor between cell number and the levels of PI, to plot the amount of each lipid as 'nmol/250 000 cells'. Due to our inability

to resolve PIP regioisomers by HPLC, the total PIP was plotted, corrected for the number of cells.

4.2.2.1 PI(3,4,5)P_3 dephosphorylation is shared between the 3- and 5-phosphatases

Unstimulated PI(3,4,5)P_3 levels remain broadly similar across genotypes and the slight variations observed are within the error of measurement (Figure 4.3). In WT Mcf10a cells, EGF stimulates a ~3-4 fold increase in PI(3,4,5)P_3 measured at 1min, which then gradually drops to near basal level by 15min. Depletion of SHIP2 from Mcf10a cells leads to an almost doubling of the peak amount of PI(3,4,5)P_3 before it starts to decay.

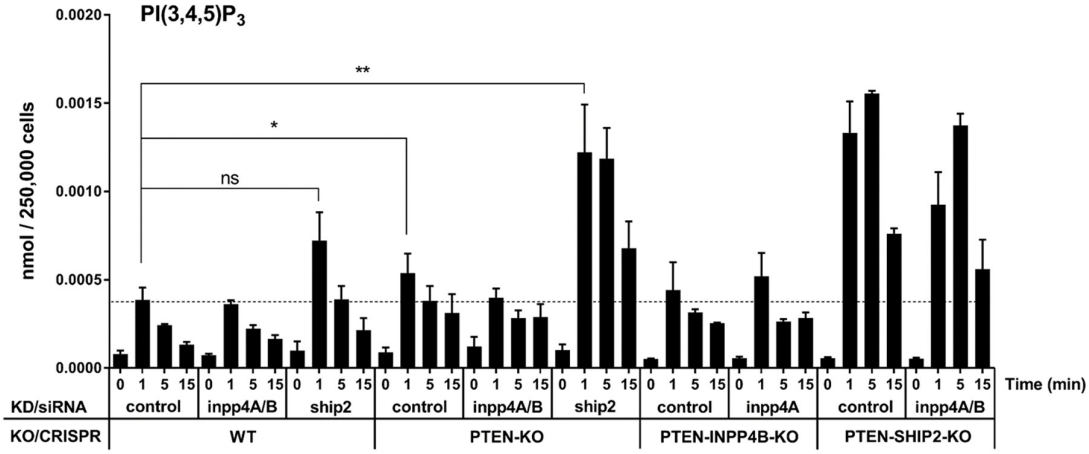

Figure 4.3 PI(3,4,5)P_3 levels in Mcf10a cells

Isogenic WT or PTEN$^{-/-}$ Mcf10a cells were genetically manipulated through siRNA-mediated suppression or CRISPR-gene editing, as indicated, then starved and stimulated with EGF. Measurement of PI(3,4,5)P_3 was performed by HPLC-ESI MS/MS using a c4 column and data represent means ± SD of 3 biological replicates (for siRNA suppression in WT or PTEN-KO cells) or 3 technical replicates (for PTEN-INPP4B-KO or PTEN-SHIP2-KO cells). One-way repeated measures ANOVA followed by post-hoc Dunnett's test were applied to the data to compare the groups of interest against control (see Materials and Methods).

PTEN-KO Mcf10a cells, on the other hand, show a slightly smaller increase in the peak stimulated PI(3,4,5)P_3 levels and the kinetics of its removal from the cell is relatively slower. Importantly, EGF stimulation of PTEN-KO Mcf10a cells with suppressed SHIP2 shows a substantial accumulation of PI(3,4,5)P_3 at 1min but even under such conditions, more than 30% of the lipid is lost by 15min. This suggests other phosphatases operate in Mcf10a cells, which are able to hydrolyse PI(3,4,5)P_3 in the absence of PTEN and SHIP2.

It is worth noting, that neither suppression of INPP4B by siRNA, nor its CRISPR-mediated deletion, cause a measurable increase in the levels of $PI(3,4,5)P_3$ in Mcf10a cells, thus putting into perspective the previously reported role of this 4-phosphatase against $PI(3,4,5)P_3$ (Kofuji, Kimura et al. 2015). If anything, INPP4B seems to negatively regulate $PI(3,4,5)P_3$ levels, via an unknown mechanism. INPP4A does not seem to have a role in $PI(3,4,5)P_3$ hydrolysis. The data depicted in Figure 4.3 represents $PI(3,4,5)P_3$ response patterns of the major species in Mcf10a cells, i.e. with the stearoyl (C18:0) fatty acyl chain on position *sn1* and arachidonoyl (C20:4) on position *sn2*. Comparing this C38:4 $PI(3,4,5)P_3$ data against the less abundant species, e.g. C36:3 or C36:2 $PI(3,4,5)P_3$, showed similar patterns in response to EGF and genetic alterations (data not shown). This gave us confidence that the C38:4 $PI(3,4)P_2$ and C38:4 $PI(4,5)P_2$ measured by the new HPLC-ESI MS/MS method should accurately represent the total $PI(3,4)P_2$ and total $PI(4,5)P_2$ present in the Mcf10a cells.

4.2.2.2 Unexpectedly high levels of $PI(3,4)P_2$ accumulate in EGF-stimulated Mcf10a cells depleted of PTEN and INPP4B

The basal levels of $PI(3,4)P_2$ in starved Mcf10a cells were apparently higher than the equivalent $PI(3,4,5)P_3$ levels, irrespective of the genotype (Figure 4.4A). This was an interesting observation and our attempts to determine the origin of basal $PI(3,4)P_2$ in Mcf10a cells will be discussed in more detail in Chapter 5. EGF did not stimulate a measurable increase in $PI(3,4)P_2$ levels above this high basal level. Moreover, neither depletion of SHIP2 nor combined depletion of INPP4A and INPP4B in these cells

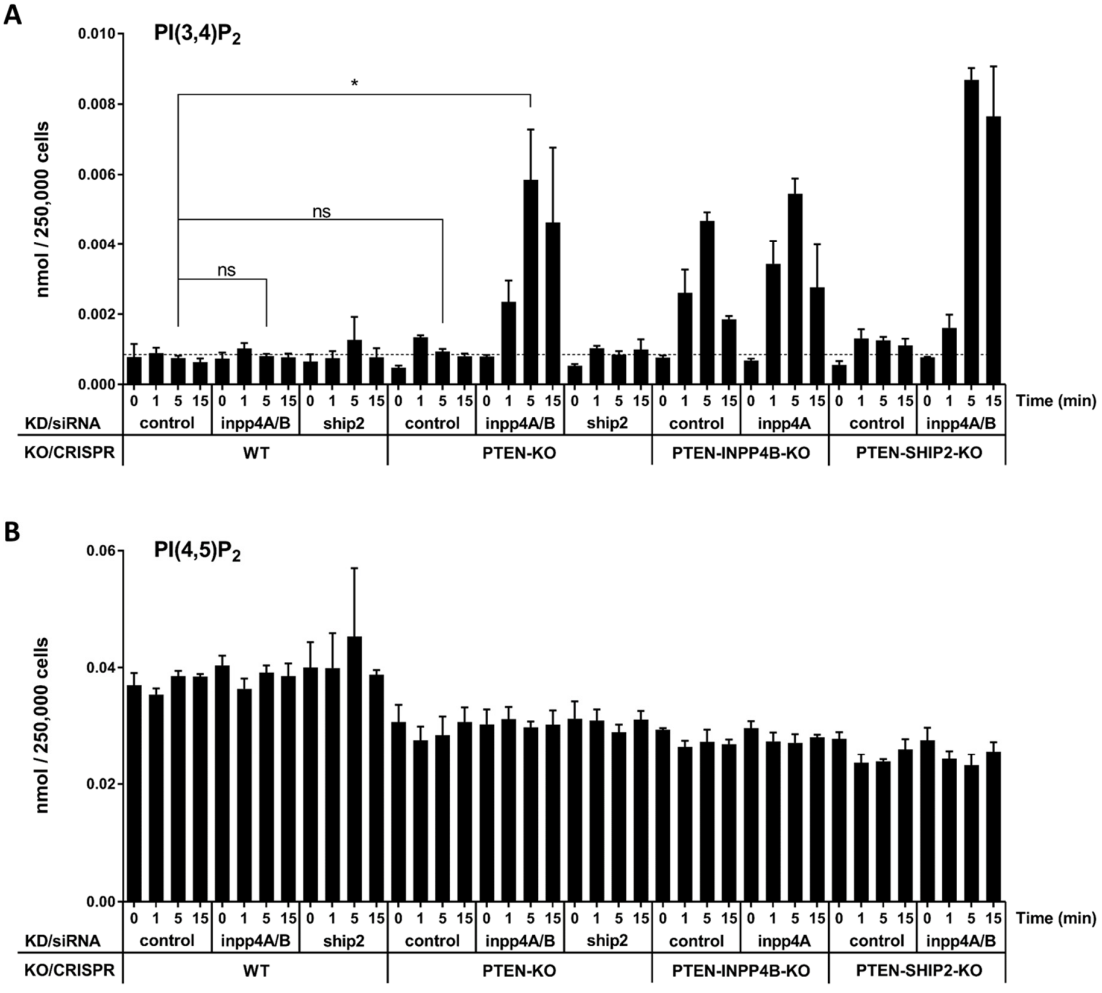

Figure 4.4 $PI(3,4)P_2$ and $PI(4,5)P_2$ levels in Mcf10a cells

*Isogenic WT or PTEN$^{-/-}$ Mcf10a cells were genetically manipulated through siRNA-mediated suppression or CRISPR-gene editing, as indicated, then starved and stimulated with EGF. Measurement of $PI(3,4)P_2$ (**A**) and $PI(4,5)P_2$ (**B**) was performed by HPLC-ESI MS/MS using a c18 column and data represent means ± SD of 3 biological replicates (for siRNA suppression in WT or PTEN-KO cells) or 3 technical replicates (for PTEN-INPP4B-KO or PTEN-SHIP2-KO cells). One-way repeated measures ANOVA followed by post-hoc Dunnett's test were applied to the data to compare the groups of interest against control (see Materials and Methods).*

elevated $PI(3,4)P_2$, which was surprising in the latter case, as INPP4A and INPP4B are both well-defined $PI(3,4)P_2$ 4-phosphatases. Similarly, PTEN deletion in the cells, which would be expected to shift the burden of $PI(3,4,5)P_3$ dephosphorylation onto 5-phosphatases, did not lead to a significant change in the $PI(3,4)P_2$ time course.

Strikingly, INPP4A and INPP4B depletion in the PTEN-KO Mcf10a cells resulted in the accumulation of large amounts of $PI(3,4)P_2$ post EGF stimulation, which at 5min was estimated to represent 15-20% of endogenous $PI(4,5)P_2$. Furthermore, generation of PTEN-INPP4B-KO cells via CRISPR gene editing confirmed this observation and suggested that INPP4B and not INPP4A, is responsible for $PI(3,4)P_2$ hydrolysis in PTEN-KO cells. Finally, we noted that loss of SHIP2 did not have a significant impact on the accumulation of EGF-stimulated $PI(3,4)P_2$ in PTEN-KO cells with knock-down of INPP4A and INPP4B.

From the data gathered, we noticed a decrease in $PI(4,5)P_2$ and a slight increase in PIP levels, related to *PTEN* loss in Mcf10a cells (Figure 4.4B and Figure 4.5). These measurements refer to the C38:4 species of these lipids only, but when the total PIP_2 and total PIP levels, i.e. a sum of all acyl chain variants routinely measured in each sample, were compared between WT and PTEN-KO Mcf10a cells, no significant differences were

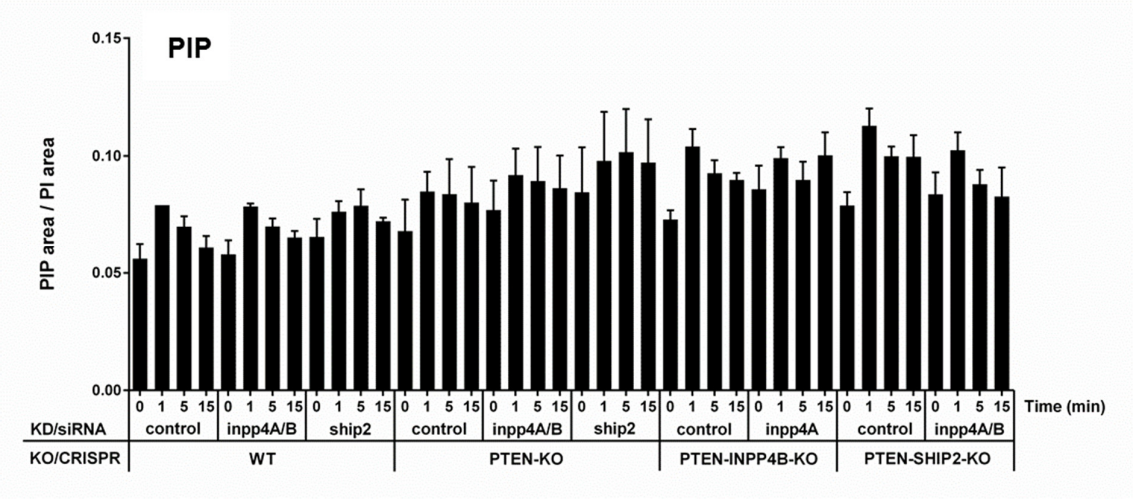

Figure 4.5 PIP levels in Mcf10a cells with altered phosphatase expression

Isogenic WT or PTEN-/- Mcf10a cells were genetically manipulated through siRNA-mediated suppression or CRISPR-gene editing, as indicated, then starved and stimulated with EGF. Measurement of PIP was performed by HPLC-ESI MS/MS using a C4 column and data represent means ± SD of 3 biological replicates (for siRNA suppression in WT or PTEN-KO cells) or 3 technical replicates (for PTEN-INPP4B-KO or PTEN-SHIP2-KO cells).

seen (data not shown). Parallel studies performed in our laboratory suggest that acyl remodelling processes may be occurring in Mcf10a cells, which are decoupled from class I PI3K signalling but emerge upon *PTEN* deletion.

4.2.3 Phosphorylation levels of EGFR in genetically modified Mcf10a cells

The next step was to test the essential elements of the PI3K signalling pathway for potential rewiring processes that might have occurred in Mcf10a cells challenged by our genetic manipulations. EGFR monomer, upon association with the growth factor ligand, undergoes dimerization and conformational changes, which activate its intrinsic, protein kinase activity. The autophosphorylation reactions that occur on several cytosolic tyrosine residues are crucial to efficiently transduce the original signal to the cell interior. In order to be able to judge whether signal amplification, and effectively cell responsiveness, is comparable across different Mcf10a genotypes, we assessed the level

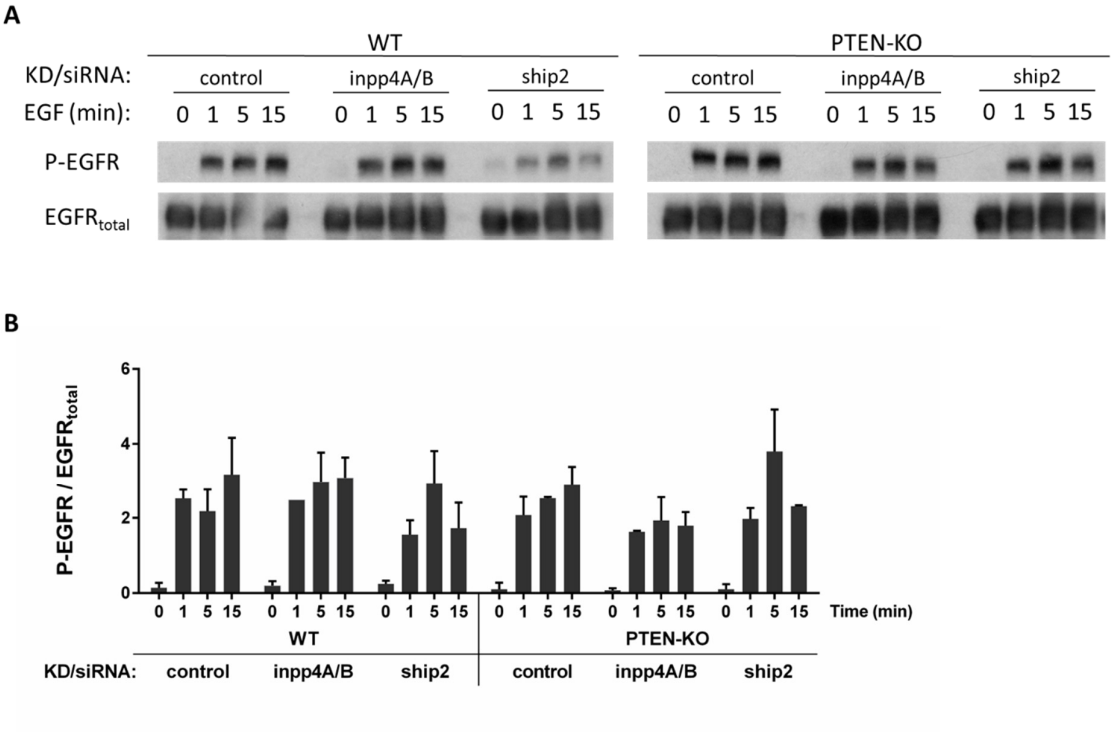

Figure 4.6 Phosphorylation of the EGFR in genetically modified Mcf10a cells

*The phosphorylation of the EGFR in Mcf10a cells treated with the indicated siRNAs, starved and then stimulated for the indicated times with EGF. Representative Western blots (**A**) are shown, together with the result of quantifying analogous blots using Aida software (**B**); data are for the phospho-EGFR levels normalised to total EGFR levels, expressed as means ± SD of three independent experiments.*

of EGF receptor phosphorylation on ^{1068}Tyr, known to associate with GAB and GRB adaptors (Figure 4.6). We did not observe significant differences in the levels of EGFR phosphorylation between genotypes.

4.2.4 The effect of siRNA suppression and CRSIPR/Cas9 gene editing on the expression level of phosphatases in Mcf10a cells

We next performed a series of experiments to evaluate the expression levels of relevant lipid phosphatases in Mcf10a cells exposed to treatment with siRNA (Figure 4.7) or gene deletion by CRISPR/Cas9 (Figure 4.8). As can be seen from Figure 4.7, the efficiency of mRNA targeting was satisfactory for all selected phosphatases, and was estimated to reach 70-80% across multiple experiments.

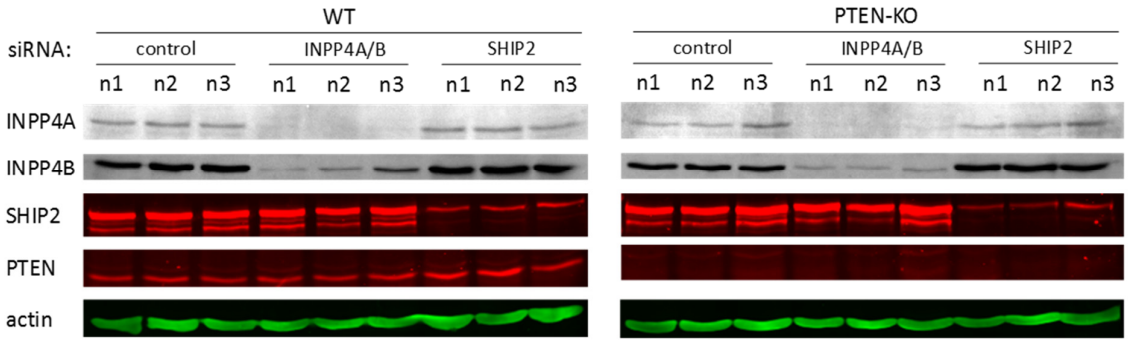

Figure 4.7 Expression of phosphatases in cell populations treated with siRNA

Expression of phosphatases in Mcf10a cell clones derived by siRNA gene suppression. A panel of Western blots is shown with data coming from three individual biological experiments.

The primary purpose for generation of CRISPR/Cas9 knockout clones in WT and PTEN-KO Mcf10a cells, was to repeat the most crucial mass spectrometry experiments, by performing phosphatidylinositol lipid quantitation in independently derived cells (see section 4.2.2.1 and 4.2.2.2), and to compare these findings to the results obtained by an siRNA knock-down approach. The Western blot analysis confirmed a successful knockout of SHIP2 or INPP4B in these cells and validated an overall lack of compensation by other lipid phosphatases. The only observation independent of our direct genetic intervention was a substantial decrease in INPP4B expression in PTEN-KO Mcf10a cells compared to the WT control.

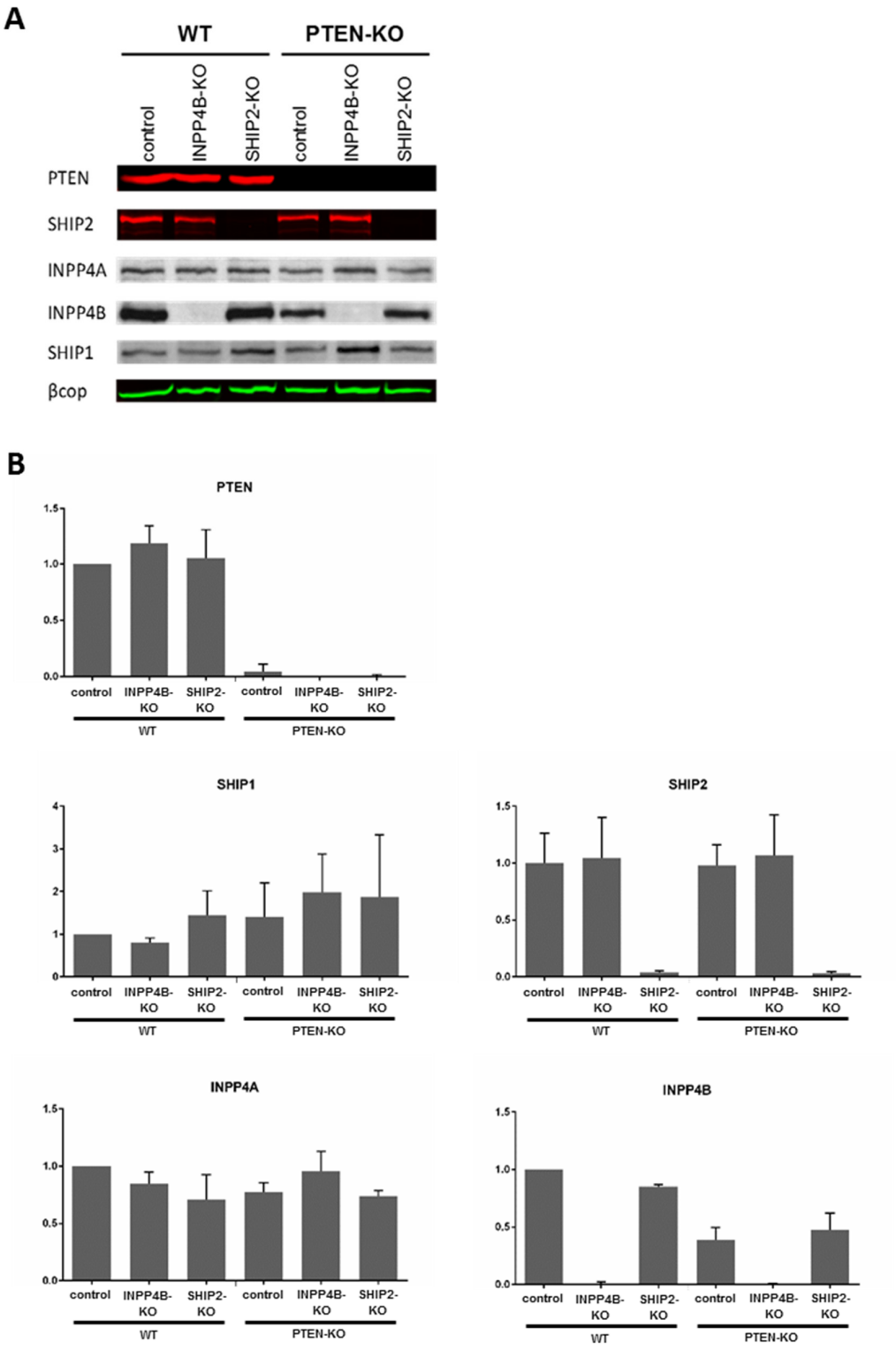

Figure 4.8 Expression of phosphatases in Mcf10a clones derived by CRISPR/Cas9 gene editing

*Expression of phosphatases in Mcf10a cell clones derived by CRISPR/Cas9 gene editing. A representative Western blot (**A**) is shown, together with the results of quantifying analogous blots using LiCor or Aida software (**B**); data are for expression levels of the indicated protein normalised to WT and are means ± SD of three independent experiments.*

4.3 Discussion

Combining the two HPLC-ESI MS/MS methods: 1) the well-established one, which in our laboratory has been routinely used for phosphatidylinositol lipid profiling, i.e. detection of PI, PIP, PIP_2 and $PI(3,4,5)P_3$ lipids that vary in acyl chain composition with good specificity and sensitivity, and 2) the newly established one that allows regioisomer-specific detection of C38:4 $PI(3,4)P_2$ and $PI(4,5)P_2$, proved to be successful in providing an insight into phosphatidylinositol lipid dynamics that occurs in EGF-stimulated Mcf10a cells. The added value of careful experimental design and preparation of calibration curves, gave us confidence in the quality of $PI(3,4)P_2$, $PI(4,5)P_2$ and $PI(3,4,5)P_3$ quantitation and provided a solid basis for the forthcoming experiments.

We confirmed that PTEN and SHIP2 are the major phosphatases, which in the EGF-stimulated class I PI3K-driven signalling pathway, control the levels of $PI(3,4,5)P_3$ in Mcf10a cells. Moreover, a substantial level of functional redundancy exists between these two proteins and $PI(3,4,5)P_3$ hydrolysis becomes re-routed to predominant 3- or predominant 5-dephosphorylation, in the absence of the other alternative. Interestingly, our initial siRNA screen did not predict the fact, that in the absence of both PTEN and SHIP2, $PI(3,4,5)P_3$ accumulation is still transient, implying the activity of another lipid phosphatase in such conditions - this is discussed further in Chapter 5. Finally, the measured basal and EGF-stimulated $PI(3,4,5)P_3$ levels, fall within the range previously described in the literature and confirm the highly dynamic behaviour of this second messenger.

Our observations suggested a surprisingly high basal level of $PI(3,4)P_2$ and an apparently insignificant accumulation of this lipid upon EGF-stimulation in WT cells. However, the most striking observation was the implied high flux through $PI(3,4)P_2$ that was revealed by blocking both PTEN and INPP4B. This surprisingly large accumulation of $PI(3,4)P_2$ raised an immediate question as to its origin and, more importantly, to its biological relevance in the context of cellular physiology and pathology.

In parallel, confocal and wide-field fluorescence microscopy using $PI(3,4,5)P_3$-specific (eGFP-GRP1-PH) or PI(3,4)P2-specific (mCherry-TAPP1-PH) reporters, or an anti-$PI(3,4)P_2$ antibody, was used by M. Malek in our laboratory to investigate the

localisation of PI(3,4,5)P_3 and PI(3,4)P_2 in Mcf10a cells and to independently evaluate the levels of these lipids generated upon EGF stimulation. These studies confirmed the core observations reported here using mass spectrometry, that loss of both PTEN and INPP4B leads to dramatic PI(3,4)P_2 accumulation in EGF-stimulated cells. Moreover, these studies indicated this PI(3,4)P_2 accumulation was in the plasma membrane (data not shown).

Chapter 5 EGF stimulates PI(3,4)P_2 accumulation via 5-phosphatase-mediated dephosphorylation of PI(3,4,5)P_3 in Mcf10a cells

5.1 Introduction

An important biological question that emerged from the mass spectrometry quantitation analyses was the identity of the catalytic pathways utilised by Mcf10a cells to generate the large amounts of PI(3,4)P_2 that appeared in EGF-stimulated PTEN-INPP4B-KO Mcf10a cells and to identify the key enzymes which control the process. Over 40 lipid phosphatases and kinases, with overlapping substrate preferences, have been suggested to act in the interconversion of phosphatidylinositol lipids and phosphates (Figure 1.5)(Balla 2013). In most cases, the extent to which any one of them is responsible for a defined reaction *in vivo* is not yet clear. Further, while several alternative pathways may coexist in the cell, some appear to become activated only under certain conditions, possibly when a significant 'biological pressure' is exerted and the cell needs to react to prevent from developing cytotoxicity. One such example may be the case of INPP4B, which under physiological conditions is a weak PI(3,4,5)P_3 phosphatase, but has been shown to regulate the levels of this lipid in the thyroid tissue of *Pten*$^{+/-}$ mice, and when inactive, leads to tumour development and metastasis (Kofuji, Kimura et al. 2015).

Several arguments have been raised in the past for different pathways leading to PI(3,4)P_2 accumulation. There is substantial evidence that PI(3,4,5)P_3 produced by activation of class I PI3Ks can be dephosphorylated by 5-phosphatases to produce a lagged accumulation of PI(3,4)P_2 (Stephens, Hughes et al. 1991, Hawkins, Jackson et al. 1992). The best studied of these 5-phosphatases is the SHIP family, but we found that knock-down of SHIP2 expression in PTEN-INPP4B-KO Mcf10a cells had little apparent effect on EGF-stimulated PI(3,4)P_2 accumulation (see previous Chapter), suggesting either other 5-phosphatases are involved in the generation of this lipid or, that this

hypothesis is incorrect. In support of the former, we also noted that PI(3,4,5)P_3 accumulation was still transient in PTEN-SHIP2-KO cells.

There is also very good evidence that PI(3,4)P_2 can be generated directly by PI3K-C2α (Posor, Eichhorn-Gruenig et al. 2013). Although the process was described in the context of clathrin-mediated endocytosis, and other work in our laboratory indicates that the PI(3,4)P_2 we measure in EGF-stimulated Mcf10a cells lacking both PTEN and INPP4B accumulates at the plasma membrane, we cannot rule out a class II PI3K in this process, especially given that previous work has indicated class II PI3Ks can be activated by EGF (Arcaro, Zvelebil et al. 2000).

We therefore sought to establish the source of PI(3,4)P_2 in our experiments, with a focus on investigating both class I PI3K/5-phosphatase and class II PI3K-mediated routes.

5.2 Results

The era of initial discoveries uncovering the mechanistic and physiological roles of PI3K was dominated by the use of two broadly specific inhibitors, wortmannin and LY294002. However, the division of the PI3K family into three classes based on their divergent regulatory mechanisms, protein architecture and substrate preference, and a unique role of class I PI3K in tumorigenesis, created the urgent need for the development of isoform specific inhibitors. Such molecules not only confirmed the observations coming from mice with deletions/mutations in the specific PI3K genes, but continue to refine our knowledge about critical functions of each of these proteins. We therefore decided to make use of the commercially available small molecule inhibitors to assess the relative contributions of class I and class II PI3K isoforms in the EGF-driven generation of PI(3,4,5)P_3 and PI(3,4)P_2 in Mcf10a cells.

5.2.1 The effect of isoform-selective and pan-class I PI3K inhibitors on the accumulation of PI(3,4,5)P_3 and PI(3,4)P_2 in EGF-stimulated Mcf10a cells

The parental and PTEN-KO Mcf10a cells were previously profiled in our laboratory for the expression levels of class I PI3K and other genes by RNA sequencing (Juvin, Malek et al. 2013). The analysis of mRNA data, subsequently confirmed by Western blots, showed that p110β is the major isoform expressed in Mcf10a cells, followed by p110α, p110δ and undetectable p110γ. In contrast, EGF-stimulation pointed towards a predominant contribution of p110α in the ^{308}Thr/^{473}Ser phosphorylation of AKT. Two members of class II PI3K - PI3K-C2α and PI3K-C2β - were detected as the only isoforms expressed in Mcf10a cells (as judged by the mRNA sequencing data) and were selected as the hypothetical kinases capable of producing PI(3,4)P_2 (Kiselev, Juvin et al. 2015). In order to maximally discriminate between class I versus class II PI3K inhibition in Mcf10a cells, we decided to use a combination of two small molecule inhibitors which show high potency against p110α (PIK75) or p110β (TGX115) but inhibit PI3K-C2α and PI3K-C2β at substantially higher doses (Knight, Gonzalez et al. 2006). We investigated the effect of these inhibitors on PTEN-KO cells with depleted INPP4A/B, which on EGF stimulation produce substantial amounts of PI(3,4)P_2 and PI(3,4,5)P_3, and therefore

A

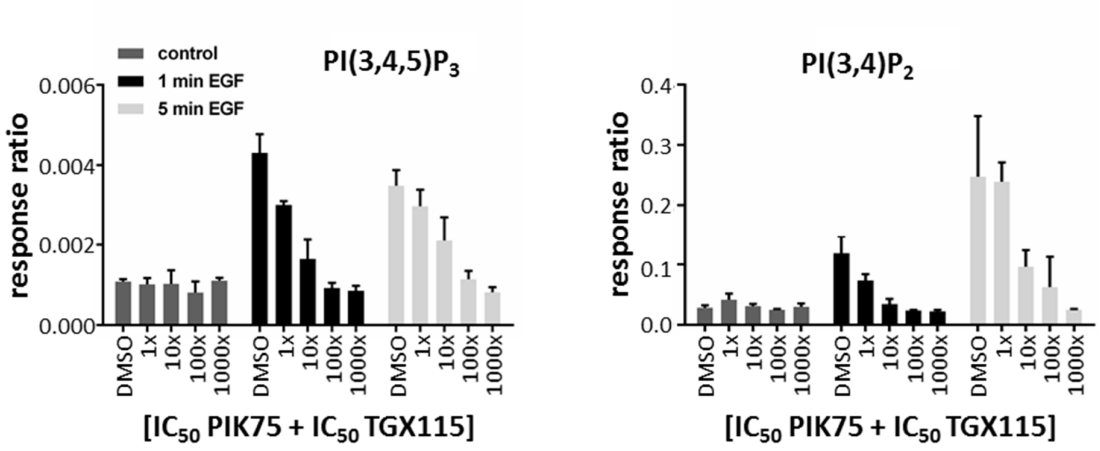

B

IC50 Values (uM)

	PIK75	TGX115
P110a	0.0058	61
P110b	1.3	0.13
P110d	0.51	0.63
PI3KC2a	10	>100
PI3KC2b	1	50

Figure 5.1 Inhibition of class I PI3K in [PTEN-KO, INPP4A/B-KD] Mcf10a cells

*Measurements by HPLC-ESI MS/MS of PI(3,4,5)P_3 or PI(3,4)P_2 (**A**) in [INPP4BA/B-KD, PTEN-KO] Mcf10a cells that were starved, pretreated for 20 min with the indicated dilutions of a mixture of PIK75 and TGX115 (1x represents 0.0058 μM PIK75 and 0.13 μM TGX115) and then stimulated with EGF (10 ng/ml) for 0, 1 or 5 min. Data are means ± SD of 3 technical replicates. The table shows IC50s of PIK75 and TGX115 against relevant PI3K activities assayed in vitro (**B**).*

generate a good dynamic range of the relevant lipids for accurate observations. Thus, cells preincubated with a mixture of PIK75 and TGX115 of increasing concentration (where 1x represents the concentration of each inhibitor in the final solution that corresponds to its IC50; see Figure 5.1B) were stimulated with EGF and the effect of PI(3,4)P_2 accumulation relative to PI(3,4,5)P_3 was monitored by HPLC-ESI MS/MS (Figure 5.1A). The inhibition profile for PI(3,4)P_2 closely resembled that for PI(3,4,5)P_3, with almost complete inhibition achieved at the 100x condition, i.e. below the IC50 values for PI3K-C2α or PI3K-C2β. This result strongly indicated that both phosphatidylinositol lipids are produced in the cell due to activity of class I PI3K.

This conclusion was supported by two parallel studies, using inhibitors of different specificity and potency. PI-103 is a commonly used pan-class I PI3K inhibitor while Byl-719 belongs to new generation compounds with documented high potency and selectivity towards p110α (Furet, Guagnano et al. 2013). Mcf10a treatment with PI-103

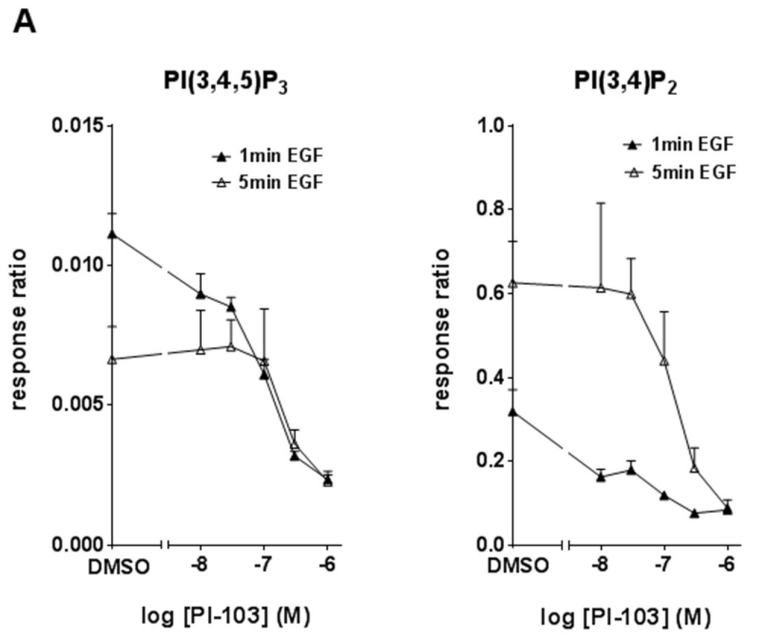

B

PI-103 IC50 values (nM)	
DNA-PK	2
p110α	8
mTORC1	20
PI 3-KC2β	26
p110δ	48
mTORC2	83
p110β	88
p110γ	150
ATR	850
ATM	920
PI 3-KC2α	~1000
hsVPS34	2300

Figure 5.2 The effect of PI-103 on the accumulation of PI(3,4,5)P_3 and PI(3,4)P_2 in EGF-stimulated [PTEN-KO, INPP4A/B-KD] Mcf10a cells

*PI(3,4,5)P_3 and PI(3,4)P_2 measurements in [INPP4A/B-KD, PTEN-KO] Mcf10a cells starved, treated with the indicated concentration of PI-103 for 20 min and then stimulated with EGF (10ng/ml) for 1 min or 5 min. Data are means ± SD of 3 technical replicates (**A**). The table shows IC50s of PI-103 against relevant PI3K activities assayed in vitro (**B**).*

produced an analogous effect to the one observed with combined PIK75/TGX115 inhibition, i.e. the extent to which class I PI3K becomes inhibited at a certain PI-103 concentration is manifested by an equivalent drop in PI(3,4,5)P_3 and PI(3,4)P_2 levels,

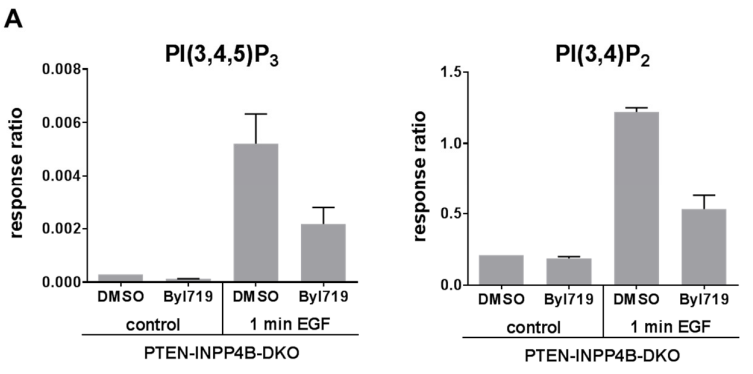

B

Byl-719 IC50 values (nM)	
p110a	5
p110b	1200
p110g	250
p110d	290

Figure 5.3 The effect of Byl-719 on the accumulation of PI(3,4,5)P_3 and PI(3,4)P_2 in EGF-stimulated [PTEN-INPP4B-KO] Mcf10a cells

*(**A**) PI(3,4,5)P_3 and PI(3,4)P_2 measurements in [PTEN-INPP4B-KO] cells starved, treated with 2μM BYL-719 or vehicle for 10 min and then stimulated with EGF (10ng/ml) or vehicle for 1 min. Data are means ± SD of three biological replicates. The table shows IC50s of Byl-719 against relevant PI3K activities assayed in vitro (**B**).*

relative to respective DMSO controls (Figure 5.2). Furthermore, the equivalent drop in levels of both phosphatidylinositol lipids upon treatment with Byl-719 strengthened our hypothesis and, as discussed earlier, corroborated p110α's role as the primary isoform driving class I PI3K signalling in Mcf10a cells (Figure 5.3).

5.2.2 The effect of class II PI3K suppression on $PI(3,4)P_2$ and $PI(3,4,5)P_3$ accumulation in EGF-stimulated Mcf10a cells

Although extensive mass spectrometry analysis using a selection of PI3K inhibitors did not imply the involvement of class II PI3K in EGF-stimulated production of $PI(3,4)P_2$, we performed an independent study, in which changes in the level of $PI(3,4,5)P_3$ and $PI(3,4)P_2$ were tested under conditions of PI3K-C2α or PI3K-C2β depletion (Figure 5.5). The suppression efficiency of targeted proteins was assessed in parallel by Westen blots (Figure 5.4), but the unsatisfactory quality of blotting data provided only a weak evidence for the level of suppression of PI3K-C2α or PI3K-C2β by the respective siRNA treatment. However, coherent with previous analyses, no discrepancy was observed in the relative effect of siRNA treatment on the accumulation of $PI(3,4,5)P_3$ versus $PI(3,4)P_2$ nor a drop in the $PI(3,4)P_2$ levels, which confirmed the lack of any apparent role for the two class II PI3K isoforms in the process. The apparent increase in $PI(3,4)P_2$ and $PI(3,4,5)P_3$ levels observed consistently in Mcf10a cells depleted of PI3K-C2α, is possibly a result of substantial growth inhibition observed in these cells and technical difficulties in normalising the mass spectrometry data between these conditions.

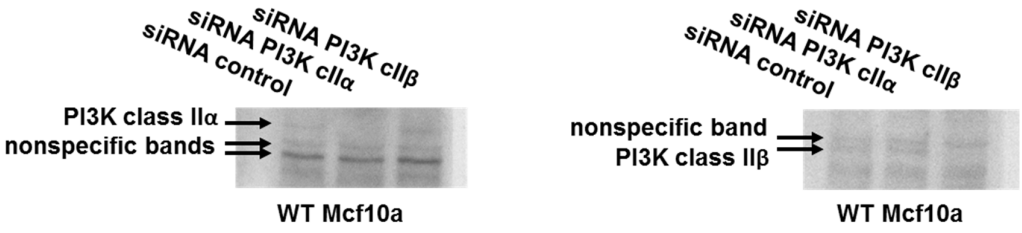

Figure 5.4 PI3K-C2α and PI3K-C2β suppression in Mcf10a cells

Exemplary Western blots showing expression of PI3K-C2α or PIK-C2β in analogous experiments to those shown in Figure 5.5.

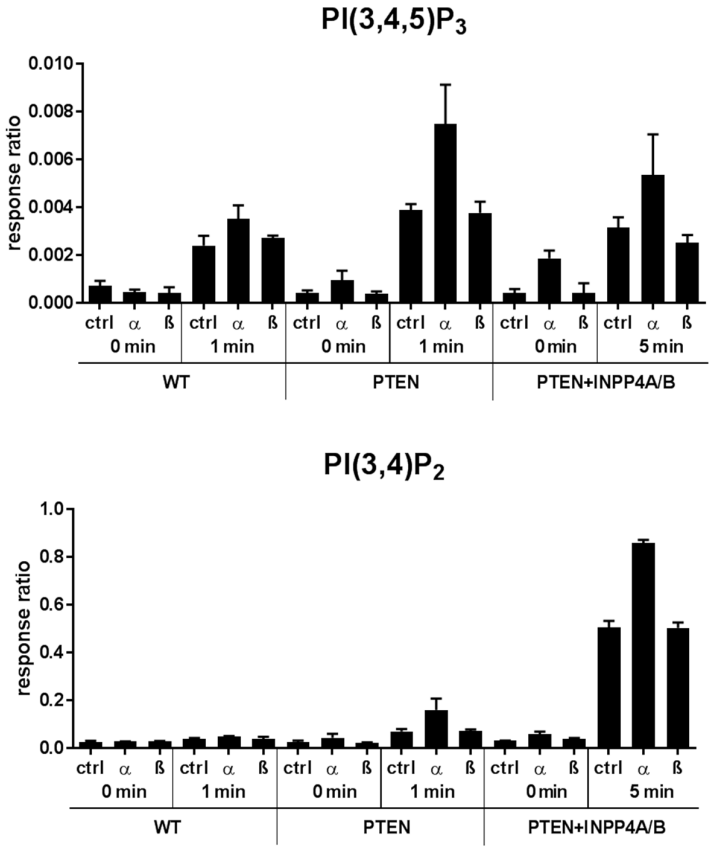

Figure 5.5 The effect of siRNA-directed suppression of Class II PI3Kα or ß on the accumulation of PI(3,4,5)P_3 and PI(3,4)P_2 in EGF-stimulated Mcf10a cells

PI(3,4,5)P_3 and PI(3,4)P_2 measurements in WT, PTEN-KO and [PTEN-KO, INPP4A/B-KD] cells incubated with the indicated siRNAs directed against Class II PI3Kα or ß, starved, and then stimulated with EGF (10ng/ml) for 5 min. Representative data of 1 of 3 biological replicates is shown, as means ± SD of 3 technical replicates.

5.2.3 The role of 5-phosphatases in PI(3,4,5)P_3 hydrolysis in Mcf10a cells

By accepting the hypothesis that PI(3,4)P_2 and PI(3,4,5)P_3 are linked together by a single, class I PI3K driven dephosphorylation reaction, one passes the burden of supplying the levels of PI(3,4)P_2 in Mcf10a cells onto the family of 5-phosphatases. Additionally, the fact that time-dependent accumulation of PI(3,4,5)P_3 in the PTEN-SHIP2-KO Mcf10a cells was transient and that INPP4B depletion in these cells led to comparable, elevated PI(3,4)P_2 levels to those seen in the PTEN-INPP4B-KO condition, suggested the existence of additional 5-phosphatases. Following this reasoning, we applied siRNA methodology to deplete multiple 5-phosphatases in [PTEN-SHIP2-KO, INPP4B-KD] cells and carried out a routine HPLC-ESI MS/MS analysis (Figure 5.6). Out

of all possibilities tested, only a combined suppression of SHIP1, SYNJ1/2, INPP5F and INPP5B showed a noticeable change in the levels of the two relevant lipids, i.e. a small increase in $PI(3,4,5)P_3$ and a small decrease of $PI(3,4)P_2$ levels. Due to the lack of a more pronounced effect, technical challenges inherent to global suppression of 5-phosphatases and the potential role of yet undiscovered 5-phosphatases in the process, we decided to look at the problem from a different angle.

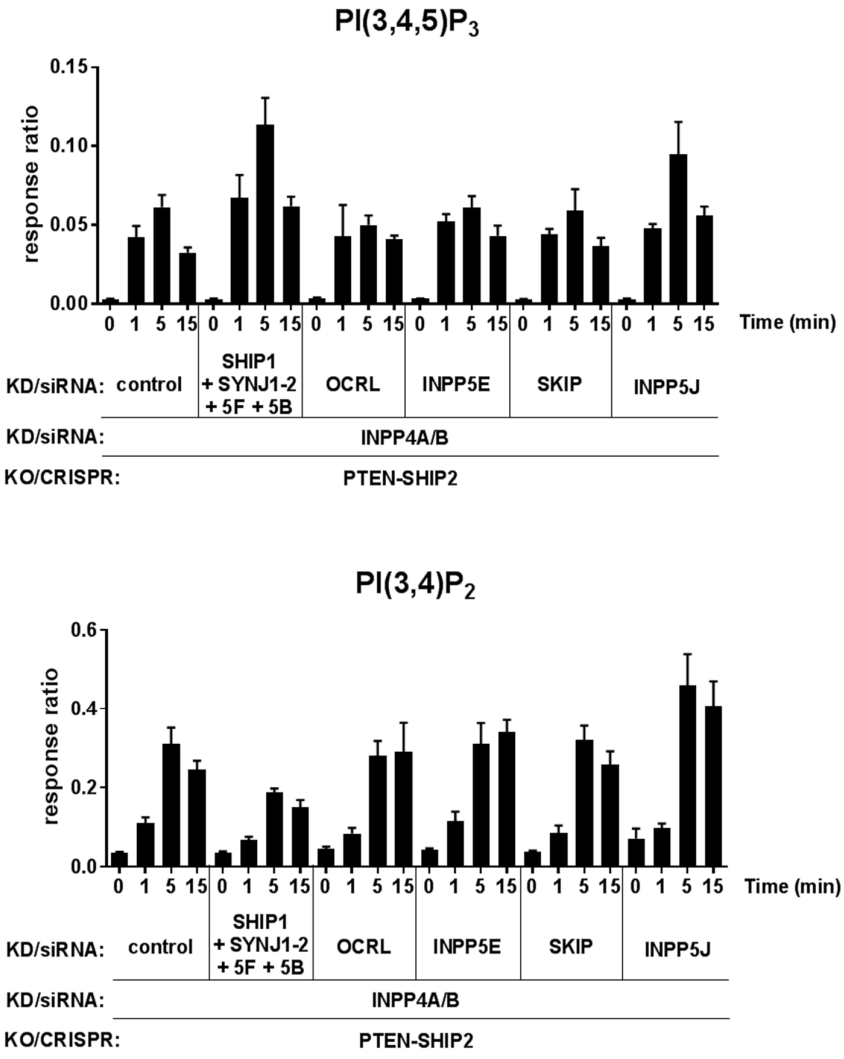

Figure 5.6 The effect of reduced 5-phosphatase expression on EGF-stimulated $PI(3,4,5)P_3$ and $PI(3,4)P_2$ accumulation in EGF-stimulated [PTEN-SHIP2-KO, INPP4A/B-KD] Mcf10a cells

$PI(3,4,5)P_3$ and $PI(3,4)P_2$ measurements in PTEN-SHIP2-KO Mcf10a cells treated with the indicated siRNAs and then starved and stimulated with EGF (10 ng/ml) for 0, 1, 5 or 15 min. Data are means ± SD of 3 technical replicates.

5.2.4 The kinetics of EGF-mediated PI(3,4,5)P_3 and PI(3,4)P_2 dephosphorylation in Mcf10a cells

Given the lack of direct evidence for the existence of a defined group of 5-phosphatases able to maintain the hydrolytic origin of PI(3,4)P_2 and the lack of any role for class II PI3K in this context, it remained possible that the source of PI(3,4)P_2 may be coming via direct 3-phosphorylation of PI4P by class I P3K. In order to evaluate the potential flux through PI(3,4,5)P_3 dephosphorylation, a series of experiments was performed, where 1μM PI-103 was added to the system 60 seconds post EGF-stimulation and the rate of PI(3,4,5)P_3 and PI(3,4)P_2 disappearance was followed by phosphatidylinositol lipid quantitation by HPLC-ESI MS/MS (Figure 5.7). This approach allowed us to monitor the speed of hydrolytic processes that in a selection of Mcf10a mutants led to PI(3,4,5)P_3 and PI(3,4)P_2 removal from the cell, and were decoupled from PI(3,4,5)P_3 production by class I PI3K. The rate of PI(3,4,5)P_3 hydrolysis in WT Mcf10a cells was very fast (with an initial half-life of < 10 sec) and within ~50 sec returned to

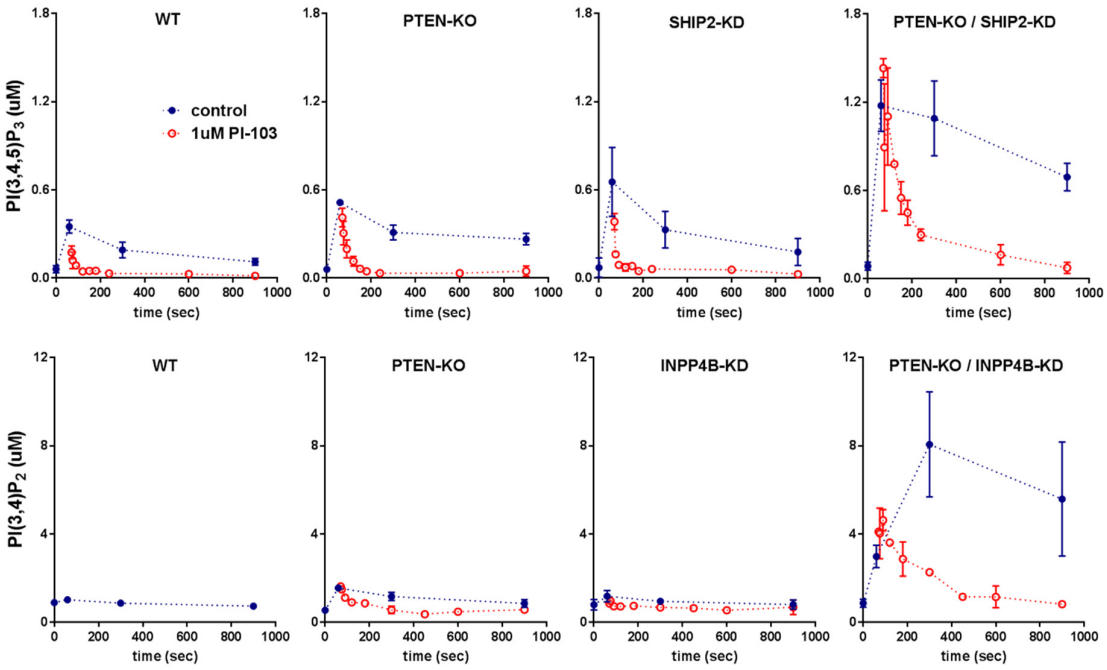

Figure 5.7 Timecourses of PI(3,4)P_2 and PI(3,4,5)P_3 hydrolysis in Mcf10a cells in response to PI-103

Time courses of PI(3,4,5)P_3 (top) and PI(3,4)P_2 (bottom) accumulation during EGF stimulation of WT, PTEN-KO, SHIP2-KD, INPP4A/B-KD, [PTEN-KO, SHIP2-KD] and [PTEN-KO, INPP4A/B-KD] cells. Cells were starved and stimulated with EGF (10ng/ml) at time 0. 60 sec post EGF-stimulation, samples were treated with either vehicle (DMSO; blue solid circles) or PI-103 (1 μM; red open circles) and incubations continued for the times indicated. Data are represented as means ±SD of 3 biological replicates.

the unstimulated level. The loss of PTEN appeared to slow the fractional rate of $PI(3,4,5)P_3$ depletion by more than loss of SHIP2, but this was very difficult to assess given the speed of $PI(3,4,5)P_3$ hydrolysis and the error in the data. However, the combined loss of both PTEN and SHIP2 did clearly lead to a substantial slowing in the fractional rate of $PI(3,4,5)P_3$ depletion, confirming that functional redundancy exists between these two phosphatases, but also directly implicating further phosphatases in $PI(3,4,5)P_3$ hydrolysis.

The kinetics of $PI(3,4,5)P_3$ decay after the addition of PI-103 to [PTEN-KO, SHIP2-KD] cells was best fitted by at least two exponential processes, with the faster process impacting less as $PI(3,4,5)P_3$ levels fell and/or time increased. This made it very difficult to derive a simple estimate for the maximum rate of $PI(3,4,5)P_3$ hydrolysis that might potentially contribute to $PI(3,4)P_2$ formation. An additional complication was that the rate of $PI(3,4)P_2$ hydrolysis could be measured accurately only in the condition of its significant accumulation in Mcf10a cells (PTEN-KO with additional suppression of INPP4B) and, further, that $PI(3,4)P_2$ levels did decay after addition of PI-103 under this condition, suggesting that the accumulation of $PI(3,4)P_2$ will be an underestimate of its true rate of formation.

We therefore collaborated with a mathematical modelling group at the Babraham Institute (N. le Novere) to model our kinetic data and evaluate the probability of a scenario in which EGF-mediated class I PI3K signalling supplies sufficient flux through $PI(3,4,5)P_3$ to support $PI(3,4)P_2$ synthesis. They modelled the core reactions involving EGFR activation, class I PI3K activation, 5- and 3- phosphatase pathways for $PI(3,4,5)P_3$ hydrolysis and 3- and 4-phosphatase pathways for $PI(3,4)P_2$ hydrolysis (not shown). They were guided by parameter limits described in the literature and assumed dephosphorylation pathways operated under substrate-limiting conditions. A good fit to our data was obtained under conditions where: $PI(3,4,5)P_3$ was dephosphorylated by PTEN and 5-phosphatases in similar proportions; 5-phosphatases supply sufficient $PI(3,4)P_2$ to account for its accumulation; these 5-phosphatases include SHIP2 and at least one other enzyme in similar proportions (the somewhat counter-intuitive lack of effect of the SHIP2-KO on $PI(3,4)P_2$ synthesis is explained by the accumulation of more $PI(3,4,5)P_3$ under this condition, driving increased dephosphorylation through other phosphatases, hence maintaining a similar absolute rate of $PI(3,4)P_2$ formation); PTEN

directly hydrolyses PI(3,4)P_2 (its actions could not be modelled by its impact on PI(3,4,5)P_3 levels alone); PTEN and INPP4B regulate PI(3,4)P_2 hydrolysis in similar proportions, with a much smaller contribution from an unknown phosphatse(s); the model could not simulate basal PI(3,4)P_2 levels in WT Mcf10a cells without introducing an independent, PI-103-insensitive route of PI(3,4)P_2 formation.

We interrogated the nature of a potentially separate, PI-103 insensitive pool of PI(3,4)P_2 further.

5.2.5 Comparison between HPLC-ESI MS/MS and ^{33}P labelling methods

The significance of predictions which came from the computational modelling was reassessed by a parallel phosphatidylinositol lipid quantification in Mcf10a cells using HPLC-ESI MS/MS and the well-established radioisotope-labelling method (Guillou, Stephens et al. 2007). ^{33}P instead of the classically used ^{32}P was selected for labelling of the inositol phosphate groups due to lower energy electrons emitted during β^- decay and a longer half-life. As a result, two types of chromatograms were obtained, when lipids extracted from EGF-treated Mcf10a cells were run through a reverse-phase HPLC column, or deacylated and headgroups separated on a strong anion-exchange column (Figure 5.8). Furthermore, independent quantitation of phosphatidylinositol lipids was performed by ^{33}P radioactivity measurements of [^{33}P]P_i-labelled headgroups or detection of the glycerol fragments of certain *m/z* in the triple-quadrupole mass spectrometer (Figure 5.9). Although siRNA-mediated suppression of INPP4A/B in WT and PTEN-KO cells showed similar patterns of EGF-stimulated PI(3,4)P_2 accumulation, the amplitude of changes appeared to vary between the ^{33}P-labelling and HPLC-ESI MS/MS approach. Comparing methods that are based on different chemical modifications (C38:4 PIP_2's reaction with ozone versus methylamine-mediated deacylation of all acyl chain variants of PIP_2), different potential pools (total versus radiolabelled pools) and different analytical methods (reverse-phase HPLC separations leading into ESI-MS/MS versus normal phase HPLC leading into scintillation counting) is difficult. However, there are no immediately obvious reasons why these differences would not be corrected by a ratio of PI(3,4)P_2/PI(4,5)P_2.

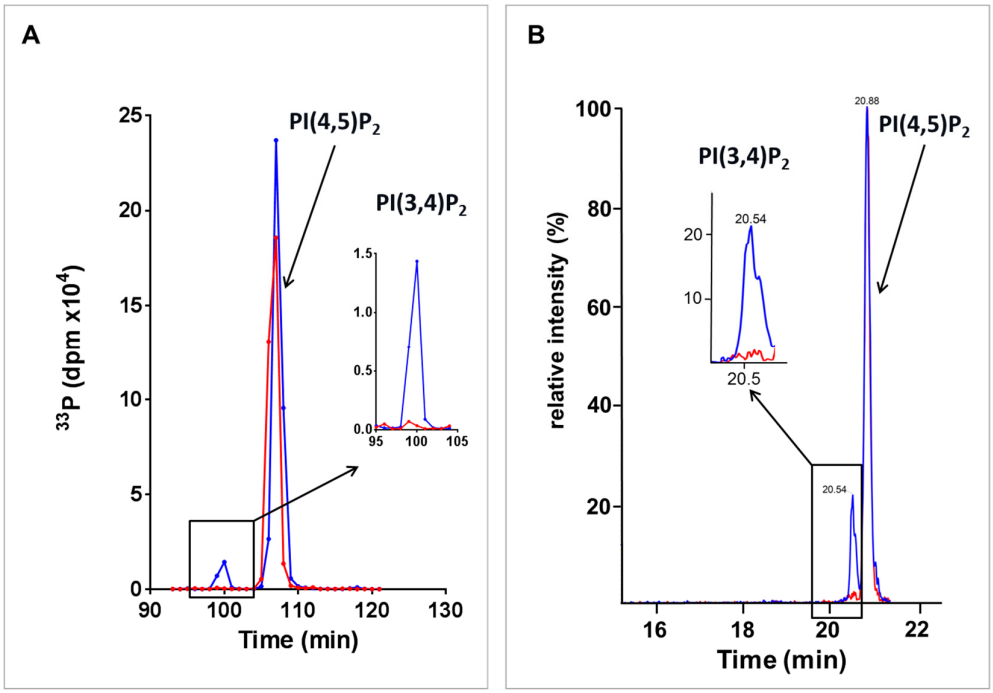

Figure 5.8 Comparison between HPLC-ESI MS/MS and ^{33}P-labelling: example HPLC traces

Example HPLC traces illustrating the raw data derived from the analysis of parallel samples of unlabelled or [^{33}P]Pi-labelled, WT or [PTEN-KO, INPP4A/B-KD] Mcf10a cells. Cells were starved and then left unstimulated or stimulated with EGF (10ng/ml) for 5 min and analysed by HPLC-ESI MS/MS (right panel) or via deacylation and anion-exchange chromatography (left panel).

Another approach, is to make the comparison based on the biological activity of class I PI3K and in this context, respective measurements were made from equivalent samples. Following this argument, we may assume that EGF stimulation should lead to a similar accumulation of PI(3,4)P_2, irrespective of the analytical method used for quantification. This implies that the HPLC-ESI MS/MS method overestimates the levels of PI(3,4)P_2 in both starved and PI-103-treated Mcf10a cells. The most likely explanation for this observation is the presence of contaminants under the chromatographic peak of PI(3,4)P_2. We also note that the radiolabelling method allowed quantification of different PIP regioisomers including PI3P. Levels of PI3P did not change significantly upon *PTEN* deletion, which suggests that PTEN does not control the total cellular levels of PI3P in Mcf10a cells (Figure 5.9C).

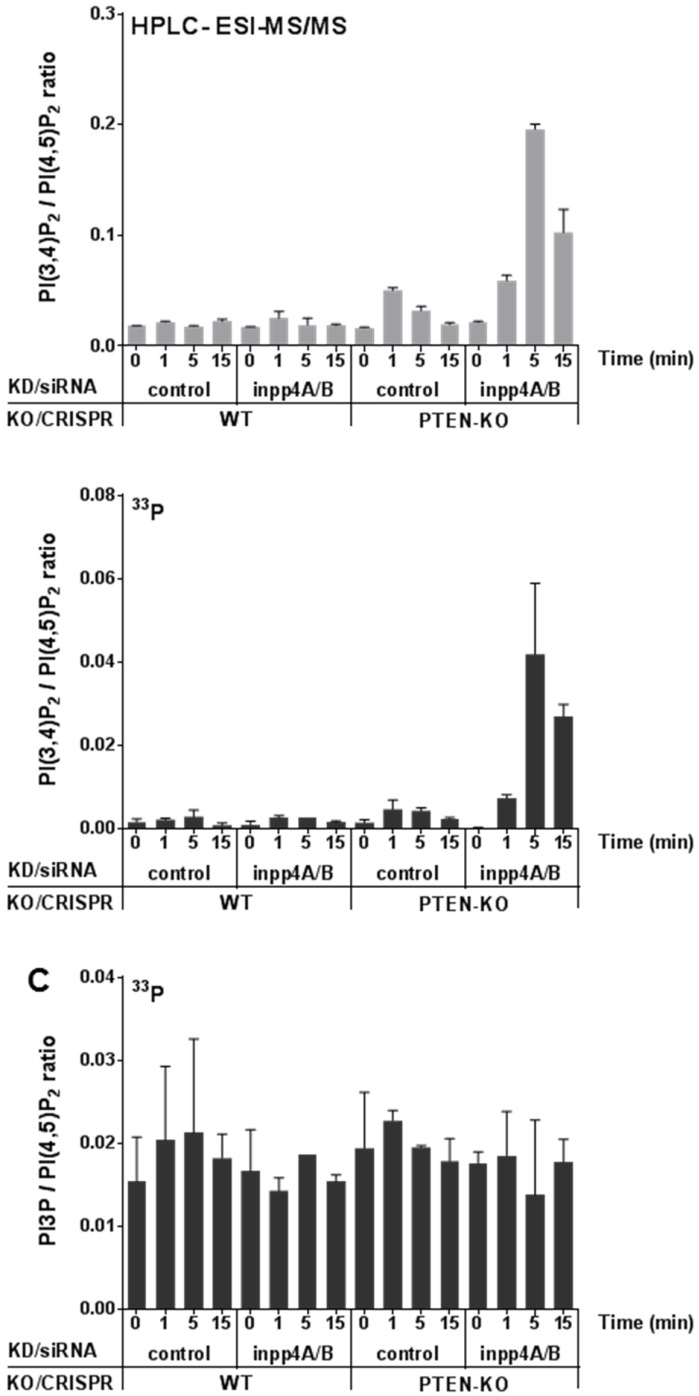

Figure 5.9 Comparison of [^{33}P]P_i-labelling and HPLC-ESI MS/MS methods for phosphatidylinositol lipid quantitation

*Quantitation of traces analogous to those shown in Figure 5.8. WT or PTEN-KO cells treated with the indicated siRNA were starved and then stimulated with EGF for 0, 1, 5 or 15 min. For the HPLC-ESI MS/MS values, peak areas derived from molecules corresponding to C38:4 PI(3,4)P_2 and PI(4,5)P_2 were first corrected for the recovery of internal deuterated standards before calculating a PI(3,4)P_2/PI(4,5)P_2 ratio (**A**). For the ^{33}P-labelling values, HPLC fractions corresponding to the appropriate glycerophosphoinositide species were summed, background radioactivity subtracted, and then a simple PI(3,4)P_2/PI(4,5)P_2 (**B**) or PI3P/PI(4,5)P_2 (**C**) ratio derived. The data shown are means ± SD of two biological replicates.*

5.2.6 Different mass spectrometry approaches for measuring PI(3,4)P_2 levels in Mcf10a cells

Since the analysis above implied that contaminants may contribute to our HPLC-ESI MS/MS measurements of PI(3,4)P_2, we investigated this further. The resolving power of the mass spectrometry machine is one of the most important parameters that should be taken into consideration when designing experiments. The triple quadrupole mass spectrometer routinely used in our laboratory for lipidomics analyses is a robust and reliable machine that is able to resolve peaks with FWHM ~0.2, which is very often insufficient to distinguish between the isobars, i.e. the molecules of the same integer mass but different atomic composition. In order to exclude the presence of contaminants in the basal PI(3,4)P_2 chromatographic peak, we ran parallel analyses on a machine equipped with a high-resolution Orbitrap detector. The most accurate approach, which involved detection of fragment ions on the Orbitrap machine (i.e. 'Orbitrap MS2'), gave consistently lower PI(3,4)P_2 levels across tested conditions, but the difference was not significant to report on the presence of a contaminant with confidence (Figure 5.10).

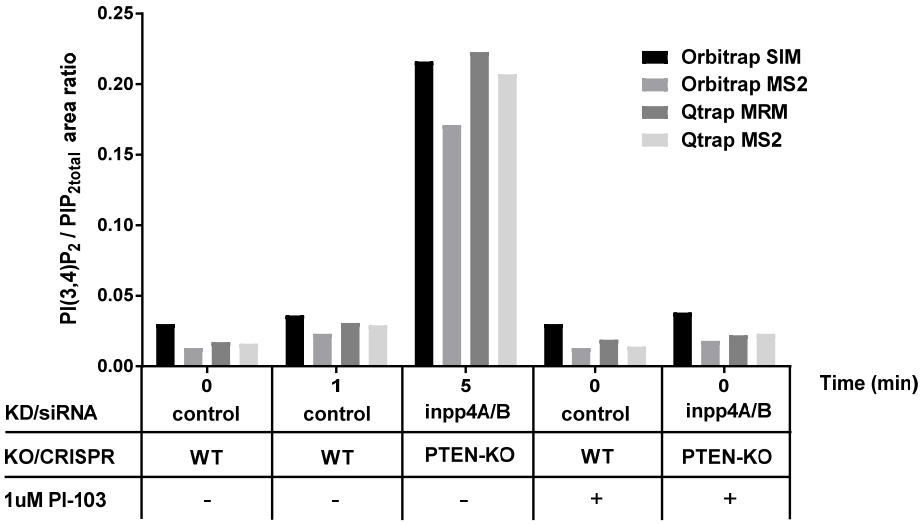

Figure 5.10 Comparison between different mass spectrometry methods

A comparison of the values obtained for PI(3,4)P_2 using identical HPLC chromatography conditions but different fragmentation strategies. WT or PTEN-KO Mcf10a cells were incubated with the indicated siRNAs, starved, treated with or without PI-103 (1 μM) for 20 min and then stimulated with EGF (10ng/ml) for 0, 1 or 5 min. Levels of PI(3,4)P_2 were measured using triple quadrupole mass spectrometer (AB SCIEX 4000 QTrap) and fragment ions were detected in multiple reaction monitoring (MRM) or MS/MS mode. Parallel measurements were performed on an orbitrap mass spectrometer (Thermo Scientific Orbitrap Elite), where ions' m/z was measured with high accuracy using single ion monitoring (SIM) or MS/MS approach.

5.3 Discussion

This part of the project focused on trying to determine the catalytic source of $PI(3,4)P_2$ in Mcf10a cells responding to receptor stimulation by EGF. We utilised a variety of small molecule inhibitors with divergent potency with respect to different classes and isoforms of PI3K, to test their effect on $PI(3,4)P_2$ accumulation relative to $PI(3,4,5)P_3$. Selective inhibition of p110α and p110β (via a mixture of PIK75 and TGX115) affected EGF-stimulated accumulation of $PI(3,4)P_2$ and $PI(3,4,5)P_3$ in a parallel, concentration-dependent manner and led to almost complete depletion of these two phosphatidylinositol lipids at concentrations which are lower than those predicted to significantly inhibit PI3K-C2α or PI3K-C2β. This suggested a common, class I PI3K-specific source of $PI(3,4)P_2$ and $PI(3,4,5)P_3$. Further, two types of class I PI3K inhibitors - PI-103 and Byl-719 - were used to support the hypothesis and showed the dominant role of p110α. In an independent experiment, we selectively reduced the expression of PI3K-C2α or PI3K-C2β and confirmed the lack of any major role for these two class II PI3K isoforms. Next, we used an siRNA strategy in an attempt to define additional 5-phosphatase/s which reveal their hydrolytic activity under elevated $PI(3,4,5)P_3$ conditions, generated by EGF-stimulation of [PTEN-SHIP2-KO, INPP4B-KD] Mcf10a cells. The results did not lead to a decisive conclusion but suggested that either we supressed the wrong combination of 5-phosphatases or that an as yet unknown $PI(3,4,5)P_3$ 5-phosphatase is expressed in Mcf10a cells.

Kinetic data from an analysis of PI-103-induced $PI(3,4,5)P_3$ and $PI(3,4)P_2$ decay in genetically manipulated Mcf10a cells indicated that the rate of $PI(3,4,5)P_3$ hydrolysis in EGF-stimulated WT cells is very high ($t_{1/2}$ < 10sec). This suggests that the accumulation of class I PI3K generated $PI(3,4,5)P_3$ represents a sensitive balance between very high rates of synthesis and degradation. A high rate of $PI(3,4,5)P_3$ hydrolysis was also seen in PTEN-KO cells. If it is assumed this is mediated via 5-phosphatases, then this must feed substantial synthesis of $PI(3,4)P_2$. Further, *in sillico* modelling of class I PI3K-controlled phosphatidylinositol lipid fluxes suggested this rate of $PI(3,4)P_2$ formation may be sufficient to explain EGF-stimulated $PI(3,4)P_2$ accumulation in cells lacking both PTEN and INPP4B. Additional conclusions from this modelling were that other 5-phosphatases may be able to sustain this flux in the absence of SHIP2, due to the elevated concentration of $PI(3,4,5)P_3$, and that PTEN may act as a direct $PI(3,4)P_2$ phosphatase.

The model also suggested the presence of a PI-103-insensitive pool of $PI(3,4)P_2$. Parallel HPLC-ESI MS/MS and $[^{33}P]P_i$-radiolabelling approaches were used to validate the time-dependent EGF accumulation of $PI(3,4)P_2$ in Mcf10a cells and the observations from both methods broadly overlapped but, the radiolabelling approach suggested a much lower basal value for $PI(3,4)P_2$ in unstimulated cells. However, high resolution mass spectrometry did not provide convincing evidence for the existence of significant contaminants within our measurements of $PI(3,4)P_2$ by HPLC-ESI MS/MS and thus we were unable to either confirm or dismiss the idea of a PI-103-insensitive pool of $PI(3,4)P_2$ in Mcf10a cells.

Chapter 6 PTEN acts as a direct PI(3,4)P_2 3-phosphatase in Mcf10a cytosol

6.1 Introduction

Enzymatic activity of a protein within a cell is not a simple, fixed, intrinsic property of its amino-acid sequence, but a resultant of the complex cellular environment, including its subcellular localisation, post-translational modification and interaction with other partners. The attempt to faithfully reconstruct such a multicomponent system in an Eppendorf tube requires substantial biochemical knowledge and a series of optimisation steps, and makes studying enzymatic reactions *in vitro* a nontrivial task. One of the classical mechanisms of enzymatic activation relies on allosteric regulation - a noncovalent interaction with a small molecule activator/inhibitor. An equally important mechanism utilised by the cells involves modification of specific amino acids with a phosphate group, either by the protein itself or by a specialised family of protein kinases. Finally, protein-protein interactions can act to switch on enzymatic activity by releasing the inhibitory conformation of a protein and/or its relocalisation within the cell.

PTEN represents a critical node in cellular regulation and a multitude of regulatory mechanisms need to converge to grant the protein its phosphatase activity. Such a system most probably developed to provide the cell with a 'continuum' of PTEN activity that allows appropriate flexibility, fidelity and robustness. Most importantly for the design of kinetic assays, PTEN is an interfacial enzyme, i.e. it manifests its catalytic activity at the surface of a cellular membrane and in association with it. PTEN is generally accepted as the main cellular PI(3,4,5)P_3 3-phosphatase but its activity towards PI(3,4)P_2 has not been convincingly shown in the cellular/organismal context and the available *in vitro* data does not offer a definitive answer. McConnachie et al. performed an extensive study of PTEN's catalytic properties by modelling biological membranes as phosphatidylcholine-based unilamellar vesicles enriched in PI(3,4,5)P_3 or PI(3,4)P_2 substrate (McConnachie, Pass et al. 2003). The behaviour of recombinant PTEN towards such substrate presentation showed ~200 fold higher catalytic efficiency

towards PI(3,4,5)P_3 relative to PI(3,4)P_2 (judged by comparing the ratios of k_{cat}/interfacial-K_m for each substrate), making the latter a negligible substrate for PTEN. Interestingly, the presence of PI(4,5)P_2 in the vesicles potentiated PI(3,4,5)P_3 hydrolysis, suggesting that PTEN may preferentially interact with and become activated by regions of the plasma membrane enriched in PI(4,5)P_2. Furthermore, a mechanism through which proper orientation of PTEN's active site against its substrate enhances the efficiency of the dephosphorylation step was proposed, after a much weaker phosphatase-vesicle interaction was observed in PTEN with a mutation in its C2 domain, which is believed to be at least partially responsible for interaction with the membrane.

The motivation to reassess PTEN's activity towards PI(3,4)P_2 was a result of several observations. Cell lines with mutations in *PTEN* have been characterised by enhanced phosphorylation of AKT and elevated levels of PI(3,4,5)P_3 and PI(3,4)P_2, when compared to cells expressing wild-type phosphatase (Haas-Kogan, Shalev et al. 1998, Taylor, Wong et al. 2000). Treatment with LY294002 or re-expression of wild-type PTEN reduced the level of phosphorylated AKT and the levels of both phosphatidylinositol lipids in these cells. Moreover, although the substantial accumulation of PI(3,4)P_2 that we observed in PTEN-INPP4B-KO Mcf10a cells post EGF-stimulation may be solely a result of increased flux through 5-dephosphorylation of PI(3,4,5)P_3, we could not disregard a more direct role of PTEN in this process. Indeed, our *in silico* analysis pointed strongly towards a dual function of PTEN, as both a PI(3,4,5)P_3 and PI(3,4)P_2 phosphatase in this system.

6.2 Results

Biochemical assays employing recombinant proteins give the advantage of studying biological processes in isolation and as such have undoubtedly contributed to some of the major discoveries in the field of PI3K. However, such cell-free approaches are not well suited to model multiprotein interactions and are inevitably prone to artefacts and over-interpretations. Thus, care should be taken when drawing conclusions from any *in vitro* assay, as it represents an attempt to mimic the natural cellular environment and may be stripped of factors that play an important role in the studied process. Likewise, no universal assay conditions exist that can be blindly applied without prior optimisation steps and evaluation of the biological relevance of obtained results. In light of this, we decided to use cytosol preparations from Mcf10a mutant cells and phosphatidylinositol lipid-containing liposomes to re-evaluate the importance of PTEN as a lipid phosphatase.

6.2.1 Dephosphorylation of PI(3,4,5)P_3 and PI(3,4)P_2 by Mcf10a cytosol

One of the critical stages in designing the biochemical assay for PTEN activity was preparation of enzymatically active Mcf10a cytosol. The initial tests with detergents, such as NP-40, suggested it was difficult to measure substantial PI(3,4,5)P_3 and PI(3,4)P_2 phosphatase activity when extracts were recombined with lipid substrates in the form of micelles, and therefore we decided to switch to detergent-free conditions. Thus, our final protocol involved cell lysis and sonication at 4°C, followed by ultracentrifugation to separate cell debris and nuclei from the cytosolic fraction. The second challenge was creation of liposomes that faithfully resemble the composition of biological plasma membrane and can serve as a carrier for phosphatidylinositol substrates. Following several optimisation steps, liposomes were prepared by sonication of a complex mixture containing naturally derived phospholipids and synthetic phosphatidylinositol lipids (Figure 6.1A). We used D6-PI(3,4,5)P_3 and D6-PI(3,4)P_2 as substrates to initially enable mass separation from endogenous, non-deuterated analogues that would be present in detergent extracts of cells, but they then remained our substrates as we moved to detergent-free conditions. For the assay, cytosol from WT, PTEN-KO or the indicated CRISPR Mcf10a clones was incubated with liposomes containing deuterated forms of

$PI(3,4,5)P_3$ or $PI(3,4)P_2$ at 30°C and the reaction was quenched at different time intervals. HPLC-ESI MS/MS was used to follow the products of enzymatic activity of different cytosol preparations (Figure 6.1 and Figure 6.2). Cytosol from Mcf10a cells

A

Lipid component	% of the total 0.33 mg/ml	Concentration [mM]
PI	26.5	0.100
PE	26.5	0.100
PC	12	0.461
PS	25.1	0.096
Sphingomyelin	3	0.011
Cholesterol	2	0.00769
$PI(4,5)P_2$	2.3	0.00885
D6-$PI(3,4)P_2$	2.6	0.01
TOTAL	100	0.384

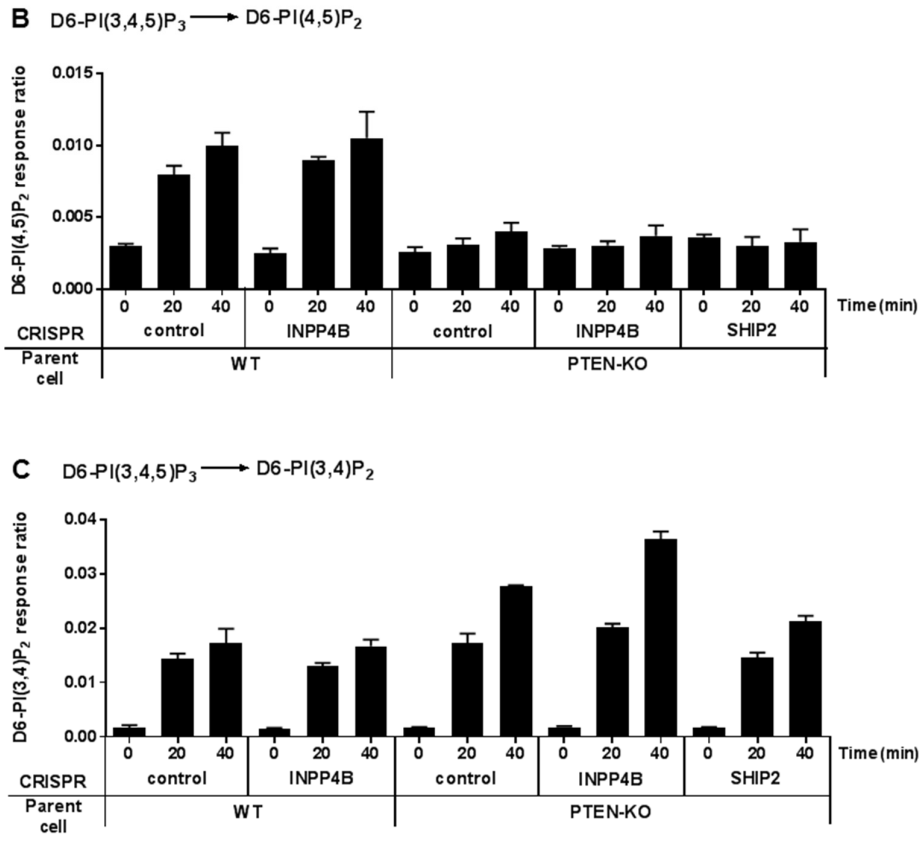

Figure 6.1 Dephosphorylation of $PI(3,4,5)P_3$ by Mcf10a cytosol

*(**A**) Lipid composition of liposomes. Measurement of: (**B**) 3-phosphatase activity against D6-$PI(3,4,5)P_3$ and (**C**) 5-phosphatase activity against D6-$PI(3,4,5)P_3$ present in cytosol prepared from the indicated Mcf10a cell genotypes. Data are means ± SD of 3 technical replicates.*

expressing wild-type PTEN showed a time-dependent conversion of D6-PI(3,4,5)P_3 to D6-PI(4,5)P_2 (Figure 6.1B). This activity was abolished in Mcf10a cytosols depleted of PTEN, which, apart from suggesting PTEN is the major 3-phosphatase operating under these conditions, is an important validation of the assay. WT Mcf10a cytosol also converted D6-PI(3,4,5)P_3 to D6-PI(3,4)P_2, indicating 5-phosphatases were also active under these conditions (Figure 6.1C). The lack of any clear effect of the loss of SHIP2 also emphasises the potential redundancy that may exist amongst the members of the family of 5-phosphatases.

Mcf10a cytosols prepared from cells expressing normal levels of PTEN and incubated with D6-PI(3,4)P_2-containing liposomes showed clear hydrolytic activity towards this phosphatidylinositol lipid (Figure 6.2A,B). Remarkably, cytosols from cells lacking PTEN showed an undetectable accumulation of D6-PIP (Figure 6.2B). This was the first and most compelling set of data supporting the hypothesis that PI(3,4)P_2 may

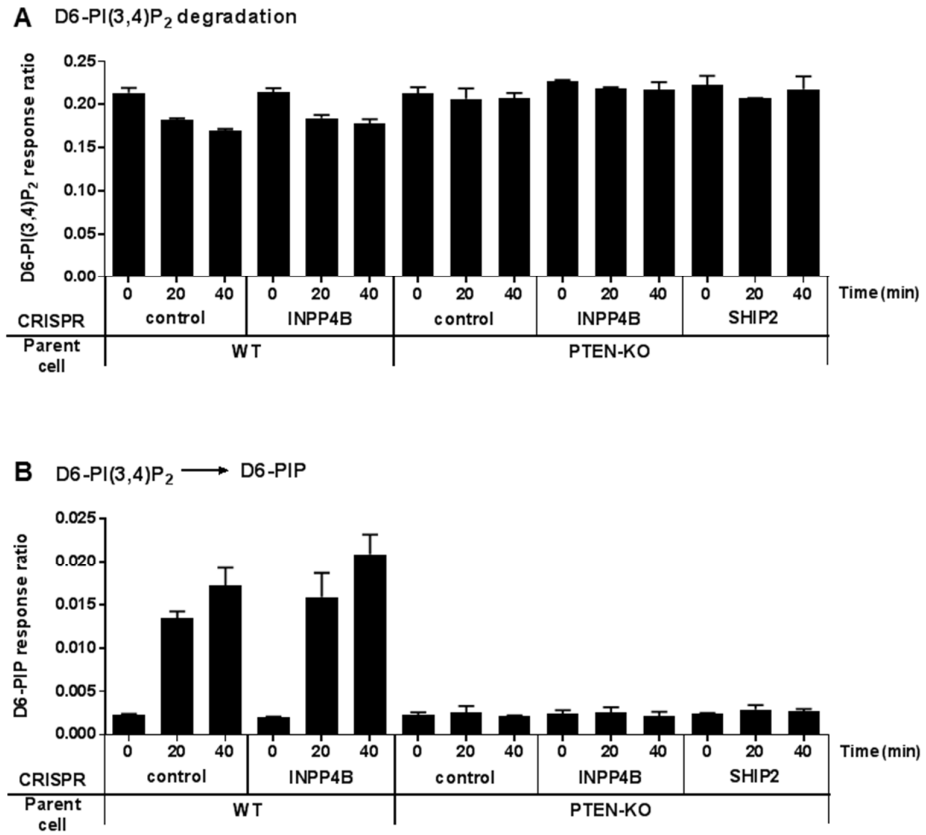

Figure 6.2 Dephosphorylation of PI(3,4)P_2 by Mcf10a cytosol

*Measurement of: (**A**) D6-PI(3,4)P_2 and (**B**) D6-PI(3,4)P_2 phosphatase activity present in cytosol prepared from the indicated Mcf10a cell genotypes. Data are means ± SD of 3 technical replicates.*

indeed be a physiological target of PTEN. Also of note, is the lack of effect of deleting INPP4B on the conversion of D6-PI(3,4)P_2 to D6-PIP, suggesting it is not an active D6-PI(3,4)P_2 4-phosphatase under these assay conditions.

6.2.2 PTEN's activity towards PI(3,4)P_2 is related to its intrinsic lipid phosphatase identity

The question that still required a formal answer was whether D6-PIP produced by WT Mcf10a cytosol from D6-PI(3,4)P_2 is a consequence of PTEN's phosphatase activity or an indirect, non-catalytic function, e.g. through involvement in protein-protein interactions with an unknown enzyme. Multiple germline mutations of *PTEN* have been identified in sufferers of Cowden's syndrome and in patients with tumours, e.g. G129E or C124S missense mutations localised in the protein's catalytic signature motif. Experiments using recombinant G129E and C124S PTEN variants have previously been performed to test their ability to dephosphorylate polyGluTyr peptide or release inorganic phosphate from [^{32}P]Pi-labelled PI(3,4,5)P_3 (Myers, Pass et al. 1998). The results indicated that the C124S mutation completely ablates PTEN's catalytic activity, while the G129E PTEN mutant is unable to recognize PI(3,4,5)P_3 but retains the ability to dephosphorylate polyGluTyr. We performed a rescue experiment, by exogenous addition of recombinant wild-type, C124S or G129E PTEN to PTEN-KO Mcf10a cytosol

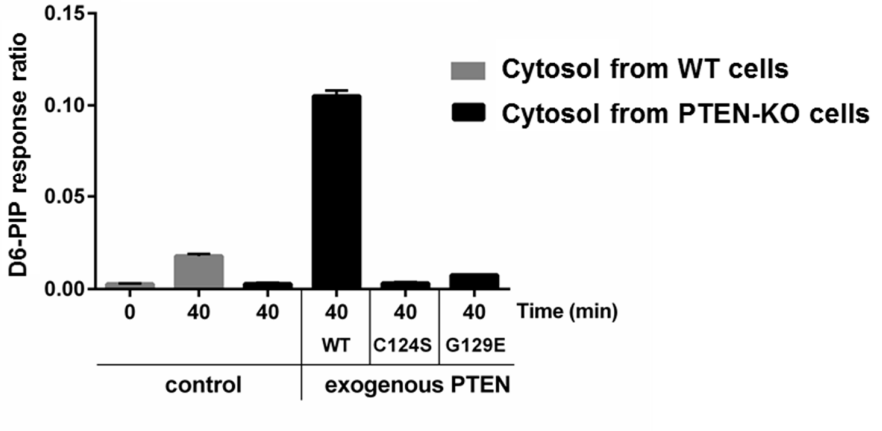

Figure 6.3 Recombinant PTEN acts as PI(3,4)P_2 phosphatase in Mcf10a cytosol

The formation of D6-PIP by Mcf10a cytosol incubated with D6-PI(3,4)P_2. Cytosol was prepared from WT or PTEN-KO cells, and supplemented with 30nM recombinant WT or mutant PTEN, as indicated. Data are means ± SD of 3 technical replicates. Recombinant PTEN was provided by Glenn Masson, University of Cambridge.

and monitored the impact it had on the accumulation of D6-PIP derived from D6-PI(3,4)P_2-containing liposomes (Figure 6.3). Reintroduction of wild-type but not mutant PTEN phosphatase restored cytosol's hydrolytic function to generate D6-PIP. A non-negligible amount of D6-PIP produced by G129E PTEN may come from incomplete inhibition of PTEN's ability to recognize PI(3,4)P_2.

6.2.3 PTEN is a PI(3,4)P_2 3-phosphatase

PTEN is a well-characterised 3-phosphatase of PI(3,4,5)P_3. In order to determine which phosphate group of PI(3,4)P_2 is preferentially hydrolysed by PTEN, we revisited the HPLC conditions optimised for PI(3,4)P_2 and PI(4,5)P_2 separation. The new HPLC method allowed sufficient separation between PI3P and PI4P that it could be used to identify these molecules in a simplified system. Cytosol from INPP4B-KO Mcf10a cells incubated with D6-PI(3,4)P_2, generated a single peak at a retention time consistent with the elution of PIP lipids (Figure 6.4). Furthermore, synthetic D6-PI4P added to the primary extraction phase of an identical lipid mixture produced a single peak, whereas spiking in D6-PI3P led to a clear peak separation. In conclusion, the phosphatidylinositol lipid generated due to PTEN's hydrolytic activity on D6-PI(3,4)P_2 was identified as D6-PI4P.

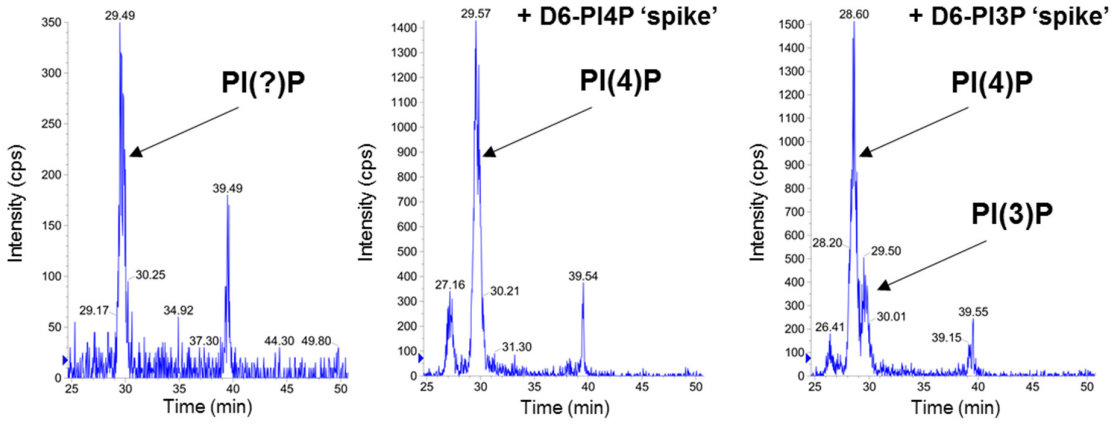

Figure 6.4 Identification of PIP derived from PI(3,4)P_2 by Mcf10a cytosol as PI4P

HPLC-ESI MS/MS separation of the products of D6-PI(3,4)P_2 dephosphorylation by [INPP4B CRSIPR-KO] Mcf10a cytosol (left panel), together with analogous separations of samples in which additional D6-PI4P (middle) or D6-PI3P (right panel) had been added after reactions were terminated. The HPLC-ESI MS/MS method to separate PI3P and PI4P regioisomers was developed by Jonathan Clark, Babraham Institute.

6.3 Discussion

Functional redundancy between proteins, although perceived as energetically unfavourable, has been utilised by the cells to control critical signalling pathways and in this respect includes the components of PI3K/AKT signalling, e.g. p110/p85 subunits of class I PI3K or isoforms of AKT. At the level of phosphatidylinositol lipid regulation, the family of lipid phosphatases is one of the most abundant and most diverse in terms of tissue-specific expression and substrate selectivity. PTEN's function as a tumour suppressor and PI(3,4,5)P_3 3-phosphatase has been fully accepted by the scientific community but it's importance with respect to PI(3,4)P_2 has been unclear. Motivated by phosphatidylinositol lipid flux analysis in Mcf10a cells and subsequent *in sillico* predictions, we designed a biochemical *in vitro* assay to re-probe PTEN's activity towards PI(3,4)P_2. Cytosols derived from various Mcf10a mutant cells provided a useful set of samples with variable phosphatase composition and thus a system to assess the role of defined phosphatases within a diluted-cytosol context. Moreover, the use of a complex lipid mixture, including PI(4,5)P_2, provided our best attempt to mimic the endogenous membrane interface. Nevertheless, the rates of phosphatidylinositol lipid accumulation/degradation in our biochemical assay will obviously differ from those within cells, as the catalytic PI3K component was absent and phosphatases were exposed to an initial, high level of phosphatidylinositol lipid substrate. Moreover, lipid distribution in liposomes was (theoretically) homogenous and therefore artificial, in contrast to more complex and dynamic distributions observed in cells. Nevertheless, the overall assay conditions were probably a better mimic of the cellular environment compared to previous studies performed using recombinant PTEN. Results obtained from our biochemical assay were strengthened by a rescue experiment with exogenous PTEN and indicated a genuine role for PTEN as PI(3,4)P_2 phosphatase under these conditions. Finally, a detailed HPLC analysis of the character of the D6-PIP generated by dephosphorylation of D6-PI(3,4)P_2 identified PTEN as PI(3,4)P_2 3-phosphatase.

Rigorous biochemical studies will be required to ascribe the real kinetic values to PTEN and INPP4B in the context of hydrolytic activity against PI(3,4)P_2, but our data in Mcf10a cells suggest that at least a certain level of redundancy may exist between these two enzymes in a cellular context, despite the apparent lack of activity of INPP4B in our *in vitro* assays. Thus, PTEN was able to keep EGF-stimulated PI(3,4)P_2 levels low in an

INPP4B depleted condition and, likewise, PTEN-KO cells show only moderate accumulation of $PI(3,4)P_2$ in the presence of INPP4B. It required the combined deletion of both phosphatases to see substantial accumulation of $PI(3,4)P_2$ in response to EGF-mediated class I PI3K signalling.

Chapter 7 PTEN and INPP4B regulate invadopodia formation in Mcf10a cells

7.1 Introduction

Joint efforts of scientists and clinicians, as well as increasing social awareness, have vastly contributed to improved curability of some of the most common cancers due to early diagnosis, supported by highly specialised therapeutic regimens. Nevertheless, metastasis persists as the major cause of death in patients with cancer disease and therefore remains one of the pressing topics of cancer research. The process of metastasis, through which invasive cells colonise secondary tissues and organs, involves communication between multiple cell types. Increasing amounts of data reveal the major reprograming mechanisms triggered by tumour cells in the cells of the tumour microenvironment to support growth and evade immune recognition. Consequently, metastasis is a complex and heterogeneous process, with cancers showing different patterns of metastatic spread and varying in lag between dormancy and metastasis formation (Wan, Pantel et al. 2013). Several stages mark this invasive process: crossing the basement layer by a disseminated cell, traveling through stroma and entering the blood stream, cell survival in the blood stream, and finally cell extravasation and proliferation in the foreign organ. Thus, enhanced proliferation and survival under nutrient- and oxygen-limiting conditions, the common features of tumorigenic cells, do not in themselves define their invasive potential.

Invasion is an intrinsic property of several types of cells and an essential mechanism during embryonic development and throughout lifetime. Osteoclasts develop podosomes to allow adhesion to bone matrix during bone resorption and several members of the haematopoietic lineage (e.g. macrophages) use the proteolytic activity of podosomes to manoeuvre through extracellular matrix (ECM) to the site of infection. Aggressive cancer cells have adapted this molecular machinery and are able to form podosome-like structures called invadopodia - F-actin-rich membrane protrusions, which by localised release of proteases are able to degrade, remodel and invade into ECM. Classically, invadopodia are able to protrude deeper into the ECM and can persist

up to hours, compared to shorter and short-lived podosomes (Revach and Geiger 2013). Moreover, several proteins are obligate components of invadopodia, e.g. cortactin, TKS5, Neural Wiskott–Aldrich syndrome protein (N-WASP) and matrix metalloproteinase MMP14, which in a coordinated way control invadopodium formation and maturation (Paterson and Courtneidge 2017). Extracellular cues that stimulate invadopodium formation include EGF, VEGF, PDGF or transforming growth factor beta (TGFβ). More importantly, functional studies on MDA-MB-231 breast cancer cells provided a link between the activity of the class I PI3K isoform p110α and a cell's intrinsic metastatic potential (Yamaguchi, Yoshida et al. 2011).

TKS5 is one of the scaffolding proteins, which via SH3 domains interacts with actin-remodelling proteins or ADAM family proteases, and is thus critical for invadopodium formation and function. Moreover, the PX domain of TKS5 is essential for the protein's localisation at invadopodia and for invadopodium stability (Abram, Seals et al. 2003, Sharma, Eddy et al. 2013). This function was shown to be controlled by SHIP2-mediated enrichment in $PI(3,4)P_2$ at the invadopodium core in response to EGF stimulation and a PX - $PI(3,4)P_2$ interaction. Finally, a pivotal role of invadopodia and TKS5 was shown *in vivo*, in the process of lung cancer cell extravasation from blood vessels (Leong, Robertson et al. 2014) (discussed in more detail in Chapter 1.4.2.1).

At this stage of the project, we decided to investigate the potential functional roles of increased $PI(3,4)P_2$ that may result from loss of PTEN. We first examined the cumulative effect of $PI(3,4)P_2$ and $PI(3,4,5)P_3$ on the phosphorylation of AKT in genetically manipulated Mcf10a cells. Next, we explored the potential link that exists in the literature between $PI(3,4)P_2$ and invadopodia. A key comparison in these studies was between the loss of PTEN and the loss of both PTEN and INPP4B, conditions which resulted in equivalent accumulation of $PI(3,4,5)P_3$, but radically different accumulations of $PI(3,4)P_2$.

7.2 Results

Regardless of their hereditary or environmental character, oncogenic alterations lay at the origin of cell transformation and as such are the major determinants of tumour development and progression. Such molecular transformations have been reported in the isoforms of PI3K, its upstream/downstream regulators (e.g. EGFR, PTEN, PIPP, INPP4B), as well as downstream effector AKT. Additional levels of complexity come from the fact that 'equivalent' mutations may lead to tumour development in one tissue but require accumulation of additional mutations to become tumourigenic in another tissue. In effect, the molecular bases of cellular transformation are cell- and context-dependent, and require in-depth analysis to avoid drawing hasty conclusions.

7.2.1 AKT phosphorylation levels in Mcf10a mutant cells

Class I PI3K activity is manifested by allosteric- and/or phosphorylation-driven activation of its downstream effectors, upon interaction of their PH domains with the second messenger $PI(3,4,5)P_3$ and/or $PI(3,4)P_2$. Aberrant AKT-mediated pro-growth signalling in cancer cells can result from oncogenic transformations that lead to excessive accumulation of $PI(3,4,5)P_3$ and $PI(3,4)P_2$ at the plasma membrane. Hence, the phosphorylation level of two important residues of AKT, ^{308}Thr and ^{473}Ser, is commonly used to report on the degree of this disturbance. Gewinner et al. in their studies on human mammary epithelial cells (HMEC) showed that collective suppression of INPP4B and PTEN leads to hyperactivation of AKT, when compared to ^{308}Thr phosphorylation levels in individual suppressions of the two respective phosphatases (Gewinner, Wang et al. 2009). We performed an analogous analysis and assessed the extent of AKT phosphorylation in Mcf10a cells with different genetic modifications (Figure 7.1). EGF stimulated an increase in AKT phosphorylation in both PTEN-KO and INPP4A/B-KD Mcf10a cells, though the scale of change was more substantial in the former. In line with previous observations, combined deletion of PTEN and INPP4A/B-KD further augmented the level of AKT phosphorylation but the dynamics of the process remained unchanged. These results suggest $PI(3,4)P_2$ regulates AKT in this system but neither P-^{308}Thr nor P-^{473}Ser closely reflect the EGF-stimulated $PI(3,4)P_2$ levels previously observed in the analogous Mcf10a genotypes. However, as discussed earlier, this might

be predicted from our still incomplete understanding of the relative importance of $PI(3,4,5)P_3$ and $PI(3,4)P_2$ in the regulation of AKT.

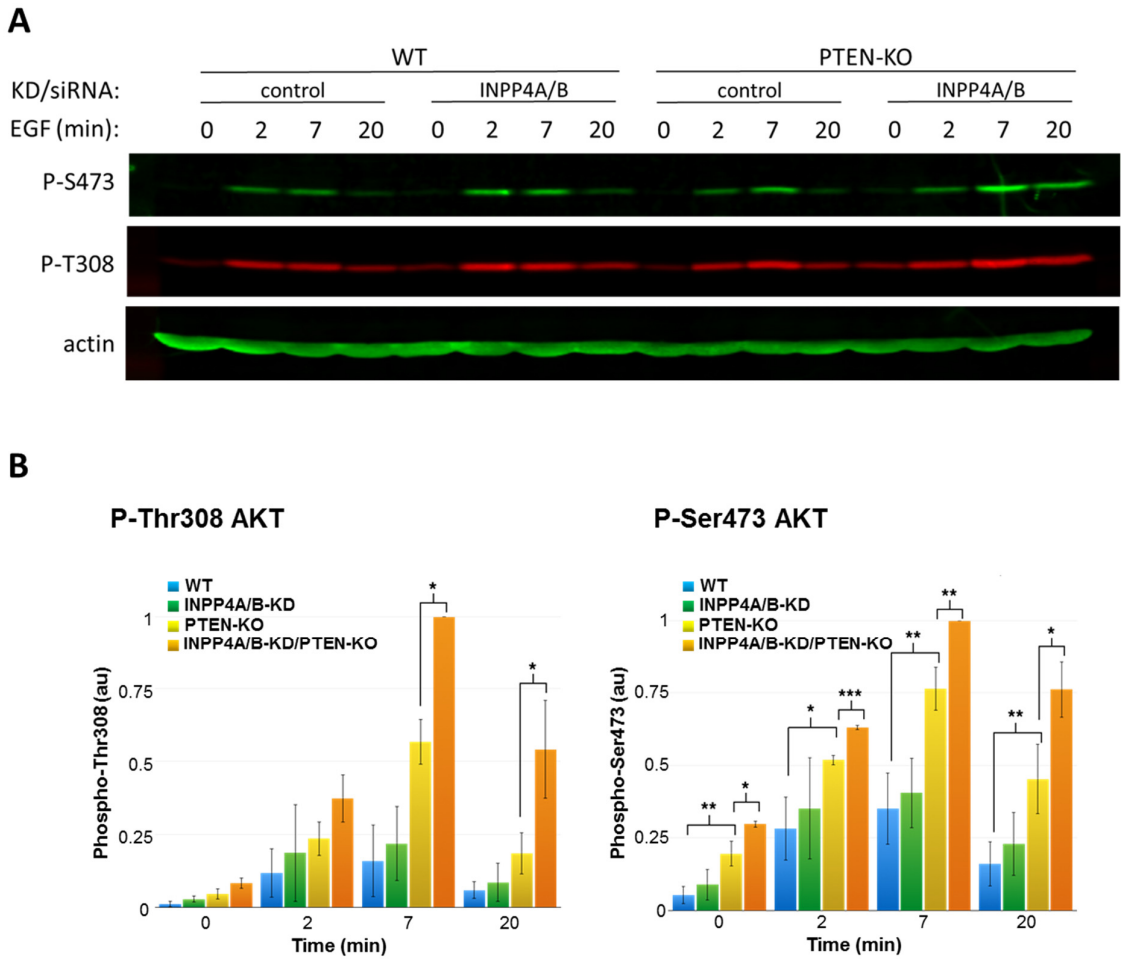

Figure 7.1 AKT phosphorylation in Mcf10a cells

*Phosphorylation of ^{308}Thr-AKT and ^{473}Ser-AKT in WT or PTEN-KO Mcf10a cells treated with either control or INPP4A/B siRNA, starved and stimulated for the indicated times with EGF (0.3 ng/ml). AKT phosphorylation was measured in cell lysates after SDS-PAGE and Western blotting with the relevant antibody. Representative Western blots (**A**) are shown, together with the result of quantifying analogous blots using LiCor software (**B**); data are for the ^{308}Thr-AKT and ^{473}Ser-AKT levels normalised to actin and expressed as means ± SD of three independent experiments. The experiment was performed by Mouhannad Malek and Karen Anderson, Babraham Institute.*

7.2.2 Invadopodia formation in Mcf10a cells

Epithelial-to-mesenchymal transition (EMT) is another molecular mechanism hijacked by transformed cells, through which they lose cell-cell adhesion, polarity and transform into mesenchymal cells with enhanced migratory potential. One of the signalling pathways known to reversibly induce EMT in cancer cells is mediated by

transforming growth factor (TGFβ). *In vivo* modelling of breast cancer metastasis showed that TGFβ is heterogeneously and transiently expressed to promote single-cell motility in a small population of cancer cells (Giampieri, Manning et al. 2009). Interestingly, such 'TGFβ positive' cells showed suppressed proliferation and were unable to promote lung metastases.

In normal Mcf10a cells, TGFβ was shown to induce the mesenchymal phenotype by promoting expression of the adaptor protein HIC-5 (Pignatelli, Tumbarello et al. 2012). Moreover, HIC-5 alone was able to promote invadopodia in these cells through activation of ROCK and p38 MAPK pathways. We decided to use this TGFβ-inducible invasive phenotype in our WT and genetically modified Mcf10a cells and follow the effect of class I PI3K signalling on invadopodia formation. During these experiments, Mcf10a cells primed with rhTGFβ-1 were seeded onto the surface of fluorescently labelled gelatin, starved and stimulated with EGF. To ensure sufficient statistical power, three coverslips per condition were prepared in each of three experiments, with 15 images obtained per cover slip. Invadopodia were identified by correlating cortactin-positive staining with holes in the gelatin formed due to proteolytic degradation (Figure 7.2). Although cortactin is not a unique marker of invadopodia, it gave better staining of the actin-rich core compared to anti-TKS5 antibodies we tested, and was supported by invasion-specific gelatin degradation. Quantitative analysis showed that upon stimulation with EGF, the number of invadopodia significantly increased across Mcf10a genotypes, which confirmed the role of this signalling pathway in supporting the

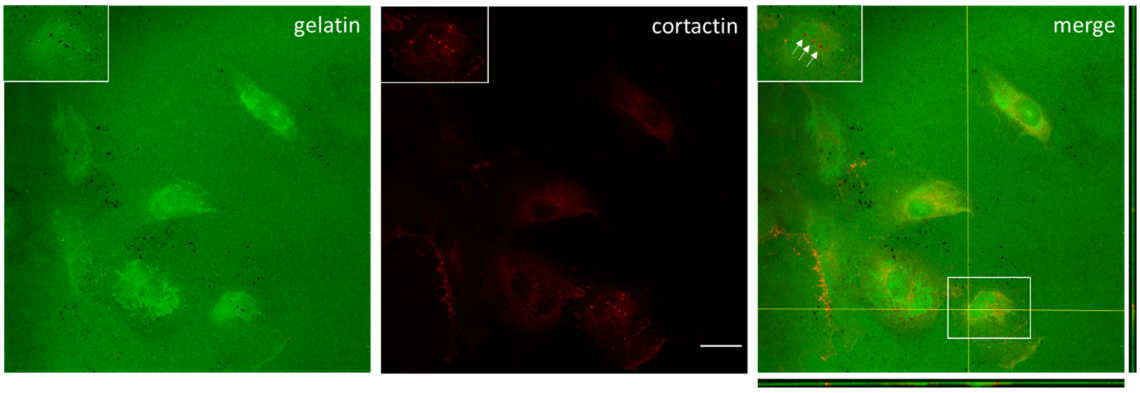

Figure 7.2 Identification of invadopodia in Mcf10a cells

An example of images taken of WT Mcf10a cells grown for 6 days in the presence of hTGF-β1 (10 ng/mL), plated on fluorescent gelatin for 2 hr, starved (4 hr) and then stimulated with EGF (20 ng/ml; 6 hr), before fixing and staining with an anti-cortactin antibody. Invadopodia were identified by the co-localisation of holes in the gelatin (green) with accumulations of cortactin (red); see arrows. Orthogonal projection of z-stacked images shows crossection through the gelatin surface (typically 1.5-2μm) and invadopodia labelled with antibody against cortactin. The scale bar represents 24 μm.

invasive process (Figure 7.3). More importantly, cells with combined deletion of PTEN and INPP4B showed a significantly higher potential to form stable, gelatin-degrading membrane protrusions when stimulated with EGF than cells with only deletion of PTEN.

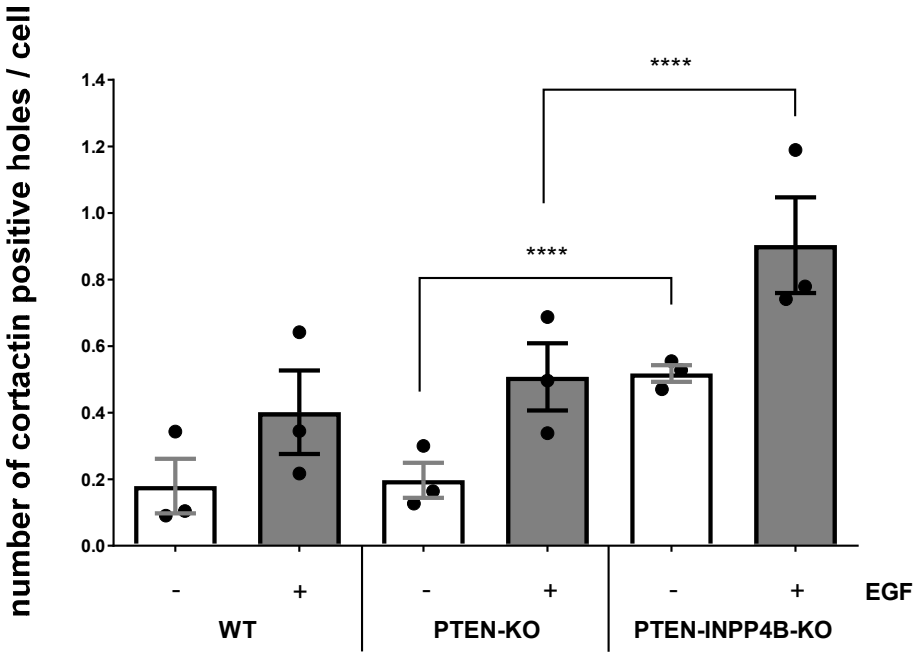

Figure 7.3 Invadopodia quantification in Mcf10a cells

Quantification of invadopodia formed in Mcf10a cells of the indicated genotype. The data represent means ± SD of 3 biological replicates. Statistical analysis was performed by applying two-way repeated measures ANOVA analysis followed by post-hoc Tukey's test to look for the effect of EGF on each genotype and to compare genotypes, with and without EGF (see Materials and Methods). The effect of EGF treatment was significant in all compared genotypes.

7.3 Discussion

Mcf10a cells lacking both PTEN and INPP4B showed hyperactivation of AKT in response to EGF. This result not only confirmed the importance of both PI(3,4,5)P_3 and PI(3,4)P_2 as signalling inputs into this pathway but relates to one of the hallmarks of transformed cells. However, we cannot comment on the 'cell-transforming' impact of combined PTEN and INPP4B deletion on Mcf10a cells without formal confirmation through a series of additional experiments, e.g. colony formation in soft agar, Ki67 index or invasion through a Boyden chamber. Previous studies reported an enhanced growth of acini in a 3D cell culture model when PTEN or INPP4B were knocked-down in Mcf10a cells (Gewinner, Wang et al. 2009). However, as yet, we have been unable to reproduce these findings in our laboratory.

A major motivation at this stage of the project was to challenge the view that PI(3,4)P_2 is merely a by-product of class I PI3K activity, which lacks a unique functional significance. The most convincing evidence thus far for a PI(3,4)P_2-selective role has been provided by a potential negative feedback loop in class I PI3K-mediated activation of AKT fulfilled by TAPP1/2, possibly via competing for PI(3,4)P_2 (Landego, Jayachandran et al. 2012). Although evidence is starting to emerge for other PI(3,4)P_2 - specific roles in endocytosis, cell migration and invasion, these processes rely on PI(3,4)P_2 binding to scaffolding proteins with varying specificity (e.g. SNX9, LPD, TKS5) and it is difficult to quantify how indispensable these interactions are to the overall phenotype (discussed in more detail in Chapter 1.4). Nevertheless, the data available in the literature which links PI(3,4)P_2 and invadopodia-dependent aspects of cancer metastasis seem cohesive, especially in the context of the tumour suppressive function of PTEN and our recent observations. Hence, we decided to set up a gelatin-degradation assay and monitor the invasive potential of genetically modified Mcf10a cells. We observed a highly significant increase in the number of EGF-stimulated invadopodia in PTEN-INPP4B-KO cells compared to PTEN-KO cells, which we interpret as a clear indication that PI(3,4)P_2 may contribute to invadopodia formation in these cells. Further experiments will be needed however to confirm the importance of PI(3,4)P_2 binding to the PX domain of TKS5 in this process.

Chapter 8 PTEN regulates the accumulation of $PI(3,4)P_2$ in mouse prostate

8.1 Introduction

Mice are one of the most common model organisms used to study human biology and have been instrumental in developing disease models, pharmacokinetic analyses of drug candidates or as donors of antibodies. Scientific hypotheses that arise from observations in humans are tested at the molecular level in biochemical or cell-based assays, but to gain an organismal perspective, very often require validation in mice. Although genetically similar, environmental adaptation has obviously led to differences between mice and humans, which will result in different physiological reactions to similar stimuli. Thus, a thorough understanding of differences between signalling pathways in mice and complementary studies in human-derived cancer cell lines are essential to prevent simplistic or false conclusions. Nevertheless, mouse models of human cancer are very often the most informative way to study tumour initiation, progression and metastasis, without losing the impact of an immune system or tumour microenvironment. Moreover, biological variability observed during tumour initiation and progression in mice reflects an analogous natural diversity that occurs in human cancers. Thus, a variety of methodological approaches, including generation of conditional knockout mice, intra-vital imaging and mouse xenografts, have been developed to study selected aspects of tumour biology. Notably, the recently described CRSIPR/Cas9 technique for targeted genome editing, has a huge potential to revolutionise cancer research and modern oncology (Cong, Ran et al. 2013).

PTEN is undoubtedly one of the most powerful known tumour suppressors. This activity is generally accepted to stem predominantly from its antagonism of the PI3K/AKT pathway – one of the major signalling networks that promote cellular growth and proliferation. Intense research on PTEN-related cancer has revealed a complex regulatory network that, depending on the mechanism, may cause downregulation or complete loss of functional PTEN (i.e. deregulation may occur at the gene, mRNA or protein level (Song, Salmena et al. 2012); discussed in more detail in Chapter 1.3.3).

Hence, there is a need for a better understanding of PTEN's role as a lipid phosphatase, which could aid in developing new biological markers and therapeutic strategies. Several transgenic mouse models have been generated to produce a spectrum of PTEN concentrations and relate these to cancer susceptibility in different organs. Hypermorphic *Pten* mice (*Pten*$^{hy/+}$, with ~80% of PTEN expressed) showed high incidence of breast tumours which revealed substantial sensitivity of this tissue to subtle PTEN variations (Alimonti, Carracedo et al. 2010). *Pten*$^{+/-}$ mice, on the other hand, showed high probability of developing breast and endometrial cancer, and high grade prostatic intraepithelial neoplasia (PIN) (Stambolic, Tsao et al. 2000). However, the high lethality of *Pten*$^{+/-}$ animals, and related to this, an inability to predict long term consequences of *Pten* heterozygosity, supported the need for generation of genetically modified mice with *Pten* alterations restricted to a single tissue. Further, mice with ~70-80% suppression of PTEN, i.e. hypomorphic *Pten*$^{hy/-}$ mice, developed prostate cancer with full penetrance (Trotman, Niki et al. 2003). Therefore, by tracing the functional outcome of PTEN deregulation, i.e. trying to increase our understanding of phosphatidylinositol lipid biology, we may be able to pinpoint the processes/proteins that drive this tissue-specific heterogeneity and identify targets for pharmacological intervention.

We selected a prostate cancer mouse model as a system to evaluate the potential impact of *Pten* deletion on the accumulation of PI(3,4)P_2 *in vivo*. Next, we used mice with individual or combined deletion of *Inpp4b* and *Pten* in prostate to compare their respective impacts on PI(3,4)P_2 accumulation and, through H&E staining, tried to relate these observations to cancer progression. Finally, we examined a panel of human prostate cancer cell lines with defined deletions of *PTEN* or *INPP4B* to evaluate their effects on EGF- and IGF1-dependent accumulation of PI(3,4)P_2 and PI(3,4,5)P_3.

8.2 Results

We utilised a mouse model harbouring prostate-specific deletion of *Pten*, where a modified rat-derived probasin promoter (ARR2PB; (Zhang, Thomas et al. 2000)) drives Cre-recombinase-mediated deletion of *Pten* specifically in prostate epithelial cells (Trotman, Niki et al. 2003). In this model, ARR2PB-driven expression of Cre-recombinase (PB-Cre4) occurs from the onset of prostate development in newborn mice (Wu, Wu et al. 2001). Deletion of PTEN leads to hyperplasic growth of epithelial cells, followed by prostatic intraepithelial neoplasia (PIN) at 6-8 weeks of age, and adenocarcinoma by 4 months, where tumour progression is fastest in the lateral prostate and slowest in the ventral prostate (C. Sandi and S. Cosulich, personal communication; Figure 8.1).

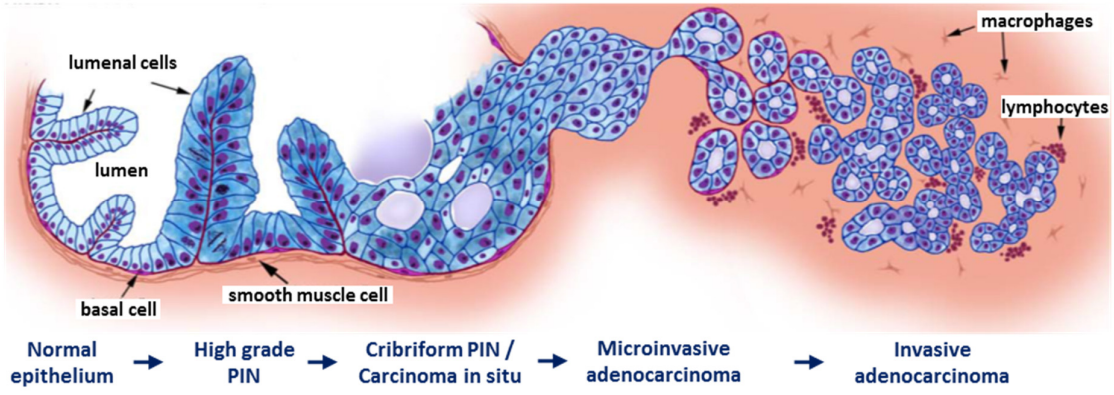

Figure 8.1 Model of cancer progression in mouse prostate

During tumorigenesis, normal prostate epithelium undergoes hyperplastic growth to progress through high-grade prostatic intraepithelial neoplasia (PIN) into cribriform PIN - considered as prostate carcinoma in situ. In later stages of disease progression, cancer cells cross the barrier of smooth muscle cells, which leads to development of microinvasive adenocarcinoma and effectively invasive carcinoma. Adapted from (Iwata, Schultz et al. 2010).

8.2.1 Phosphatidylinositol lipid quantitation in mouse prostate by HPLC-ESI MS/MS

Through a collaboration established with Takehiko Sasaki's group at Akita University, we were able to measure total levels of selected phosphatidylinositol lipids in 10 week [*Pten*$^{flox/flox}$, *PbCre*$^{-/-}$] ('WT') and [*Pten*$^{flox/flox}$, *PbCre*$^{+/-}$] ('PTEN-KO') prostate

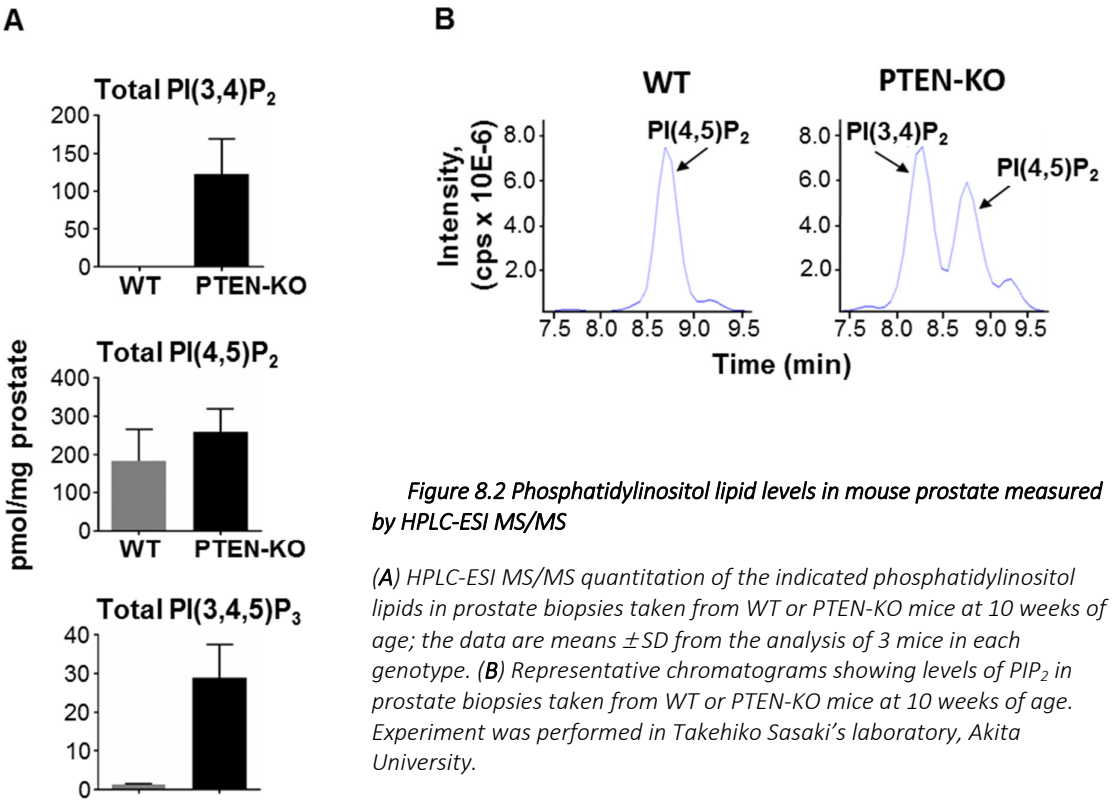

Figure 8.2 Phosphatidylinositol lipid levels in mouse prostate measured by HPLC-ESI MS/MS

*(**A**) HPLC-ESI MS/MS quantitation of the indicated phosphatidylinositol lipids in prostate biopsies taken from WT or PTEN-KO mice at 10 weeks of age; the data are means ± SD from the analysis of 3 mice in each genotype. (**B**) Representative chromatograms showing levels of PIP_2 in prostate biopsies taken from WT or PTEN-KO mice at 10 weeks of age. Experiment was performed in Takehiko Sasaki's laboratory, Akita University.*

biopsies by HPLC-ESI MS/MS (Figure 8.2). Epithelium-specific *Pten* deletion in prostate led to an ~25 fold increase in PI(3,4,5)P_3 compared to the WT condition. More surprisingly, we noted a substantial accumulation of PI(3,4)P_2 in PTEN-KO prostate, with levels of this phosphatidylinositol lipid reaching ~50% of PI(4,5)P_2 (Figure 8.2A). This was an unexpected observation, especially in the context of our previous studies in Mcf10a cells, where EGF-stimulated PI(3,4)P_2 levels in PTEN-KO cells never exceed 5% with respect to PI(4,5)P_2. This immediately suggested PTEN may have a highly significant pathophysiological role in regulating not only PI(3,4,5)P_3, but also PI(3,4)P_2 levels in mouse prostate.

8.2.2 The impact of deleting PTEN and INPP4B in mouse prostate

In order to better understand the function of PTEN and INPP4B in PI(3,4)P_2 homeostasis in mouse prostate, we generated a series of tissue cryosections from mice of different genetic background and at different ages. In pilot experiments, freshly dissected prostates from 12 week WT or PTEN-KO animals were fixed in paraformaldehyde and after incubation in sucrose, slowly frozen in the embedding

medium (refer to Methods section for more detail). Embedded prostates were then sectioned to give 12 µm specimens, followed by labelling of representative sections with anti-PI(3,4)P_2 antibody and a nuclear stain - Hoechst (Figure 8.3). The acini in WT prostate looked normal, with a clear layer of luminal cells at the periphery and no detectable PI(3,4)P_2-specific staining. In contrast, cryosections from PTEN-KO prostate

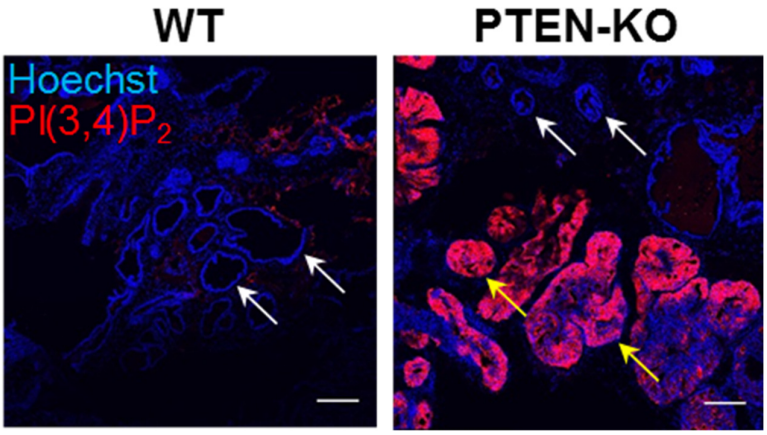

Figure 8.3 PI(3,4)P_2 staining in 12 week mouse prostate cryosections

An example of Hoechst and anti-PI(3,4)P_2 stained sections of prostates taken from WT and PTEN-KO mice at 12 weeks of age. White arrows indicate normal acini and yellow arrows indicate regions in the prostate where acini exhibit HG-PIN. Images are confocal sections of a 12 µm specimen and scale bars represent 0.2 mm.

were more heterogeneous. Some areas displayed characteristics of WT sections, which was probably due to lack of Cre recombinase activity and resulting from this, differences in disease progression between different lobes. These 'normal' areas of PTEN-KO prostate contrasted with neighbouring regions, in which very intense PI(3,4)P_2 staining correlated with acini showing signs of high grade PIN. These results were the first *in vivo* demonstration of aberrant growth that correlated with PI(3,4)P_2-rich, prostatic epithelial cells lacking PTEN expression.

These initial observations were a motivation to extend the study and compare PTEN's role in mouse prostate versus that of INPP4B. To achieve this, we used an analogous approach and prepared cryosections from 16 week mice with four different genetic backgrounds: [*Pten*$^{flox/flox}$, *PbCre*$^{-/-}$] ('WT'), [*Pten*$^{flox/flox}$, *PbCre*$^{+/-}$] ('PTEN-KO'), [*Pten*$^{flox/flox}$, *PbCre*$^{-/-}$, *Inpp4b*$^{-/-}$] ('INPP4B-KO') and [*Pten*$^{flox/flox}$, *PbCre*$^{+/-}$ *Inpp4b*$^{-/-}$] ('PTEN-INPP4B-KO') mice. Two adjacent sections were chosen per condition: the first was labelled with anti-PI(3,4)P_2 antibody and the second was subject to standard H&E

staining for histopathological examination (Figure 8.4A). Analysis of immunofluorescence images from WT and INPP4B-KO prostates showed no significant difference in PI(3,4)P_2 staining. Conversely, prostate sections from PTEN-KO and PTEN-INPP4B-KO mice showed very high accumulation of PI(3,4)P_2 in the acini, with signal intensity indiscernible between the two genotypes. Moreover, PI(3,4)P_2 signal maxima

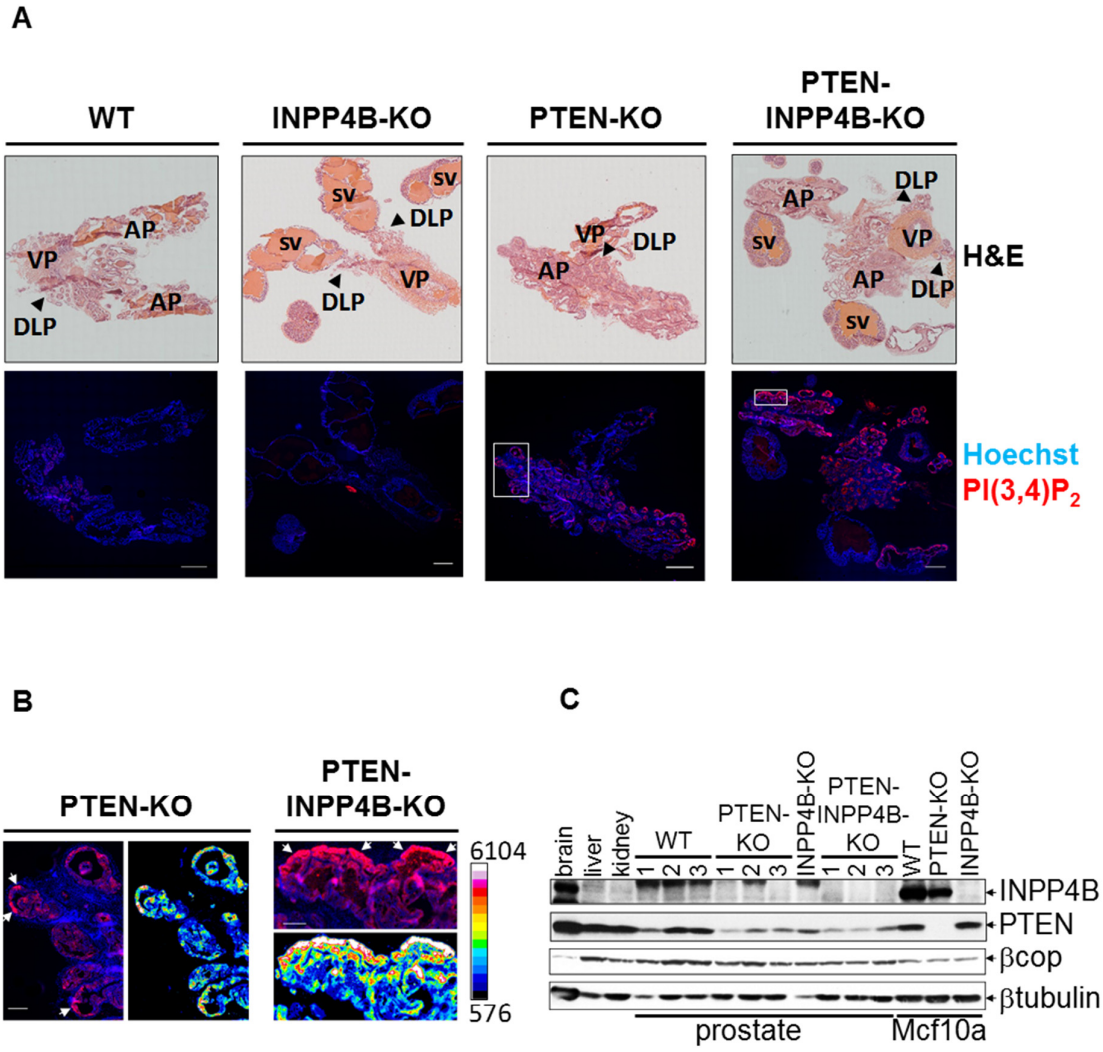

Figure 8.4 The impact of deleting Pten and Inpp4b in mouse prostate

*(**A**) H&E, Hoechst and anti-PI(3,4)P_2 stained sections of prostates taken from WT; PTEN-KO; INPP4B-KO or PTEN-INPP4B-KO mice at 16 weeks of age (scale bar represents 1 mm). (**B**) Some areas of PTEN-KO and PTEN-INPP4B-KO sections are shown at higher magnification (scale bar represents 0.2 mm) and levels of anti-PI(3,4)P_2 staining are represented on the pseudo-colour scale shown; examples of the tips of growing acini are indicated by white arrows. The images shown are typical of 3 prostate sections analysed from 3 mice in each genotype. Seminal vesicles (SV), anterior (A), dorsolateral (DLP) and ventral (V) lobes of the prostate are indicated by black arrows. (**C**) A representative Western blot is shown describing the relative expression of INPP4B and PTEN in the indicated mouse tissues (estimated 20 μg total protein loaded per lane) and human Mcf10a cell clones (15 μg total protein loaded per lane). This experiment was repeated 3 times with similar results. Note: in PTEN-KO prostates, Cre expression and hence PTEN deletion is restricted to prostate epithelial cells which represent only approx 70% of total cellular content. Western Blot analysis performed by Tamara Chessa, Babraham Institute.*

in these two genotypes seemed to localize at the tips of fast proliferating acini (Figure Figure 8.4B).

The lack of effect of *Inpp4b* depletion on $PI(3,4)P_2$ levels and a negligible difference between PTEN and PTEN-INPP4B-KO genotypes, implied that PTEN may be the major $PI(3,4)P_2$ phosphatase in mouse prostate. To test this, we measured protein levels of PTEN and INPP4B in mouse prostate and compared these to expression levels in other mouse organs and Mcf10a cells (Figure 8.4C). The results indicate that the protein level of INPP4B in mouse prostate is very low, which would explain why loss of *Pten*, and not *Inpp4b*, has a very large impact on $PI(3,4)P_2$ accumulation in this organ.

8.2.3 Pathophysiological significance of PTEN deletion in mouse prostate

Phosphatidylinositol lipid analysis in mouse prostate provided us with an insight into the molecular mechanisms that regulate $PI(3,4)P_2$ levels in this tissue. However, the more challenging task was to correlate these observations with a pathophysiological outcome, in situations when the PI3K pathway becomes deregulated. For this, similar to previous studies in Mcf10a cells, we tried to evaluate the levels of AKT phosphorylation resulting from $PI(3,4)P_2$ phosphatase deletion in mouse prostate. Staining of WT prostate with anti-phospho-^{473}Ser-AKT gave a weak signal, which substantially

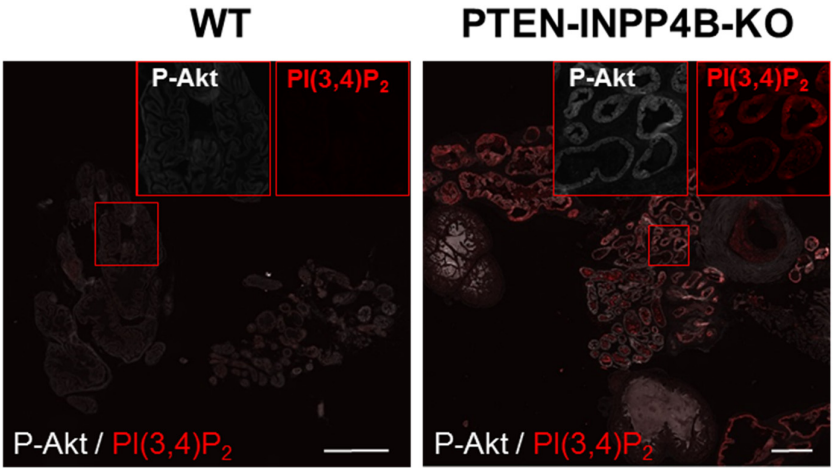

Figure 8.5 $PI(3,4)P_2$ and pAKT levels in 16 week mouse prostate

An example of anti-phospho-^{473}Ser-AKT and anti-$PI(3,4)P_2$ stained sections of prostates taken from [$PTEN^{flox/flox}$, $PbCre^{-/-}$] ('WT') and [$PTEN^{flox/flox}$, $PbCre^{+/-}$ $INPP4B^{-/-}$] ('PTEN-INPP4B-KO') mice at 16 weeks of age (12mm sections). Some areas in anterior prostate of WT and PTEN-INPP4B-KO wide field images are shown at higher magnification, to show localisation of antibody staining. Scale bar represents 1 mm.

increased in analogous staining of PTEN-INPP4B-KO prostate (Figure 8.5). Significantly, increased phosphorylated-AKT levels overlapped with increased anti-PI(3,4)P_2 labelling in this genotype. Although ^{473}Ser-AKT is not an exclusive PI(3,4)P_2 marker, it was a good indication that increased AKT activity is indeed observed in the epithelial cells which undergo hyperplastic growth and are a hallmark of the disease state that evolves in mouse prostate.

Histopathology is one of the most utilised microscopy techniques for comparative examination of tissue biopsies and an important diagnostic tool used in oncology and other areas of medicine. Labelling methods vary depending on the cell type and subject of investigation, but the most broadly used among them is a classical haematoxylin and eosin (H&E) staining. In order to evaluate disease progression in mouse prostates with deleted *Pten*, we performed H&E staining of prostate cryosections from 16 week mice of four different genotypes, i.e. WT, PTEN-KO, INPP4B-KO and PTEN-INPP4B-KO. We also established a collaboration with Sergio Felisbino from the University of Sao Paulo, to gain an independent and unbiased opinion about the changes that occur in genetically modified mouse prostates. Normal mouse prostate is characterised by acini surrounded by a continuous layer of smooth muscle cells and dispersed in the connective tissue of the stroma (Figure 8.6). In such tissue, PI(3,4)P_2 was virtually undetectable by the anti-PI(3,4)P_2 antibody. Acini in INPP4B-KO prostate sections showed no signs of hyperplasia and, to the level of confidence provided by H&E and anti-PI(3,4)P_2 staining,

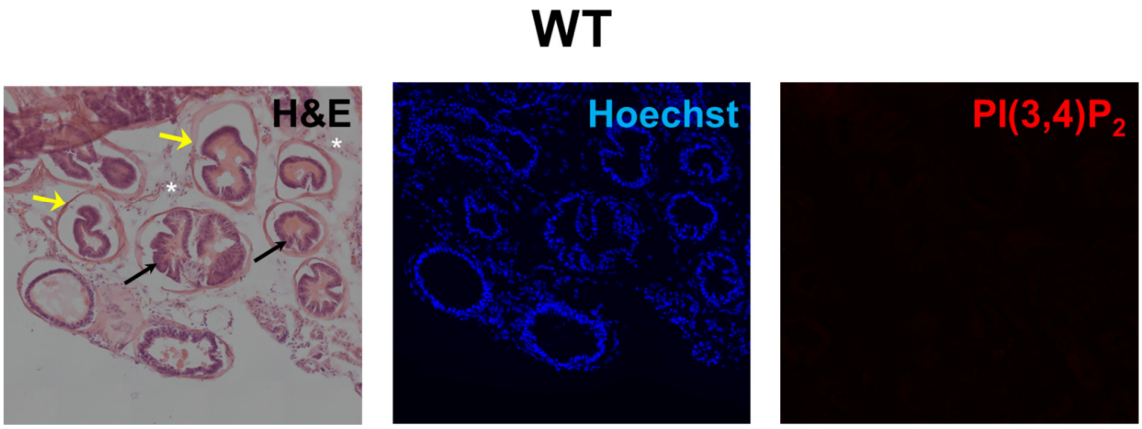

Figure 8.6 H&E staining and PI(3,4)P_2 levels in WT mouse prostate

H&E, Hoechst and anti-PI(3,4)P_2 stained sections of prostates taken from [PTEN$^{flox/flox}$, PbCre$^{-/-}$]('WT') mice at 16 weeks of age. In the H&E panel, yellow arrows indicate smooth muscle cell layer, black arrows indicate luminal cells of the acini and asterisks indicate cells of the stroma. The images shown are typical of 3 prostate sections analysed from 3 mice in each genotype.

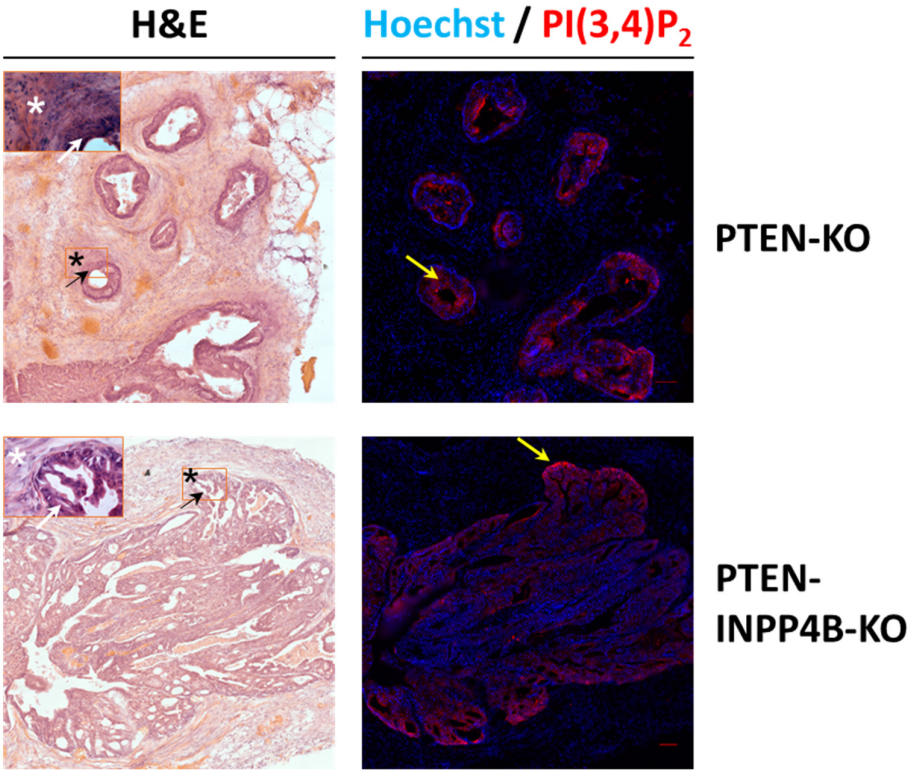

Figure 8.7 H&E staining and PI(3,4)P_2 levels in PTEN and PTEN-INPP4B-KO mouse prostate

H&E, Hoechst and anti-PI(3,4)P_2 stained sections of prostates taken from [PTEN$^{flox/flox}$, PbCre$^{+/-}$]('PTEN-KO') and [PTEN$^{flox/flox}$, PbCre$^{+/-}$ INPP4B$^{-/-}$] ('PTEN-INPP4B-KO') mice at 16 weeks of age (scale bar represents 69 µm). In the H&E panel and insets, arrows indicate position of hyperproliferative epithelium and asterisks indicate reactive stroma and loss of the smooth muscle cell layer. In the Hoechst/PI(3,4)P_2 panel, yellow arrows indicate high PI(3,4)P_2 levels in the acini that correspond to the insets in the H&E images. The images shown are typical of 3 prostate sections analysed from 3 mice in each genotype. Histopathological expertise obtained from Sergio Felisbino, University of Sao Paulo.

they did not differ significantly from WT prostates (data not shown). Deletion of *Pten*, on the other hand, had a significant impact on mouse prostate morphology. Hyperproliferative growth of acinar epithelial cells was accompanied by co-evolution of reactive stroma and, in some cases, gradual infiltration of immune cells. This, and the apparent loss of the smooth muscle cell layer around acini, were indications of initial stages of microinvasion occurring in the prostate from PTEN-KO mice (Figure 8.7). Subsequent histopathological examination of prostates from PTEN-INPP4B-KO mice led to similar observations. Notably, prostates from PTEN-KO and PTEN-INPP4B-KO mice showed elevated levels of PI(3,4)P_2 which strongly correlated with acini in the lobes characterised by most pronounced disease progression.

8.2.4 Role of PTEN as a PI(3,4)P_2 phosphatase in human prostate cancer cell lines

PTEN deregulation is one of the primary molecular drivers of prostatic neoplasia in men, with genetic abnormalities detected in nearly 1 in 3 cases of advanced primary tumours (Wang, Gao et al. 2003). Due to its haploinsufficient character, consequences of loss of one functional *PTEN* allele are clearly manifested by elevated AKT phosphorylation. Human prostate cancer cell lines have been extensively used as tools to study prostate cancer biology, especially in the context of functional overlap between PI3K/AKT and AR signalling axes. Unlike in mice, INPP4B has an important role in human prostate and its expression seems to be androgen-regulated (Hodgson, Shao et al. 2011).

We chose a panel of human prostate cancer cell lines and examined the impact of INPP4B or PTEN absence on the EGF- or IGF1-stimulated accumulation of PI(3,4,5)P_3 and PI(3,4)P_2 (Figure 8.8A, B). In parallel, we performed Western blot analysis to assess INPP4B and PTEN expression in these cells (Figure 8.8C). EGF and IGF1 stimulated PI(3,4,5)P_3 accumulation in BPH1 ('WT' control) and DU145 ('INPP4B-KO') cells, but did not lead to a detectable increase in PI(3,4)P_2. Cells lacking PTEN, i.e. LNCaP, LNCaP95 and PC3, showed elevated, basal PI(3,4,5)P_3 levels and accumulated significant amounts of both PI(3,4,5)P_3 and PI(3,4)P_2 in response to EGF. Interestingly, the kinetics and relative amounts of phosphatidylinositol lipids differed between the three 'PTEN-KO' cell lines, which may be related to availability and/or activation of 5-phosphatases in each cell type or additional factors (e.g. mutations), which are common in transformed cells. Surprisingly, IGF1 stimulation did not result in significant increases in PI(3,4)P_2 or PI(3,4,5)P_3 in 'PTEN-KO' cells. This phenomenon may be partly explained by negative feedback within the IGF-signalling pathway caused by hyperactivation of the PI3K pathway upon *PTEN* deletion – an observation made in a parallel project in our lab. Unfortunately we did not find a prostate line in which both PTEN and INPP4B were mutated.

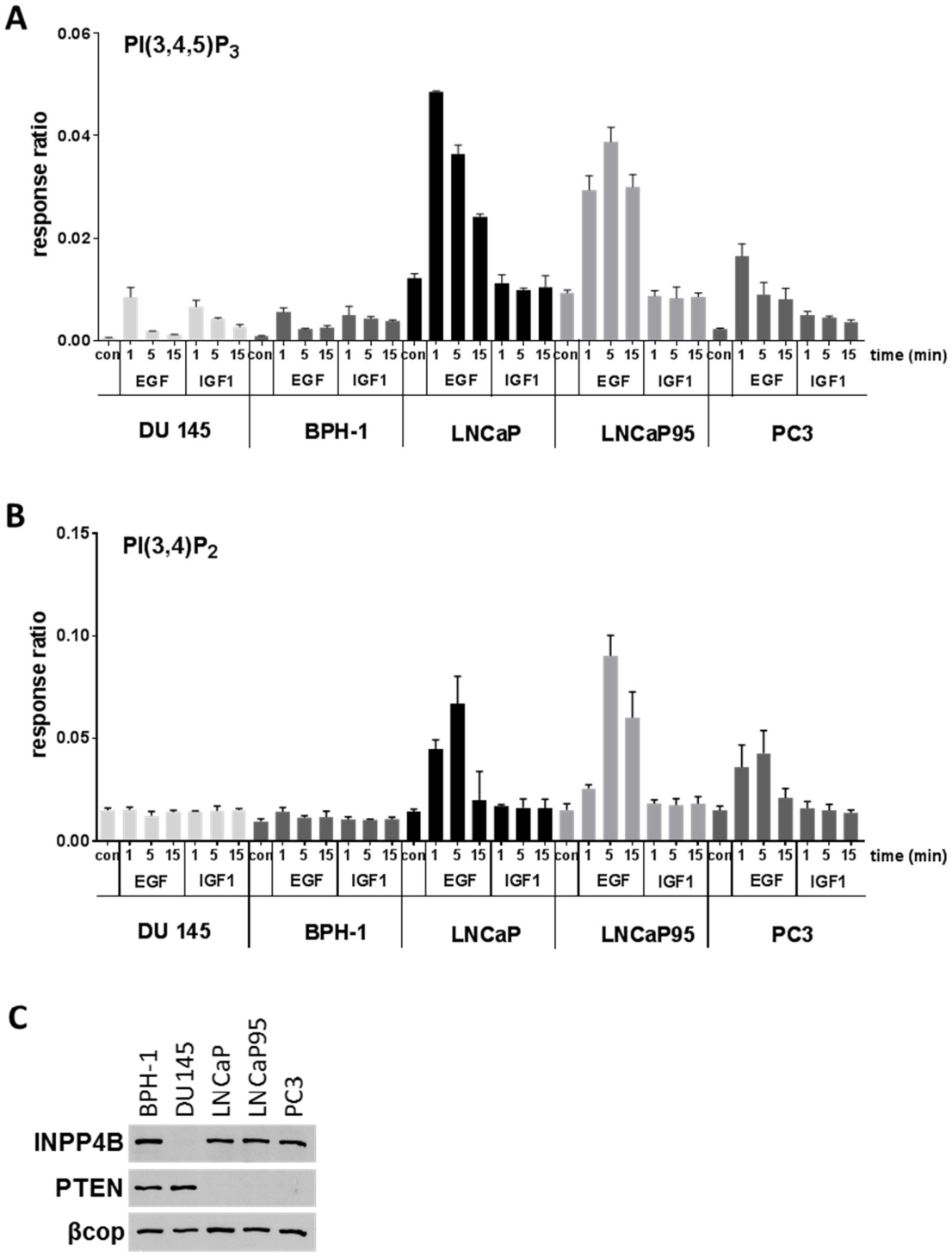

Figure 8.8 PI(3,4,5)P_3 and PI(3,4)P_2 in prostate cancer cells

*(**A**) PI(3,4,5)P_3 and (**B**) PI(3,4)P_2 levels in human prostate cancer cell lines starved and then stimulated with EGF (10ng/ml) or IGF1 (50ng/ml) for 0, 1, 5 or 15 min. Phosphatidylinositol lipids were analysed by HPLC-ESI MS/MS using a C4 or C18 column for measurement of PI(3,4,5)P_3 and PI(3,4)P_2, respectively. Data are means ± SD of at least two independent experiments. (**C**) Western blot showing relative expression of INPP4B, PTEN and beta-COP in the indicated human prostate cancer cell lines (20mg total protein loaded per lane). Western blot analysis was performed by Tamara Chessa, Babraham Institute.*

8.3 Discussion

We demonstrated here a critical role for PTEN in controlling cellular processes that underpin normal prostate development and function. By using a conditional mouse knock-out model, we were able to restrict our observations to *Pten-null*, prostatic epithelial cells and exclude other systemic effects. Importantly, $PI(3,4)P_2$ levels were significantly elevated in PTEN-KO prostates from early stages of tumour development (10 weeks) to a pre-invasive state (16 weeks) and we were able to detect these levels reliably by HPLC-ESI MS/MS as well as using an anti-$PI(3,4)P_2$ antibody. We were surprised by the high accumulation of $PI(3,4)P_2$, reaching almost equivalent levels to $PI(4,5)P_2$ in prostates from 10 week PTEN-KO animals. Since then, we have also observed comparably high levels of $PI(3,4)P_2$ accumulation in PTEN-KO prostate organoids grown in acidic pH for extended periods of time (data not shown). Further, we demonstrated very low expression of INPP4B in mouse prostate compared to other mice tissues or Mcf10a cells with comparable expression of PTEN.

Histopathological examination of mouse prostate sections revealed that elevated $PI(3,4)P_2$ marks the tips of growing acini and acini which show early stages of microinvasion. Finally, we correlated high $PI(3,4)P_2$ levels with regions in mouse prostate with enhanced phospho-^{473}Ser-AKT - a marker suggested to positively correlate with high Gleason grade in patients with advanced prostate cancer (Ayala, Thompson et al. 2004).

Prostate cancer cell lines with reported *PTEN* deletion have been characterised by hyperactivation of AKT (Nacerddine, Beaudry et al. 2012). We demonstrated that cells lacking PTEN, but not INPP4B, accumulate significant levels of $PI(3,4,5)P_3$ and $PI(3,4)P_2$ in response to stimulation with EGF. Unfortunately, we were unable to identify a prostate cancer cell line with low INPP4B expression in addition to a *PTEN-null* background (our best candidate, the NCI H660 cell line, expressed ~30% of INPP4B relative to 'WT' cells).

Overall, our analysis of mouse prostate was consistent with our observations in Mcf10a cells. Conditions in which both PTEN and INPP4B are absent, mouse PTEN-KO prostate or PTEN-INPP4B-KO Mcf10a cells, result in substantial accumulation of $PI(3,4)P_2$. In contrast to mouse prostate, human prostate cell lines express significant levels of INPP4B. However, several studies have now shown that advanced, androgen-

ablation-resistant prostate cancer is characterised by a high incidence of PTEN mutation and relatively low levels of INPP4B expression. This has obvious implications for a potential role for $PI(3,4)P_2$ in tumorigenesis and this is discussed further in the next Chapter.

Chapter 9 General discussion

Since the initial discovery of PTEN in the late 90s, our understanding of its central role in modulating physiological processes driven by class I PI3K signalling has significantly advanced. Although the intellectual link between PTEN, PI(3,4,5)P_3 and AKT remains fully justifiable, the work presented in this dissertation describes PTEN as a dual PI(3,4,5)P_3/PI(3,4)P_2 lipid phosphatase, which not only emphasizes its importance in cellular homeostasis but raises an immediate question about the overlapping/divergent functions of these two phosphatidylinositol lipids. Inevitably, time limitations of this project restricted our ability to explore some of the observations that emerged during its course, hence, several important questions still need resolving. Nevertheless, I hope that our initial attempts to characterise PTEN as a physiological PI(3,4)P_2 3-phosphatase in Mcf10a cells and mouse prostate will stimulate a scientific discussion and create a driving force for future studies to fully appreciate PTEN's importance as a tumour suppressor.

The newly developed HPLC-ESI MS/MS method for measuring two regioisomers - PI(3,4)P_2 and PI(4,5)P_2 - was instrumental in performing the core experiments of this project and in demonstrating PTEN's direct role as a PI(3,4)P_2 phosphatase. However, its restriction to the measurement of the C38:4 molecular species of these lipids, together with the need for a separate method to measure PI(3,4,5)P_3, are significant limitations. The C38:4 species is the most abundant form of inositol lipids in primary mammalian cells (Clark, Anderson et al. 2011, Anderson, Juvin et al. 2016), but recent papers have started to suggest that the acyl composition of these lipids may be under tight regulation (Naguib, Bencze et al. 2015). Furthermore, analysing these lipids in other eukaryotes would require significant further development of the method described here. This method was also unable to sufficiently resolve PI(3,5)P_2 from PI(4,5)P_2, or the regioisomers of PIPs (PI3P, PI4P, PI5P) to allow their measurement in cell extracts. Thus, future efforts should focus on developing a universal mass spectrometry method, one that would allow quantification of the eight phosphatidylinositol lipid members, irrespective of their headgroup or acyl chain characteristics.

The HPLC-ESI MS/MS method gave a much higher value for PI(3,4)P_2 in basal Mcf10a cells than parallel labelling studies with [^{33}P]Pi. We do not understand the reason for this discrepancy, but a slowly turning over pool of PI(3,4)P_2 or some form of

mass contaminant seem the most plausible explanations. Labelling cells to equilibrium with radiolabelled and/or isotope enriched inositol would seem to be the next logical step to resolving this.

Our studies in human mammary epithelial cells (Mcf10a), prostate cancer cell lines and mouse prostate supported previous observations suggesting substantial functional redundancy exists amongst the lipid phosphatases that are a result of complex regulatory mechanisms which are organism-, cell- and stimulus-specific. LPS-activated B cells from *Ship1*$^{-/-}$ mice were shown to express SHIP2 as a compensatory mechanism to antagonise BCR-mediated AKT phosphorylation via interaction with the tyrosine-phosphorylated ITIM motifs of cytosolic FcγRIIB tails (Brauweiler, Tamir et al. 2001). In contrast, human platelets seem to rely on SHIP1's activity to dephosphorylate PI(3,4,5)P_3, with a marginal contribution from SHIP2 and PTEN (Giuriato, Pesesse et al. 2003). Keeping this in mind, our inability to define a group of 5-phosphatases with a dominant role in the dephosphorylation of class I PI3K-generated PI(3,4,5)P_3 in EGF-stimulated Mcf10a cells was still surprising. On the other hand, PI(3,4,5)P_3 levels generated in EGF-stimulated [PTEN-SHIP2-KO, INPP4A/B-KD] cells represent a highly abnormal situation, where phosphatases may become enrolled in the dephosphorylation of PI(3,4,5)P_3 that would not normally contribute under more physiological circumstances. This is precisely what has previously been proposed to be the role of INPP4B in the dephosphorylation of PI(3,4,5)P_3 in PTEN-deficient mouse thyroid (Kofuji, Kimura et al. 2015), although we observed no such role for this protein in Mcf10a cells.

Our results describing PTEN as a direct PI(3,4)P_2 phosphatase has evolved the current perception of its role in the context of class I PI3K signalling. There are two main reasons why this role may have been under-appreciated in the past. Firstly, it is difficult to study PI(3,4)P_2, a secondary product of class I PI3K activity, decoupled from transiently generated PI(3,4,5)P_3. Hence, arguments such as increased flux through PI(3,4,5)P_3 5-dephosphorylation were probably the most intuitive explanation in cases where elevated PI(3,4)P_2 and PI(3,4,5)P_3 levels were observed in cells lacking PTEN activity. Secondly, whilst PI(3,4)P_2 was recognised as a potential substrate for PTEN in early *in vitro* experiments (Maehama and Dixon 1998), the most sophisticated analyses suggested it was a very poor substrate compared to PI(3,4,5)P_3 (McConnachie, Pass et al. 2003). We don't yet understand why PTEN was such an effective PI(3,4)P_2 3-phosphatase in our Mcf10a cytosol assays, but a clue may be the inclusion of substantial

amounts of PI(4,5)P_2 in all of our assays, which is an important co-factor for PTEN and which would be autologously generated from PI(3,4,5)P_3, but not PI(3,4)P_2, in assays containing only these substrates. A strategy to circumvent the coupling of PTEN's effects on PI(3,4,5)P_3 and PI(3,4)P_2, would be to generate a PTEN mutant capable of hydrolysing PI(3,4,5)P_3 but not PI(3,4)P_2. In this regard, it would also be extremely interesting to evaluate whether specific missense mutations in PTEN observed in cancer or overgrowth syndromes differ in their relative abilities to hydrolyse PI(3,4)P_2 versus PI(3,4,5)P_3.

Our results draw into focus the potential role for PI(3,4)P_2 as a signalling molecule in its own right and its contribution to the phenotypes observed when PTEN function is impaired. The recently described class I PI3K-mediated endocytic recycling of agonist-activated RTKs and GPCRs (i.e. endophilin-specific 'FEME', see Introduction) is an example of a physiological process that depends on cellular PI(3,4)P_2 (Boucrot, Ferreira et al. 2015). Here, INPP4A/B suppression in cells was shown to increase endophilin-positive endosomes/lysosomes and it would be interesting to carefully test PTEN's contribution to this process, particularly given PTEN's best characterised roles as a lipid phosphatase acting on PI(4,5)P_2-rich plasma membranes. This would also help put into perspective the level of redundancy between PI(3,4)P_2-specific phosphatases - a question that we did not answer exhaustively during this project.

The interaction between PH domain-containing AKT and PI(3,4,5)P_3/PI(3,4)P_2 is an obligatory step to trigger kinase catalytic activity and many experiments have shown that chemical inhibition of class I PI3K terminates AKT-driven processes. However, the precise relative contribution of PI(3,4,5)P_3 versus PI(3,4)P_2 to the activation of AKT in any given pathophysiological context is still unclear. Further, the interaction between scaffolding proteins like LPD, TKS5 or SNX9 and PI(3,4)P_2, is only one of several stages during the assembly of multicomponent protein-complexes in the vicinity of the plasma membrane, which makes it very difficult to isolate the specific contribution that PI(3,4)P_2 makes and hence its indispensability to the physiological process. Nevertheless, PI(3,4)P_2 is starting to emerge as an important modulator of processes which influence cellular motility, signalling efficiency and tumour progression. Our studies show a strong correlation between EGF-stimulated PI(3,4)P_2 formation, which in Mcf10a cells accumulates as a consequence of combined deletion of its two direct phosphatases, PTEN and INPP4B, and an increased number of gelatin-degrading

invadopodia. Whilst additional experiments are required to relate this observation to the TKS5-PI(3,4)P_2 interaction described in the literature, our experiments suggest that an invasive phenotype can be induced in Mcf10a cells driven by the presence of PI(3,4)P_2 and thus implies a new potential role for the PTEN tumour suppressor. The involvement of PI(3,4)P_2 in the class I PI3K-mediated invasive potential of mutated Mcf10a cells is also in line with the most recent work performed in breast cancer cells (Fukumoto, Ijuin et al. 2017). Fukumoto et al. described SHIP2 as a 'phenotypic switch', which when supressed, transforms highly motile, lamellipodia-forming MDA-MB-231 cells into cells with increased number of mature focal adhesions and extended surface area. The invasive phenotype of 'native' MDA-MB-231 cells was shown to depend on class I PI3K activity, combined with SHIP2's generation of PI(3,4)P_2. Interestingly, PTEN knock-down did not affect focal adhesion formation but led to decreased cell size and increased cell penetration through matrigel, indicating enhanced invasive character compared to control MDA-MB-231 cells. Further, cells with combined suppression of PTEN and SHIP2, i.e. cells with impeded PI(3,4,5)P_3 hydrolytic activity, showed decreased matrigel-penetration ability, similar to SHIP2-KD cells. In light of this recent work, it would be interesting to test the effect of SHIP2 depletion on Mcf10a's ability to form invadopodia, especially in the [PTEN-KO, INPP4B-KD] mutant cells, where SHIP2 deletion had a negligible effect on total cellular PI(3,4)P_2 levels. Finally, future experiments should focus on validating the molecular mechanisms that link the phosphatidylinositol lipid PI(3,4)P_2, PTEN and cellular invasiveness in the *in vivo* setting of invadopodia formation by cancer cells.

Tumourigenesis can be described as process in which normal cells escape tight regulatory mechanisms controlling proliferation and programmed cell death through acquired mutations. Unrestrained cellular growth and division, as well as survival under limiting nutrient conditions due to reprogrammed metabolic pathways, are some of the characteristics of transformed cells. It is therefore perhaps unsurprising that a powerful tumour suppressor such as PTEN turned out to be a direct antagonist of class I PI3K-signalling. Despite this, the differential susceptibility of tissues to PTEN-driven carcinogenesis and the complex mechanisms that underpin PTEN's expression and activity are the subject of an ongoing debate. PTEN's function as the major phosphatase regulating PI(3,4)P_2 levels in mouse prostate and PI(3,4)P_2's correlation with the regions of most advanced disease progression (i.e. exhibiting high grade PIN and in

some cases the first signs of microinvasion), substantiated our previous findings in Mcf10a cells and provoked a consideration about PI(3,4)P_2's role in tumourigenesis. Advanced cancers are characterised by outgrowth beyond the initiation site and/or by their potential to metastasize. The potential for INPP4B to act as a conditional tumour suppressor in mouse thyroid was demonstrated by crossing mice lacking both alleles of *Inpp4b* with mice lacking one allele of *Pten* (Kofuji, Kimura et al. 2015, Li Chew, Lunardi et al. 2015). Our results indicating both INPP4B and PTEN can act in a partially redundant manner in the dephosphorylation of PI(3,4)P_2 provides a potential explanation for these observations. Further, the importance of INPP4B as a tumour suppressor in humans is supported by studies showing that loss of INPP4B expression correlated with advanced breast and poorly-prognosing ovarian cancer (Gewinner, Wang et al. 2009, Fedele, Ooms et al. 2010). Moreover, coincidental downregulation at the gene and/or protein level of PTEN and INPP4B was revealed by the analysis of human thyroid and endometrial cancer databases (Kofuji, Kimura et al. 2015). In human prostate, loss of expression of PTEN or INPP4B has been associated with poor prognosis in advanced tumours but no significant correlation between these two events has been reported (Rynkiewicz, Fedele et al. 2015). However, due to INPP4B's transcriptional regulation downstream of androgen receptor signalling, the relationship between PTEN and INPP4B, and their potential impact on PI(3,4)P_2 levels in patients subject to androgen-ablation therapy is more complex (Hodgson, Shao et al. 2011). Considering these findings, one could hypothesize that in advanced tumours a hyperproliferative phenotype co-exists with an activated invasive phenotype due, at least in part, to enhanced PI(3,4)P_2 accumulation. This is especially interesting in light of SHIP2's control of the invasive phenotype in MDA-MB-231 cells (discussed earlier in this Chapter (Fukumoto, Ijuin et al. 2017)) and emerging reports that postulate a correlation between SHIP2's overexpression and poor outcome in metastatic breast cancer (Prasad, Tandon et al. 2008). If followed up in future studies, this may bring a new functional significance to the 5-dephosphorylation route of PI(3,4,5)P_3 removal and specific 5-phosphatase's role within it. With this in mind, it becomes more important than ever to better understand the fine balance that exists between PI(3,4,5)P_3 and PI(3,4)P_2 in normal cells, as well as the changes that occur at different stages of tumour progression and the role of PTEN and other relevant phosphatidylinositol lipid phosphatases entangled in class I PI3K-mediated signalling. These considerations may have a pivotal impact on helping identify new targets along the class I PI3K/AKT signalling axis, or

other yet unidentified pathways, and may potentially lead to therapy strategies suited for cancers of different cellular origin and different stages of advancement.

References

Abram, C. L., D. F. Seals, I. Pass, D. Salinsky, L. Maurer, T. M. Roth and S. A. Courtneidge (2003). "The adaptor protein fish associates with members of the ADAMs family and localizes to podosomes of Src-transformed cells." J Biol Chem **278**(19): 16844-16851.

Agoulnik, I. U., M. C. Hodgson, W. A. Bowden and M. M. Ittmann (2011). "INPP4B: the new kid on the PI3K block." Oncotarget **2**(4): 321-328.

Agranoff, B. W., R. M. Bradley and R. O. Brady (1958). "The enzymatic synthesis of inositol phosphatide." J Biol Chem **233**(5): 1077-1083.

Alessi, D. R., S. R. James, C. P. Downes, A. B. Holmes, P. R. Gaffney, C. B. Reese and P. Cohen (1997). "Characterization of a 3-phosphoinositide-dependent protein kinase which phosphorylates and activates protein kinase Balpha." Curr Biol **7**(4): 261-269.

Alimonti, A., A. Carracedo, J. G. Clohessy, L. C. Trotman, C. Nardella, A. Egia, L. Salmena, K. Sampieri, W. J. Haveman, E. Brogi, A. L. Richardson, J. Zhang and P. P. Pandolfi (2010). "Subtle variations in Pten dose determine cancer susceptibility." Nat Genet **42**(5): 454-458.

Alvarez-Nunez, F., E. Bussaglia, D. Mauricio, J. Ybarra, M. Vilar, E. Lerma, A. de Leiva and X. Matias-Guiu (2006). "PTEN promoter methylation in sporadic thyroid carcinomas." Thyroid **16**(1): 17-23.

Anderson, K. E., K. B. Boyle, K. Davidson, T. A. Chessa, S. Kulkarni, G. E. Jarvis, A. Sindrilaru, K. Scharffetter-Kochanek, O. Rausch, L. R. Stephens and P. T. Hawkins (2008). "CD18-dependent activation of the neutrophil NADPH oxidase during phagocytosis of Escherichia coli or Staphylococcus aureus is regulated by class III but not class I or II PI3Ks." Blood **112**(13): 5202-5211.

Anderson, K. E., V. Juvin, J. Clark, L. R. Stephens and P. T. Hawkins (2016). "Investigating the effect of arachidonate supplementation on the phosphoinositide content of MCF10a breast epithelial cells." Adv Biol Regul **62**: 18-24.

Anderson, K. E., A. Kielkowska, T. N. Durrant, V. Juvin, J. Clark, L. R. Stephens and P. T. Hawkins (2013). "Lysophosphatidylinositol-acyltransferase-1 (LPIAT1) is required to maintain physiological levels of PtdIns and PtdInsP(2) in the mouse." PLoS One **8**(3): e58425.

Angulo, I., O. Vadas, F. Garcon, E. Banham-Hall, V. Plagnol, T. R. Leahy, H. Baxendale, T. Coulter, J. Curtis, C. Wu, K. Blake-Palmer, O. Perisic, D. Smyth, M. Maes, C. Fiddler, J. Juss, D. Cilliers, G. Markelj, A. Chandra, G. Farmer, A. Kielkowska, J. Clark, S. Kracker, M. Debre, C. Picard, I. Pellier, N. Jabado, J. A. Morris, G. Barcenas-Morales, A. Fischer, L. Stephens, P. Hawkins, J. C. Barrett, M. Abinun, M. Clatworthy, A. Durandy, R. Doffinger, E. R. Chilvers, A. J. Cant, D. Kumararatne, K. Okkenhaug, R. L. Williams, A. Condliffe and S. Nejentsev (2013). "Phosphoinositide 3-kinase delta gene mutation predisposes to respiratory infection and airway damage." Science **342**(6160): 866-871.

Arcaro, A., M. J. Zvelebil, C. Wallasch, A. Ullrich, M. D. Waterfield and J. Domin (2000). "Class II phosphoinositide 3-kinases are downstream targets of activated polypeptide growth factor receptors." Mol Cell Biol **20**(11): 3817-3830.

Auger, K. R., L. A. Serunian, S. P. Soltoff, P. Libby and L. C. Cantley (1989). "PDGF-dependent tyrosine phosphorylation stimulates production of novel polyphosphoinositides in intact cells." Cell **57**(1): 167-175.

Axe, E. L., S. A. Walker, M. Manifava, P. Chandra, H. L. Roderick, A. Habermann, G. Griffiths and N. T. Ktistakis (2008). "Autophagosome formation from membrane compartments enriched in phosphatidylinositol 3-phosphate and dynamically connected to the endoplasmic reticulum." The Journal of Cell Biology **182**(4): 685-701.

Ayala, G., T. Thompson, G. Yang, A. Frolov, R. Li, P. Scardino, M. Ohori, T. Wheeler and W. Harper (2004). "High levels of phosphorylated form of Akt-1 in prostate cancer and non-neoplastic prostate tissues are strong predictors of biochemical recurrence." Clin Cancer Res **10**(19): 6572-6578.

Balla, T. (2013). "Phosphoinositides: tiny lipids with giant impact on cell regulation." Physiol Rev **93**(3): 1019-1137.

Banerjee, S. and S. Mazumdar (2012). "Electrospray ionization mass spectrometry: a technique to access the information beyond the molecular weight of the analyte." Int J Anal Chem **2012**: 282574.

Bassi, C., J. Ho, T. Srikumar, R. J. Dowling, C. Gorrini, S. J. Miller, T. W. Mak, B. G. Neel, B. Raught and V. Stambolic (2013). "Nuclear PTEN controls DNA repair and sensitivity to genotoxic stress." Science **341**(6144): 395-399.

Blero, D., B. Payrastre, S. Schurmans and C. Erneux (2007). "Phosphoinositide phosphatases in a network of signalling reactions." Pflugers Arch **455**(1): 31-44.

Boucrot, E., A. P. Ferreira, L. Almeida-Souza, S. Debard, Y. Vallis, G. Howard, L. Bertot, N. Sauvonnet and H. T. McMahon (2015). "Endophilin marks and controls a clathrin-independent endocytic pathway." Nature **517**(7535): 460-465.

Branch, K. M., D. Hoshino and A. M. Weaver (2012). "Adhesion rings surround invadopodia and promote maturation." Biol Open **1**(8): 711-722.

Bratton, D. L., V. A. Fadok, D. A. Richter, J. M. Kailey, L. A. Guthrie and P. M. Henson (1997). "Appearance of phosphatidylserine on apoptotic cells requires calcium-mediated nonspecific flip-flop and is enhanced by loss of the aminophospholipid translocase." J Biol Chem **272**(42): 26159-26165.

Brauweiler, A., I. Tamir, J. Dal Porto, R. J. Benschop, C. D. Helgason, R. K. Humphries, J. H. Freed and J. C. Cambier (2000). "Differential regulation of B cell development, activation, and death by the src homology 2 domain-containing 5' inositol phosphatase (SHIP)." J Exp Med **191**(9): 1545-1554.

Brauweiler, A., I. Tamir, S. Marschner, C. D. Helgason and J. C. Cambier (2001). "Partially Distinct Molecular Mechanisms Mediate Inhibitory Fc RIIB Signaling in Resting and Activated B Cells." The Journal of Immunology **167**(1): 204-211.

Brown, J. R., J. C. Byrd, S. E. Coutre, D. M. Benson, I. W. Flinn, N. D. Wagner-Johnston, S. E. Spurgeon, B. S. Kahl, C. Bello, H. K. Webb, D. M. Johnson, S. Peterman, D. Li, T. M. Jahn, B. J. Lannutti, R. G. Ulrich, A. S. Yu, L. L. Miller and R. R. Furman (2014). "Idelalisib, an inhibitor of phosphatidylinositol 3-kinase p110delta, for relapsed/refractory chronic lymphocytic leukemia." Blood **123**(22): 3390-3397.

Burgering, B. M. and P. J. Coffer (1995). "Protein kinase B (c-Akt) in phosphatidylinositol-3-OH kinase signal transduction." Nature **376**(6541): 599-602.

Burke, J. E. and R. L. Williams (2015). "Synergy in activating class I PI3Ks." Trends Biochem Sci **40**(2): 88-100.

Cariaga-Martinez, A. E., P. Lopez-Ruiz, M. P. Nombela-Blanco, O. Motino, A. Gonzalez-Corpas, J. Rodriguez-Ubreva, M. V. Lobo, M. A. Cortes and B. Colas (2013). "Distinct and specific roles of AKT1 and AKT2 in androgen-sensitive and androgen-independent prostate cancer cells." Cell Signal **25**(7): 1586-1597.

Carracedo, A., A. Alimonti and P. P. Pandolfi (2011). "PTEN level in tumor suppression: how much is too little?" Cancer Res **71**(3): 629-633.

Chen, W. T. (1989). "Proteolytic activity of specialized surface protrusions formed at rosette contact sites of transformed cells." J Exp Zool **251**(2): 167-185.

Clark, J., K. E. Anderson, V. Juvin, T. S. Smith, F. Karpe, M. J. Wakelam, L. R. Stephens and P. T. Hawkins (2011). "Quantification of PtdInsP3 molecular species in cells and tissues by mass spectrometry." Nat Methods **8**(3): 267-272.

Clark, J., R. R. Kay, A. Kielkowska, I. Niewczas, L. Fets, D. Oxley, L. R. Stephens and P. T. Hawkins (2014). "Dictyostelium uses ether-linked inositol phospholipids for intracellular signalling." EMBO J **33**(19): 2188-2200.

Clarke, N. G. and R. M. Dawson (1981). "Alkaline O leads to N-transacylation. A new method for the quantitative deacylation of phospholipids." Biochem J **195**(1): 301-306.

Cong, L., F. A. Ran, D. Cox, S. Lin, R. Barretto, N. Habib, P. D. Hsu, X. Wu, W. Jiang, L. A. Marraffini and F. Zhang (2013). "Multiplex genome engineering using CRISPR/Cas systems." Science **339**(6121): 819-823.

Damen, J. E., L. Liu, P. Rosten, R. K. Humphries, A. B. Jefferson, P. W. Majerus and G. Krystal (1996). "The 145-kDa protein induced to associate with Shc by multiple cytokines is an inositol tetraphosphate and phosphatidylinositol 3,4,5-triphosphate 5-phosphatase." Proc Natl Acad Sci U S A **93**(4): 1689-1693.

David-Pfeuty, T. and S. J. Singer (1980). "Altered distributions of the cytoskeletal proteins vinculin and alpha-actinin in cultured fibroblasts transformed by Rous sarcoma virus." Proc Natl Acad Sci U S A **77**(11): 6687-6691.

Deladeriere, A., L. Gambardella, D. Pan, K. E. Anderson, P. T. Hawkins and L. R. Stephens (2015). "The regulatory subunits of PI3Kgamma control distinct neutrophil responses." Sci Signal **8**(360): ra8.

Di Cristofano, A., B. Pesce, C. Cordon-Cardo and P. P. Pandolfi (1998). "Pten is essential for embryonic development and tumour suppression." Nat Genet **19**(4): 348-355.

Dillon, R. L., R. Marcotte, B. T. Hennessy, J. R. Woodgett, G. B. Mills and W. J. Muller (2009). "Akt1 and akt2 play distinct roles in the initiation and metastatic phases of mammary tumor progression." Cancer Res **69**(12): 5057-5064.

Doherty, G. J. and H. T. McMahon (2009). "Mechanisms of endocytosis." Annu Rev Biochem **78**: 857-902.

Domin, J., F. Pages, S. Volinia, S. E. Rittenhouse, M. J. Zvelebil, R. C. Stein and M. D. Waterfield (1997). "Cloning of a human phosphoinositide 3-kinase with a C2 domain that displays reduced sensitivity to the inhibitor wortmannin." Biochem J **326 (Pt 1)**: 139-147.

Dove, S. K., K. Dong, T. Kobayashi, F. K. Williams and R. H. Michell (2009). "Phosphatidylinositol 3,5-bisphosphate and Fab1p/PIKfyve underPPIn endo-lysosome function." Biochem J **419**(1): 1-13.

Dowler, S., R. A. Currie, D. G. Campbell, M. Deak, G. Kular, C. P. Downes and D. R. Alessi (2000). "Identification of pleckstrin-homology-domain-containing proteins with novel phosphoinositide-binding specificities." Biochem J **351**(Pt 1): 19-31.

Ellson, C. D., S. Gobert-Gosse, K. E. Anderson, K. Davidson, H. Erdjument-Bromage, P. Tempst, J. W. Thuring, M. A. Cooper, Z. Y. Lim, A. B. Holmes, P. R. Gaffney, J. Coadwell, E. R. Chilvers, P. T. Hawkins and L. R. Stephens (2001). "PtdIns(3)P regulates the neutrophil oxidase complex by binding to the PX domain of p40(phox)." Nat Cell Biol **3**(7): 679-682.

Endersby, R., X. Zhu, N. Hay, D. W. Ellison and S. J. Baker (2011). "Nonredundant functions for Akt isoforms in astrocyte growth and gliomagenesis in an orthotopic transplantation model." Cancer Res **71**(12): 4106-4116.

Engelman, D. M. (2005). "Membranes are more mosaic than fluid." Nature **438**(7068): 578-580.

Eramo, M. J. and C. A. Mitchell (2016). "Regulation of PtdIns(3,4,5)P3/Akt signalling by inositol polyphosphate 5-phosphatases." Biochem Soc Trans **44**(1): 240-252.

Fedele, C. G., L. M. Ooms, M. Ho, J. Vieusseux, S. A. O'Toole, E. K. Millar, E. Lopez-Knowles, A. Sriratana, R. Gurung, L. Baglietto, G. G. Giles, C. G. Bailey, J. E. Rasko, B. J. Shields, J. T. Price, P. W. Majerus, R. L. Sutherland, T. Tiganis, C. A. McLean and C. A. Mitchell (2010). "Inositol polyphosphate 4-phosphatase II regulates PI3K/Akt signaling and is lost in human basal-like breast cancers." Proc Natl Acad Sci U S A **107**(51): 22231-22236.

Ferguson, K. M., M. A. Lemmon, J. Schlessinger and P. B. Sigler (1995). "Structure of the high affinity complex of inositol trisphosphate with a phospholipase C pleckstrin homology domain." Cell **83**(6): 1037-1046.

Ferron, M., M. Boudiffa, M. Arsenault, M. Rached, M. Pata, S. Giroux, L. Elfassihi, M. Kisseleva, P. W. Majerus, F. Rousseau and J. Vacher (2011). "Inositol polyphosphate 4-phosphatase B as a regulator of bone mass in mice and humans." Cell Metab **14**(4): 466-477.

Franke, T. F., D. R. Kaplan, L. C. Cantley and A. Toker (1997). "Direct regulation of the Akt proto-oncogene product by phosphatidylinositol-3,4-bisphosphate." Science 275(5300): 665-668.

Franke, T. F., S. I. Yang, T. O. Chan, K. Datta, A. Kazlauskas, D. K. Morrison, D. R. Kaplan and P. N. Tsichlis (1995). "The protein kinase encoded by the Akt proto-oncogene is a target of the PDGF-activated phosphatidylinositol 3-kinase." Cell 81(5): 727-736.

Frech, M., M. Andjelkovic, E. Ingley, K. K. Reddy, J. R. Falck and B. A. Hemmings (1997). "High affinity binding of inositol phosphates and phosphoinositides to the pleckstrin homology domain of RAC/protein kinase B and their influence on kinase activity." J Biol Chem 272(13): 8474-8481.

Freeburn, R. W., K. L. Wright, S. J. Burgess, E. Astoul, D. A. Cantrell and S. G. Ward (2002). "Evidence That SHIP-1 Contributes to Phosphatidylinositol 3,4,5-Trisphosphate Metabolism in T Lymphocytes and Can Regulate Novel Phosphoinositide 3-Kinase Effectors." The Journal of Immunology 169(10): 5441-5450.

Fruman, D. A. and C. Rommel (2011). "PI3Kdelta inhibitors in cancer: rationale and serendipity merge in the clinic." Cancer Discov 1(7): 562-572.

Fukumoto, M., T. Ijuin and T. Takenawa (2017). "PI(3,4)P2 plays critical roles in the regulation of focal adhesion dynamics of MDA-MB-231 breast cancer cells." Cancer Sci 108(5): 941-951.

Funamoto, S., R. Meili, S. Lee, L. Parry and R. A. Firtel (2002). "Spatial and temporal regulation of 3-phosphoinositides by PI 3-kinase and PTEN mediates chemotaxis." Cell 109(5): 611-623.

Furet, P., V. Guagnano, R. A. Fairhurst, P. Imbach-Weese, I. Bruce, M. Knapp, C. Fritsch, F. Blasco, J. Blanz, R. Aichholz, J. Hamon, D. Fabbro and G. Caravatti (2013). "Discovery of NVP-BYL719 a potent and selective phosphatidylinositol-3 kinase alpha inhibitor selected for clinical evaluation." Bioorganic & Medicinal Chemistry Letters 23(13): 3741-3748.

Gan, X., J. Wang, B. Su and D. Wu (2011). "Evidence for direct activation of mTORC2 kinase activity by phosphatidylinositol 3,4,5-trisphosphate." J Biol Chem 286(13): 10998-11002.

Garcia, J. M., J. Silva, C. Pena, V. Garcia, R. Rodriguez, M. A. Cruz, B. Cantos, M. Provencio, P. Espana and F. Bonilla (2004). "Promoter methylation of the PTEN gene is a common molecular change in breast cancer." Genes Chromosomes Cancer 41(2): 117-124.

Gaullier, J. M., A. Simonsen, A. D'Arrigo, B. Bremnes, H. Stenmark and R. Aasland (1998). "FYVE fingers bind PtdIns(3)P." Nature 394(6692): 432-433.

Gewinner, C., Z. C. Wang, A. Richardson, J. Teruya-Feldstein, D. Etemadmoghadam, D. Bowtell, J. Barretina, W. M. Lin, L. Rameh, L. Salmena, P. P. Pandolfi and L. C. Cantley (2009). "Evidence that inositol polyphosphate 4-phosphatase type II is a tumor suppressor that inhibits PI3K signaling." Cancer Cell 16(2): 115-125.

Giampieri, S., C. Manning, S. Hooper, L. Jones, C. S. Hill and E. Sahai (2009). "Localized and reversible TGFbeta signalling switches breast cancer cells from cohesive to single cell motility." Nat Cell Biol 11(11): 1287-1296.

Giuriato, S., X. Pesesse, S. Bodin, T. Sasaki, C. Viala, E. Marion, J. Penninger, S. Schurmans, C. Erneux and B. Payrastre (2003). "SH2-containing inositol 5-phosphatases 1 and 2 in blood platelets: their interactions and roles in the control of phosphatidylinositol 3,4,5-trisphosphate levels." Biochem J **376**(Pt 1): 199-207.

Gligorijevic, B., A. Bergman and J. Condeelis (2014). "Multiparametric classification links tumor microenvironments with tumor cell phenotype." PLoS Biol **12**(11): e1001995.

Gratacap, M. P., J. Guillermet-Guibert, V. Martin, G. Chicanne, H. Tronchere, F. Gaits-Iacovoni and B. Payrastre (2011). "Regulation and roles of PI3Kbeta, a major actor in platelet signaling and functions." Adv Enzyme Regul **51**(1): 106-116.

Guertin, D. A. and D. M. Sabatini (2007). "Defining the role of mTOR in cancer." Cancer Cell **12**(1): 9-22.

Guillou, H., L. R. Stephens and P. T. Hawkins (2007). "Quantitative Measurement of Phosphatidylinositol 3,4,5-trisphosphate." Methods Enzymol **434**: 117-130.

Gurung, R., A. Tan, L. M. Ooms, M. J. McGrath, R. D. Huysmans, A. D. Munday, M. Prescott, J. C. Whisstock and C. A. Mitchell (2003). "Identification of a novel domain in two mammalian inositol-polyphosphate 5-phosphatases that mediates membrane ruffle localization. The inositol 5-phosphatase skip localizes to the endoplasmic reticulum and translocates to membrane ruffles following epidermal growth factor stimulation." J Biol Chem **278**(13): 11376-11385.

Haas-Kogan, D., N. Shalev, M. Wong, G. Mills, G. Yount and D. Stokoe (1998). "Protein kinase B (PKB/Akt) activity is elevated in glioblastoma cells due to mutation of the tumor suppressor PTEN/MMAC." Curr Biol **8**(21): 1195-1198.

Hammond, G. R. and T. Balla (2015). "Polyphosphoinositide binding domains: Key to inositol lipid biology." Biochim Biophys Acta **1851**(6): 746-758.

Hankins, H. M., R. D. Baldridge, P. Xu and T. R. Graham (2015). "Role of flippases, scramblases and transfer proteins in phosphatidylserine subcellular distribution." Traffic **16**(1): 35-47.

Harlan, J. E., P. J. Hajduk, H. S. Yoon and S. W. Fesik (1994). "Pleckstrin homology domains bind to phosphatidylinositol-4,5-bisphosphate." Nature **371**(6493): 168-170.

Hawkins, P. T., K. E. Anderson, K. Davidson and L. R. Stephens (2006). "Signalling through Class I PI3Ks in mammalian cells." Biochem Soc Trans **34**(Pt 5): 647-662.

Hawkins, P. T., T. R. Jackson and L. R. Stephens (1992). "Platelet-derived growth factor stimulates synthesis of PtdIns(3,4,5)P3 by activating a PtdIns(4,5)P2 3-OH kinase." Nature **358**(6382): 157-159.

Hawkins, P. T. and L. R. Stephens (2015). "PI3K signalling in inflammation." Biochim Biophys Acta **1851**(6): 882-897.

Hawkins, P. T. and L. R. Stephens (2016). "Emerging evidence of signalling roles for PI(3,4)P2 in Class I and II PI3K-regulated pathways." Biochem Soc Trans **44**(1): 307-314.

Helgason, C. D., J. E. Damen, P. Rosten, R. Grewal, P. Sorensen, S. M. Chappel, A. Borowski, F. Jirik, G. Krystal and R. K. Humphries (1998). "Targeted disruption of SHIP leads to hemopoietic perturbations, lung pathology, and a shortened life span." Genes Dev **12**(11): 1610-1620.

Hiles, I. D., M. Otsu, S. Volinia, M. J. Fry, I. Gout, R. Dhand, G. Panayotou, F. Ruiz-Larrea, A. Thompson, N. F. Totty and et al. (1992). "Phosphatidylinositol 3-kinase: structure and expression of the 110 kd catalytic subunit." Cell **70**(3): 419-429.

Hodgson, M. C., L. J. Shao, A. Frolov, R. Li, L. E. Peterson, G. Ayala, M. M. Ittmann, N. L. Weigel and I. U. Agoulnik (2011). "Decreased expression and androgen regulation of the tumor suppressor gene INPP4B in prostate cancer." Cancer Res **71**(2): 572-582.

Hollander, M. C., G. M. Blumenthal and P. A. Dennis (2011). "PTEN loss in the continuum of common cancers, rare syndromes and mouse models." Nat Rev Cancer **11**(4): 289-301.

Iwata, T., D. Schultz, J. Hicks, G. K. Hubbard, L. N. Mutton, T. L. Lotan, C. Bethel, M. T. Lotz, S. Yegnasubramanian, W. G. Nelson, C. V. Dang, M. Xu, U. Anele, C. M. Koh, C. J. Bieberich and A. M. De Marzo (2010). "MYC overexpression induces prostatic intraepithelial neoplasia and loss of Nkx3.1 in mouse luminal epithelial cells." PLoS One **5**(2): e9427.

Jia, S., Z. Liu, S. Zhang, P. Liu, L. Zhang, S. H. Lee, J. Zhang, S. Signoretti, M. Loda, T. M. Roberts and J. J. Zhao (2008). "Essential roles of PI(3)K-p110beta in cell growth, metabolism and tumorigenesis." Nature **454**(7205): 776-779.

Juvin, V., M. Malek, K. E. Anderson, C. Dion, T. Chessa, C. Lecureuil, G. J. Ferguson, S. Cosulich, P. T. Hawkins and L. R. Stephens (2013). "Signaling via class IA Phosphoinositide 3-kinases (PI3K) in human, breast-derived cell lines." PLoS One **8**(10): e75045.

Kanai, F., H. Liu, S. J. Field, H. Akbary, T. Matsuo, G. E. Brown, L. C. Cantley and M. B. Yaffe (2001). "The PX domains of p47phox and p40phox bind to lipid products of PI(3)K." Nat Cell Biol **3**(7): 675-678.

Kennedy, E. P. and S. B. Weiss (1956). "The function of cytidine coenzymes in the biosynthesis of phospholipides." J Biol Chem **222**(1): 193-214.

Kielkowska, A., I. Niewczas, K. E. Anderson, T. N. Durrant, J. Clark, L. R. Stephens and P. T. Hawkins (2014). "A new approach to measuring phosphoinositides in cells by mass spectrometry." Adv Biol Regul **54**: 131-141.

Kinross, K. M., K. G. Montgomery, M. Kleinschmidt, P. Waring, I. Ivetac, A. Tikoo, M. Saad, L. Hare, V. Roh, T. Mantamadiotis, K. E. Sheppard, G. L. Ryland, I. G. Campbell, K. L. Gorringe, J. G. Christensen, C. Cullinane, R. J. Hicks, R. B. Pearson, R. W. Johnstone, G. A. McArthur and W. A. Phillips (2012). "An activating Pik3ca mutation coupled with Pten loss is sufficient to initiate ovarian tumorigenesis in mice." J Clin Invest **122**(2): 553-557.

Kiselev, V. Y., V. Juvin, M. Malek, N. Luscombe, P. Hawkins, N. Le Novere and L. Stephens (2015). "Perturbations of PIP3 signalling trigger a global remodelling of mRNA landscape and reveal a transcriptional feedback loop." Nucleic Acids Res **43**(20): 9663-9679.

Klein, D. E., A. Lee, D. W. Frank, M. S. Marks and M. A. Lemmon (1998). "The pleckstrin homology domains of dynamin isoforms require oligomerization for high affinity phosphoinositide binding." J Biol Chem **273**(42): 27725-27733.

Knight, Z. A., B. Gonzalez, M. E. Feldman, E. R. Zunder, D. D. Goldenberg, O. Williams, R. Loewith, D. Stokoe, A. Balla, B. Toth, T. Balla, W. A. Weiss, R. L. Williams and K. M. Shokat (2006). "A pharmacological map of the PI3-K family defines a role for p110alpha in insulin signaling." Cell **125**(4): 733-747.

Knobbe, C. B., V. Lapin, A. Suzuki and T. W. Mak (2008). "The roles of PTEN in development, physiology and tumorigenesis in mouse models: a tissue-by-tissue survey." Oncogene **27**(41): 5398-5415.

Kofuji, S., H. Kimura, H. Nakanishi, H. Nanjo, S. Takasuga, H. Liu, S. Eguchi, R. Nakamura, R. Itoh, N. Ueno, K. Asanuma, M. Huang, A. Koizumi, T. Habuchi, M. Yamazaki, A. Suzuki, J. Sasaki and T. Sasaki (2015). "INPP4B Is a PtdIns(3,4,5)P3 Phosphatase That Can Act as a Tumor Suppressor." Cancer Discov **5**(7): 730-739.

Koren, S. and M. Bentires-Alj (2013). "Mouse models of PIK3CA mutations: one mutation initiates heterogeneous mammary tumors." FEBS J **280**(12): 2758-2765.

Landego, I., N. Jayachandran, S. Wullschleger, T. T. Zhang, I. W. Gibson, A. Miller, D. R. Alessi and A. J. Marshall (2012). "Interaction of TAPP adapter proteins with phosphatidylinositol (3,4)-bisphosphate regulates B-cell activation and autoantibody production." Eur J Immunol **42**(10): 2760-2770.

Lands, W. E. (1958). "Metabolism of glycerolipides; a comparison of lecithin and triglyceride synthesis." J Biol Chem **231**(2): 883-888.

Lee, H. C., T. Inoue, R. Imae, N. Kono, S. Shirae, S. Matsuda, K. Gengyo-Ando, S. Mitani and H. Arai (2008). "Caenorhabditis elegans mboa-7, a member of the MBOAT family, is required for selective incorporation of polyunsaturated fatty acids into phosphatidylinositol." Mol Biol Cell **19**(3): 1174-1184.

Lee, J. O., H. Yang, M. M. Georgescu, A. Di Cristofano, T. Maehama, Y. Shi, J. E. Dixon, P. Pandolfi and N. P. Pavletich (1999). "Crystal structure of the PTEN tumor suppressor: implications for its phosphoinositide phosphatase activity and membrane association." Cell **99**(3): 323-334.

Lemmon, M. A. (2007). "Pleckstrin homology (PH) domains and phosphoinositides." Biochem Soc Symp(74): 81-93.

Leong, H. S., A. E. Robertson, K. Stoletov, S. J. Leith, C. A. Chin, A. E. Chien, M. N. Hague, A. Ablack, K. Carmine-Simmen, V. A. McPherson, C. O. Postenka, E. A. Turley, S. A. Courtneidge, A. F. Chambers and J. D. Lewis (2014). "Invadopodia are required for cancer cell extravasation and are a therapeutic target for metastasis." Cell Rep **8**(5): 1558-1570.

Leslie, N. R., N. Kriplani, M. A. Hermida, V. Alvarez-Garcia and H. M. Wise (2016). "The PTEN protein: cellular localization and post-translational regulation." Biochem Soc Trans **44**(1): 273-278.

Li Chew, C., A. Lunardi, F. Gulluni, D. T. Ruan, M. Chen, L. Salmena, M. Nishino, A. Papa, C. Ng, J. Fung, J. G. Clohessy, J. Sasaki, T. Sasaki, R. T. Bronson, E. Hirsch and P. P. Pandolfi (2015). "In Vivo Role of INPP4B in Tumor and Metastasis Suppression through Regulation of PI3K-AKT Signaling at Endosomes." Cancer Discov **5**(7): 740-751.

Li, H. and A. J. Marshall (2015). "Phosphatidylinositol (3,4) bisphosphate-specific phosphatases and effector proteins: A distinct branch of PI3K signaling." Cell Signal **27**(9): 1789-1798.

Li, J., C. Yen, D. Liaw, K. Podsypanina, S. Bose, S. I. Wang, J. Puc, C. Miliaresis, L. Rodgers, R. McCombie, S. H. Bigner, B. C. Giovanella, M. Ittmann, B. Tycko, H. Hibshoosh, M. H. Wigler and R. Parsons (1997). "PTEN, a putative protein tyrosine phosphatase gene mutated in human brain, breast, and prostate cancer." Science **275**(5308): 1943-1947.

Liaw, D., D. J. Marsh, J. Li, P. L. Dahia, S. I. Wang, Z. Zheng, S. Bose, K. M. Call, H. C. Tsou, M. Peacocke, C. Eng and R. Parsons (1997). "Germline mutations of the PTEN gene in Cowden disease, an inherited breast and thyroid cancer syndrome." Nat Genet **16**(1): 64-67.

Lindsay, Y., D. McCoull, L. Davidson, N. R. Leslie, A. Fairservice, A. Gray, J. Lucocq and C. P. Downes (2006). "Localization of agonist-sensitive PtdIns(3,4,5)P3 reveals a nuclear pool that is insensitive to PTEN expression." J Cell Sci **119**(Pt 24): 5160-5168.

Ma, K., S. M. Cheung, A. J. Marshall and V. Duronio (2008). "PI(3,4,5)P3 and PI(3,4)P2 levels correlate with PKB/akt phosphorylation at Thr308 and Ser473, respectively; PI(3,4)P2 levels determine PKB activity." Cell Signal **20**(4): 684-694.

Maehama, T. and J. E. Dixon (1998). "The tumor suppressor, PTEN/MMAC1, dephosphorylates the lipid second messenger, phosphatidylinositol 3,4,5-trisphosphate." J Biol Chem **273**(22): 13375-13378.

Manning, B. D. and L. C. Cantley (2007). "AKT/PKB signaling: navigating downstream." Cell **129**(7): 1261-1274.

Martin, K. H., K. E. Hayes, E. L. Walk, A. G. Ammer, S. M. Markwell and S. A. Weed (2012). "Quantitative measurement of invadopodia-mediated extracellular matrix proteolysis in single and multicellular contexts." J Vis Exp(66): e4119.

Maxwell, M. J., Y. Yuan, K. E. Anderson, M. L. Hibbs, H. H. Salem and S. P. Jackson (2004). "SHIP1 and Lyn Kinase Negatively Regulate Integrin alpha IIb beta 3 signaling in platelets." J Biol Chem **279**(31): 32196-32204.

McConnachie, G., I. Pass, S. M. Walker and C. P. Downes (2003). "Interfacial kinetic analysis of the tumour suppressor phosphatase, PTEN: evidence for activation by anionic phospholipids." Biochem J **371**(Pt 3): 947-955.

Mueller, H., A. Stadtmann, H. Van Aken, E. Hirsch, D. Wang, K. Ley and A. Zarbock (2010). "Tyrosine kinase Btk regulates E-selectin-mediated integrin activation and neutrophil recruitment by controlling phospholipase C (PLC) gamma2 and PI3Kgamma pathways." Blood **115**(15): 3118-3127.

Myers, M. P., I. Pass, I. H. Batty, J. Van der Kaay, J. P. Stolarov, B. A. Hemmings, M. H. Wigler, C. P. Downes and N. K. Tonks (1998). "The lipid phosphatase activity of PTEN is critical for its tumor supressor function." Proc Natl Acad Sci U S A **95**(23): 13513-13518.

Myers, M. P., J. P. Stolarov, C. Eng, J. Li, S. I. Wang, M. H. Wigler, R. Parsons and N. K. Tonks (1997). "P-TEN, the tumor suppressor from human chromosome 10q23, is a dual-specificity phosphatase." Proc Natl Acad Sci U S A **94**(17): 9052-9057.

Nacerddine, K., J. B. Beaudry, V. Ginjala, B. Westerman, F. Mattiroli, J. Y. Song, H. van der Poel, O. B. Ponz, C. Pritchard, P. Cornelissen-Steijger, J. Zevenhoven, E. Tanger, T. K. Sixma, S. Ganesan and M. van Lohuizen (2012). "Akt-mediated phosphorylation of Bmi1 modulates its oncogenic potential, E3 ligase activity, and DNA damage repair activity in mouse prostate cancer." J Clin Invest **122**(5): 1920-1932.

Naguib, A., G. Bencze, D. D. Engle, Chio, II, T. Herzka, K. Watrud, S. Bencze, D. A. Tuveson, D. J. Pappin and L. C. Trotman (2015). "p53 mutations change phosphatidylinositol acyl chain composition." Cell Rep **10**(1): 8-19.

Naylor, T. L., J. Greshock, Y. Wang, T. Colligon, Q. C. Yu, V. Clemmer, T. Z. Zaks and B. L. Weber (2005). "High resolution genomic analysis of sporadic breast cancer using array-based comparative genomic hybridization." Breast Cancer Res **7**(6): R1186-1198.

Nishio, M., K. Watanabe, J. Sasaki, C. Taya, S. Takasuga, R. Iizuka, T. Balla, M. Yamazaki, H. Watanabe, R. Itoh, S. Kuroda, Y. Horie, I. Forster, T. W. Mak, H. Yonekawa, J. M. Penninger, Y. Kanaho, A. Suzuki and T. Sasaki (2007). "Control of cell polarity and motility by the PtdIns(3,4,5)P3 phosphatase SHIP1." Nat Cell Biol **9**(1): 36-44.

Norris, F. A., R. C. Atkins and P. W. Majerus (1997). "The cDNA cloning and characterization of inositol polyphosphate 4-phosphatase type II. Evidence for conserved alternative splicing in the 4-phosphatase family." J Biol Chem **272**(38): 23859-23864.

Okkenhaug, K., M. Graupera and B. Vanhaesebroeck (2016). "Targeting PI3K in Cancer: Impact on Tumor Cells, Their Protective Stroma, Angiogenesis, and Immunotherapy." Cancer Discov **6**(10): 1090-1105.

Ooms, L. M., L. C. Binge, E. M. Davies, P. Rahman, J. R. Conway, R. Gurung, D. T. Ferguson, A. Papa, C. G. Fedele, J. L. Vieusseux, R. C. Chai, F. Koentgen, J. T. Price, T. Tiganis, P. Timpson, C. A. McLean and C. A. Mitchell (2015). "The Inositol Polyphosphate 5-Phosphatase PIPP Regulates AKT1-Dependent Breast Cancer Growth and Metastasis." Cancer Cell **28**(2): 155-169.

Ooms, L. M., C. G. Fedele, M. V. Astle, I. Ivetac, V. Cheung, R. B. Pearson, M. J. Layton, A. Forrai, H. H. Nandurkar and C. A. Mitchell (2006). "The inositol polyphosphate 5-phosphatase, PIPP, Is a novel regulator of phosphoinositide 3-kinase-dependent neurite elongation." Mol Biol Cell **17**(2): 607-622.

Ooms, L. M., K. A. Horan, P. Rahman, G. Seaton, R. Gurung, D. S. Kethesparan and C. A. Mitchell (2009). "The role of the inositol polyphosphate 5-phosphatases in cellular function and human disease." Biochem J **419**(1): 29-49.

Papayannopoulos, V., C. Co, K. E. Prehoda, S. Snapper, J. Taunton and W. A. Lim (2005). "A polybasic motif allows N-WASP to act as a sensor of PIP(2) density." Mol Cell **17**(2): 181-191.

Paterson, E. K. and S. A. Courtneidge (2017). "Invadosomes are coming: new insights into function and disease relevance." FEBS J.

Patki, V., D. C. Lawe, S. Corvera, J. V. Virbasius and A. Chawla (1998). "A functional PtdIns(3)P-binding motif." Nature **394**(6692): 433-434.

Pesesse, X., S. Deleu, F. De Smedt, L. Drayer and C. Erneux (1997). "Identification of a second SH2-domain-containing protein closely related to the phosphatidylinositol polyphosphate 5-phosphatase SHIP." Biochem Biophys Res Commun **239**(3): 697-700.

Pignatelli, J., D. A. Tumbarello, R. P. Schmidt and C. E. Turner (2012). "Hic-5 promotes invadopodia formation and invasion during TGF-beta-induced epithelial-mesenchymal transition." J Cell Biol **197**(3): 421-437.

Pomorski, T. and A. K. Menon (2006). "Lipid flippases and their biological functions." Cell Mol Life Sci **63**(24): 2908-2921.

Posor, Y., M. Eichhorn-Gruenig, D. Puchkov, J. Schoneberg, A. Ullrich, A. Lampe, R. Muller, S. Zarbakhsh, F. Gulluni, E. Hirsch, M. Krauss, C. Schultz, J. Schmoranzer, F. Noe and V. Haucke (2013). "Spatiotemporal control of endocytosis by phosphatidylinositol-3,4-bisphosphate." Nature **499**(7457): 233-237.

Prasad, N. K., M. Tandon, A. Handa, G. E. Moore, C. F. Babbs, P. W. Snyder and S. Bose (2008). "High expression of obesity-linked phosphatase SHIP2 in invasive breast cancer correlates with reduced disease-free survival." Tumour Biol **29**(5): 330-341.

Ran, F. A., P. D. Hsu, J. Wright, V. Agarwala, D. A. Scott and F. Zhang (2013). "Genome engineering using the CRISPR-Cas9 system." Nat Protoc **8**(11): 2281-2308.

Revach, O.-Y. and B. Geiger (2013). "The interplay between the proteolytic, invasive, and adhesive domains of invadopodia and their roles in cancer invasion." Cell Adhesion & Migration **8**(3): 215-225.

Rodgers, S. J., D. T. Ferguson, C. A. Mitchell and L. M. Ooms (2017). "Regulation of PI3K effector signalling in cancer by the phosphoinositide phosphatases." Biosci Rep **37**(1).

Rokhlin, O. W., A. F. Taghiyev, N. V. Guseva, R. A. Glover, S. I. Syrbu and M. B. Cohen (2002). "TRAIL-DISC formation is androgen-dependent in the human prostatic carcinoma cell line LNCaP." Cancer Biol Ther **1**(6): 631-637.

Rudolph, M., T. Anzeneder, A. Schulz, G. Beckmann, A. T. Byrne, M. Jeffers, C. Pena, O. Politz, K. Kochert, R. Vonk and J. Reischl (2016). "AKT1 (E17K) mutation profiling in breast cancer: prevalence, concurrent oncogenic alterations, and blood-based detection." BMC Cancer **16**: 622.

Rynkiewicz, N. K., C. G. Fedele, K. Chiam, R. Gupta, J. G. Kench, L. M. Ooms, C. A. McLean, G. G. Giles, L. G. Horvath and C. A. Mitchell (2015). "INPP4B is highly expressed in prostate

intermediate cells and its loss of expression in prostate carcinoma predicts for recurrence and poor long term survival." Prostate 75(1): 92-102.

Saal, L. H., K. Holm, M. Maurer, L. Memeo, T. Su, X. Wang, J. S. Yu, P. O. Malmstrom, M. Mansukhani, J. Enoksson, H. Hibshoosh, A. Borg and R. Parsons (2005). "PIK3CA mutations correlate with hormone receptors, node metastasis, and ERBB2, and are mutually exclusive with PTEN loss in human breast carcinoma." Cancer Res 65(7): 2554-2559.

Samuels, Y., Z. Wang, A. Bardelli, N. Silliman, J. Ptak, S. Szabo, H. Yan, A. Gazdar, S. M. Powell, G. J. Riggins, J. K. Willson, S. Markowitz, K. W. Kinzler, B. Vogelstein and V. E. Velculescu (2004). "High frequency of mutations of the PIK3CA gene in human cancers." Science 304(5670): 554.

Sarbassov, D. D., D. A. Guertin, S. M. Ali and D. M. Sabatini (2005). "Phosphorylation and regulation of Akt/PKB by the rictor-mTOR complex." Science 307(5712): 1098-1101.

Sarker, D., A. H. Reid, T. A. Yap and J. S. de Bono (2009). "Targeting the PI3K/AKT pathway for the treatment of prostate cancer." Clin Cancer Res 15(15): 4799-4805.

Sasaki, J., S. Kofuji, R. Itoh, T. Momiyama, K. Takayama, H. Murakami, S. Chida, Y. Tsuya, S. Takasuga, S. Eguchi, K. Asanuma, Y. Horie, K. Miura, E. M. Davies, C. Mitchell, M. Yamazaki, H. Hirai, T. Takenawa, A. Suzuki and T. Sasaki (2010). "The PtdIns(3,4)P(2) phosphatase INPP4A is a suppressor of excitotoxic neuronal death." Nature 465(7297): 497-501.

Scheid, M. P., M. Huber, J. E. Damen, M. Hughes, V. Kang, P. Neilsen, G. D. Prestwich, G. Krystal and V. Duronio (2002). "Phosphatidylinositol (3,4,5)P3 is essential but not sufficient for protein kinase B (PKB) activation; phosphatidylinositol (3,4)P2 is required for PKB phosphorylation at Ser-473: studies using cells from SH2-containing inositol-5-phosphatase knockout mice." J Biol Chem 277(11): 9027-9035.

Schu, P. V., K. Takegawa, M. J. Fry, J. H. Stack, M. D. Waterfield and S. D. Emr (1993). "Phosphatidylinositol 3-kinase encoded by yeast VPS34 gene essential for protein sorting." Science 260(5104): 88-91.

Seals, D. F., E. F. Azucena, Jr., I. Pass, L. Tesfay, R. Gordon, M. Woodrow, J. H. Resau and S. A. Courtneidge (2005). "The adaptor protein Tks5/Fish is required for podosome formation and function, and for the protease-driven invasion of cancer cells." Cancer Cell 7(2): 155-165.

Sezgin, E., I. Levental, S. Mayor and C. Eggeling (2017). "The mystery of membrane organization: composition, regulation and roles of lipid rafts." Nat Rev Mol Cell Biol 18(6): 361-374.

Sharma, V. P., R. Eddy, D. Entenberg, M. Kai, F. B. Gertler and J. Condeelis (2013). "Tks5 and SHIP2 regulate invadopodium maturation, but not initiation, in breast carcinoma cells." Curr Biol 23(21): 2079-2089.

Singer, S. J. and G. L. Nicolson (1972). "The fluid mosaic model of the structure of cell membranes." Science 175(4023): 720-731.

Sleeman, M. W., K. E. Wortley, K. M. Lai, L. C. Gowen, J. Kintner, W. O. Kline, K. Garcia, T. N. Stitt, G. D. Yancopoulos, S. J. Wiegand and D. J. Glass (2005). "Absence of the lipid phosphatase SHIP2 confers resistance to dietary obesity." Nat Med **11**(2): 199-205.

Song, M. S., L. Salmena and P. P. Pandolfi (2012). "The functions and regulation of the PTEN tumour suppressor." Nat Rev Mol Cell Biol **13**(5): 283-296.

Soule, H. D., T. M. Maloney, S. R. Wolman, W. D. Peterson, Jr., R. Brenz, C. M. McGrath, J. Russo, R. J. Pauley, R. F. Jones and S. C. Brooks (1990). "Isolation and characterization of a spontaneously immortalized human breast epithelial cell line, MCF-10." Cancer Res **50**(18): 6075-6086.

Stambolic, V., A. Suzuki, J. L. de la Pompa, G. M. Brothers, C. Mirtsos, T. Sasaki, J. Ruland, J. M. Penninger, D. P. Siderovski and T. W. Mak (1998). "Negative regulation of PKB/Akt-dependent cell survival by the tumor suppressor PTEN." Cell **95**(1): 29-39.

Stambolic, V., M.-s. Tsao, D. Macpherson, A. Suzuki, W. B. Chapman and T. W. Mak (2000). "High incidence of breast and endometrial neoplasia resembling human Cowden syndrome in pten+/- mice." Cancer Res **60**(13): 3605-3611.

Steck, P. A., M. A. Pershouse, S. A. Jasser, W. K. Yung, H. Lin, A. H. Ligon, L. A. Langford, M. L. Baumgard, T. Hattier, T. Davis, C. Frye, R. Hu, B. Swedlund, D. H. Teng and S. V. Tavtigian (1997). "Identification of a candidate tumour suppressor gene, MMAC1, at chromosome 10q23.3 that is mutated in multiple advanced cancers." Nat Genet **15**(4): 356-362.

Stephens, L., K. Anderson, D. Stokoe, H. Erdjument-Bromage, G. F. Painter, A. B. Holmes, P. R. Gaffney, C. B. Reese, F. McCormick, P. Tempst, J. Coadwell and P. T. Hawkins (1998). "Protein kinase B kinases that mediate phosphatidylinositol 3,4,5-trisphosphate-dependent activation of protein kinase B." Science **279**(5351): 710-714.

Stephens, L. R., K. T. Hughes and R. F. Irvine (1991). "Pathway of phosphatidylinositol(3,4,5)-trisphosphate synthesis in activated neutrophils." Nature **351**(6321): 33-39.

Stokoe, D., L. R. Stephens, T. Copeland, P. R. Gaffney, C. B. Reese, G. F. Painter, A. B. Holmes, F. McCormick and P. T. Hawkins (1997). "Dual role of phosphatidylinositol-3,4,5-trisphosphate in the activation of protein kinase B." Science **277**(5325): 567-570.

Suzuki, A., J. L. de la Pompa, V. Stambolic, A. J. Elia, T. Sasaki, I. del Barco Barrantes, A. Ho, A. Wakeham, A. Itie, W. Khoo, M. Fukumoto and T. W. Mak (1998). "High cancer susceptibility and embryonic lethality associated with mutation of the PTEN tumor suppressor gene in mice." Curr Biol **8**(21): 1169-1178.

Taylor, B. S., N. Schultz, H. Hieronymus, A. Gopalan, Y. Xiao, B. S. Carver, V. K. Arora, P. Kaushik, E. Cerami, B. Reva, Y. Antipin, N. Mitsiades, T. Landers, I. Dolgalev, J. E. Major, M. Wilson, N. D. Socci, A. E. Lash, A. Heguy, J. A. Eastham, H. I. Scher, V. E. Reuter, P. T. Scardino, C. Sander, C. L. Sawyers and W. L. Gerald (2010). "Integrative genomic profiling of human prostate cancer." Cancer Cell **18**(1): 11-22.

Taylor, V., M. Wong, C. Brandts, L. Reilly, N. M. Dean, L. M. Cowsert, S. Moodie and D. Stokoe (2000). "5' phospholipid phosphatase SHIP-2 causes protein kinase B inactivation and cell cycle arrest in glioblastoma cells." Mol Cell Biol **20**(18): 6860-6871.

Thomas, C. C., S. Dowler, M. Deak, D. R. Alessi and D. M. van Aalten (2001). "Crystal structure of the phosphatidylinositol 3,4-bisphosphate-binding pleckstrin homology (PH) domain of tandem PH-domain-containing protein 1 (TAPP1): molecular basis of lipid specificity." Biochem J **358**(Pt 2): 287-294.

Thomas, M. P., C. Erneux and B. V. L. Potter (2017). "SHIP2: Structure, Function and Inhibition." ChemBioChem **18**(3): 233-247.

Tibarewal, P., G. Zilidis, L. Spinelli, N. Schurch, H. Maccario, A. Gray, N. M. Perera, L. Davidson, G. J. Barton and N. R. Leslie (2012). "PTEN protein phosphatase activity correlates with control of gene expression and invasion, a tumor-suppressing phenotype, but not with AKT activity." Sci Signal **5**(213): ra18.

Traynor-Kaplan, A. E., A. L. Harris, B. L. Thompson, P. Taylor and L. A. Sklar (1988). "An inositol tetrakisphosphate-containing phospholipid in activated neutrophils." Nature **334**(6180): 353-356.

Trimboli, A. J., C. Z. Cantemir-Stone, F. Li, J. A. Wallace, A. Merchant, N. Creasap, J. C. Thompson, E. Caserta, H. Wang, J. L. Chong, S. Naidu, G. Wei, S. M. Sharma, J. A. Stephens, S. A. Fernandez, M. N. Gurcan, M. B. Weinstein, S. H. Barsky, L. Yee, T. J. Rosol, P. C. Stromberg, M. L. Robinson, F. Pepin, M. Hallett, M. Park, M. C. Ostrowski and G. Leone (2009). "Pten in stromal fibroblasts suppresses mammary epithelial tumours." Nature **461**(7267): 1084-1091.

Trotman, L. C., M. Niki, Z. A. Dotan, J. A. Koutcher, A. Di Cristofano, A. Xiao, A. S. Khoo, P. Roy-Burman, N. M. Greenberg, T. Van Dyke, C. Cordon-Cardo and P. P. Pandolfi (2003). "Pten dose dictates cancer progression in the prostate." PLoS Biol **1**(3): E59.

Vadas, O., J. E. Burke, X. Zhang, A. Berndt and R. L. Williams (2011). "Structural basis for activation and inhibition of class I phosphoinositide 3-kinases." Sci Signal **4**(195): re2.

van Meer, G., D. R. Voelker and G. W. Feigenson (2008). "Membrane lipids: where they are and how they behave." Nat Rev Mol Cell Biol **9**(2): 112-124.

Vance, J. E. (2015). "Phospholipid synthesis and transport in mammalian cells." Traffic **16**(1): 1-18.

Vanhaesebroeck, B., J. Guillermet-Guibert, M. Graupera and B. Bilanges (2010). "The emerging mechanisms of isoform-specific PI3K signalling." Nat Rev Mol Cell Biol **11**(5): 329-341.

Vanhaesebroeck, B., L. Stephens and P. Hawkins (2012). "PI3K signalling: the path to discovery and understanding." Nat Rev Mol Cell Biol **13**(3): 195-203.

Wada, T., T. Sasaoka, M. Funaki, H. Hori, S. Murakami, M. Ishiki, T. Haruta, T. Asano, W. Ogawa, H. Ishihara and M. Kobayashi (2001). "Overexpression of SH2-containing inositol

phosphatase 2 results in negative regulation of insulin-induced metabolic actions in 3T3-L1 adipocytes via its 5'-phosphatase catalytic activity." Mol Cell Biol **21**(5): 1633-1646.

Wan, L., K. Pantel and Y. Kang (2013). "Tumor metastasis: moving new biological insights into the clinic." Nat Med **19**(11): 1450-1464.

Wang, S., J. Gao, Q. Lei, N. Rozengurt, C. Pritchard, J. Jiao, G. V. Thomas, G. Li, P. Roy-Burman, P. S. Nelson, X. Liu and H. Wu (2003). "Prostate-specific deletion of the murine Pten tumor suppressor gene leads to metastatic prostate cancer." Cancer Cell **4**(3): 209-221.

Whitman, M., C. P. Downes, M. Keeler, T. Keller and L. Cantley (1988). "Type I phosphatidylinositol kinase makes a novel inositol phospholipid, phosphatidylinositol-3-phosphate." Nature **332**(6165): 644-646.

Worby, C. A. and J. E. Dixon (2014). "Pten." Annu Rev Biochem **83**: 641-669.

Wu, X., J. Wu, J. Huang, W. C. Powell, J. Zhang, R. J. Matusik, F. O. Sangiorgi, R. E. Maxson, H. M. Sucov and P. Roy-Burman (2001). "Generation of a prostate epithelial cell-specific Cre transgenic mouse model for tissue-specific gene ablation." Mech Dev **101**(1-2): 61-69.

Yamaguchi, H., S. Yoshida, E. Muroi, N. Yoshida, M. Kawamura, Z. Kouchi, Y. Nakamura, R. Sakai and K. Fukami (2011). "Phosphoinositide 3-kinase signaling pathway mediated by p110alpha regulates invadopodia formation." J Cell Biol **193**(7): 1275-1288.

Ye, Y., L. Jin, J. S. Wilmott, W. L. Hu, B. Yosufi, R. F. Thorne, T. Liu, H. Rizos, X. G. Yan, L. Dong, K. H. Tay, H. Y. Tseng, S. T. Guo, C. E. de Bock, C. C. Jiang, C. Y. Wang, M. Wu, L. J. Zhang, P. Hersey, R. A. Scolyer and X. D. Zhang (2013). "PI(4,5)P2 5-phosphatase A regulates PI3K/Akt signalling and has a tumour suppressive role in human melanoma." Nat Commun **4**: 1508.

Zhang, J., T. Z. Thomas, S. Kasper and R. J. Matusik (2000). "A small composite probasin promoter confers high levels of prostate-specific gene expression through regulation by androgens and glucocorticoids in vitro and in vivo." Endocrinology **141**(12): 4698-4710.

Zhao, L. and P. K. Vogt (2008). "Helical domain and kinase domain mutations in p110alpha of phosphatidylinositol 3-kinase induce gain of function by different mechanisms." Proc Natl Acad Sci U S A **105**(7): 2652-2657.